QUANTUM EFFECTS IN THE HMF MODEL

QUANTUM EFFECTS IN THE HAMILTONIAN MEAN FIELD MODEL

By RYAN PLESTID, B. Sc. , M. Sc.

A Thesis Submitted to the School of Graduate Studies in Partial Fulfilment of the Requirements for the Degree Doctor of Philosophy

McMaster University DOCTOR OF PHILOSOPHY (2019) Hamilton, Ontario (Physics and Astronomy)
TITLE: Quantum Effects in the Hamiltonian Mean Field Model
AUTHOR: Ryan Plestid, B.Sc. (University of Guelph), M.Sc. (McMaster University)
SUPERVISOR: Professor Duncan H. J. O'Dell
NUMBER OF PAGES: ix, 104

Lay Abstract

The Hamiltonian Mean Field (HMF) model was initially proposed as a simplified description of self-gravitating systems. Its simplicity shortens calculations and makes the underlying physics more transparent.This has made the HMF model a key tool in the study of systems with long-range interactions.

In this thesis we study a quantum extension of the HMF model. The goal is to understand how quantum effects can modify the behaviour of a system with long-range interactions. We focus on how the model relaxes to equilibrium, the existence of special "solitary waves", and whether quantum fluctuations can prevent a second order (quantum) phase transition from occurring at zero temperature.

Abstract

We consider a gas of indistinguishable bosons, confined to a ring of radius R, and interacting via a pair-wise cosine potential. This may be thought of as the quantized Hamiltonian Mean Field (HMF) model for bosons originally introduced by Chavanis as a generalization of Antoni and Ruffo's classical model.

This thesis contains three parts: In part one, the dynamics of a Bose-condensate are considered by studying a generalized Gross-Pitaevskii equation (GGPE). Quantum effects due to the quantum pressure are found to substantially alter the system's dynamics, and can serve to inhibit a pathological instability for repulsive interactions. The non-commutativity of the large-N, long-time, and classical limits is discussed.

In part two, we consider the GGPE studied above and seek static solutions. Exact solutions are identified by solving a non-linear eigenvalue problem which is closely related to the Mathieu equation. Stationary solutions are identified as solitary waves (or solitons) due to their small spatial extent and the system's underlying Galilean invariance. Asymptotic series are developed to give an analytic solution to the non-linear eigenvalue problem, and these are then used to study the stability of the solitary wave mentioned above.

In part three, the exact solutions outlined above are used to study quantum fluctuations of gapless excitations in the HMF model's symmetry broken phase. It is found that this phase is destroyed at zero temperature by large quantum fluctuations. This demonstrates that mean-field theory is *not* exact, and can in fact be qualitatively wrong, for long-range interacting quantum systems, in contrast to conventional wisdom.

Acknowledgements

It has been a long time since I started, and its hard to think back to what it felt like when I first moved to Hamilton to start my M.Sc. Everything seemed so overwhelming at the time, and its kind of crazy to look back and see how far I have come. For my most formative years I have a lot of people to thank. First my peers: Shouvik for being a great office mate and someone I could always talk physics with, Sedigh for always checking in to make sure things were going alright, Matt and Ross for always being ready to lend a hand, Wen for his positivity, and Gabriel for challenging me and keeping me honest. I am also endebted to my mentors. To Itay, Cliff, Sung-Sik and Brian: the learning curve was steep but you helped me climb it. I probably learned more in the PI-shuttle than in any class room, and so thank you Werner for working fourteen hour days andslogging through bad weather.

For my time during the Ph.D. I also have many people to thank. First and foremost thank you Duncan for your flexibility, and the freedom it offered me. I was able to see the world, meet a lot of great people, and work on a lot of great physics because of your support and I will always remember that. Of course I have to thank Gabriel twice, and Maxim, Cliff, and Richard also, because without them I would never have had the options that I have today, and I certainly wouldn't be moving on to Fermilab and U. Kentucky.

My Ph.D. was more than just a list of papers, and I have spent more time at McMaster than I have anywhere else in my adult life. There were a lot of good times that I will look back fondly upon, and a lot of friendships I won't forget. Tina, Cheryl, Mara, and Hope: the department would go up in flames without you, thank you so much. To Joey, Wyatt, James, Alex, and later Dan, thank you for the the clown-car parties at Winston Place. James, Anton, Greg, Laszlo, Peter, Ivy, Zhiqiang, Jon, and Micheal, thank you for helping out with the Journal Club. Ian, Ashley, Joey, and especially Wyatt, it was a pleasure working with you planning department events. A huge shout out to Sarah, Joey, Anton, and everyone else who helped out with the the SWL-math club. To Carmen, Thanasis, Lilli, James, Connor, Jesse, Sririam, Matt, Sebastian, Adam, Markus, Paolo, Mel, Dalini, Mahsa, Gwen, Sean, Andreas(es), Faiyaz, Mark,

Gandhali, and everybody else I met in the department over the years; your good people, thanks for being you.

The people I met in Hamilton and abroad over the past four years have a special place in my heart. Kate I am so happy I stumbled across you at that pub crawl, and Annica I am even happier that we became such good friends. Kevin, I can't believe we became so close in only a few short weeks together at Weizmann. I did not expect to gain a new friend from that trip, but I am elated that I did. Ramsha and Pip, I never met any people as easy to talk to as you two, and you guys are the real reason I enjoyed Kevlahan's class as much as I did. To all the Goal Diggers, but especially Mack, Fred, Paul, Hailey, Joe, and Kylie, no matter how much we sucked, I don't think I've ever had a better time playing soccer than I did with you guys. Rober and Sunny, it was great getting to know you, and all the times we spent together hanging out with Vincent. Catherine, you were a great neighbour and you're maybe the easiest person to talk to I have ever met. And Jitka, I don't think anyone has ever felt so much like family to me, even more so after Martin and Elishka took care of us in Brno. My Ph.D. flew by with you around, and I hope I get to see you as often as possible in the next chapter of our lives.

Finally, I wanted to thank the people who have been in my life since before this all started. First and foremost: Leanne, thank you for coming to live in Hamilton, and enduring the GO-train for two and a half years, and thank you even more for being so happy to come with me to Chicago. To my family: you have been more supportive and helpful than I ever could have hoped for. Its crazy to think about all of the opportunities you provided me, and crazier still that so many people do not get the same. Katie and Andrea, you are my closest friends, and I am going to miss the hell out of you. Marcus, Vanessa, Dylan, and Ben, I love that we still see each other, even without a common circle of friends; you guys are friends for life. To my friends from Guelph; I can't express how much it means to me that we have all stuck together Kaya (and Pat), Tan, Kristen, Alex, Boris, Emily, Willem, Phil, Stephen, Steph, Dan, and Shayan. The same for Gresham, Andrew, Liam, Doorn (even if you live in Woodstock), Slater, Kyle, and Jason.

Contents

List of Figures

List of Abbreviations and Symbols

BEC Bose-Einstein condensate

GGPE Generalized Gross-Pitaevskii equation

GPE Gross-Pitaevskii equation

HMF Hamiltonian Mean Field Model

LRI(s) Long-range interaction(s)

LRI-MB Long-range interacting many-body

QSS Quasi-stationary state

Declaration of Academic Achievement

- **Chapter 2:** is based on
  R. Plestid, D. H. J. O'Dell, and P. Mahon, *Violent relaxation in quantum fluids with long-range interactions*, Phys. Rev. E. **98**, 012112, (2018).

  Ryan Plestid wrote the code for the numerical simulations, ran the simulations, wrote the majority of the manuscript, performed all of the calculations, and made all of the figures except for Figs. 2 & 7 (made by Dr. Duncan O'Dell). Fig. 6 was made jointly by Ryan and Dr. Duncan O'Dell.

  Dr. Duncan O'Dell concieved of the idea for the project and oversaw the calculations and simulations. He also provided edits to the entire manuscript, and contributed significantly to the writing of the introduction (especially the connections to cavity-QED experiments and dipolar BECs) and Sec. VII.

  Perry Mahon performed exploratory numerical simulations in the early stages of this project, and provided final comments on the manuscript before submission.

- **Chapter 3:** is based on
  R. Plestid, and D. H. J. O'Dell, *Balancing long-range interactions and quantum pressure: solitons in the HMF model*, Phys. Rev. E. **100**, 022216, (2019)

  Ryan Pletid performed all of the calculations, made all of the figures, wrote the full manuscript, and was involved in all final edits.

  Dr. Duncan O'Dell suggested mapping the problem onto the Mathieu equation, and provided useful guidance on the analytic properties of the Mathieu functions which were essential in obtaining the central results of the paper. helped to edit the manuscript, suggested the inclusion of Figs. 3 & 4, and contributed significantly to the introduction, conclusion, and the discussion surrounding Figs. 3 & 4.

- **Chapter 4:** is based on
  R. Plestid, and J. Lambert, *Goldstone modes destroy order in a long-range interacting Bose Gas*, in prep.

  Ryan Plestid developed and performed all of the calculations, and helped to make all of the figures. Ryan also wrote the majority of the manuscript.

  James Lambert reproduced/checked important calculations and found a crucial error that changed the qualitative conclusions of the paper. James also edited parts of the manuscript and was involved in important discussions that shaped the future outlook in the final section of the paper.

  Sung-Sik Lee suggested the project initially and was constantly available for feedback. His input was extremely valuable.

Complete List of Publications

During my Doctorate, in addition to my work on the HMF model, I have worked on particle physics phenomenology both within and beyond the Standard Model, and on the development and application of point particle effective field theory. Below is a comprehensive list of my publications since September 2015 organized by subject area, daggers[†] denote first author or equivalent.

The Hamiltonian Mean-Field Model

1. R. Plestid[†], D.H.J. O'Dell, and P. Mahon, *Violent Relaxation in Quantum Fluids with Long-Range Interactions*, Phys. Rev. E **98**, 012112 (2018)

2. R. Plestid[†], and D.H.J. O'Dell, *Balancing Long-Range Interactions and Quantum Pressure: Solitons in the HMF Model*, Phys. Rev. E **100**, 022216 (2019)

Point Particle Effective Field Theory

1. R. Plestid[†], C.P. Burgess, and D.H.J. O'Dell, *Fall to the Centre in Atom Traps and Point-Particle EFT for Absorptive Systems*, JHEP 2018:08, (2018)

2. M. Rummel[†], R. Plestid, and C.P. Burgess, *Effective Field Theory of Black Hole Echoes*, JHEP 2018:09, (2018)

Particle Phenomenology

1. R. Plestid[†], G. Magill[†], M. Pospelov, Y.D. Tsai, *Millicharged Particles in Neutrino Experiments*, Phys. Rev. Lett. **122** 071801 (2019)

2. R. Plestid[†], G. Magill[†], M. Pospelov, Y.D. Tsai, *Dipole Portal to Heavy Neutral Leptons*, Phys. Rev. D. **98** 115015 (2018)

3. R. Plestid[†], G. Magill[†], *Probing New Charged Scalars with Neutrino Trident Production* , Phys. Rev. D. **97** 055003 (2018)

4. R. Plestid[†], G. Magill[†], *Neutrino Trident Production at the Intensity Frontier*, Phys. Rev. D. **95** (2017) 073004 (2017)

"It [thermodynamics] is the only physical theory of universal content which I am convinced will never be overthrown, within the framework of applicability of its basic concepts."

—Albert Einstein

CHAPTER 1

Introduction

Long-range interacting many-body (LRI-MB) systems are poorly understood in the context of statistical physics, especially compared to their short-range interacting counterparts. A wide range of theorems, formalisms, and basic results assume, and heavily rely upon, the constituent degrees of freedom interacting via a short-range force and are often invalid in the presence of long-range interactions (LRIs); in these situations proofs need to be re-evaluated on a case-by-case basis. This is true of both the Mermin-Wagner [1, 2] and Goldstone theorems [3], and also of basic fundamental building blocks such as the equivalence of ensembles [4–6] and even the concept of additive energies [7]. These issues are further compounded by dynamical features of LRI-MB systems. Conventional statistical mechanics is founded on ergodic theory which postulates that, after any reasonably long time scale, a macroscopic system will explore its energetically accessible phase space such that time averaged measurements are equivalent to microcanonical averages. LRI-MB systems, however, are characterized by extremely slow relaxation rates (taking a timescale $t \sim \mathcal{O}(\log N)$ to relax to equilibrium [8–10]) and their late time behaviour, being far from equilibrium, often disagrees with microcanonical predictions [11]; their behaviour, therefore, often resembles that of integrable systems.

These features were well known in the astrophysical community as early as the 1920s [14], but were strongly emphasized in the 1960s by Donald Lynden-Bell [15, 16] (see [17–19] for a more contemporary discussion). Other communities have noted the importance of long-range interactions. This includes the study of non-neutral plasmas [20–24], long-range interacting spin chains [25–32], dipolar Bose gases [33–41], Rydberg atoms [42–49], and atoms interacting via (spatially extended) electromagnetic modes in an optical cavity [50–61]. Nevertheless, certain peculiarities specific to LRI-MB systems

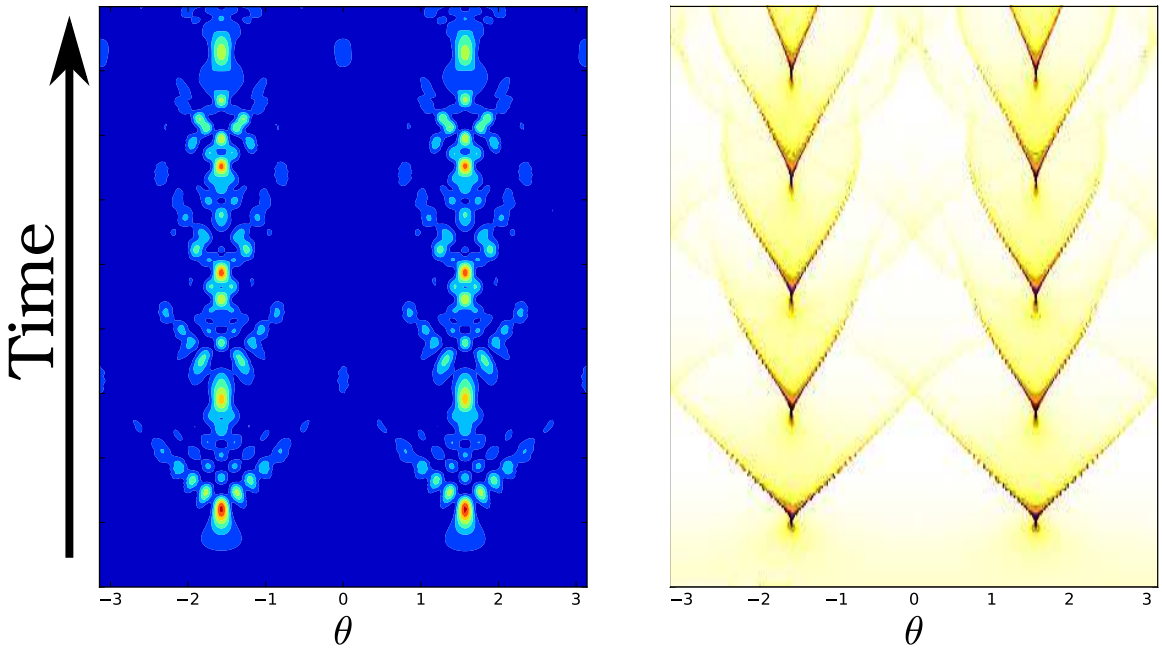

Figure 1.1: Comparison of the formation of a bi-cluster in the quantum and classical HMF model with repulsive interactions. An initial (nearly) homogeneous gas of particles (defined on a ring of unit radius) undergoes rapid, but small amplitude fluctuations. Due to long-range interactions, this leads to an effective time-averaged focusing potential that results in a bi-cluster. Quantum effects modify this behaviour leading to either a dressed interference pattern or a lack of focusing altogether (depending on the strength of the quantum effects). The left figure is taken from [12] (i.e. Chapter 2), while the right figure is taken from [13] and has been re-scaled, and cropped to match the figure on the left.

(such as negative specific heats) were ignored or dismissed as being peculiar features of gravitational systems by the statistical physics community [18]. Consequently a unified approach to understand LRI-MB systems has largely emerged only in the past twenty-five years (see [5, 11, 62] for reviews). Much of the recent progress in this field can be attributed to the development of a group of exactly solvable[1] toy models that have served as testing grounds for new ideas and provided litmus tests to identify generic behavior common across a wide range of LRI-MB systems [5]. These toy models can provide rigorous tests for general statistical theories of LRI-MB systems, but are also extremely useful for exploring the connection between their dynamics and their approach towards (or stubborn resistance to) equilibrium.

From the intense research activity over the past twenty years, the Hamiltonian Mean Field (HMF) model has emerged as the most prominent toy model for LRI-MB physics [5, 7, 11, 63]. Often referred to as paradigmatic, the HMF model has shown a remarkable ability to capture dynamical properties that appear across a wide range of LRI-MB systems, whilst simultaneously exhibiting non-trivial behaviour such as a symmetry breaking phase transition that is naively forbidden by the Mermin-Wagner theorem. Nevertheless, its hallmark, when compared to other exactly solvable models of LRI-MB systems (such as the Blume-Emery-Grifiths model [4], the long-range Ising model [13], or the mean-field ϕ^4 model [64]), is that it has non-trivial dynamics. Better yet, these dynamics closely mimic those of a self-gravitating system, reproducing the same dynamical behaviour that leads to Lynden-Bell [15] and core-halo statistics [11, 65–67]. Furthermore, due to its simplicity, the HMF model is amenable to large-scale numerical simulations allowing for a direct comparison between molecular dynamics simulations and new proposals for statistical theories of LRI-MB systems' late-time behaviour [11].

The HMF model describes a system of N particles of mass m on a ring of radius R interacting via a pairwise cosine potential. It is therefore a full many-body description of a LRI-MB system. This is equivalent to an infinite-range kinetic-XY (or $O(2)$ rotor) model, and this correspondence informs much of the model's nomenclature. The HMF

[1] In this context this refers to a model whose canonical free-energy or microcanonical internal energy can be found exactly in the $N \to \infty$ limit.

model's Hamiltonian can be written as

$$H = \frac{1}{2mR^2}\sum_i L_i^2 + \frac{\epsilon}{N}\sum_{i<j}\cos(\theta_i - \theta_j) \tag{1.1}$$

where L_i is the conjugate momentum to the position variable θ_i, ϵ characterizes the interaction strength, and the $\frac{1}{N}$ factor (known as the Kac prescription [68]) preserves extensivity of the energy in the thermodynamic limit. The case of $\epsilon > 0$ corresponds to repulsive (or anti-ferromagnetic) interactions, while $\epsilon < 0$ corresponds instead to attractive (or ferromagnetic) interactions. As alluded to above, the HMF model has attracted substantial attention, and its classical behaviour, both dynamical and statistical, has been extremely well studied [13, 62, 63, 66, 69–81]. Despite this progress, the HMF model's quantum behaviour has remained relatively unexplored with only preliminary studies having taken place [82, 83].

The focus of this thesis is to extend our knowledge of the HMF model and its properties to the quantum regime, where the Hamiltonian takes the (first quantized) form [82]

$$\hat{H} = \frac{\hbar^2}{2mR^2}\sum_i\left(-\mathrm{i}\frac{\partial^2}{\partial\theta_i^2}\right) + \frac{\epsilon}{N}\sum_{i<j}\cos(\theta_i - \theta_j)\ . \tag{1.2}$$

At the time of this writing, very little research has been conducted on the extension of known results in the HMF model to the quantum regime (which is generally true of the theory of LRI-MB systems). This thesis focuses on three different consequences of quantum effects for the HMF models dynamical and statistical behaviour. First, in Chapter 2 a well known dynamical instability of the model is investigated whose presence is related to the (lack of) thermalization in the model. Quantum effects are found to modify this behaviour and a schematic dynamical phase diagram is constructed. In Chapter 3 the mean-field (i.e. Gross-Pitaevskii) equations of the model are studied and all possible stationary states are identified. Exact solutions are found, with a fully analytic (non-trivial) solution available in two distinct scaling limits. Finally, in Chapter 4, the exact solution of the lowest energy stationary state is used to construct a variational ansatz for the ground state wavefunction. We find that quantum fluctuations inhibit the formation of the clustered phase that is known to exist classically, and was predicted on the grounds of mean-field theory. Chapter 5 summarizes the current state of affairs for the quantum HMF model, and outlines

what we feel are crucial open questions and next steps that can be taken to address them.

Literature Review and Background Material

The remainder this chapter will serve as an introduction to the motivations for, and techniques used in, each of the three papers mentioned above. First in Section 1.1 we give a short introduction to the (relatively) newly developed theory of LRI-MB systems at equilibrium. This includes a short discussion of extensivity, additivity, ensemble inequivalence, and the role of LRIs in modifying key theorems related to spontaneous symmetry breaking. Next, in Section 1.2 we focus on the dynamical features of long-range interacting systems. The focus here is on the derivation of the Vlasov equation, and its implications for (non-)thermalization in LRI-MB physics. The Vlasov equation, has emergent symmetries and conservation laws whose presence can drastically alter a system's dynamical behavior. We discuss how the Vlasov equation's dynamics can lead to the formation of so-called quasi-stationary states (QSSs), via a process known as violent relaxation (VR). Then, in Section 1.3 we give a short-introduction to the conventional theory of a dilute Bose-gas, paying specific attention to the case of a finite sized system. We also overview non-local mean-field theories (i.e. a generalized Gross-Pitaevskii equation [GGPE]) for Bose systems. Finally, in Section 1.4 we turn our attention towards the HMF model, and the existing literature surrounding it. This includes existing results regarding the HMF model's quantum behaviour as well as its features in the classical regime.

1.1 Statistical Features of Long-Range Interactions

Why can LRIs undermine the foundations of conventional statistical mechanics? The simplest, and most fundamental, reason is that energy cannot be additive for a LRI-MB system. This idea is most easily illustrated by considering a simple model; namely the

all-to-all (or infinite ranged) ferromagnetic Ising model [84]

$$H = -\frac{J}{N}\sum_{j=1}^{N}\sum_{i<j}\sigma_i\sigma_j \ , \tag{1.3}$$

where $\sigma_i \in \{0,1\}$ is a classical spin pointing either up or down, $J > 0$ is a coupling with dimensions of energy, and the factor of $1/N$ has been included to make the Hamiltonian extensive (this is known as the Kac-prescription [68])

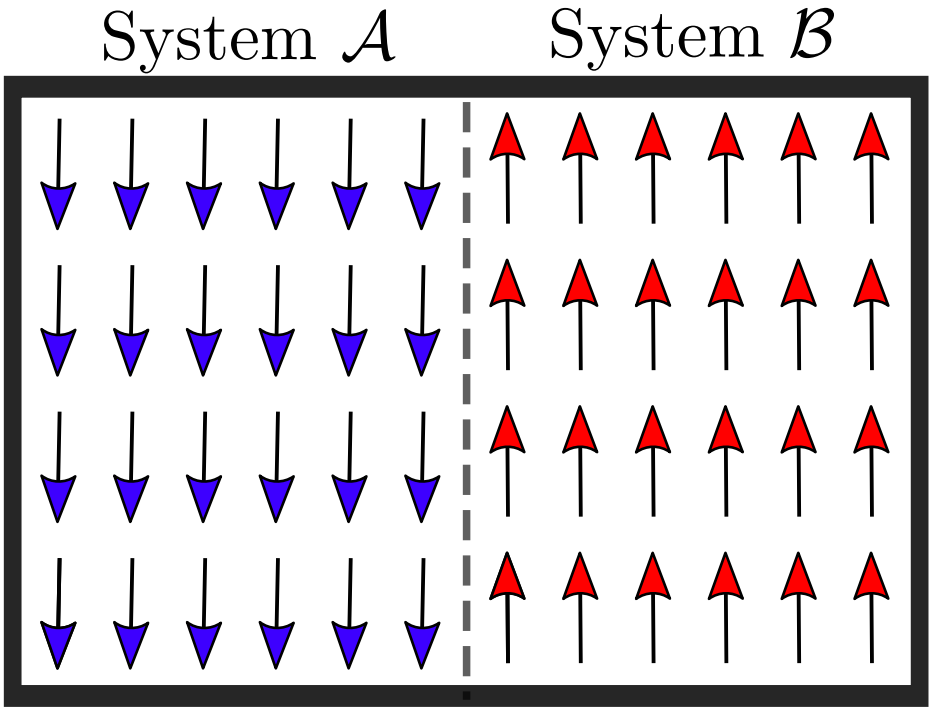

Figure 1.2: Spin configuration for the all-to-all Ising model for $2N$ spins partitioned into two blocks of N spins. In this case of all-to-all interactions the energy of the left block is minimal, $E_{\mathcal{A}} = -J(N-1)/2$, as is the energy of the right block, $E_{\mathcal{B}} = -J(N-1)/2$, and yet the system's energy is $E = 0 \neq E_{\mathcal{A}} + E_{\mathcal{B}}$, and is thus non-additive. This is the interaction between $\mathcal{A}$ and $\mathcal{B}$ is extensive, $E_{\text{int}} \sim \mathcal{O}(N)$.

We will consider a system of spins, $\mathcal{S}$, that has been bi-partitioned, $\mathcal{S} = \mathcal{S}_A \otimes \mathcal{S}_B$. We will be interested in calculating the energy of the full system, E, and of the isolated sub-systems, E_A and E_B respectively. This idea is illustrated for a particular spin configuration in Figure 1.2, where it can be easily seen that $E \neq E_A + E_B$, even in the thermodynamic limit. This is because the interaction energy between $\mathcal{S}_A$ and $\mathcal{S}_B$ scales extensively $E_{\text{int}} \sim \mathcal{O}(N)$; the interaction can "reach acrosss" the boundary. This

is to be contrasted with the short-ranged Ising model, where the interaction between the two blocks is limited to their shared boundary. This kind of infinite ranged model seems pathological at first sight, however it serves to illustrate key concepts and ideas that appear in more realistic models.

1.1.1 Scaling of Entropy

Boltzmann famously connected thermodynamics and microscopic physics, by realizing that entropy could be defined by counting microstates via his celebrated formula

$$S = k_B \ln \Omega \tag{1.4}$$

where Ω is the number of accessible states given a set of constraints (such as fixed energy). As we have discussed above, for a short-range interacting systems, the local nature of the interactions guarantees that the energy is additive. For a microcanonical state this has important ramifications for the entropy.

To be concrete, suppose a large system (hereafter called "the universe") is composed of N identical particles and is described by the Hamiltonian $H(u)$ (where u is a microstate of the universe). Suppose $\mathcal{U}$ has an energy $E_{\mathcal{U}}$, and is at equilibrium (defined as a maximum entropy state). There are a large number, $\Omega_{\mathcal{U}}(E_{\mathcal{U}})$, of microstates, u, with energy $H(u) = E_{\mathcal{U}}$.

We will be interested in partitioning the universe into two systems $\mathcal{A}$ and $\mathcal{B}$. In a short-range interacting system, for microstates a and b we have that $H(u) = H(a, b) = H(a) + H(b)$ because the energy is additive in the thermodynamic limit. Therefore we find that if our two sub-systems have average energy $E_{\mathcal{A}}$ and $E_{\mathcal{B}}$ respectively then

$$\Omega(E_{\mathcal{U}}) = \sum_{E_{\mathcal{A}}} \Omega(E_{\mathcal{A}})\Omega(e_{\mathcal{U}} - E_{\mathcal{A}}) \quad \text{(short-range systems)}. \tag{1.5}$$

In the thermodynamic limit the most probable energy of each sub-system dominates the sum, and we can approximate Equation (1.5) as

$$\Omega(E_{\mathcal{U}}) \approx \Omega(E_{\mathcal{A}})\Omega(E_{\mathcal{B}}) \quad \text{(short-range systems)}. \tag{1.6}$$

which, when coupled with Equation (1.4), immediately implies that

$$S(E) = S(E_{\mathcal{A}}) + S(E_{\mathcal{B}}) \quad \text{(short-range systems)} \; . \tag{1.7}$$

Consider, in contrast the case of a LRI-MB system. For microstates a and b we have instead that

$$H(a,b) = H(a) + H(b) + H_{\text{int}}(a,b) \tag{1.8}$$

where $H_{\text{int}}(a,b)$ describes the long-range interactions between sub-system a and sub-system b.

For concreteness let us consider the infinite-range Ising model, Equation (1.3), and specifically consider the case of $E_{\mathcal{U}} = 0$. Let us take the universe to contain $2N$ spins that are bi-paritioned into equal sub-systems composed of N spins. The criterion that $E_{\mathcal{U}} = 0$ demands that half of all spins in the universe point down, and that the other half point up; note that the spin configuration shown in Figure 1.2 is one example of a configuration that satisfies $E_{\mathcal{U}} = 0$ but there are many more (most of which have a mixture of up and down spins in both $\mathcal{A}$ and $\mathcal{B}$). We can calculate the total number of microstates, u, satisfying this criterion explicitly

$$\Omega_{\mathcal{U}} = \binom{2N}{N} = \frac{(2N)!}{N!N!} \approx \sqrt{2} \times \frac{2^{2N}}{\sqrt{N}} \tag{1.9}$$

where we have used Stirling's formula $N! \sim \sqrt{2\pi N}(N/e)^N$. Within this ensemble $E_{\mathcal{A}} = 0$ and $E_{\mathcal{B}} = 0$, and so applying the above formula to each of these sub-systems containing N spins we find

$$\Omega_{\mathcal{B}} = \Omega_{\mathcal{A}} = \binom{N}{N/2} = \frac{(N)!}{\frac{N}{2}!\frac{N}{2}!} \approx 2 \times \frac{2^N}{\sqrt{N}} \tag{1.10}$$

We can then compute $S(E_{\mathcal{U}})$ and compare it to $S(E_{\mathcal{A}}) + S(E_{\mathcal{B}}) = 2S(E_{\mathcal{A}})$

$$S(E_{\mathcal{U}}) \sim k_B 2N \ln 2 - \frac{1}{2}\ln N + \frac{1}{2}\ln 2 + \mathcal{O}\Big(\frac{1}{N}\Big) \tag{1.11}$$

$$2S(E_{\mathcal{A}}) \sim k_B 2N \ln 2 - \ln N + \ln 2 + \mathcal{O}\Big(\frac{1}{N}\Big) \tag{1.12}$$

Thus, in this extreme example of infinite range interactions, the entropy is additive up to errors of $\mathcal{O}(\log N)$, and similar errors are present in short-range interacting systems

when approximating Equation (1.5) by Equation (1.6), such that in the thermodynamic limit

$$S(E) \approx S(E_{\mathcal{B}}) + S(E_{\mathcal{A}}) \ . \tag{1.13}$$

Notice, for example, that the spin configuration shown in Figure 1.2 contributes to the entropy of the universe (as it has energy $E_{\mathcal{U}} = 0$) but not to the entropy of the sub-systems (since $E_{\mathcal{A}} \ll 0$ and $E_{\mathcal{B}} \ll 0$).

1.1.2 Additivity of Energy

A more realistic situation is a spatially dependent two-body interaction potential whose long-range behaviour is that of a power law decay i.e.

$$V_{\text{LR}}(r) \sim \frac{V_\infty}{r^\alpha} \quad \text{as} \quad r \to \infty \ . \tag{1.14}$$

Consider a smoothly varying density profile $\rho(x) \sim \mathcal{O}(1)$, describing a system of particles each of which interact via the pair-wise potential $V(r)$; for simplicity we will take $\rho(\mathbf{x}) = \rho(|\mathbf{x}|)$ to be spherically symmetric[2] and the system to have a finite radial extent R. The total potential energy of the system is given by

$$\begin{aligned} U &= \int \mathrm{d}^d x_1 \mathrm{d}^d x_2 \rho(x_1)\rho(x_2) V(|x_1 - x_2|) \\ &= \int \mathrm{d}^d x \rho(x) \int \mathrm{d}^d y V(|\mathbf{y}|)\rho(\mathbf{x}+\mathbf{y}) \\ &= N\Omega_{d-1} \int_0^R \mathrm{d}r r^{d-1} V(r)\rho(r) \ . \end{aligned} \tag{1.15}$$

where, here, Ω_{d-1} denotes the surface area of the $d-1$ sphere and should not be confused with the number of microstates. For a short-range interacting system, the remaining integral would evaluate to some finite $\mathcal{O}(1)$ number, but for a long-range interacting system this need not be the case. Splitting the integral into two pieces, we

[2]The following can be trivially generalized to spherically asymmetric densities by expanding in spherical harmonics. This does not affect the scaling argument presented below.

find

$$\begin{aligned} U &= N\Omega_{d-1}\left[\int_0^{\mathfrak{R}} \mathrm{d}r r^{d-1} V(r)\rho(r) + \int_{\mathfrak{R}}^{R} \mathrm{d}r r^{d-1} V(r)\rho(r)\right] \\ &\approx N\tilde{U}_0(\mathfrak{R}) + \frac{V_\infty}{d-\alpha}\Big(R^{d-\alpha} - \mathfrak{R}^{d-\alpha}\Big) N\Omega_{d-1} \\ &\approx N\tilde{U}_0(\mathfrak{R}) - \frac{V_\infty N\Omega_{d-1}}{d-\alpha}\mathfrak{R}^{d-\alpha} + \frac{V_\infty N\Omega_{d-1}}{d-\alpha}R^{d-\alpha} \\ &= NU_0 + \frac{V_\infty N\Omega_{d-1}}{d-\alpha}R^{d-\alpha}\ . \end{aligned} \tag{1.16}$$

where U_0 is some order one number (with dimensions of energy) that is independent[3] of $\mathfrak{R}$. If $\rho \sim \mathcal{O}(1)$ then this implies that $R \sim \mathcal{O}(N^{1/d})$, and so we find that the energy scales in three different ways depending on whether or not the interactions are long-ranged

$$U \sim \begin{cases} \mathcal{O}(N) & \text{for} \quad \alpha > d \\ \mathcal{O}(N\log N) & \text{for} \quad \alpha = d \\ \mathcal{O}\Big(N^{2-\frac{\alpha}{d}}\Big) & \text{for} \quad \alpha < d \end{cases} \tag{1.17}$$

these three cases are referred to as short-range, marginal, and long-range. Thus, the criterion for defining LRIs is dimensionally dependent [5, 85, 86].

Importantly, LRI-MB systems are characterized by energy scaling that is super-linear with respect to N. Just like in the all-to-all Ising model studied above, this leads to non-additive energies. A fundamental consequence of non-additive energies is that the microcanonical and canonical ensembles need not be equivalent even in the thermodynamic limit.

[3] Since $\mathfrak{R}$ was introduced spuriously into the problem, the left hand side of Equation (1.16) cannot depend on $\mathfrak{R}$, and so, therefore, neither can the combination $\tilde{U}_0\mathfrak{R} - V_\infty/(d-\alpha) \times \mathfrak{R}^{d-\alpha} := NU_0$.

1.1.3 Ensemble Inequivalence

Typically the microcanonical ensemble is justified by appealing to ergodicity[4]. The canonical ensemble is then derived by considering a large universe, $\mathcal{U}$, with microcanonical statistics. The universe is then partitioned into two macroscopic sub-systems; one a bath, $\mathcal{B}$, and the other our system of interest $\mathcal{S}$.

The microcanonical ensemble describes the probability for the universe to be in a microstate, u, given that the universe has an energy $E_{\mathcal{U}}$. It is defined by

$$\rho_{\text{mc}}(u; E_{\mathcal{U}}) = P(u|E_{\mathcal{U}}) = \frac{1}{\Omega(E_{\mathcal{U}})}\delta(H(u) - E_{\mathcal{U}}) \tag{1.18}$$

where $\delta(x)$, is the Dirac-delta function, and $\Omega(E_{\mathcal{U}})$ represent the number of microstates, u, with energies, $H(u) = E_{\mathcal{U}}$. Note that $\rho_{\text{mc}}(u; E_{\mathcal{U}})$ assigns a uniform probability weight to every state satisfying the energetic constraints imposed by the delta function.

We are interested in the probability of our system, $\mathcal{S}$, being in microstate s, conditioned on the universe having energy $E_{\mathcal{U}} = E$, $P(s|E)$. Since the super-system is describable by the microcanonical ensemble, we may trade energy for temperature by using

$$T = \left(\frac{\partial E}{\partial S}\right)_V \tag{1.19}$$

where S is the entropy, and the subscript denotes that volume, V, has been held fixed. Note, that this is only permissible if $S(E, V)$ is a concave function of energy. With this caveat in mind, we proceed and introduce the canonical ensemble defined by

$$\rho_c(s; T) = P(s|E) \quad \text{where} \quad T = \frac{\partial E}{\partial S}\ . \tag{1.20}$$

Since all microstates are equally likely in the canonical ensemble we have that

$$\rho_c(s; T) = \rho_{\text{mc}}\Omega_{\mathcal{B}}(E_{\mathcal{B}}) = \rho_{\text{mc}}\text{e}^{S(E_{\mathcal{B}})/k_B}\ . \tag{1.21}$$

where we have used Boltzmann's famous result $S = k_B \ln \Omega$. Now, the energy, E_b, of the bath's microstate, b, depends on the energy of the system E_s. *If the energy is*

[4] Although for some long-range interacting systems even this seemingly innocuous assumption can break down [see Section 1.2].

additive then $E_b = E - E_s$, and since the bath is macroscopic we may replace E_b by $E_{\mathcal{B}}$. Then since $E_s \ll E$ we may Taylor expand the entropy

$$\begin{aligned} S(E_{\mathcal{B}}) &\approx S(E) - E_s \frac{\partial S}{\partial E} \quad \text{if energy is additive} \\ &= S(E) - E_s/T \ . \end{aligned} \tag{1.22}$$

We can therefore conclude that

$$\rho_c(s;T) \propto \exp\left[-\frac{E_s}{k_B T}\right] , \tag{1.23}$$

with $\beta = 1/k_B T$ the inverse temperature. Notice that two crucial assumptions were made:

1. Energy is additive. We have shown above via microscopic considerations, that this is not true for a LRI-MB system.

2. Entropy is a concave function of energy. This also need not be true for a LRI-MB system, as we will discuss below.

This second feature has far reaching implications that can be understood purely at the level of thermodynamics (i.e. without recourse to statistical physics). Since different state functions are defined as Legendre transforms of one another, (e.g. $F = E - TS$), information is lost if the entropy is not concave. This is because a Legendre transform trades the argument of a function, for that function's derivative. If the function is not concave, then then there is no longer a one-to-one mapping between these two quantities, and the transformation can not be inverted without a loss of information [6].

In a standard course on statistical mechanics, a simple proof is given that establishes entropy as a concave function. It goes as follows: Consider a large short-range interacting system, $\mathcal{U}$, (once again called the universe) at equilibrium that can be partitioned into p subsystems, all with equal energy E. Next, consider an out-of-equilibrium configuration where r of the partitions have energy E_r and q of the partitions have energy E_q. Energy is additive (due to short-range interactions) such that $rE_r + qE_q = pE$. Since the entropy of an equilibrium state is maximal we can

guarantee that

$$pS(E) \geq rS(E_r) + qS(E_q). \tag{1.24}$$

Dividing through by p and introducing $\lambda = r/p$, we have, equivalently,

$$S(\lambda E_r + (1-\lambda)E_q) \geq \lambda S(E_r) + (1-\lambda)S(E_q) \quad \text{(short-range systems)} \quad , \tag{1.25}$$

which proves that entropy is a concave function of energy (with a similar argument proving it to be a concave function of any of its arguments).

This proof does not hold up for long-range interacting systems precisely because energy is not additive. We do not have the condition that $rE_r + qE_q = pE$, but instead that $rE_r + qE_q + H'_{\text{int}} = pE + H_{\text{int}}$ where H'_{int} is the net interaction energy of the various sub-sytems. This prevents us from taking Equation (1.24) and re-expressing it in the form Equation (1.24). Rather, we arrive at

$$S(\lambda E_r + (1-\lambda)E_q + H'_{\text{int}} - H_{\text{int}}) \geq \lambda S(E_r) + (1-\lambda)S(E_q) \quad \text{(long-range systems)} \quad , \tag{1.26}$$

and this does not imply concavity.

Thus the lack of additivity in LRI-MB systems both invalidates the typical proof of ensemble equivalence, and can lead to non-concave entropies. This is reminiscent of (but conceptually distinct from) the Maxwell construction for a non-concave pressure curve as a function of the energy. The (generalized) Legendre transform of a non-concave function will itself be concave, and so if a system has an entropy function with a convex intruder, its free energy will not contain the information about this intruder. Thus, upon inverting the Legendre transform, we find a different internal energy U' than we started with. This loss of information is what underlies the inequivalence of ensembles as emphasized in [5, 6].

1.1.4 Thermodynamic Limit

In the prototypical example of a short-range interacting gas the thermodynamic limit is derived by considering a finite sized system, of volume V, with a fixed number of particles N. Then, the limit is defined by considering $N \to \infty$, $L \to \infty$, with $N/L^d = \rho$ fixed. What is the appropriate limit for a system with LRIs?

The range of a long-range interaction introduces a new length scale into the problem whose influence persists in the $L \to \infty$ limit. Furthermore, the number of interacting pairs scales faster than $\mathcal{O}(N)$ [and as fast as $\mathcal{O}(N^2)$], whereas the kinetic energy scales linearly with N. This precludes a naive $N \to \infty$ scaling as it would lead to a trivial limit that is entirely dominated by the interaction energy; this is, of course, not physical. The underlying dynamics allow for the exchange of kinetic and potential energy, and identities such as the virial ratio for self-gravitating systems guarantees that both the interaction and kinetic energies will be of the same order.

Indeed, as will be discussed in Section 1.2, a long-range interacting system's momentum can be trivially re-scaled by choosing a dynamical time scale. For long-range interacting systems the dynamical time-scale is naturally N-dependent (because energy is non-extensive). One simple way to both ensure that energy is extensive, and that there is a non-trivial thermodynamic limit (where the kinetic and potential energies are allowed to compete with one another) is the so-called Kac prescription, wherein the long-ranged potential is rescaled $V_{\text{LR}} \to V_{\text{LR}}/N$. In this case, the volume should be held fixed while $N \to \infty$. For instance, if we considered a Hamiltonian

$$H = \sum_i \frac{p_i^2}{2m} + G \sum_{i<j} V(x_i - x_j) \ , \tag{1.27}$$

the Kac prescription would dictate that we introduce a new parameter $g = GN$ such that the Hamiltonian could be written as

$$H = \sum_i \frac{p_i^2}{2m} + \frac{g}{N} \sum_{i<j} V(x_i - x_j) \ , \tag{1.28}$$

then the thermodynamic limit would correspond to $N \to \infty$, with the volume V, and coupling, g, held fixed. Then, the sum $\sum_{i<j} V_{ij}$ is manifestly $\mathcal{O}(N^2)$ and the interaction energy is $\mathcal{O}(N)$ such that energy is extensive and the potential and kinetic energies are of the same order.

1.1.5 Mean-Field Theory and Symmetry Breaking

One powerful technique in statistical mechanics is mean-field theory whose, simplifying assumption involves ignoring statistical fluctuations and correlations. By imposing an

extraneous constraint on a statistical system its analysis is often greatly simplified. The successes and limitations of mean-field theory for short-range interacting systems are well understood and reviewed elsewhere [87, 88]. It is generically expected that long-range interacting systems are better described by mean-field theory, with many authors claiming that mean-field theory is exact [70, 82, 83, 89–94] (although see [81, 95, 96] for some interesting counter-examples). In this section we discuss mean-field theory contrasting its implications for long- and short-range interacting systems.

As an illustrative example of a short-range interacting system let us consider the mean-field treatment of the nearest-neighbour Ising model. Interactions between neighbouring spins are replaced by an averaged value, namely the magnetization M,

$$H = -J\sum_{\langle ij\rangle}\sigma_i\sigma_j \to -JzM\sum_i \sigma_i \tag{1.29}$$

where z is the coordination number of the lattice (e.g. $z = 2d$ for a d-dimensional square lattice), and $\bar{m} = \langle\sigma_i\rangle$.

This simplifying assumption can allow us to understand certain qualitative features of the model's behaviour *if fluctuations are small*. Famously, in the Ising model, mean-field theory predicts a second-order phase transition from a disordered to an ordered state that breaks the model's underlying $\mathbb{Z}_2$ symmetry. Within mean-field theory, the transition is predicted to occur for any lattice geometry and in any dimension. This can be seen straightforwardly by considering the related single-particle problem of a single Ising spin in a magnetic field B_{eff}. For an inverse-temperature β this implies that

$$\bar{m} = \langle\sigma\rangle = \frac{\sum_\sigma \sigma \mathrm{e}^{-\beta B\sigma}}{\sum_{\sigma_i} \mathrm{e}^{-\beta B\sigma}} = \tanh(-\beta B_{\text{eff}}). \tag{1.30}$$

In our original problem the effective-, or mean-field, magnetic field B is generated by the nearest neighbour spins such that $B_{\text{eff}} = -J\sum_{\langle ij\rangle}\sigma_j$. Assuming that $\sum_{\langle ij\rangle}\sigma_j = z\bar{m}$, and demanding that this solution is self-consistent requires that

$$\tanh(-B_{\text{eff}}\bar{m}) = \tanh(\beta Jz\bar{m}) = \bar{m} \tag{1.31}$$

This can only happen if the slope of the tanh curve at the origin is greater than unity (see Figure 1.3), and so predicts that if $\beta Jz > 1$ there is an ordered phase, while if

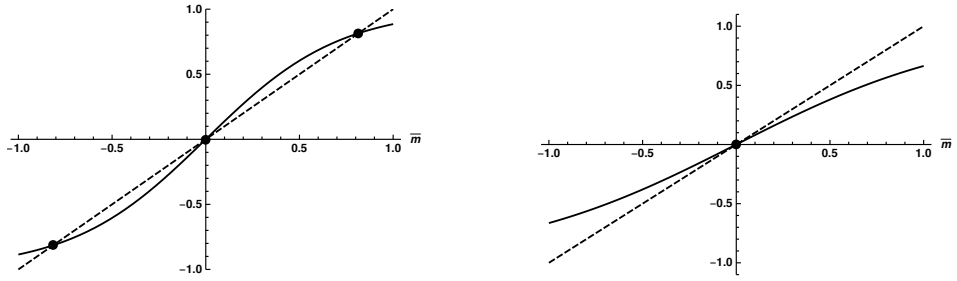

(a) $\beta J z = 1.4$ (b) $\beta J z = 0.8$

Figure 1.3: Two possible solutions to Equation (1.31). If, as in (a), $z\beta J > 1$, then three solutions exist, whereas if $z\beta J < 1$, as in (b), then only one solution exists.

$\beta J z < 1$ there is not. Famously, this prediction fails completely in one-dimension [87, 88], as we will discuss below.

We can make this kind of mean-field argument less ad hoc to better understand its limitations. Consider re-writing the Ising model's partition function, by re-organizing the sum over microstates $s = \{\sigma_i\}$ into a set of conditional sums

$$Z = \int_{-1}^{1} \mathrm{d}m \sum_{s|m} \mathrm{e}^{-\beta H[s]} := \int_{-1}^{1} \mathrm{d}m \mathrm{e}^{-\beta \mathcal{F}(m,\beta)} \tag{1.32}$$

where a conditional microstate $s|m$ denotes any collection of spins $\{\sigma_i\}$ satisfying $\frac{1}{N}\sum_i \sigma_i = m$, and where we have introduced an effective free-energy $\mathcal{F}(m,\beta)$. This is the Landau free-energy, typically inferred from phenomenological considerations, although it could in principle be calculated from first principles. The Landau free energy is more powerful than the mean-field theory outlined in the previous section. Once give, the Landau free energy, also allows us to compute fluctuations such as $\langle m^2\rangle_\beta - \langle m\rangle_\beta^2$, and can therefore serve to diagnose problems with mean-field theory (which completely neglects fluctuations).

Using the Landau free-energy the average value of the magnetization $\bar{m}$ is then given by

$$\bar{m} := \langle m\rangle_\beta = \frac{\int_{-1}^{1} \mathrm{d}m \; m \mathrm{e}^{-\beta\mathcal{F}(m,\beta)}}{Z} \tag{1.33}$$

The mean-field theory of the preceding paragraph is equivalent to minimizing the Landau free energy (i.e. it is a saddle-point approximation). If the free-energy becomes

very flat, then a saddle-point approximation may be unjustified. This can lead to not only quantitative disagreement but also qualitatively wrong predictions. For example, as mentioned above, in one-dimension the predictions of mean-field theory are brutally wrong for the Ising model. This is a generic consequence of short-range interacting systems, because the energetic cost of excitations will be dwarfed by the entropy created by producing them. For instance, in the context of the Ising model the failure of mean-field theory can be attributed to the proliferation of domain walls whose energetic cost is simply J, but whose entropy scales as $k_B \log(L/a)$ (since the boundary of a domain wall can occur at any lattice site). For $L \gg a$ domain walls (i.e. disorder) will proliferate because the entropic profit will always outweigh the energetic penalty [87]. Thus, as was first pointed out by Landau, in a one dimensional short-range interacting system, at finite temperatue no phase transitions can take place (although at zero temperature phase transitions are possible with the Ising model providing an explicit example).

Notice that this argument crucially relies on the scaling of the energy (being $\mathcal{O}(1)$) and the entropy (being $\mathcal{O}(\log L)$]. As we have already outlined, for even marginal interactions where $V(r_1 - r_2) \sim 1/(r_1 - r_2)^d$ the energy per-particle scales logarithmically. In contrast, the entropy is largely insensitive to the range of interactions. Consequently, the entropy gain disorder can, in certain cases, be balanced by its energetic cost.

A different kind of behaviour can also lead to the invalidation of mean-field theory. If a system has low-lying excitations then their fluctuations can lead to mean-field theory being qualitatively wrong. This idea is most easily illustrated by considering a generalization of the Ising model known as the $O(2)$ vector, or XY, model. Instead of decorating a lattice with discrete variables σ_i we will instead consider a two-component vector, $\vec{s}_i = (\cos\theta_i, \sin\theta_i)^T$, of unit length, $\vec{s}\cdot\vec{s} = 1$. The model is defined, for nearest neighbour interactions, by the Hamiltonian

$$H = -J \sum_{\langle ij \rangle} \vec{s}_i \cdot \vec{s}_j \tag{1.34}$$

In this case, using the same arguments as above, but allowing for a spatially varying order parameter $\vec{\phi}(\mathbf{x})$, we can construct an effective free-energy functional given by

$$\mathcal{F}[\phi(x)] = \int \mathrm{d}^d x K(T) \nabla_i \phi_\alpha \nabla_i \phi_\alpha + M(T)\phi_\alpha\phi_\alpha + \Lambda\phi_\alpha\phi_\alpha\phi_\beta\phi_\beta + ... \tag{1.35}$$

where K, M, are phenomenological parameters that can in principle be calculated from the underlying microscopic Hamiltonian, and the ellipsis represent terms that are of $\mathcal{O}(\phi^6)$ or higher, or that contain higher powers of derivatives; assuming that $\phi(x)$ is small, and smooth, theses terms are of lesser importance and can be neglected in our discussion. Suppose that for some value of $T = T_c$, the parameter M vanishes becoming negative for $T < T_c$ and positive for $T > T_c$, such that $M = m(1 - \frac{T}{T_c})$ and that $K(T_c) = \kappa \neq 0$, and $\Lambda(T_c) = \lambda \neq 0$, the system will minimize its effective free energy, $\mathcal{F}$, by acquiring a non-zero homogeneous profile

$$\phi_\alpha(\mathbf{x})\phi_\alpha(\mathbf{x}) = v^2 = \frac{m\left(1 - \frac{T}{T_c}\right)}{2\lambda} \ . \tag{1.36}$$

This condition defines a degenerate manifold of states each of which corresponds to a different orientation of the spins. Importantly, each of these distinct states is connected to one-another by a continuous $O(2)$ symmetry transformation.

To study this we can assume that a given direction has been spontaneously chosen, and then study fluctuations about this point. Let us assume (without loss of generality) that $\vec{\phi}_0(x) = (v, 0)^T$, then let us write

$$\vec{\phi} = \sqrt{v + \rho} \begin{pmatrix} \cos\theta(x) \\ \sin\theta(x) \end{pmatrix} \tag{1.37}$$

such that the effective free energy can be re-written

$$\mathcal{F} = \int \mathrm{d}^d x (2v\lambda - 2v^2\lambda)\rho + \lambda\rho^2 + \frac{\kappa(\nabla\rho)^2}{4(v+\rho)} + \kappa v(\nabla\theta)^2 + \kappa\rho(\nabla\theta)^2 \tag{1.38}$$

Notice that θ never appears without an accompanying derivative. This is a direct consequence of the "broken" $O(2)$ symmetry. In fact the symmetry has not been broken at all, but is rather being realized non-linearly via a shift symmetry; Equation (1.38) is invariant under $\theta(\mathbf{x}) \to \theta(\mathbf{x}) + \alpha$.

If we assume that terms appearing in the free-energy that are of quartic-order in the fields or higher (such as $|\nabla\theta|^4$) then we can approximate $\mathcal{F}$ by keeping only the lowest-order terms; this is often referred to as the Gaussian approximation. Then, since a term such as $\frac{1}{2}m^2\theta^2$ is forbidden by the shift symmetry, $\theta(\mathbf{x}) \to \theta(\mathbf{x}) + \alpha$, the

only term that can appear inside the free-energy at quadratic order is $|\nabla\theta|^2$. This line of reasoning then suggests that the two-point correlation function is given in momentum space by

$$\langle|\theta(k)|^2\rangle = \int \mathcal{D}\theta \mathrm{e}^{-\beta\mathcal{F}}\theta(\mathbf{k})\theta(-\mathbf{k}) \tag{1.39}$$

Approximating the free energy by $\mathcal{F} \approx \int \mathrm{d}^d x \frac{1}{2}|\nabla\theta|^2 = \int \mathrm{d}^d k \frac{1}{2}k^2|\theta(\mathbf{k})|^2$ then reduces the above integral into a product of independent Gaussian integrals over different Fourier modes. $\langle|\theta(\mathbf{k})|^2\rangle$ is the variance of the mode labeled by $\mathbf{k}$ and is therefore $\langle|\theta(\mathbf{k})|^2\rangle = 1/(\beta k^2)$.

The application of the Gaussian approximation at very small values of k, however, is somewhat suspect. Since $|\nabla\theta|^2 \to k^2|\theta(\mathbf{k})|^2$, the limit of $k \to 0$ naively invalidates the Gaussian approximation; the saddle-point becomes less and less steep in this limit, and eventually one would expect quartic corrections to modify the integral's behaviour. In fact (surprisingly) if a continuous symmetry is spontaneously broken, the naive reasoning applied above turns out to be exactly correct. This result is known as Goldstone's theorem [3, 97], which states that if a continuous symmetry is spontaneously broken, then there must be an accompanying gapless excitation (often called a Goldstone boson).

One consequence of Goldstone's theorem is that the energy cost of fluctuations in the radial direction (i.e. the Higgs mode ρ) is much higher than in the angular direction. We may therefore neglect fluctuations of ρ and replace it by its average value $\langle\rho\rangle = 0$ leading to

$$\mathcal{F} \approx \kappa v \int \mathrm{d}^d x \ (\nabla\theta)^2 \tag{1.40}$$

from which we can calculate fluctuations in the angular direction (assuming the background configuration ϕ_0)

$$\begin{aligned}\langle\theta(\mathbf{x})\theta(\mathbf{x})\rangle_{\beta,\phi_0} &= \int \frac{\mathrm{d}^d k}{(2\pi)^d}\langle|\theta(\mathbf{k})|^2\rangle_{\beta,\phi_0} \\ &= \frac{1}{\beta\kappa v}\int \mathrm{d}^d k \frac{1}{\mathbf{k}^2} \\ &\propto T\int_0^Q \mathrm{d}k k^{d-3}\end{aligned} \tag{1.41}$$

where Q is a cut-off that we have introduced. We are mostly interested in the role

played contributions to the integral from low-kS modes, and we see that in sufficiently low-dimensional systems the contributions from such modes is sufficiently large to render fluctuations in the angular direction to be infinite. Thus, our assumption of a symmetry broken state ϕ_0, is not self-consistent. If such a state were prepared, thermal fluctuations would rapidly explore the entirety of the low-energy manifold resulting in a state with a restored $O(2)$ symmetry.

This result is a special case of the Mermin-Wagner theorem [1], which states that for short-range interacting systems spontaneously broken symmetries are not allowed in $d \leq 2$ at any finite temperature. Why is this the case? It is true that in any dimension, at low temperatures, low-lying states can be excited, so what makes low-dimensional systems so prone to their effects?. What is crucially different in $d = 1$ or $d = 2$ is the *number* or *density* of such low-lying states. For states labeled by momentum k, with dispersion $E(k) \sim k^2$ the density of states in d dimensions is scales as $\rho(E) \sim E^{d/2-1}$ and so in higher dimensions low-lying excitations are comparatively rare.

This situation changes when long-range interactions are taken into consideration (see e.g. [5, 25, 26, 98–100]). Notice that, as far as a lattice model is concerned, the role of higher dimensionality is to increase the coordination number of each lattice site. Thus, the suppression of fluctuations in higher dimensional systems may be ascribed to the greater connectivity between neighbouring lattice sites. In this way, it is intuitive to expect that long-range interactions may have a similar effect as an increased dimensionality. Thus, a long-range interacting system is less susceptible to low-lying excitations, and it is possible for a LRI-MB system to spontaneously break continuous symmetries in any dimension.

1.2 Dynamical Features of Long-Range Interactions

In the last section we focused on the ways in which LRIs can modify a system's equilibrium behaviour. In reality the applicability of statistical mechanics rests on the assumption that ensemble averages are equivalent to time averaged quantities for a many-body system. Typically this is justified by appealing to ergodicity; if a system can sample all of its energetically available phase space within the duration of

one measurement, then a time average will be equivalent to a microcanonical average. Studies of the Boltzmann equation provide important evidence that short-range collisions will drive a classical short-range interacting system towards equilibrium.

This is not the case for LRI-MB systems. Although the microscopic laws governing their dynamics appear only superficially different when compared to a short-range interacting system, the equations governing their average behaviour in phase space are fundamentally distinct. Because the interactions from far-distant particles can dominate over local short-range interactions, a mean-field description is justified; this is known as the Vlasov equation [5, 9, 10, 24]. Importantly, distributions which are stable with respect to the Vlasov equation need not be equilibrium states. Thus, the thermalization of long-range interacting systems is very different than short-range interacting systems. They tend to flow to so-called quasi-stationary states (QSS) which are stable over very long time scales [often of $\mathcal{O}(\log N)$]. Only after this very long time scale do short-range collisional effects then drive the system to its thermodynamic equilibrium. In this section we will introduce the Vlasov equation, and emphasize one of its associated relaxation mechanisms known as violent relaxation.

1.2.1 The Vlasov Equation

We begin by considering a phase space distribution for N point particles in Eulerian phase space coordinates Q and P,

$$f(Q,P,t) = \frac{1}{N}\sum_{i=1}^{N}\delta(Q-q_i(t))\delta(P-p_i(t)) \tag{1.42}$$

where Q and P are Eulerian coordinates and $q_i(t)$ and $p_i(t)$ are to be thought of as Lagrangian coordinates evolving according to Hamilton's equations for a Hamiltonian

$$H = \sum_i \frac{p_i^2}{2m} + \sum_{i<j} V(q_i - q_j) \tag{1.43}$$

$$\dot{q}_i = \frac{\partial H}{\partial p_i} \qquad \dot{p}_i = -\frac{\partial H}{\partial q_i}\ . \tag{1.44}$$

Taking the total time derivative of Equation (1.42) we find

$$\begin{aligned}\frac{\mathrm{d}}{\mathrm{d}t}f(q,p,t) &= \frac{\partial f}{\partial t} + \frac{1}{N}\sum_{i=1}^{N}\delta(Q-q_i)\frac{\mathrm{d}}{\mathrm{d}t}\delta(P-p_i) + \delta(P-p_i)\frac{\mathrm{d}}{\mathrm{d}t}\delta(Q-q_i) \\ &= \frac{\partial f}{\partial t} + \frac{1}{N}\sum_{i=1}^{N}\delta(Q-q_i)\frac{\mathrm{d}p_i}{\mathrm{d}t}\delta'(P-p_i) + \delta(P-p_i)\frac{\mathrm{d}q_i}{\mathrm{d}t}\delta'(Q-q_i) \\ &= \frac{\partial f}{\partial t} - \frac{1}{N}\sum_{i=1}^{N}\delta(Q-q_i)\frac{\partial H}{\partial q_i}\delta'(P-p_i) + \frac{p_i}{m}\delta(P-p_i)\delta'(Q-q_i)\end{aligned} \tag{1.45}$$

where we have applied the time derivatives only to the Lagrangian coordinates $q_i(t)$ and $p_i(t)$. Next, we have

$$\begin{aligned}\delta(Q-q_i)\frac{\partial H}{\partial q_i} &= \sum_j \delta(Q-q_i)\frac{\partial V(q_i-q_j)}{\partial q_i} \\ &= \sum_j \delta(Q-q_i)\frac{\partial V(Q-q_j)}{\partial Q} \\ &= \sum_j \int \mathrm{d}Q'\frac{\partial V(Q-Q')}{\partial Q}\delta(Q-q_i)\delta(Q'-q_j) \\ &= \delta(Q-q_i)\int \mathrm{d}Q'\frac{\partial V(Q-Q')}{\partial Q}\sum_j \delta(Q'-q_j) \\ &= \delta(Q-q_i)\frac{\partial}{\partial Q}\Big[N\int \mathrm{d}Q' V(Q-Q')\mathrm{d}P' f(P',Q',t)\Big]\,,\end{aligned} \tag{1.46}$$

and we therefore define the mean-field potential $\Phi(Q,P,t)$ via

$$\Phi(Q,t) = N\int \mathrm{d}Q\mathrm{d}P' f(P',Q',t)V(Q-Q') \tag{1.47}$$

we then find

$$\begin{aligned}\frac{\mathrm{d}}{\mathrm{d}t}f(q,p,t) &= \frac{\partial f}{\partial t} + \frac{1}{N}\sum_i^N\left(-\frac{\partial\Phi}{\partial Q}\right)\delta(Q-q_i)\delta'(P-p_i) + \frac{P}{m}\delta(P-p_i)\delta'(Q-q_i) \\ &= \frac{\partial f}{\partial t} - \frac{\partial\Phi}{\partial Q}\frac{\partial f}{\partial P} + \frac{P}{m}\frac{\partial f}{\partial Q}\,.\end{aligned} \tag{1.48}$$

Since the total number of particles $N = \int \mathrm{d}Q\mathrm{d}P f(Q,P,t)$ is conserved, so too must $\frac{\mathrm{d}}{\mathrm{d}t}f$. We then find the exact relation

$$\frac{\partial f}{\partial t} + \frac{P}{m}\frac{\partial f}{\partial Q} - \frac{\partial \Phi}{\partial Q}\frac{\partial f}{\partial P} = 0. \tag{1.49}$$

This is referred to as the Klimontovich equation and its solution is equivalent to the full N-body solution of Newton's or Hamilton's equations. If we average over an ensemble of initial conditions it is useful to decompose a given distribution into its ensemble average, and its deviation from that average

$$f^{(\alpha)}(Q,P,t) = \langle f(Q,P,t)\rangle + \frac{1}{\sqrt{N}}\delta f^{(\alpha)}(Q,P,t) \tag{1.50}$$

where α indexes different members of the ensemble such that

$$f_0(Q,P,t) := \langle f(Q,P,t)\rangle = \frac{1}{M}\sum_{\alpha=1}^{M} f^{(\alpha)}(Q,P,t)\ . \tag{1.51}$$

Substituting Equation (1.50) into Equation (1.49) and using the fact that $\langle \delta f\rangle = 0$ (while $\langle \delta f \delta\Phi\rangle$ does not) we find that the average distribution then satisfies the following equation

$$\frac{\partial f_0}{\partial t} + \frac{P}{m}\frac{\partial f_0}{\partial Q} - \frac{\partial \Phi_0}{\partial Q}\frac{\partial f_0}{\partial P} = \frac{1}{N}\left\langle \frac{\partial \delta\Phi}{\partial Q}\frac{\partial \delta f}{\partial P}\right\rangle. \tag{1.52}$$

with $\Phi_0 = \Phi[f_0]$ and where we have introduced the fluctuations of the mean-field potential defined via

$$\Phi[f^\alpha] = \Phi[f_0] + \frac{1}{\sqrt{N}}\delta\Phi^{(\alpha)}\ . \tag{1.53}$$

Equation (1.52) provides an exact description of the dynamics. Notice that this has the same form as the Boltzmann equation with the terms on the right hand side, being analogous to a collision integral, and the averaged mean-field potential Φ_0 playing the role of a fluctuating background potential. The Vlasov equation emerges as the leading order approximation to this equation in the $N \to \infty$ limit, and is given by

$$\frac{\partial f_0}{\partial t} + \frac{P}{m}\frac{\partial f_0}{\partial Q} - \frac{\partial \Phi_0}{\partial Q}\frac{\partial f_0}{\partial P} = 0. \tag{1.54}$$

This constitutes a kind of dynamical mean-field approximation in which fluctuations about a dynamical background are neglected. This approximation can be justified by

showing that the difference between two sets of initial data $f_0^{(a)}$ and $f_0^{(b)}$ is bounded in time, and will grow at most exponentially in time [8]. Since the averaged phase space distribution is related to the exact (i.e. discrete) one by a finite error (of size $1/\sqrt{N}$) this implies that the exact dynamics are well approximated by the Vlasov equation up to times at least of $\mathcal{O}(\log N)$ [11]. Numerical investigations of explicit examples have shown that most LRI-MB systems are described by the Vlasov equation up until times of $\mathcal{O}(N^\nu)$ with ν a system specific exponent; for example in the HMF model $\nu \approx 1.7$ [73]. Finite size "collisional" effects appearing on the right-hand side of Equation (1.52) could also serve to influence the late time behaviour of the exact solution, however their influence will only appear at polynomialy late times. This argument has been made rigourous with the most famous proof being given by Hepp and Braun [8].

1.2.2 Collisionless Relaxation

The Vlasov equation has been extensively studied [10, 20, 21] and its consequences for the dynamics of a long-range interacting system are very important for understanding relaxation and thermalization. Given that thermalization is typically attributed to short-range collisions, and that we have just argued that the influence of these collisions is subdominant, a simple picture for thermalization emerges. First, the system evolves according to Equation (1.52), early time dynamics may be highly non-trivial, however after a long time (but sufficiently short such that Equation (1.52) still applies), the system will tend towards an *attractor* of the Vlasov equation. Many such attractors are stable, and can be infinitely long-lived with respect to the Vlasov equation; these are the aforementioned QSS. Eventually, the QSS will undergo "collisional" relaxation, whether due to sub-dominant short-range interactions, or finite-N statistical fluctuations that can mimic their effects. On extremely long time scales, these collisional dynamics will eventually lead to the system relaxing to microcanonical equilibrium as described in Section 1.1. This picture can be formalized as a perturbative solution to the kinetic theory in a series in $1/N$ see e.g. [10, 101].

This section will focus on the regime of collisionless relaxation. Collisionless relaxation occurs via three distinct mechanisms: phase mixing, violent relaxation, and Landau damping [11, 19]. Phase mixing is effectively a static, non-interacting effect. Violent relaxation involves an interplay between phase mixing, and energy transfer via coherent

oscillations of the mean-field potential $\Phi(Q, P, t)$. Landau damping results from energetic exchange between wave-like excitations and single particles which results in a non-dissipative damping mechanism. While interesting in its own right, the mechanism of Landau damping will not concern us for the rest of this thesis and, in what follows, we will focus on violent relaxation, which is important in the context of Chapter 2.

Phase mixing is the simplest of the three mechanisms, being essentially a relaxation mechanism driven by a fixed background potential. For example, consider an initial phase space distribution for an ensemble of pendula. Suppose the distribution lies between two phase space orbits of the pendulum, as sketched in Figure 1.4. Since neighbouring points in phase space evolve with differing velocities they will separate linearly in time and form filiments. Strictly speaking this does not lead to relaxation until we consider a coarse graining procedure where phase space is averaged over cells of size $\Delta Q \times \Delta P$. This coarse grained distribution will relax to an equilibrium. A similar phenomenon may occur in a system exhibiting chaos,

Violent relaxation, is *not* a single-body effect. In contrast to phase mixing, energy transfer is mediated by the *time-dependance* of the mean-field potential. To understand this consider a test particle moving in the dynamical background potential $U(Q, t)$. The energy of the test particle is conserved for a static potential, however, for a time-dependent potential the energy of our test particle can change $\mathrm{d}E/\mathrm{d}t = \partial U/\partial t$. In a LRI-MB system the background potential becomes our mean-field potnetial $U \to \Phi$, and there are many such test particles. Furthermore, the time-dependance of $\Phi(Q, t)$ is modified based on the energy gained, or lost, by the full ensemble of test particles; Φ mediates energy transfer, which modifies the dynamics, which in turn modifies the dynamics of Φ.

How does this energy transfer lead to relaxation? Consider a gas of particles interacting via an attractive interaction potential, whose mean-field pontential, for simplicity, will be assumed to have a fixed shape but whose depth changes with time. Suppose at $t = 0$ the distribution of energies is tightly peaked around $E = 0$, and that the mean-field potential is negiligbly small. Attractive interactions will lead to a collapse instability, and the mean-field potential will develop minimum, and its depth will increase. As time proceeds, some of the particles will sit in the well of the mean-field potential, without gaining energy; they will represent a large population with $E < 0$.

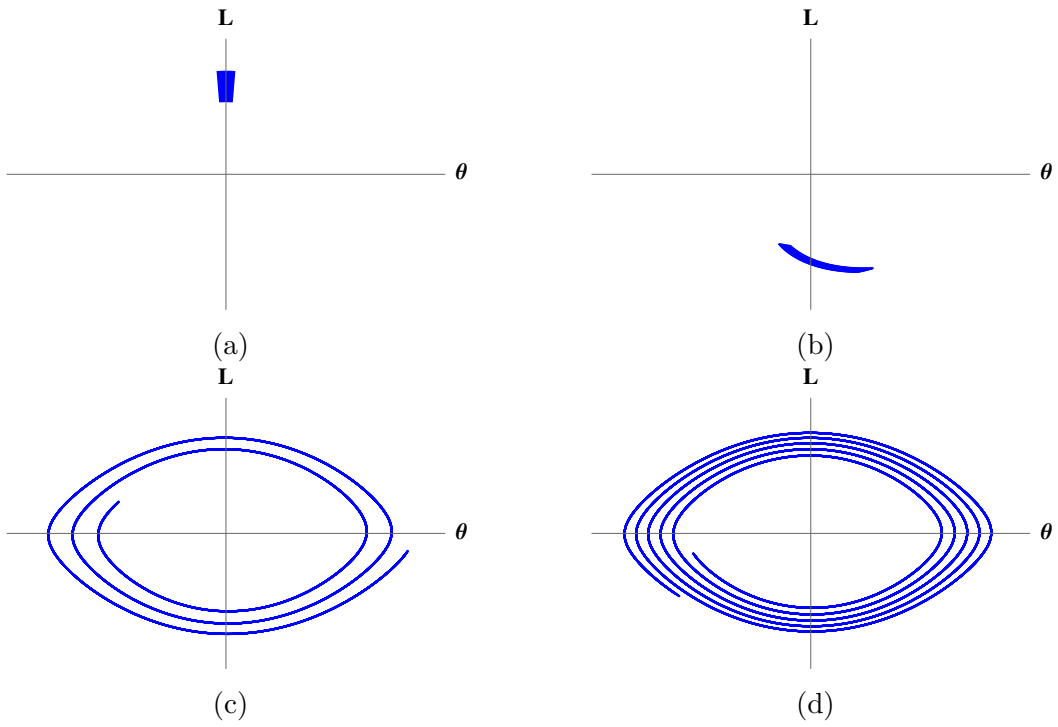

Figure 1.4: Sketch of an initial phase space distribution for an ensemble of pendula at early times (a) and (b), intermediate times (c), and late times (d). Due to the asychronous orbits the distribution forms filaments over time tending towards a space-filling curve that paints the entire space between the orbits. On a coarse grained scale of resolution $\Delta Q \times \Delta P$ this is well approximated by the microcanonical ensemble.

Other particles will fall into the well, which grows deeper and deeper, these particles will have large kinetic energies. After some time t, those collapsed particles will begin escaping the well, but as they do so the system will become more homogeneous. The well, therefore, will become less deep as these particles escape, and they will exit with more kinetic energy than they entered with; these particles represent a population of particles with $E > 0$. These kind of dynamics are illustrated in the HMF model in Chapter 2. Thus, a time-varying potential can widen the distribution of particle energies in much the same way that short-range collisions can in a conventional gas.

The key ingredient in violent relaxation is a time varying potential. During periods of rapid change in the phase space distribution, energy can be re-distributed, and in periods during with the dynamics are more calm, can relax via phase mixing (or Landau damping). As we will see in Chapter 2 (and as was first elucidated in [13, 72] *c.f.* Section 1.4.2) for a repulsive LRI-MB system such as the HMF model with $\epsilon > 0$, the argument outlined above does not lead to rapid violent relaxation because negative energy states cannot be easily accessed. Nevertheless, a time varying potential can still transfer energy, and, because this energy transfer is correlated with the dynamics, this can lead to coherent formation of structures that are completely absent in an equilibrium statistical treatment.

1.2.3 Quasi-Stationary States

As outlined above, LRI-MB systems described by the Vlasov equation have a variety of relaxation mechanisms at their disposal, however, unlike a short-range system they do not necessarily relax towards a Maxwell-Boltzmann (or otherwise "equilibrium") steady state. Instead the Vlasov equation has an *infinite* number of stationary states [11] many of which are stable with respect to the Vlasov equation. Since on very long-time scales (of $\mathcal{O}(N)$) we expect collisional relaxation, the stablizers of the Vlasov equation are often refered to as QSS. Unlike a short-range system, which of these states the system is driven towards can be sensitive to initial conditions and cannot necessarily be inferred from statistical considerations alone. Nevertheless there are some statistical theories that can successfully describe the late-time behaviour of LRI-MB systems.

One such theory is Lynden-Bell statistics. Motivated by the incompressible nature of Vlasov flow ($\mathrm{d}f_0/\mathrm{d}t = 0$) Donald Lynden-Bell conjectured that the late time limit of a

self-gravitating system would tend towards a Fermi-Dirac like phase space density with a temperature set by the mass of the distribution [11, 15]. This kind of generalized statistics was later found to be broadly applicable to LRI-MB systems, although noticeable disagreement with numerical simulations was noted for initial data that was far from virialized [102]. In more recent years it has been discovered that Lynden-Bell statistics can be modified to account for non-virial distributions with the resultant statistics being known as core-halo statistics [11, 67]. Although inessential for the rest of this thesis it is worth mentioning that the HMF model played a key role in illustrating the physical mechanism underlying core-halo formation [66].

In certain cases certain dynamical features can drive a model towards a given QSS. For example in the case of core-halo statistics, where the core refers to an ensemble of low energy states that are well-described by Lynden-Bell statistics, and the halo to an ensemble of high energy particles that are not. This high-energy halo is formed dynamically due to residual fluctuations in the mean-field potential that resonantly eject particles from the Lynden-Bell core, which removes kinetic energy from the core, and damps the mean-field potential's oscillations. Without these oscillations the Lynden-Bell core stabilizes. In Section 1.4.2 we discuss a particular QSS of the HMF model which is driven by rapid fluctuations in the mean-field potential, but whose formation time is very slow.

1.3 Theory of Bose Gases

Gases are amongst the simplest many-body systems and understanding the role played by weak interactions in these systems has often served as bedrock upon which to build theories of generic, and often times more complicated, systems. Historically important examples include Boltzmann's H-theorem for a collisional quasi-ideal gas, the free Fermi-gas and its extension to the theory of Landau Fermi-liquids, and non-neutral plasmas which were responsible for the derivation of the Valsov equation. One further example is given by dilute Bose gases. For short-ranged weak interactions a microscopic theory can be constructed whose perturbative solution yields tremendous insight into the formation of quasi-particles in quantum many-body system.

In this section we will review some key concepts underlying the theory of a Bose gas,

and explain how the theory is extended to account for long-range interactions. This will include a description of Bose-Einstein condensates (BECs) and Gross-Pitaevskii theory, which can be interpreted as the classical field equations for a Bose gas. This theory will be generalized to incorportate long-range interactions, and a brief review of two famous applications of the generalized Gross-Pitaevskii equation (GGPE) equation, one to Bose stars, and the other to dipolar BECs.

1.3.1 The Ideal Bose Gas

We will begin by considering the (grand-canonical) thermodynamics of an ideal non-relativistic Bose-gas confined to a finite sized box of length L, of definite particle number N_{tot}. The system is described by the Hamiltonian

$$\hat{H} = \int_0^L \mathrm{d}^d x \frac{\hbar^2}{2m} \nabla_i \hat{\Psi}^\dagger(\mathbf{x}) \nabla_i \hat{\Psi}(\mathbf{x}). \tag{1.55}$$

Strictly speaking the correct ensemble for describing this system is the canonical ensemble, however the system is short-range interacting, and we should expect that the grand-canonical and canonical ensembles will give equivalent results. Being an ideal Bose gas, if the system is described by the grand canonical ensemble with a chemical potential μ, then the average occupation number of each momentum mode k is given by

$$n_{\text{gc}}(k, T, z) = \frac{1}{z \exp[\beta E] - 1} \ , \tag{1.56}$$

independent of dimension, where $z = \mathrm{e}^{\beta\mu}$ is the fugacity. The chemical potential μ is both restricted to be negative $\mu \leq 0$[5], and to be self consistent such that the grand-canonical average of the total particle number agrees with the total number of particles $\langle N \rangle_{\text{gc}} = N_{\text{tot}}$. Mathematically this is expressed as

$$\sum_k n(k, T, z) = N_{\text{tot}} \ . \tag{1.57}$$

[5]The chemical potential is defined as $\mu = \partial E / \partial N$ at fixed entropy and volume. Naively adding a particle will increase the entropy and energy of the system, and thus to keep the entropy constant the energy must decrease.

If the grand-canonical ensemble is a good description of the system then $n(k,T,\mu) = n_{\rm gc}(k,T,\mu)$, and the chemical potential can be found by solving

$$\sum_k n_{\rm gc}(k,T,z) = N_{\rm tot} \ . \tag{1.58}$$

At sufficiently low temeperatures, solutions to this equation are not compatible with the constraint that $\mu \geq E_0$. Notice that $n_{\rm gc}(k,T,z)$ is a monotonically increasing function of z for all values of k. Therefore, if z is decreased, the sum on the left-hand side of Equation (1.58) will also decrease. Since $z \in (0,1]$), if

$$\sum_k n_{\rm gc}(k,T,z=1) \geq N_{\rm tot} \ , \tag{1.59}$$

then there will always exist a fugacity $z' < 1$ such that $\sum_k n_{\rm gc}(k,T,z') \geq N_{\rm tot}$ If, instead, for $z = 1$ we find that the sum over all states is *less* than the total number of particles in the gas

$$\sum_k n_{\rm gc}(k,T,z=1) < N_{\rm tot} \ , \tag{1.60}$$

then no value of the fugacity (or chemical potential) can consistently describe our gas of $N_{\rm tot}$ particles within the grand-canonical ensemble. This implies that the number distributions are not described by the grand-canonical ensemble $n(k,T,z) \neq n_{\rm gc}(k,T,z)$. Rather, in addition to the thermal population of states, there must be an $\mathcal{O}(N)$ contribution arising from a macroscopic occupation of a single particle state, i.e.

$$n(k,t,z) = n_0\delta(k) + n_{\rm ex}(k,T) \tag{1.61}$$

where $n_{\rm ex}(k,T) = n_{\rm gc}(k,T,z=1)$.

To make our discusion more explicit we can consider the $L \to \infty$ limit in three dimensions for a cubic box of length L. Dividing both sides of Equation (1.57) by L^3, the sum tends towards an integral and we find that the total number of particles per unit volume $n_{\rm tot} = N_{\rm tot}/L^3$, in the grand-canonical ensemble for $z = 0$ is given by

[103]

$$\begin{aligned} n_{\text{tot}}(z=0) &= \frac{4\pi}{(2\pi)^3}\int_0^\infty \mathrm{d}k k^2 n_{\text{gc}}(k,T,z=0) \\ &= \zeta(\tfrac{3}{2})\left(\frac{mk_BT}{2\pi\hbar^2}\right)^{3/2} \end{aligned} \tag{1.62}$$

where ζ is the Riemann-Zeta function. Thus, for a fixed number density n_{tot} this identifies a critical temperature

$$k_BT_c = \frac{2\pi\hbar^2}{m}\left[n_{\text{tot}}\zeta(\tfrac{3}{2})\right]^{3/2} \tag{1.63}$$

such that for temperatures below the critical temperature $T < T_c$ the condensate franction scales as

$$n_0 = n_{\text{tot}}\left[1-\left(\frac{T}{T_c}\right)^{3/2}\right] . \tag{1.64}$$

The above discussion can be generalized to an arbitrary dimension, or instead to an arbitrary density of states $g(E)$. In this case Equation (1.62) becomes

$$n_{\text{tot}}(z=0) = \int_0^\infty \mathrm{d}E g(E) n_{\text{gc}}(k,T,z=0) . \tag{1.65}$$

For a density of states $g(E) = C_\alpha E^\alpha$, we find

$$n_{\text{tot}}(z=0) = C_\alpha \Gamma(\alpha)\zeta(\alpha)(k_BT)^\alpha , \tag{1.66}$$

with the case of $d = 3$ corresponding to $\alpha = 3/2$. Importantly, in the limit that $\alpha \to 1_+$ (i.e. taking the limit from above), the right-hand side diverges since $\zeta(1+\epsilon) \sim 1/\epsilon + \mathcal{O}(1)$. Thus, as $\alpha \to 1$ the critical temperture tends to zero. This is a reflection of the Mermin-Wagner theorem. A BEC way be interpreted as a spontaneous breaking of the $U(1)$ symmetry ($\Psi \to \mathrm{e}^{\mathrm{i}\theta}\Psi$) of Equation (1.55), and this is formally equivalent to the $O(2)$ symmetry in the XY model Equation (1.34), In the next section we will see this same result re-appear in the presence of short-ranged repulsive interactions.

1.3.2 The Dilute Bose Gas

Real Bose gases are not ideal, for instance a gas of hydrogen (or Lithium, or Rubidium) interacts via the van der Waals interaction as well as other short-range forces. If, however, the gas is dilute then collisions will be relatively rare and this justifies neglecting the interactions. In fact, the dilute Bose gas can be solved via perturbation theory, as demonstrated by Bogoliubov [104] in 1947 and this solution allows us to critically evaluate the validity of the dilute gas approximation *a posteori*.

We are, in principle, interested in studying the following Hamiltonian

$$H = \int \mathrm{d}^d x \frac{\hbar^2}{2m} \nabla_i \hat{\Psi}^\dagger(\mathbf{x}) \nabla_i \hat{\Psi}(\mathbf{x}) + \frac{1}{2} \int \mathrm{d}^d x \mathrm{d}^d y \hat{\Psi}^\dagger(\mathbf{y}) \hat{\Psi}^\dagger(\mathbf{x}) \hat{\Psi}(\mathbf{x}) \hat{\Psi}(\mathbf{y}) V(\mathbf{x}-\mathbf{y}) \quad (1.67)$$

The perturbative solution to the many-body problem for this Hamiltonian may be obtained diagramatically via a resummation of an infinite series of Feynman diagrams [105]. Such an approach, while intellectually satisfying, is equivalent to using an effective Hamiltonian; this is the approach we will outline below.

We may construct an effective Hamiltonian capable of reproducing all of the behaviour of Equation (1.67) when it is applied within its regime of validity; namely low temperatures, low energies, long wavelengths, and low densities. The effects of interactions can be mimicked, at leading order in a long-wavelength expansion, by an effective contact interaction [106]. This may be phrased in terms of effective field theory [107] as has been outlined in detail for dilute Bose gases [108–112]. The first two terms in the low energy expansion are given by

$$H = \int \mathrm{d}^d x \frac{\hbar^2}{2m} \nabla_i \hat{\Psi}^\dagger(\mathbf{x}) \nabla_i \hat{\Psi}(\mathbf{x}) + \frac{g}{2} \int \mathrm{d}^d x \hat{\Psi}^\dagger(\mathbf{x}) \hat{\Psi}^\dagger(\mathbf{x}) \hat{\Psi}(\mathbf{x}) \hat{\Psi}(\mathbf{x}) \ . \quad (1.68)$$

This Hamiltonian must reproduce all of the physics of Equation (1.67), order-by-order in perturbation theory, and this requirement can allow us to determine g. The simplest such matching calculation can be found in the two-body sector. Working to leading order in g one finds [103, 113]

$$g = \frac{4\pi\hbar^2 a}{m} \quad \text{for} \quad d = 3 \ , \quad (1.69)$$

where a is the three-dimensional scattering length that can be measured in a two-body scattering experiment. The algebraic relationship between g and the scattering length varies with dimension, however the requirement is always that scattering length obtained using the first order Born approximation for Equation (1.68) reproduces the scattering length obtained from the full two-body potential in Equation (1.67). For the rest of this section we will use Equation (1.68) with the understanding that it is an effective Hamiltonian valid at low energies and long-wavelengths.

1.3.3 Bogoliubov Theory

To study the influence of interactions on a BEC, it is convenient to re-express $\hat{\Psi}$ in the Fourier basis

$$\hat{\Psi}(\mathbf{x}) = \sum_{\mathbf{k}} \frac{1}{\sqrt{V}} \mathrm{e}^{\mathrm{i}\mathbf{k}\cdot\mathbf{x}} \hat{a}_{\mathbf{k}} \tag{1.70}$$

which leads to the momentum-space representation of Equation (1.68)

$$H = \sum_{\mathbf{k}} \frac{\hbar^2 \mathbf{k}^2}{2m} \hat{a}^\dagger_{\mathbf{k}} \hat{a}_{\mathbf{k}} + \frac{g}{2V} \sum_{\mathbf{k},\mathbf{q},\mathbf{p}} \hat{a}^\dagger_{\mathbf{p}+\mathbf{q}-\mathbf{k}} \hat{a}^\dagger_{\mathbf{k}} \hat{a}_{\mathbf{q}} \hat{a}_{\mathbf{p}} \tag{1.71}$$

For a condensed state $|\Omega\rangle$, the expectation value $\langle\Omega| \hat{a}^\dagger_0 \hat{a}_0 |\Omega\rangle \sim \mathcal{O}(N)$ while all other operators' expecation values $\langle\Omega| \hat{a}_{\mathbf{k}\neq 0} |\Omega\rangle \sim \mathcal{O}(1)$. It is therefore convenient, to replace $\hat{a}_0$ by $\sqrt{N_0}$ which is equivalent to working with a set of coherent states[6]. This the leads to

$$H = \sum_{\mathbf{k}} \frac{\hbar^2 \mathbf{k}^2}{2m} \hat{a}^\dagger_{\mathbf{k}} \hat{a}_{\mathbf{k}} + \frac{g N_0^2}{2V} + \frac{g N_0}{2V} \sum_{\mathbf{k}} \hat{a}_{-\mathbf{k}} \hat{a}_{\mathbf{k}} + \hat{a}^\dagger_{-\mathbf{k}} \hat{a}^\dagger_{\mathbf{k}} + 4 \hat{a}^\dagger_{\mathbf{k}} \hat{a}_{\mathbf{k}} + \mathcal{O}\Big(n_0 / \sqrt{N_0} \Big) \tag{1.72}$$

[6] A Bogoliubov theory can also be constructed for Fock states of definite total particle number N. Although technical details differ, the physical conclusions are the same [114].

trading N_0 for $N = N_0 + \sum_{\mathbf{k}\neq 0} \hat{a}^\dagger_{\mathbf{k}}\hat{a}_{\mathbf{k}}$ we find

$$\begin{aligned} H = &\sum_{\mathbf{k}} \frac{\hbar^2\mathbf{k}^2}{2m}\hat{a}^\dagger_{\mathbf{k}}\hat{a}_{\mathbf{k}} \\ &\qquad + \frac{1}{2}g\frac{g\Big(N^2 - 2N\sum_{\mathbf{k}}\hat{a}^\dagger_{\mathbf{k}}\hat{a}_{\mathbf{k}}\Big)}{2V} + \frac{1}{2}gn\sum_{\mathbf{k}}\Big(\hat{a}_{-\mathbf{k}}\hat{a}_{\mathbf{k}} + \hat{a}^\dagger_{-\mathbf{k}}\hat{a}^\dagger_{\mathbf{k}} + 2\hat{a}^\dagger_{\mathbf{k}}\hat{a}_{\mathbf{k}}\Big) + \mathcal{O}\Big(\sqrt{N}\Big) \\ = &\frac{gN^2}{2V} + \sum_{\mathbf{k}}\left(\frac{\hbar^2\mathbf{k}^2}{2m} + gn\right)\hat{a}^\dagger_{\mathbf{k}}\hat{a}_{\mathbf{k}} + \frac{1}{2}gn\sum_{\mathbf{k}}\Big(\hat{a}_{-\mathbf{k}}\hat{a}_{\mathbf{k}} + \hat{a}^\dagger_{-\mathbf{k}}\hat{a}^\dagger_{\mathbf{k}} + 4\hat{a}^\dagger_{\mathbf{k}}\hat{a}_{\mathbf{k}}\Big), \end{aligned} \tag{1.73}$$

where $n = N/V$ is the density. this can be re-arranged as

$$H = \frac{gN^2}{2V} + \sum_{\mathbf{k}}\left(\frac{\hbar^2\mathbf{k}^2}{2m} + gn\right)\hat{a}^\dagger_{\mathbf{k}}\hat{a}_{\mathbf{k}} + \frac{1}{2}gn\sum_{\mathbf{k}}\Big(\hat{a}_{-\mathbf{k}}\hat{a}_{\mathbf{k}} + \hat{a}^\dagger_{-\mathbf{k}}\hat{a}^\dagger_{\mathbf{k}}\Big). \tag{1.74}$$

This Hamiltonian can be diagonalized by introducing new creation and annihilation operators via a Bogoliubov transformation

$$b_{\mathbf{k}} = \cosh\theta_{\mathbf{k}}\hat{a}_{\mathbf{k}} - \sinh\theta_{\mathbf{k}}\hat{a}^\dagger_{-\mathbf{k}} \tag{1.75}$$

where $\theta_{\mathbf{k}}$ satisifies

$$\coth 2\theta_{\mathbf{k}} = \frac{\hbar^2k^2}{2mgn} + 1 \tag{1.76}$$

Using this transformation Equation (1.71) can be re-expressed as

$$H = E^{(0)}_b + \sum_{\mathbf{k}}\hbar\omega_b(k)\hat{b}^\dagger_{\mathbf{k}}\hat{b}_{\mathbf{k}} \tag{1.77}$$

where

$$\hbar\omega_b(k) = \sqrt{\frac{\hbar^2k^2}{2m}\left(\frac{\hbar^2k^2}{2m} + gn\right)}\,, \tag{1.78}$$

and $E^{(0)}_b$ is the energy of the Bogoliubov vacuum $|0\rangle_b$ (satisfying $\hat{b}_{\mathbf{k}}|0\rangle_b = 0$).

1.3.3.1 Depletion of the Condensate

Notice that the Bogoliubov vacuum is not the same as the "atomic" vacuum,

$$\hat{a}_{\mathbf{k}} \left|0\right\rangle_b = \left(\hat{b}_{\mathbf{k}} \cosh\theta_{\mathbf{k}} + \hat{b}^\dagger_{-\mathbf{k}} \sinh\theta_{\mathbf{k}}\right) \left|0\right\rangle_b = \sinh\theta_{\mathbf{k}} \left|-\mathbf{k}\right\rangle \neq 0 \ . \tag{1.79}$$

therefore, the ground state of Equation (1.77) is not a macroscopically occupied eigenstate of $\hat{a}_0^\dagger \hat{a}_0$, nevertheless, provided that the average value occupation of this state is macroscopic [i.e. $\langle \hat{a}_0^\dagger \hat{a}_0 \rangle \sim \mathcal{O}(N)$], our assumption is justified. We can therefore test if our approach is self-consistent by computing the *quantum depletion* of the condensate at zero temperature. This is found by considering the occupation of all modes other than $\hat{a}_0^\dagger \left|0\right\rangle_a$. At $T = 0$ this is given by

$$\sum_{\mathbf{k}\neq 0} \left\langle 0\right| \hat{a}^\dagger_{\mathbf{k}} \hat{a}_{\mathbf{k}} \left|0\right\rangle_b = \sum_{\mathbf{k}\neq 0} \sinh^2\theta_k \left\langle 0\right| \hat{b}_{\mathbf{k}} \hat{b}^\dagger_{\mathbf{k}} \left|0\right\rangle_b = \sum_{\mathbf{k}\neq 0} \sinh^2\theta_{\mathbf{k}} \ . \tag{1.80}$$

while at finite temperature, where $\langle \hat{b}^\dagger_{\mathbf{k}} \hat{b}_{\mathbf{k}} \rangle_{\text{gc}} = n_{\text{gc}}(k, T, z)$ we find instead

$$\sum_{\mathbf{k}\neq 0} \langle \hat{a}^\dagger_{\mathbf{k}} \hat{a}_{\mathbf{k}} \rangle_{\text{gc}} = \sum_{\mathbf{k}\neq 0} n_{\text{gc}}(k, T, z) \Big(\cosh^2\theta_{\mathbf{k}} + \sinh^2_\theta \mathbf{k}\Big) + \sinh^2\theta_{\mathbf{k}} \tag{1.81}$$

with the added term, proportional to $n_{\text{gc}}(k, T, z)$, accounting for thermal depletion of the condensate. We must confirm the validity of our Bogoliubov approach *a posteori* by checking that the condensate fraction is still macroscopic [i.e. $\mathcal{O}(N)$]. Using

$$\cosh^2\theta_{\mathbf{k}} = \frac{\frac{\hbar^2\mathbf{k}^2}{2m} + gn + \hbar\omega_b(\mathbf{k})}{2\hbar\omega_b(\mathbf{k})} \tag{1.82}$$

$$\sinh^2\theta_{\mathbf{k}} = \frac{\frac{\hbar^2\mathbf{k}^2}{2m} + gn - \hbar\omega_b(\mathbf{k})}{2\hbar\omega_b(\mathbf{k})} \tag{1.83}$$

we can evaluate Equations (1.80) and (1.81) explicitly. For $d = 3$ focussing on just Equation (1.80) in the continuum limit we find [113]

$$n_{\text{ex}}(T = 0) = \frac{4\pi}{(2\pi)^3} \int_0^\infty \mathrm{d}k k^2 \frac{\frac{\hbar^2 k^2}{2m} + gn - \hbar\omega_b(k)}{2\hbar\omega_b(k)} = \sqrt{\frac{64na^3}{9\pi}} \tag{1.84}$$

This introduces us to an important fact. If $na^3 \ll 1$ the condensate is only slightly affected by the presence of interactions and we have validated our assumption of a

macroscopic condensate *a posteori*. If instead $na^3 \gtrsim 1$ then our approach is not self-consistent, interactions destroy the condensate, and our naive pertrubative approach is not sufficent.

By considering the same calculation in lower dimensions we can also learn something interesting about the behaviour of our gas. At low values of $\mathbf{k}$ both $\sinh^2\theta_{\mathbf{k}}$ and $\cosh^2\theta_{\mathbf{k}}$ are $\mathcal{O}(1/k)$ as $k \to 0$ as is the thermal number density $n_{\text{gc}}(k,T,z) \sim \mathcal{O}(1/k)$. Therefore, for $T \neq 0$, the thermal depletion of the condensate has a long-wavelength contribution scaling as $\int \mathrm{d}k\ k^{d-1} \times \frac{1}{k^2}$ which is divergent for $d \leq 2$. This is a manifestation of the Mermin-Wagner theorem, and in fact, Equation (1.68) can be re-written in a density-phase representation that is formally equivalent to the XY-model. Similar considerations show that the quantum depletion of the condensate scales as $\int \mathrm{d}k\ k^{d-1} \times \frac{1}{k}$ such that in one-dimension, even at zero temperature, the condensate is destroyed.

1.3.3.2 Gross-Pitaevskii equation

When the depletion of the condensate is small ($T \ll T_c$ and $na^3 \ll 1$), we can use a classical approximation to study Equation (1.68) [103, 113]. The resultant equation of motion is known as the Gross-Pitaevskii equation (GPE) and is given by

$$\mathrm{i}\hbar\partial_t\Psi = -\frac{\hbar^2}{2m}\nabla^2\Psi + g|\Psi|^2\Psi\ . \tag{1.85}$$

Importantly, it is not the bare potential $V(\mathbf{x}_1 - \mathbf{x}_2)$ of Equation (1.67) that appears in Equation (1.85). This is because if one were to study the classical field limit of Equation (1.67) one would neglect short-distance correlations. Using Equation (1.68) we include these short-range correlations implicitly in the coupling g [113].

Stationary states of the GPE correspond to minimizers of the energy functional

$$\mathcal{E}[\Psi] = \int \mathrm{d}^d x \left(\frac{\hbar^2}{2m}|\nabla\Psi|^2 + \frac{g}{2}|\Psi|^4 - \mu|\Psi|^2 \right) \tag{1.86}$$

where μ is the chemical potential of the gas. These stationary states can be written as $\Psi(\mathbf{x},t) = \mathrm{e}^{-\mathrm{i}\mu t/\hbar}\psi(\mathbf{x})$. The trivial stationary state of the GPE is homogeneous, i.e. $\psi(\mathbf{x}) = 1/\sqrt{V}$, and minimizes the energy Equation (1.86).

Given a stationary state of Equation (1.85), its stability can be investigated by a linearization procedure.

$$\Psi(\mathbf{x},t) = \left[\psi(\mathbf{x}) + \sum_{\alpha} U_\alpha(\mathbf{x})\mathrm{e}^{-\mathrm{i}\omega_\alpha t} + V_\alpha^*(\mathbf{x})\mathrm{e}^{\mathrm{i}\omega_\alpha^* t}\right]\mathrm{e}^{-\mathrm{i}\mu t/\hbar} \tag{1.87}$$

Working to linear order in U_α and V_α then leads to the coupled equations

$$\omega_\alpha U_\alpha = \left[-\frac{\hbar^2}{2m}\nabla^2 + 2g|\psi|^2 - \mu\right]U_\alpha + g\psi^2 V_\alpha \tag{1.88a}$$

$$-\omega_\alpha V_\alpha = \left[-\frac{\hbar^2}{2m}\nabla^2 + 2g|\psi|^2 - \mu\right]V_\alpha + g\psi^2 U_\alpha\ , \tag{1.88b}$$

which gives the normal modes and frequencies of excitations about a background profile. Dynamical stability can be checked by studying the spectrum of eigenvalues $\{\omega_\alpha\}$. If any eigenvalue has a non-vanishing imaginary part then the stationary state is not stable.

In addition to the ground state, there can also be non-trivial spatially varying solutions. The type of solution, stability, and general properties depends sensitively on dimensionality. For example, for $d = 2$, vortices can form, while in $d = 1$ Equation (1.85) is an integrable equation and supports solitons. For $g < 0$ Equation (1.85) supports bright solitons. In this case attractive interactions pull the particles together, and the cost of gradient energy pushes them apart. This can be easily understood in the density-phase representation where Equation (1.85) takes the form

$$\partial_t \rho + \partial_x(\rho v) = 0 \tag{1.89a}$$

$$\partial_t v + v\partial_x\theta = -\partial_x\left[-|g|\rho + \frac{\hbar^2}{2m}\frac{\partial_x^2\sqrt{\rho}}{\sqrt{\rho}}\right] \tag{1.89b}$$

where $v = \partial_x S$. The bracketed expression contains two terms: first, $-|g|\rho$ (the non-linearity) acts as a self-consistent potential; second, the Bohmian potential (whose gradient is often called the quantum pressure) reflects the energetic cost of gradients in the density profile. The competition between the attractive density-density interaction and the quantum pressure is what determines the shape of a bright soliton whose

profile is given by [113]

$$\rho(x) = \frac{n_0}{\cosh^2\left(\frac{x}{\xi}\right)} \ , \tag{1.90}$$

with $\xi = \sqrt{2m|g|n_0}$, often called the healing-length, being the natural length scale of the GPE. This result can be generalized to a moving solitary wave by performing a Galilean boost $\psi(x) \to \mathrm{e}^{\mathrm{i}kx}\psi(x - vt)$ where $k = mv/\hbar$. In this moving frame the density is given by

$$\rho(x,t) = \frac{n_0}{\cosh^2\left(\frac{x-vt}{\xi}\right)} \ . \tag{1.91}$$

1.3.4 Bose Gases with Long-Range Interactions

A system of Bosons interacting via a long-range potential is very similar to a short-range interacting one. It is also amenable to a mean-field treatment, and much of the machinery of the previous section carries over verbatim.

The key difference is that we *do not* introduce an effective Hamiltonian as we did going from Equation (1.67) to Equation (1.68). This is because for the short-range interacting systems we could re-package any short-distance correlations, and their influence on long-distance physics, into an effective coupling constant g. For a long-range potential this is no longer sensible since it is precisely the long-range effects of the potential that we wish to consider. In similar systems (such as dipolar Bose gases [115] and self-gravitating Bose stars [116, 117]), it has long been the standard of the community to work directly with the bare interaction potential .

This can be seen directly if one attempts to match scattering amplitudes in the two-body sector, because scattering amplitudes for a long-range potential are not analytic at $k = 0$ [118] and this inhibits a Taylor series expansion in momentum space. This problem of non-analytic scattering amplitudes occurs even for "short-ranged" van der Waals forces [119].

1.3.4.1 Bogoliubov Theory

If a large condensate fraction exists a Bogoliubov approach is still justified, with the only modification being that we must keep the structure of the long-range interaction

in our description. Once again we must check whether the condensate is depleted by interactions *a posteori*. Taking Equation (1.71) and promoting $g \to g_{\mathbf{q}}$ we have

$$H = \sum_{\mathbf{k}} \frac{\hbar^2 \mathbf{k}^2}{2m} \hat{a}^\dagger_{\mathbf{k}} \hat{a}_{\mathbf{k}} + \frac{1}{2V} \sum_{\mathbf{k},\mathbf{q},\mathbf{p}} g_{\mathbf{q}} \hat{a}^\dagger_{\mathbf{p}+\mathbf{q}} \hat{a}^\dagger_{\mathbf{k}-\mathbf{q}} \hat{a}_{\mathbf{p}} \hat{a}_{\mathbf{p}} \ . \tag{1.92}$$

Assuming a uniform condensate we find, in direct analogy with Equation (1.74)

$$H = \frac{g_0 N^2}{2V} + \sum_{\mathbf{k}} \left(\frac{\hbar^2 \mathbf{k}^2}{2m} + g_{\mathbf{k}} n \right) \hat{a}^\dagger_{\mathbf{k}} \hat{a}_{\mathbf{k}} + \frac{1}{2} \sum_{\mathbf{k}} g_{\mathbf{k}} n \Big(\hat{a}_{-\mathbf{k}} \hat{a}_{\mathbf{k}} + \hat{a}^\dagger_{-\mathbf{k}} \hat{a}^\dagger_{\mathbf{k}} \Big). \tag{1.93}$$

Thus, all of the equations for the dilute Bose gas carry through, but with the contact interaction being replaced by the bare interaction ($g\delta(\mathbf{x}-\mathbf{x}') \to V(\mathbf{x}-\mathbf{x}') = \sum_{\mathbf{k}} g_{\mathbf{k}} \mathrm{e}^{\mathrm{i}\mathbf{k}\cdot(\mathbf{x}-\mathbf{x}')}$). We may therefore calculate the quantum depletion by using Equation (1.80) and making the aforementioned substitution

$$n_{\mathrm{ex}}(T=0) = \frac{4\pi}{(2\pi)^3} \int \mathrm{d}k k^2 \frac{\frac{\hbar^2 \mathbf{k}^2}{2m} + g_{\mathbf{k}} n - \hbar \widetilde{\omega}_b(\mathbf{k})}{2\hbar \widetilde{\omega}_b(\mathbf{k})} \tag{1.94}$$

where we have introduce the long-range Bogoliubov frequencies

$$\hbar \widetilde{\omega}_b(\mathbf{k}) = \sqrt{\frac{\hbar^2 k^2}{2m} \left(\frac{\hbar^2 k^2}{2m} + g_{\mathbf{k}} n \right)} \ . \tag{1.95}$$

Foldy evaluated this integral for the Coulomb potential $g_{\mathbf{k}} = 4\pi e^2/\mathbf{k}^2$ and found [120]

$$n_{\mathrm{ex}}(T=0) \propto \left(\frac{1}{n a_B^3} \right)^{1/4} \tag{1.96}$$

with a_B the Bohr radius. Thus for a long-range interacting gas, the depletion of the condensate vanishes in the *high-density* limit.

1.3.4.2 Generalized Gross-Pitaevskii equation

Provided a gas is sufficiently cold and quantum fluctutations do not deplete the condensate, we may reasonably expect a mean-field theory with the bare potential, as opposed to an effective one, to provide a good description of LRI-MB system of indistinguishable bosons; this expectation has been demonstrated rigourously for

self-gravitating bosons [89], the charged Boson gas [121], and for dipolar bose gases [122]. This equation, often called a Generalized GPE (GGPE) is inherently non-local and takes the form

$$\mathrm{i}\hbar\partial_t\Psi = -\frac{\hbar^2}{2m}\nabla^2\Psi + \Phi(\mathbf{x},t)\Psi \tag{1.97a}$$

$$\Phi(\mathbf{x},t) = \int \mathrm{d}^d x V(\mathbf{x}-\mathbf{x}')|\Psi(\mathbf{x}',t)|^2 \tag{1.97b}$$

where Φ is referred to as the mean-field potential. Famous equations of this form include the GGPE for a dipolar Bose gas, where [115, 122]

$$V_{\mathrm{dd}}(\mathbf{x}-\mathbf{x}') = \frac{1-3\cos^2\theta}{4\pi|\mathbf{x}-\mathbf{x}'|^3} \tag{1.98}$$

where $\cos\theta = \mathbf{x}\cdot\mathbf{x}'/(|\mathbf{x}||\mathbf{x}'|)$, and the Schrödinger-Poisson (or Schrödinger-Newton) equation [82, 89, 117] where

$$V_{\mathrm{dd}}(\mathbf{x}-\mathbf{x}') = \frac{G}{|\mathbf{x}-\mathbf{x}'|}. \tag{1.99}$$

1.4 The Hamiltonian Mean-Field Model

Having outlined the most important features of LRI-MB systems, and reviewed the theory of a Bose gas, we are now in a position to discuss the HMF model's history in context. Originally proposed as a simple, solvable, toy model, it has shown a remarkable ability to capture and elucidate key features present in a wide range of LRI-MB systems.

Classically the model may be viewed as describing either a gas of particles confined to a periodic domain, or as an all-to-all rotor model; these two pictures are illustrated in Figure 1.5. The Hamiltonian is given by

$$H = \sum_i \frac{1}{2}L_i^2 + \frac{\epsilon}{N}\sum_{i<j}\cos(\theta_i-\theta_j)\ . \tag{1.100}$$

It is convenient to note that the Hamiltonian can be re-written in terms of the average

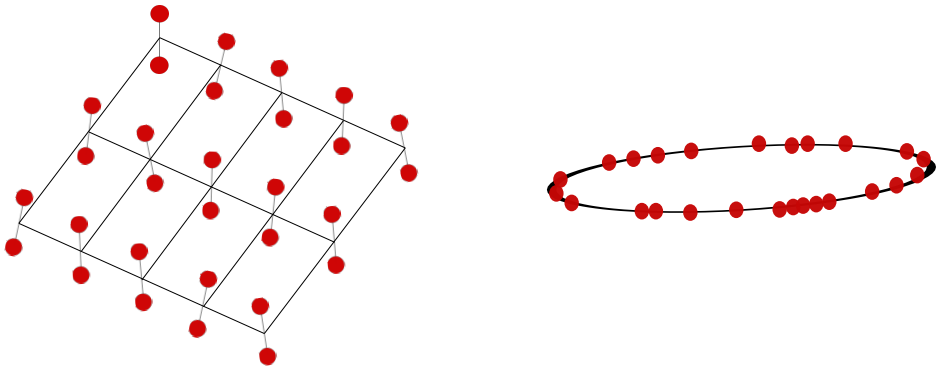

(a) (b)

Figure 1.5: Two interpretations of the HMF model. We may think of a lattice of rotors interacting via an infinite-range XY interaction (a), or equivalently of particles on a ring interacting via a pair-wise cosine potential (b).

magnetization $\mathbf{M} = \frac{1}{N}\sum_i(\cos\theta_i, \sin\theta_i)^T$

$$H = \sum_i \frac{1}{2}L_i^2 + \frac{1}{2}N\epsilon\mathbf{M}^2 \ . \tag{1.101}$$

The motivation for proposing the HMF model was to be able to find a model that was exactly solvable, but could also be easily simulated on a computer, and that isolated features of *long-range* interactions. This seems obvious in the context of this thesis, but prior to the mid-90s almost all of the interest on LRI-MB systems centred around self-gravitating fluids, and non-neutral plasmas, both containing a Coulomb-like interaction. This has the added complication of including a short-range singularity that can complicate numerics, and potentially result in "exotic" behaviour that is not cause by LRI.

The HMF model's greatest strength has been its ability to bridge the divide between dynamics and statistical mechanics. Its numerical tractability has allowed for large scale (and consequently trust worthy) molecular dynamics simulations that can be performed on a laptop. This has allowed for direct tests of microcanonical predictions, investigations into out-of-equilibrium phase transitions, and from virialized "galactic" dynamics.

In this section, we will focus on three existing studies of the HMF model. First we

will outline the earliest works on the model's canonical phase diagram. Then we will discuss a peculiar dynamical property of the HMF model, wherein it can be driven *away* from equilibrium. Finally, we will outline work done in the early 2010s on the quantum HMF model [82, 83]. This will set the stage for the rest of the thesis.

1.4.1 Canonical Phase Diagram

The HMF model can be solved exactly in the $N \to \infty$ limit [5, 63]. For $\epsilon > 0$ the model's canonical phase diagram does not exhibit a phase transition. Thus we will consider the case of $\epsilon < 0$ in this section. We begin by writing the partition function including an external field $\mathbf{B}$

$$Z = \int \prod_{i=1}^{N} \mathrm{d}\theta_i \mathrm{d}p_i \exp[-\beta(H - N\mathbf{B}\cdot\mathbf{M})] \tag{1.102}$$

the integration over the conjugate momenta can be performed easily. Then, using the magnetization representation of the Hamiltonian Equation (1.101) the partition function can be decoupled via the identity

$$\mathrm{e}^{-\beta|\epsilon|N\mathbf{M}^2/2} = \text{const} \times \int \mathrm{d}y_1 \mathrm{d}y_2 \exp\left[-N\frac{\mathbf{y}^2}{2\beta|\epsilon|} + \mathbf{M}\cdot\mathbf{y}\right] . \tag{1.103}$$

This then allows all of the integrals over the angular varibles to be carried out (since they have all be decoupled) leaving only an integral over y_1 and y_2. The partition function is then (up to irrelevant constant pre-factors)

$$Z = \int \mathrm{d}y_1 \mathrm{d}y_2 \exp\left\{ - N\left[\frac{\mathbf{y}^2}{2\beta|\epsilon|} - I_0(\mathbf{y}+\mathbf{B})\right]\right\} . \tag{1.104}$$

where $I_0(z) = \int_0^{2\pi} \exp[z\cos\theta]$ is the modified Bessel funciton of order zero. This integral can be evaluated asymptotically as $N \to \infty$ using Watson's Lemma yielding

$$\beta f = \frac{\ln Z}{N} \sim \beta f_0 + \inf_{\mathbf{y}}\left[\frac{\mathbf{y}^2}{2\beta|\epsilon|} - \ln I_0(|\mathbf{y}+\mathbf{B}|)\right] + \mathcal{O}\Big(\frac{1}{N}\Big) , \tag{1.105}$$

then, because $I_0(z)$ is monotonically increasing, this is always minimized when $\mathbf{y}$ is parallel to $\mathbf{B}$ so we find.

$$\beta f \sim \beta f_0 + \inf_y \left[\frac{y^2}{2\beta|\epsilon|} - \ln I_0(y+B) \right] \tag{1.106}$$

For $\epsilon > 0$ (repulsive interactions) the minimizing value of y is $y_\star = 0$ for all temperatures at zero field B and there is no phase transition; however, for $\epsilon < 0$ (attractive interactions) this is no longer true. In this case the minimizer, $y_\star$, solves

$$\frac{I_1(y_\star + B)}{I_0(y_\star + B)} - \frac{y_\star}{\beta|\epsilon|} = 0 \tag{1.107}$$

Giving

$$\beta f \sim \beta f_0 + \left[\frac{y_\star^2}{2\beta|\epsilon|} - \ln I_0(y_\star + B) \right] . \tag{1.108}$$

The average magnetization is given by $\langle|\mathbf{M}|\rangle = \beta \partial F/\partial B$ evaluated at $B = 0$, which gives

$$\langle|\mathbf{M}|\rangle = \frac{I_1(y_\star)}{I_0(y_\star)} = \frac{y_\star}{\beta|\epsilon|} . \tag{1.109}$$

The solution to Equation (1.107) is $y_\star = 0$ for $\beta\epsilon < 2$, whereas for $\beta\epsilon \geq 2$ a new solution appears at $y_\star \neq 0$. This results in the magnetization undergoing a second-order phase transition since $\langle|\mathbf{M}|\rangle = y_\star$. Thus, the HMF model is exactly solvable, and its equilibrium phase diagram exhibits a non-trivial phase transition for attractive interactions.

As emphasized in the introduction, different ensembles can yield different results for a LRI-MB system. In the HMF model, this turns out not to be the case, and the canonical ensemble is equivalent to the microcanonical one. In the microcanonical ensemble the phase transition is driven by the internal energy per particle u which can be related to the temperature via

$$u = \frac{1}{N}\frac{\partial \ln Z}{\partial \beta} = \frac{T}{2} - \frac{|\epsilon|}{2}\mathbf{M}^2 . \tag{1.110}$$

This allows for the canonical ensembles predictions to be compared directly with molecular dynamics simulations which can be carried out at fixed energy, and their long-time behaviour compared to our equilibrium predictions.

1.4.2 Dynamical Formation of Bi-Clusters

From the HMF model's inception it was noted that molecular dynamics simulations showed a propensity towards the formation of a bi-cluster (composed of two nearly Dirac-delta-like density peaks spaced on opposite sides of the ring). This behaviour occus for repulsive interaction ($\epsilon > 0$), for initial conditions very close to thermodynamic equilibrium (i.e. homogeneous density and vanishing velocity) [63].

As was discussed in Section 1.2.1, the dynamics of the HMF model can be expected to evolve under the Vlasov equation, and to be driven towards a QSS. The thermodynamic equilibrium is certainly one such state, and given that we are considering initial conditions very close to equilibrium, we expect that the system will relax towards thermodynamic equilibrium, or at least stay nearby, even when its dynamics are governed by the collisionless relaxation in the Vlasov equation.

Antoni and Ruffo [63] studied this question by preparing *water bag* initial data, consisting of a box-distribution of velocities $f(\theta, L, 0) = \Theta(v - |L|)\rho(\theta)$, with $\rho(\theta)$ generally taken to be very slowly varying. For $v > 0$ the expectation of quasi-equilibrium dynamics is borne out, and the state simply fluctuates around the equilibrium distribution. Shockingly, however, for smaller values of v the system is driven far away from equilibrium forming a bi-cluster. This is energetically possible because, as emphasized by Equation (1.101), the interaction energy vanishes provided that the magnetization does as well. Thus, a bi-clustered state has very low energy, since $\langle \mathbf{M} \rangle = 0$. Nevertheless, bulk quantities, such as $\langle \frac{1}{N} \sum_i \cos 2\theta_i \rangle$ differ substantially from their thermodynamic predictions.

The first analytic understanding of this phenomenon came half a decade later [13, 72] by studying the Vlasov equation in the "zero-temperature" limit corresponding to an infinitesimally thin spread in velocities. In this case the phase space distribution can be approximated (at early times) as $f(\theta, L, t) = \rho(\theta, t)\delta(L - v(\theta, t))$. This leads to a set of Euler equations (in reduced variables)

$$\partial_t \rho + \partial_\theta(\rho v) = 0 \tag{1.111a}$$

$$\partial_t v + v\partial_\theta v + \partial_\theta \Phi = 0 \tag{1.111b}$$

$$\Phi(\theta, t) = \int_0^{2\pi} \mathrm{d}\theta' \cos(\theta - \theta')\rho(\theta') \ . \tag{1.111c}$$

Perturbing around a homogeneous density distribution, these equations can be linearized and solved in a basis of Fourier modes. It is found that only the $k = \pm 1$ Fourier components oscillate, with a frequency given by $\omega_{\mathrm{pl}} = 1/\sqrt{2}$. This linear analysis does not reveal the origin of the bi-clusteron its own, but instead is a building block that can be used to construct an analysis which *does* explain the late-time bicluster.

Using multi-scale methods, and time-averaging over the fast plasma oscillations, an effective equation that governs the slow evolution of the density. For an initial departure from equilibrium of size A, the time scale on which the bi-cluster forms is $t_{\mathrm{bc}} \sim \mathcal{O}(1/A)$. We therefore introduce a slow timescale, $\mathcal{T}$ such that $\mathcal{T}_{\mathrm{bc}} \sim \mathcal{O}(1)$. We therefore define $\mathcal{T} = At$. Then, the effective equation governing the slow time dynamics is

$$\partial_{\mathcal{T}} v + v\partial_\theta v + \partial_\theta \left[\frac{\omega_{\mathrm{pl}}}{8} \cos^2 \theta \right] = 0 \ . \tag{1.112}$$

The origin of the bi-cluster is now clear. The linearized dynamics lead to fast oscillations, that, when time averaged, result in a shallow focusing potential. On very long-time scales the effect of the weak focusing potential is to drive the system towards a bi-clustered state. The mean-field potential Φ drives rapid linear dynamics which result in an energy exchange, slowly converting small amounts of potential energy into kinetic energy. The systems' dynamics prefer a bi-clustered state, despite being extremely close to the equilibrium distribution initially. This dynamical process is similar to violent relaxation in that a rapidly varying mean-field potential allows the system to transfer energy. Unlike for attractive interactions however, the time scale of energy transfer is *much longer* than the time scale governing the dynamics of the underlying mean-field potential Φ.

The formation of the bi-cluster is interesting not only because it shows marked departure from equilibrium behaviour, but also because it is persistent. The bi-cluster reoccurs and its lifetime lengthens upon each recurrence. In fact, it can be shown that if an effective time-averaged Lagrangian is constructed, in complete analogy with the multi-scale approach outlined above, that the bi-cluster is the equilibrium state of the associated effective time-averaged Hamiltonian. Thus, the bi-cluster is a state that the equilibrium state of an emergent Hamiltonian different than the HMF model.

1.4.3 The Quantum HMF Model

The bosonic quantum HMF model can be written, in second quantized notation, as [82]

$$H_{\text{Bose}} = \int \mathrm{d}\theta \hat{\Psi}^\dagger \left(-\frac{\hbar^2}{2mR^2}\partial_\theta^2 \right) \hat{\Psi} + \frac{\epsilon}{N} \int \mathrm{d}\theta \mathrm{d}\theta' \hat{\Psi}^\dagger(\theta)\hat{\Psi}^\dagger(\theta')\hat{\Psi}(\theta')\hat{\Psi}(\theta)\cos(\theta-\theta') \tag{1.113}$$

for fields satisfying the bosonic commutator identity

$$[\hat{\Psi}(\theta), \hat{\Psi}^\dagger(\theta')] = \delta(\theta-\theta') \tag{1.114}$$

or for fermions

$$H_{\text{Fermi}} = \int \mathrm{d}\theta \hat{\Phi}^\dagger \left(-\frac{\hbar^2}{2mR^2}\partial_\theta^2 \right) \hat{\Phi} + \frac{\epsilon}{N} \int \mathrm{d}\theta \mathrm{d}\theta' \hat{\Phi}^\dagger(\theta)\hat{\Phi}^\dagger(\theta')\hat{\Phi}(\theta')\hat{\Phi}(\theta)\cos(\theta-\theta') \tag{1.115}$$

with fields satisfying the fermionic anti-commutator relation

$$\{\hat{\Phi}(\theta), \hat{\Phi}^\dagger(\theta')\} = \delta(\theta-\theta') \ . \tag{1.116}$$

For the remainder of this thesis we will focus on H_{Bose}. Both Equations (1.113) and (1.115) were introduced and studied by Chavanis [82, 83]. He focused on the equilibrium properties of the HMF model drawing close analogy with the theory of Bose stars. A first step in studying Equation (1.113) is to note that the Hamiltonian is governed by one dimensionless ratio $\chi = \hbar/\sqrt{mR^2|\epsilon|}$. This governs the relative strength of the kinetic energy relative to the potential energy. Chavanis studied the GGPE associated with Equation (1.113) both with and without contact interactions (adding a term proportional to $\int \mathrm{d}\theta |\Psi|^4$ to the Hamiltonian) , written in terms of χ this is given by

$$\mathrm{i}\chi\partial_t\Psi = -\frac{\chi^2}{2}\partial_\theta^2\Psi + \mathrm{sgn}(\epsilon)\Phi(\theta,t)\Psi \tag{1.117a}$$

$$\Phi(\theta,t) = \int \mathrm{d}\theta' |\Psi(\theta',t)|^2 \cos(\theta-\theta') \tag{1.117b}$$

Chavanis was able to numerically solve these equations to find the ground state and found that for for attractive interactions (i.e. $\mathrm{sgn}(\epsilon) = -1$) if $\chi > \sqrt{2}$ then the

ground state is a homogenous gas, whereas for $\chi < \sqrt{2}$ the condensate wavefunction develops a non-trivial spatial variation. This is indicative of spontaneous symmetry breaking, and suggests that the HMF model undergoes a quantum phase transition. Chavanis was able to numerically solve for the magnetization (in this context defined as $M = \int_0^{2\pi} |\Psi(\theta)|^2 \cos\theta$) as a function of χ.

In addition to studying the lowest energy state, Chavanis also studied linearized dynamics about the homogeneous phase. For this purpose, he included not only the long-range interaction, but also short-range interactions by adding a $g|\Psi|^2$ to Equation (1.117a). The normal mode frequencies are then given by

$$\omega(k) = \widetilde{\omega}_b(k) \tag{1.118}$$

where $\widetilde{\omega}_b(k)$ is given by Equation (1.95) with $g(k) = \frac{\mathrm{sgn}(\epsilon)}{2}\delta_{|k|,1} + \frac{g}{2\pi}$. In the limit of $g \to 0$ where we recover the HMF model this gives

$$\omega^2(k) = \begin{cases} \left(\frac{\mathrm{sgn}(\epsilon)}{2} + \frac{\chi^2}{2}k^2\right)\frac{\chi^2}{2}k^2 & \text{if} \quad k = \pm 1 \\ \frac{\chi^4}{4}k^4 & \text{else} \end{cases} . \tag{1.119}$$

This result agrees with the linearized analysis of the Euler equations for the classical HMF model in the zero-temperature limit. This is not surprising since by using the density-phase representation, the GGPE for the HMF model can be re-written as

$$\partial_t \rho + \partial_\theta(\rho v) = 0 \tag{1.120a}$$

$$\partial_t v + v\partial_\theta v + \partial_\theta \Phi = -\partial_x\left[\frac{\chi^2}{2}\frac{\partial_x^2\sqrt{\rho}}{\sqrt{\rho}}\right] \tag{1.120b}$$

$$\Phi(\theta, t) = \int_0^{2\pi} \mathrm{d}\theta' \cos(\theta - \theta')\rho(\theta') \ . \tag{1.120c}$$

which are identical to the classical Euler equations but with the added quantum pressure term.

Summary

LRI-MB systems are different than those with short-range interactions. They have unique features that modify both their statistical and dynamical behaviours. A system with LRI is not restricted by the Mermin-Wagner theorem, and can spontaneously break symmetries in low-dimensions; a related topic is the improved accuracy of mean-field theory for LRI-MB systems.

The HMF model is a prolific toy model that can be used to investigate and elucidate many novel aspects of long-range interacting systems. Its dynamics display violent relaxation, and it is known to exhibit a spontaneously broken continuous symmetry providing a concrete example of "violating" the Mermin-Wagner theorem. The quantum limit of the HMF model has been seldom studied, with only its equilibrium physics (as described by mean-field theory) having been given significant attention.

In the rest of this thesis we present three different studies of the bosonic HMF model. In Chapter 2 we extend the theory of the bi-cluster the quantum regime by studying the HMF model's GGPE. In Chapter 3 we find exact solutions to the same GGPE. We classify an infinite set of stationary states, and identify them as solitons that are stabilized by long-range interactions. Finally, in Chapter 4 we use the exact solutions of Chapter 3 to go beyond mean-field theory and study many-body quantum fluctuations. We are particularly interested in understanding whether symmetry breaking persists at zero temperature.

"I consider the basic urge for for disequilibrium in self-gravitating systems to sound the death knoll of Boltzmann's hypothesis....it is probable that no equilibrium can exist even in theory!"

—Donald Lynden-Bell

CHAPTER 2

Quantum Violent Relaxation

Ryan Plestid, Perry Mahon, and D.H.J. O'Dell
Violent relaxation in quantum fluids with long-range interactions
Phys. Rev. E **98**, 012112; doi: 10.1103/PhysRevE.98.012112

As emphasized in Section 1.2, LRI-MB systems approach equilibrium in a very different way than short-range interacting systems. Rather than relaxation being driven by collisions, LRI-MB systems have a variety of relaxation mechanisms at their disposal. In this paper we study the dynamics of the HMF model's GGPE paralleling previous studies in the classical regime. We focus on initial conditions that are focusing on initial conditions that are nearly homogeneous with small sinusoidal variations in their velocity profiles (or equivalently with weak phase gradients). We focus primarily on the hydrodynamic formulation of the GGPE, as expressed in Equations (1.120a) to (1.120c), to made broader contact with other quantum fluids.

In the case of attractive interactions we study the HMF model's Jeans instability and observe what is essentially violent relaxation (as it is known within the astrophysical community). In contrast, for repulsive interactions we focus on the bi-cluster reviewed in Section 1.4.2. In both cases we find that the semi-classical limit can be understood in terms of catastrophe theory, the background of which is explained in a self contained manner in Sec. VII of the paper.

Our major focuses are as follows

- How can a semi-classical theory of trajectories be used to understand the quantum dynamics?
- Does the attractive case display behaviour remniscent of classical violent relaxation? How do quantum effects modify the dynamics?
- Do the bi-clusters of Section 1.4.2 form in the quantum HMF model? Are the classical model's biclusters diffused by quantum pressure?
- Does the $\chi \to 0$ limit commute with the $t \to \infty$ and $N \to \infty$ limits?

Violent relaxation in quantum fluids with long-range interactions

Ryan Plestid,[1,2,*] Perry Mahon,[1,3] and D. H. J. O'Dell[1,†]

[1]*Department of Physics and Astronomy, McMaster University, 1280 Main St. W. Hamilton, Ontario, Canada L8S 4M1*

[2]*Perimeter Institute for Theoretical Physics, 31 Caroline St. N., Waterloo, Ontario, Canada N2L 2Y5*

[3]*Department of Physics, University of Toronto, 60 St. George St., Toronto, Ontario, Canada M5S 1A7*

(Received 20 December 2017; revised manuscript received 2 June 2018; published 12 July 2018)

Violent relaxation is a process that occurs in systems with long-range interactions. It has the peculiar feature of dramatically amplifying small perturbations, and rather than driving the system to equilibrium, it instead leads to slowly evolving configurations known as quasistationary states that fall outside the standard paradigm of statistical mechanics. Violent relaxation was originally identified in gravity-driven stellar dynamics; here, we extend the theory into the quantum regime by developing a quantum version of the Hamiltonian mean field (HMF) model which exemplifies many of the generic properties of long-range interacting systems. The HMF model can either be viewed as describing particles interacting via a cosine potential, or equivalently as the kinetic XY model with infinite-range interactions, and its quantum fluid dynamics can be obtained from a generalized Gross-Pitaevskii equation. We show that singular caustics that form during violent relaxation are regulated by interference effects in a universal way described by Thom's catastrophe theory applied to waves and this leads to emergent length scales and timescales not present in the classical problem. In the deep quantum regime we find that violent relaxation is suppressed altogether by quantum zero-point motion. Our results are relevant to laboratory studies of self-organization in cold atomic gases with long-range interactions.

DOI: 10.1103/PhysRevE.98.012112

I. INTRODUCTION

Quantum many-body (QMB) systems with long-range interactions (LRI) are increasingly being realized in laboratory experiments with cold atomic and molecular gases where inherently long coherence times are suited to investigating dynamics. Examples include atomic Bose-Einstein condensates (BEC) with magnetic dipole-dipole interactions [1–12], cold polar molecules [13–18], trapped ions [19–22], Rydberg atoms [23–30], and atoms inside high-finesse optical cavities which interact via the cavity modes that extend over the entire cavity [31–36]. There are also new approaches in the pipeline, such as using optical waveguides or photonic band gap crystals to engineer electromagnetic modes and hence mediate highly controlled long-range interatomic interactions [37–39].

This progress in trapped atomic and molecular systems has fostered broad interest in LRI both in and out of equilibrium [40–50]. While the focus has been on spin and Hubbard models, the versatility of these systems also allows for new regimes not seen in traditional condensed matter systems, including gravitylike attractive $1/r$ interactions [51–53], and also cosine-type interactions that occur between atoms in optical cavities [54–62].

Historically, the motivation for studying LRI has come from astrophysics and plasma physics: the range of the gravitational and Coulomb interactions, respectively, are such that all particles experience a common, essentially mean field, potential. In nonequilibrium situations, this potential becomes time dependent and drives a rapid, collisionless relaxation mechanism, known as violent relaxation, which efficiently mixes phase space [63]. This process is nonergodic and hence profoundly different from relaxation in systems with short-range interactions. Nevertheless, universality still emerges: pioneering work in the 1960's by Lynden-Bell [64] on the statistical mechanics of violent relaxation in stellar and galactic dynamics introduced a fourth type of equilibrium distribution which is related to both the Fermi-Dirac distribution and equipartition of energy per unit mass. More recent research has generalized Lynden-Bell statistics to two-parameter Core-Halo distributions [65–68] which can also handle the case of far-from-virialized initial conditions and the following two-stage picture of relaxation from a nonequilibrium state has emerged [69,70]: First, there is violent relaxation, the timescale of which does not depend on the number of particles N, and results in *long-lived nonequilibrium configurations* known as quasistationary states (QSS). Second, at long times, there is the more familiar collisional relaxation towards Maxwell-Boltzmann equilibrium, however, this occurs at times of order N^{δ}, where $\delta \geqslant 1$ [71,72]. Therefore, in the thermodynamic limit $N \to \infty$ the lifetime of the QSS diverges and the system remains out of equilibrium indefinitely, which has implications for thermalization. Violent relaxation is now recognized as the cornerstone of statistical theories describing the QSS that dominate transient behavior in systems with LRI. Since these QSS are formed by nonergodic dynamics, they are not captured by conventional statistical treatments.

In this paper, we are interested in the following thematic questions: Does violent relaxation take place in quantum systems? Do QSS exist and do they display new length scales and timescales? Do these modifications survive in the

*plestird@mcmaster.ca

†dodell@mcmaster.ca

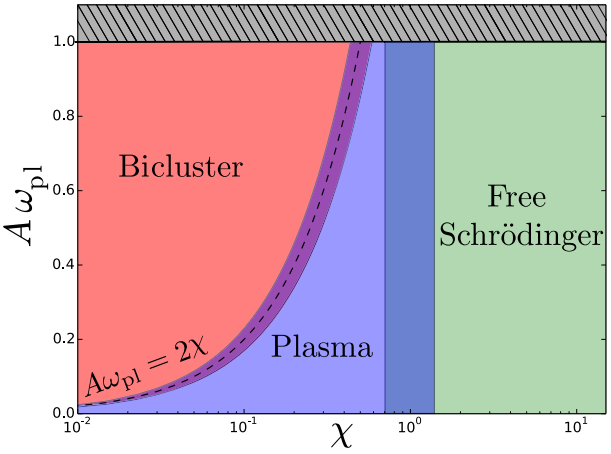

FIG. 1. Nonequilibrium phase diagram for the quantum HMF model with repulsive interactions ($\epsilon > 0$). Violent relaxation leads to quasistationary states which are very slowly evolving nonequilibrium configurations; for the HMF model these are the bicluster states. On this semilog plot, the vertical axis measures the initial deviation from equilibrium quantified by $v_0 = A\omega_{\rm pl}\cos\theta$ which is the initial velocity field due to small plasma oscillations [see Eq. (D1)]. The horizontal axis captures quantum effects via the effective Planck constant $\chi = \hbar/\sqrt{|\epsilon| m R^2}$. When $\chi \ll 1$ *and* $\chi \lesssim 2A\omega_{\rm pl}$ the system forms a bicluster at late times [see Fig. 5(f)]. By contrast, for $\chi \lesssim 1$, the $k = \pm 1$ modes dominate and the system continues to undergo plasma oscillations without relaxing [see Eq. (11) and Fig. 5(b)]. Finally, for $\chi \gtrsim 1$ all Fourier modes experience a free Schrödinger-type dispersion relation and violent relaxation is suppressed by quantum zero-point motion [see Fig. 5(a)]. The gray region denotes initial conditions that invalidate the short-time linear response procedure detailed in Eqs. (14) and (15).

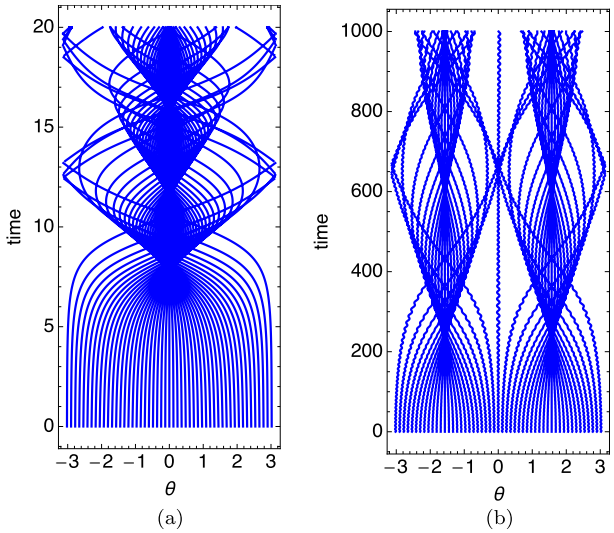

FIG. 2. Long-range interactions tend to amplify initial perturbations. We illustrate this feature here with the Newtonian trajectories of 52 particles obeying the classical HMF model with (a) attractive ($\epsilon < 0$) and (b) repulsive ($\epsilon > 0$) interactions. At $t = 0$, the particles are spaced evenly around the ring with very slightly varying initial velocities $v_i(\theta,0) = 0.005\cos\theta$. In both cases, the LRI cause the particles to cluster and this behavior repeats such that the envelopes of the trajectories form a quasiperiodic series of cusp-shaped caustics (or "chevrons"[75,76]). However, there are key differences: First, the attractive interactions give rise to a single cluster point (monocluster) around the ring whereas repulsive interactions produce two cluster points (bicluster), and second there are very different timescales associated with the two cases with the repulsive case being much slower (note the different scales on the time axes).

thermodynamic limit? We base our analysis on the Hamiltonian mean field (HMF) model [72–77] which over the last two decades has become one of the main theoretical tools for investigating many-body systems with LRI (see Refs. [69,70] for reviews). It offers the advantage of being analytically tractable at equilibrium, and is known to capture dynamical features present in more complicated systems [67,70,74,76]. Moreover, the HMF model is directly relevant to describing cold atoms in optical cavities where self-organization and the nonequilibrium Dicke phase transition have been intensively studied both theoretically [54–62] and experimentally [32,78–82]. Our work, therefore, has experimental relevance but for brevity's sake we only consider closed systems and do not include effects that would model cavity pumping and decay. However, in separate work we have shown that the type of QSS we observe (wave catastrophes) have the fundamental property of structural stability, even against decoherence, and hence survive in cavities weakly coupled to the environment [83]. Wave catastrophes can also be seen in simulations by others [84] of microcavity polaritons using a driven damped Gross-Pitaevskii equation.

A key part of our results is summarized in the nonequilibrium phase diagram in Fig. 1 which depicts the end results of violent relaxation in a quantum version of the HMF model. The vertical axis gives the magnitude of initial perturbations from equilibrium, i.e., initial velocity fluctuations v_0, and the horizontal axis measures the effective Planck constant χ which, of course, is entirely absent in classical systems. We find that quantum effects increasingly stabilize initial plasma fluctuations, thereby suppressing violent relaxation, such that by the time the deep quantum regime (designated the free Schrödinger phase) is reached quantum zero-point motion of higher lying modes dominates the plasma oscillations.

A second strand to the story we present here concerns the nature of the QSS and their connection to *caustics*. In a landmark paper on the large scale structure of the universe, Arnold, Shandarin, and Zeldovich [85] considered a self-gravitating mass distribution and showed that initially smooth perturbations evolve into singular caustics upon which the density diverges (for a recent update to this work see [86]). These caustics take universal shapes described by the so-called catastrophe theory due originally to Thom and Arnold [87–89] and include cusps, swallowtails, beak-to-beaks, and Zeldovich pancakes [90]. Likewise, as shown in Fig. 2, the dynamics of the classical HMF model also leads to cusp catastrophes [75,76,91,92] which are the structurally stable catastrophes found in two dimensions (1 space + 1 time).

One might expect quantum effects to smooth classical singularities and this is indeed what we find; however, what is remarkable is that quantum effects enter in a universal way,

replacing the caustics with characteristic interference patterns known as wave catastrophes that introduce new length scales and timescales [93,94]. For instance, cusp catastrophes become Pearcey functions (see Fig. 7). Wave catastrophes obey a set of scaling relations as the wavelength is varied, and thus, as quantum effects are switched on *the new length scales and timescales of the QSS scale in a universal way*. Once again, the nonergodic nature of the classical limit plays a crucial role as caustics are formed by the cooperative behavior of families of trajectories and are dissolved by ergodic dynamics.

The rest of this paper is organized as follows: In Sec. II we provide examples of violent relaxation in the classical HMF model and formulate a classical hydrodynamic description. In Sec. III we describe a theory for the quantum hydrodynamics for the HMF model based on a generalized Gross-Pitaevskii equation (GGPE). Our numerical solutions of the GGPE are presented in Sec. IV where we explore how quantum effects modify the QSS. In Sec. V we sketch out the multiscale analysis first used for describing QSS analytically in Ref. [76], and show how this is modified by quantum effects. In Sec. VI we explain how we arrived at the nonequilibrium phase diagram shown in Fig. 1, and in Sec. VII show how the interference patterns decorating the quantum biclusters can be understood using catastrophe theory. In Sec. VIII we argue that the thermodynamic limit $N \to \infty$ and the classical limit $\hbar \to 0$ do not commute, and we make our concluding remarks in Sec. IX. There are also five appendices covering details omitted in the main text.

II. VIOLENT RELAXATION IN THE CLASSICAL HMF MODEL

The HMF model, despite its name, provides an exact description of a many-body system in one dimension. Defined on a ring of radius R, it describes N particles interacting via a pairwise potential varying as $\cos(\theta_i - \theta_j)$, and has the Hamiltonian

$$H = \sum_i \frac{L_i^2}{2mR^2} + \frac{\epsilon}{N}\sum_{i<j}\cos(\theta_i - \theta_j), \tag{1}$$

where each angular momentum L_i and position θ_i form a canonically conjugate pair (L_i,θ_i). When two particles sit on top of one another, the potential is repulsive (attractive) when $\epsilon > 0$ ($\epsilon < 0$). The explicit $1/N$ factor in the interaction term, known as the Kac prescription [95], enforces extensivity of the Hamiltonian [69]. Experiments with cold atoms trapped in linear optical resonators formed of two mirrors where the atoms interact via the sinusoidal mode of a quasiresonant optical field [60] are described by Hamiltonians closely related to Eq. (1). A complementary interpretation of Eq. (1) is as a kinetic XY model [96] with an infinite-range interaction, and therefore, another physical realization is provided by polar molecules in optical lattices [97–99].

There are two distinct types of dynamics in the HMF model which are illustrated in Fig. 2. The first case has attractive interactions [$\mathrm{sgn}(\epsilon) = -1$] as shown in Fig. 2(a). These lead to a Jeans-type collapse into a monocluster at a single point around the ring which then spreads out and revives periodically, with a timescale that is directly determined by the strength of the interparticle interaction. The second case has repulsive interactions [$\mathrm{sgn}(\epsilon) = 1$] and is shown in Fig. 2(b). One again finds clustering but now at two points on opposite sides of the ring. Furthermore, it arises on vastly longer timescales and corresponds to a QSS.

When the number of particles becomes large, a kinetic-theory description in terms of the phase space density $f(\theta,L,t)$ becomes appropriate. The fact that the number of pairwise LRI scales as $\mathcal{O}(N^2)$ whereas collisional terms are $\mathcal{O}(N)$ suggests one can neglect collisions in this regime. In this case, $f(\theta,L,t)$ obeys the conservation law [100]

$$\frac{df}{dt} = \partial_t f + \dot\theta\partial_\theta f + \dot L\partial_L f = 0, \tag{2}$$

which is known as the collisionless Boltzmann or Vlasov equation (see [101] for a discussion of the difference between the Boltzmann and Vlasov equations.) In fact, Hepp and Braun [102] have rigorously shown that as $N \to \infty$ the Vlasov equation provides an exact description of the dynamics of an N-body classical system with pairwise LRI.

Biclustering was first identified in numerical simulations [91,92] seeded by a "water-bag"-shaped initial distribution in phase space: $f(\theta,L,t=0) \propto \Theta(\theta_0 - |\theta|) \times \Theta(L_0 - |L|)$. In this paper, we are interested in the low-temperature regime where the water bag becomes thin in the L direction. This both causes the lifetimes of the QSS to diverge in the classical theory [76], and also allows for a natural point of contact between our quantum (low-temperature) treatment and the classical dynamics. In the limit $\Delta L \to 0$, each point in space can be assigned a definite velocity, i.e., $f(\theta,L,0) = \rho(\theta)\delta[v(\theta) - L]$, and Eq. (2) can be reexpressed in a Euler (i.e., hydrodynamic) form. This is what constitutes the zero-temperature approximation. It is convenient to introduce a new time $\tau = t/\sqrt{mR^2|\epsilon|}$ and velocity $v(\theta) = v(\theta)\sqrt{mR^2|\epsilon|}$, and to normalize the density via $\int d\theta\rho = 1$. Written in terms of these quantities, the Euler equations are given by

$$\partial_\tau\rho + \partial_\theta(\rho v) = 0, \tag{3a}$$

$$\partial_\tau v + v\partial_\theta v + \mathrm{sgn}(\epsilon)\partial_\theta\Phi = 0 \tag{3b}$$

and can be interpreted as the equations of motion for a fluid undergoing adiabatic and inviscid flow [103]. Here,

$$\begin{aligned}\Phi(\theta,\tau) &= \int_{-\pi}^{\pi} d\phi\,\rho(\phi,\tau)\cos(\theta-\phi)\\ &= M(\tau)\cos[\theta - \varphi(\tau)]\end{aligned} \tag{4}$$

is the mean field potential (for the zero-temperature case) found by summing up the long-range interactions amongst all the particles. It is related to $\dot L$ in Eq. (2) via the Euler-Lagrange equation $\dot L = -\epsilon\partial_\theta\Phi$.

The last line of Eq. (4) represents a remarkable simplification that is proved in Appendix A: the mean field potential always assumes the same cosine functional form specified by just two time-dependent parameters: the depth, or magnetization $M(\tau)$, and a phase $\varphi(\tau)$. Thus, $\Phi(\theta,t)$ is highly constrained and can only change its depth and position around the ring.

III. QUANTUM FLUID DYNAMICS: GROSS-PITAEVSKII THEORY

Chavanis [104] has previously investigated the equilibrium properties of the quantum HMF model using the Gross-Pitaevskii theory, finding that when $\epsilon < 0$ quantum effects can stabilize against the Jeans instability. We focus instead on dynamics which take on a heightened importance in the presence of LRI.

The full quantum description is in terms of a many-body wave function $\psi(\theta_1,\theta_2,\ldots,\theta_N,\tau)$, where the set $\{\theta_i\}$ of N independent angles refer to the particle positions. However, if we consider indistinguishable bosons, in the large-N regime and at very low temperatures, the system can be expected to Bose condense. If all the bosons enter the condensate, then ψ can be written as a product of single-particle wave functions [i.e., $\psi = \prod_{i=1}^{N}\varphi(\theta_i)$] which must be found self-consistently due to the effect of interactions. This is the Hartree description and treats the N-particle system in terms of a condensate wave function $\psi(\theta_1,\theta_2,\ldots,\theta_N,\tau) \to \Psi(\theta,\tau)$, which depends on a single spatial coordinate and obeys a nonlinear wave equation, the Gross-Pitaevskii equation [105,106].

Bose condensation therefore naturally leads to a mean field description (equivalent to a hydrodynamic description) and we will assume this situation in our treatment of the quantum problem. In this context, it is important to point out that the Mermin-Wagner theorem [107–109], which forbids Bose condensation in infinite one-dimensional systems with short-range interactions, does not apply here because our system has both finite size and LRI. The mean field description for a Bose-condensed system is provided by the Gross-Pitaevskii theory which becomes exact in the thermodynamic limit $N \to \infty$.

A. Generalized Gross-Pitaevskii equation

Consider the Gross-Pitaevskii energy functional

$$E[\Psi,\Psi^*] = \frac{N\hbar^2}{2mR^2}\int |\partial_\theta\Psi|^2 d\theta + \frac{N\epsilon}{2}\iint |\Psi(\theta')|^2 \times \cos(\theta-\theta')|\Psi(\theta)|^2 d\theta\, d\theta'. \tag{5}$$

Here, the condensate wave function is normalized to unity: $\int d\theta|\Psi|^2 = 1$, which ensures that Eq. (5) is extensive. The equation of motion for Ψ is given by taking the functional derivative $i\hbar\partial\Psi/\partial t = \delta E/\delta\Psi^*$. One thereby obtains the GGPE for the HMF model [104]

$$i\chi\,\partial_\tau\Psi = -\frac{\chi^2}{2}\partial_\theta^2\Psi + \mathrm{sgn}(\epsilon)\Phi(\theta,\tau)\Psi, \tag{6a}$$

$$\text{where}\quad \Phi(\theta,\tau) = \int_{-\pi}^{\pi}|\Psi(\phi,\tau)|^2\cos(\theta-\phi)d\phi \tag{6b}$$

is the Hartree or mean field potential. The parameter $\chi := \hbar/\sqrt{|\epsilon|mR^2}$ serves as a dimensionless Planck's constant, and we have rescaled time by introducing $\tau = t/\sqrt{mR^2|\epsilon|}$. Using the fact that $|\Psi(\phi,\tau)|^2$ is the probability density equivalent to the particle density $\rho(\phi,\tau)$ in the zero-temperature classical theory discussed in Sec. II, the quantum Hartree potential similarly reduces to the cosine form given in Eq. (4).

For LRI, the Gross-Pitaevskii theory is valid in the high density limit where correlations are weak: for an early discussion in the context of the charged Bose gas, see Ref. [110]. The validity of the Gross-Pitaevskii treatment with LRI has also been established rigorously for boson stars [111] and most recently for dipolar BECs [112]. For a more detailed discussion of the validity of the Gross-Pitaevskii theory for our system, see Appendix B.

B. Quantum Euler equations

The GGPE can be recast in a hydrodynamic form that closely resembles the classical Euler equations. Expressing the generally complex condensate wave function as $\Psi = \sqrt{\rho}e^{iS/\chi}$ we can transform Eq. (6) into two coupled equations describing the evolution of the density ρ and a velocity profile $v = \partial_\theta S$. The dynamics is then controlled by the quantum Euler, or Madelung, equations [104]

$$\partial_\tau\rho + \partial_\theta(\rho v) = 0, \tag{7a}$$

$$\partial_\tau v + v\partial_\theta v + \mathrm{sgn}(\epsilon)\partial_\theta\Phi = -\partial_\theta\left(\frac{\chi^2}{2}\frac{\partial_\theta^2\sqrt{\rho}}{\sqrt{\rho}}\right). \tag{7b}$$

The expression on the right-hand side is often referred to as the *quantum pressure*; physically it arises from zero-point kinetic energy. Here, it is written as the gradient of the so-called quantum potential

$$Q = \frac{\chi^2}{2}\frac{\partial_\theta^2\sqrt{\rho}}{\sqrt{\rho}} \tag{8}$$

and is the only formal mathematical difference between the classical Euler equations, given in Eqs. (3a) and (3b), and the quantum ones.

The quantum versus classical aspects of the system can be better appreciated by writing the Gross-Pitaevskii energy functional (5) in terms of the hydrodynamic variables ρ and v [104]:

$$E[\Psi,\Psi^*] = \tfrac{1}{2}\langle v^2\rangle_\rho + \tfrac{1}{2}\langle\Phi\rangle_\rho + \langle Q\rangle_\rho = T_{\rm cl} + U_{\rm cl} + E_Q, \tag{9}$$

where the averages are taken over the density $\rho(\theta)$. When $\chi = 0$, this agrees with the classical result in the zero-temperature approximation. We refer to the contribution of the quantum pressure term as the quantum energy E_Q. The remaining terms resemble their classical counterparts: the kinetic energy and the mean-field potential energy are denoted by $T_{\rm cl}$ and $U_{\rm cl}$, respectively.

C. Linear response: Plasma oscillations and Bogoliubov dispersion

In this work, we focus on initial conditions that are close to equilibrium. When violent relaxation occurs, it counterintuitively moves us out of this regime, but linear response still plays a key role at short times. Linearizing the hydrodynamic equations (7a) and (7b) about a spatially homogeneous condensate with density $\rho_0 = 1/2\pi$ with zero velocity $v_0 = 0$ we obtain

$$\partial_\tau\rho_1 + \rho_0\partial_\tau v_1 = 0, \tag{10a}$$

$$\partial_\tau v_1 + \partial_\theta\left[\mathrm{sgn}(\epsilon)\Phi[\rho_1] + \frac{\chi^2}{4\rho_0}\partial_\theta^2\rho_1\right] = 0 \tag{10b}$$

which describe small excitations about the condensate. In this linear approximation, each Fourier component evolves as an independent oscillator with frequency ω_k given by the Bogoliubov dispersion relation [104]

$$\omega_k^2 = \tfrac{1}{2}\big[\tfrac{1}{2}\chi^2 k^4 + \mathrm{sgn}(\epsilon)\delta_{|k|,1}k^2\big]. \tag{11}$$

In the limit $\chi \to 0$, and for repulsive interactions ($\epsilon > 1$), we recover the classical plasma frequency $\omega_{\rm pl} = 1/\sqrt{2}$ [76], with quantum corrections only appearing at the quadratic level $\omega_{\pm 1} \approx \omega_{\rm pl} + \mathcal{O}(\chi^2)$. The $\delta_{|k|,1}$ term reflects the fact that with a uniform density only the $k = \pm 1$ modes feel the long-range cosine interaction and are therefore responsible for plasma oscillations. By contrast, the other modes ($k \neq \pm 1$) evolve as free massive particles with frequency $\omega_k = (1/2)\chi\, k^2$, which is a purely quantum effect. Referring back to the nonequilibrium phase diagram Fig. 1, these quantum modes are responsible for the "free Schrödinger" regime on the right-hand side. In the classical case, these modes have zero frequency and so take an infinite time to appear. When the interactions are attractive ($\epsilon < 1$), the frequency is imaginary in the classical limit indicating the Jeans instability, but quantum effects stabilize the system providing $\chi > \sqrt{2}$ [104].

We can estimate the importance of quantum effects by comparing the magnitude of E_Q to that of the total classical energy. During classical plasma oscillations, the energy alternates between $T_{\rm cl}$ and $U_{\rm cl}$ such that these two terms are on average of equal magnitude and we can compare E_Q against either of them. We therefore expect classical-like behavior provided

$$\left|\frac{E_Q}{U_{\rm cl}}\right| \ll 1 \quad \text{(short times)}, \tag{12}$$

where we have stressed that the above argument applies on timescales on the order of the inverse Bogoliubov frequency Eq. (11). In the classical limit, this corresponds to the timescale shown in Fig. 2(a), whereas the timescale of the bicluster in Fig. 2(b) is much longer, and so we may anticipate this criterion to be insufficient in understanding the role of quantum effects on the bicluster.

IV. NUMERICAL RESULTS: VIOLENT RELAXATION IN THE QUANTUM REGIME

We now present the results of our numerical simulations of the full GGPE for equivalent initial data to that used in Fig. 2. In the case of the bicluster we have to contend with the very different timescales provided by the fast microscopic plasma frequency and slow the revival time. This makes the computation quite challenging, but from the physical point of view this is why biclusters are examples of QSS and hence relevant to understanding late-time behavior and possible thermalization. The fate of these structures in the quantum theory is therefore of great interest. The details of our numerical methods can be found in Appendix C.

A. Attractive interactions ($\epsilon < 0$): Jeans instability in the quantum regime

In the case of attractive interactions, the mean field potential Φ favors clustering and this results in the Jeans-type instability. In the classical theory, this occurs even for infinitesimal interactions and leads to a cusp caustic with divergent density as shown in Fig. 2(a). However, the Bogoliubov dispersion relation (11) predicts that quantum zero-point motion stabilizes the system if $\chi > \sqrt{2}$. We have confirmed this threshold numerically. An explicit realization of the quantum Jeans instability is presented in Fig. 3 for $\chi = 10^{-3}$. We see that quantum effects temper the caustic and replace it with an interference pattern such that the density is always finite.

It is important to note that the classical and quantum dynamics only differ qualitatively after the formation of the first cusp, as can be seen by comparing to Fig. 4 where we plot the trajectories of noninteracting test particles which simply feel the force generated by the mean field potential $\Phi(\theta,\tau)$ obtained in making Fig. 3 (this is the quantum analog of the test-particle model discussed in Ref. [70]). This can be easily understood by appealing to energy conservation, and in particular to Eq. (9). At early times $\langle|\partial_\theta\sqrt{\rho}|^2\rangle \lesssim \mathcal{O}(1)$ and consequently $E_Q \lesssim \mathcal{O}(\chi^2) \ll |U_{\rm cl}|$. However, the classical dynamics leads to a folding of the phase space distribution (see Fig. 6), or equivalently a pointwise divergent density profile, and this eventually makes the quantum energy relevant, $E_Q \simeq U_{\rm cl}$, at which point interference effects kick in.

B. Repulsive interactions ($\epsilon > 0$): Bicluster in the quantum regime

Biclustering is surprising not only because it exists at all (in the presence of repulsive interactions), but also because it occurs at half the wavelength of the mean field cosine potential. These mysterious features can be explained within the classical theory by using a multiscale analysis [76] that will be discussed in Sec. V. However, in order to put our quantum results in context, it is worth quoting the main result now, namely, that there is an emergent single-particle (i.e., noninteracting) description with the effective potential

$$V_{\rm eff} = \frac{A^2\omega_{\rm pl}^2}{8}\cos 2\theta. \tag{13}$$

Apart from the $\cos 2\theta$ spatial dependence, we note that the depth of $V_{\rm eff}$ is proportional to the square of the amplitude of the initial plasma fluctuations, and that this predicts a periodic revival of biclusters with period $T_{\rm bc} = \pi/(\sqrt{2}A\omega_{\rm pl})$. We shall adopt this as our timescale when plotting the dynamics in the repulsive regime, and note that it is generally much longer than the plasma period used for the attractive case.

In Fig. 5, we plot solutions of the GGPE in the repulsive case. In the top row, we vary the effective Planck constant χ, and in the bottom row we vary the magnitude of the initial velocity perturbations $v_0(\theta) = A\omega_{\rm pl}\cos\theta$.

All plots have an initially homogeneous density profile $\rho_0 = 1/2\pi$. The top left-hand panel of Fig. 5(a) corresponds to the strongly quantum regime $\chi \geqslant 1$ where we see that the clustering has been almost completely eliminated. Moving to the right, χ is decreased towards the semiclassical regime and biclustering appears, although this by itself does not lead to structures closely resembling the classical case and the temporal period is quite different from the classical bicluster formation time $T_{\rm bc}$. In fact, to retrieve something resembling the classical behavior, we also need the initial plasma wave's amplitude $A\omega_{\rm pl}$ to not be too small as illustrated by the bottom

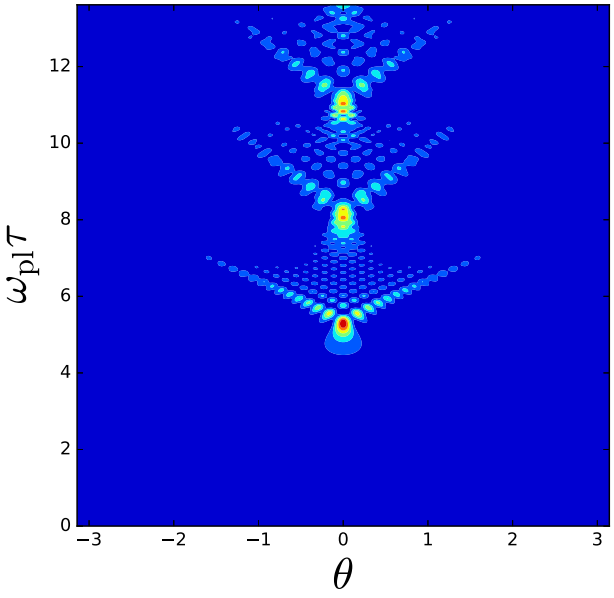

FIG. 3. Quantum Jeans instability: dynamics of the density profile $\rho(\theta,\tau)$ for attractive interactions ($\epsilon < 0$) with initial conditions $\rho_0 = (1+0.01\cos\theta)^2$ and $v_0 = 0$ with $\chi = 10^{-3}$. Interference tempers the (singular) classical caustic and replaces it with a characteristic interference pattern. The dynamical timescale is set by $\omega_{\rm pl} \approx \omega_1 = \mathrm{Im}(i/\sqrt{2})\sqrt{1-\chi^2/2}$ [Eq. (11)].

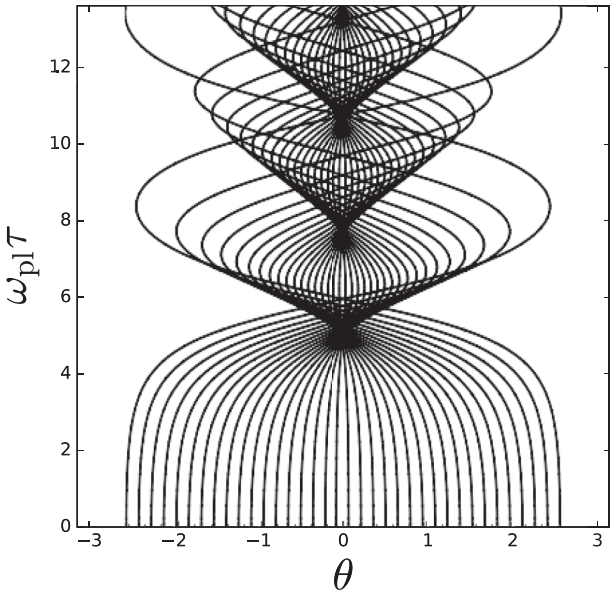

FIG. 4. Trajectories of test particles, each computed by solving Newton's equations for a particle moving in a given external potential $V(\theta,\tau) = -M_\chi[\rho(\tau)]\cos\theta$. This is exactly the mean field potential $\Phi(\theta,\tau)$ computed numerically in the quantum dynamics shown in Fig. 3, where $M_\chi[\rho(\tau)]$ is the self-consistent magnetization.

row in Fig. 5. We emphasize that this increase in classical behavior as $A\omega_{\rm pl}$ is increased occurs for a fixed value of χ.

Our numerical simulations suggest that while the semiclassical condition identified on energetic grounds in Eq. (12) may be necessary for realizing violent relaxation in the quantum regime, it is certainly not sufficient: one also needs a perturbation away from equilibrium that is large enough to overcome quantum fluctuations.

V. QUANTUM PRESSURE AND THE BICLUSTER

As alluded to above, the emergence of the Jeans instability for attractive interactions can be accurately diagnosed via a straightforward linearization of the quantum problem (Bogoliubov theory). Furthermore, the criterion for classical behavior given in Eq. (12) is also obeyed in the presence of attractive interactions. By contrast, the repulsive case is more subtle and the bicluster's underlying mechanism is inherently nonlinear. It therefore requires a more sophisticated analysis even in the classical regime. To understand this behavior, we first sketch (details are relegated to Appendix D) the derivation of the effective potential $V_{\rm eff}(\theta)$ in the classical limit, which was first presented in [75,76], and argue that the same procedure can be carried out in the quantum regime provided $\chi \lesssim 1$. This then provides an effective single-particle picture where semiclassical intuition applies.

Starting from the classical Euler equations (3a) and (3b), and performing the analogous linearization procedure to that outlined in Sec. III C, one finds a set of independent Fourier modes all of which have zero frequency, with the exception of the $k = \pm 1$ modes which oscillate with the plasma frequency $\omega_{\rm pl} = \sqrt{2}$. This defines a "fast" scale, wherein small oscillations of the first Fourier component take place. Anticipating the bicluster that takes place on long timescales, a slow variable $\mathcal{T} = A\tau$ is introduced which reflects the fact that the timescale at which nonlinear effects become important is dictated by A, the amplitude of the initial plasma wave. Next, the velocity field may be decomposed into a fast part v_1 evolving under the linear equations, and a slow part $u(\mathcal{T})$ that is influenced by nonlinear effects (the variations of the density can be neglected). A time average then yields

$$\partial_{\mathcal{T}} u + u\partial_\theta u = -\langle v_1 \partial_\theta v_1\rangle_{\mathcal{T}} := -\frac{1}{A^2}\partial_\theta V_{\rm eff}(\theta),$$
$$\text{where}\quad V_{\rm eff}(\theta) = \frac{A^2\omega_{\rm pl}^2}{8}\cos 2\theta. \tag{14}$$

This is a forced Burgers equation governing the flow of the velocity field. The forcing term involves an effective potential $V_{\rm eff}$ with half the wavelength of the mean field potential Φ. Thus, we have obtained the nontrivial result that the slow variables are governed by a different potential than the original. Burgers' equation is well known to give rise to shock waves where the velocity field becomes multivalued and hence the equation breaks down [113,114] and one needs some physical criterion for determining the fate of the system after the shockwave. In our problem, these shockwaves are the caustics associated with clustering. As depicted in Fig. 6, they occur when the "sheet" of initial data in phase space folds over. When projected onto the (θ,τ) plane, we obtain cusp-shaped caustics: there are three trajectories passing through each spatial point inside the cusp and one outside. Two of the trajectories coalesce at each point along the cusp edges (known as fold lines) and three coalesce

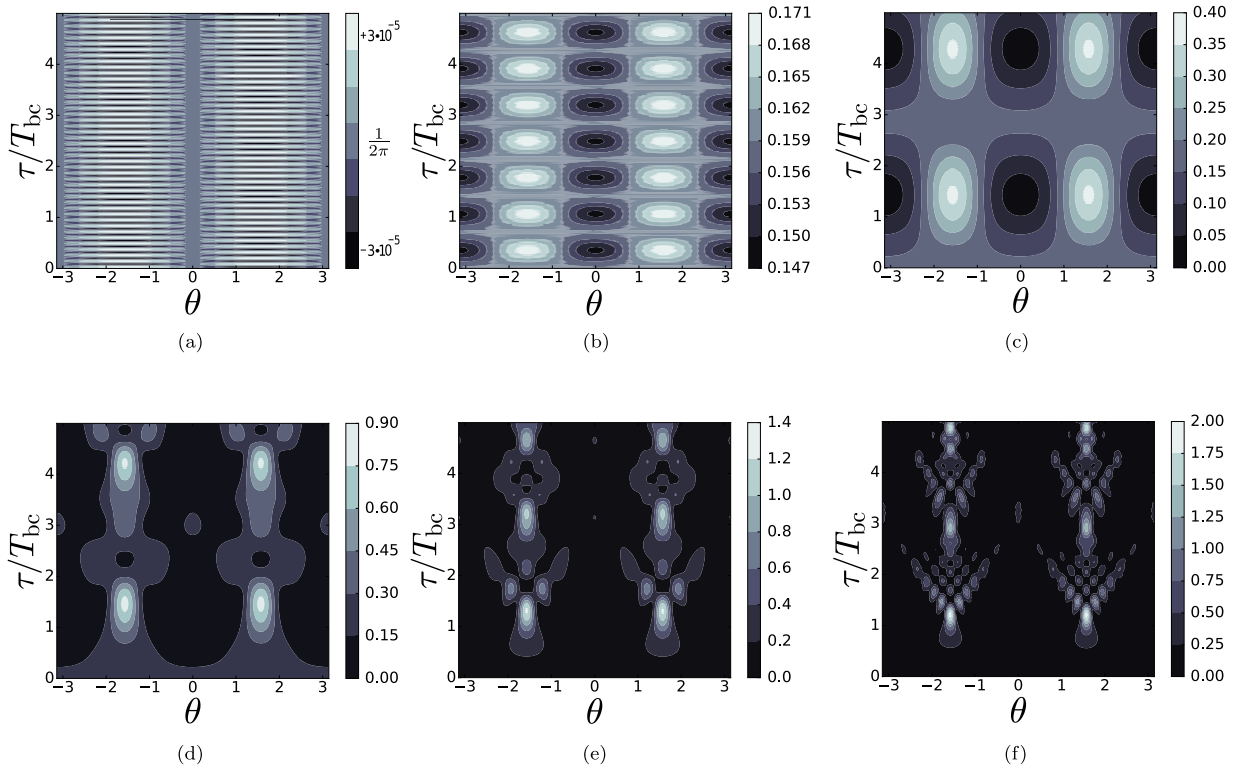

FIG. 5. Dynamics of the density profile $\rho(\theta,\tau)$ for $\epsilon > 0$ in the $\log \chi$-$A\omega_{\rm pl}$ plane in correspondence with the different regimes plotted in Fig. 1. The initial conditions in all panels are $\rho_0 = 1/2\pi$ and $v_0 = A\omega_{\rm pl}\cos\theta$ and time has been rescaled by $T_{\rm bc}$. For $\chi \gg 1$ no bicluster develops (a). For $A\omega_{\rm pl} < \chi \ll 1$ (b) classical plasma oscillations occur, and a very weak π periodic focusing occurs, but is dispersed by the quantum pressure before the classical focusing time $T_{\rm bc}$. In (c)–(f) χ is held fixed while the plasma amplitude $A\omega_{\rm pl}$ is tuned. This has the effect of a deeper effective potential $V_{\rm eff}$ [see Eq. (15)], and consequently a more classical-like pattern emerges. This change of behavior is captured by the nonequilibrium phase diagram shown in Fig. 1, and is discussed at length in Sec. VI. (a) $\chi = 5.0\times10^{1}$, $A\omega_{\rm pl} = 5.0\times10^{-3}$. (b) $\chi = 5.0\times10^{-1}$, $A\omega_{\rm pl} = 5.0\times10^{-3}$. (c) $\chi = 2.5\times10^{-3}$, $A\omega_{\rm pl} = 5.0\times10^{-3}$. (d) $\chi = 2.5\times10^{-3}$, $A\omega_{\rm pl} = 1.3\times10^{-2}$. (e) $\chi = 2.5\times10^{-3}$, $A\omega_{\rm pl} = 2.5\times10^{-2}$. (f) $\chi = 2.5\times10^{-3}$, $A\omega_{\rm pl} = 5.0\times10^{-2}$.

at the cusp tip, which is the most divergent part of the caustic. Quantum mechanically, the cusp is therefore associated with three-wave interference giving rise to the characteristic patterns we observe in Fig. 3, and in the more semiclassical panels in Fig. 5, which will be discussed further in Sec. VII. This highly coherent (nonergodic) dynamics is a consequence of the long-range nature of the two-body potential.

How do these semiclassical arguments fare in the deep quantum regime where quantum zero-point motion can dominate? The essential ingredient in obtaining the forced Burgers equation is the presence of two well-separated timescales. Therefore, provided $\omega_{k=\pm1} \gg \omega_{k\neq\pm1}$, the above analysis is valid with the caveat that we must include the effects of the quantum pressure. This condition is naturally satisfied provided $\chi \ll 1$, as can be clearly seen from Eq. (11). Naively, by appending the full quantum pressure to the right-hand side of Eq. (14) we find

$$\begin{aligned}\partial_\mathcal{T} u + u\partial_\theta u &= -\frac{1}{A^2}\partial_\theta[V_{\rm eff} + Q] \\ &= -\frac{1}{A^2}\partial_\theta\left[\frac{A^2\omega_1^2}{8}\cos 2\theta + \frac{\chi^2}{2}\frac{\partial_\theta^2\sqrt{\rho}}{\sqrt{\rho}}\right],\end{aligned} \tag{15}$$

while a more sophisticated analysis would subtract off the linearized part of the quantum pressure whose influence is accounted for by the Bogoliubov dispersion relation (11). Nevertheless, Eq. (15) correctly predicts the parametric competition between the quantum pressure and the classical effective potential induced by the time-averaged linear plasma oscillations.

We therefore have two distinct semiclassical limits governing the nonlinear dynamics of the HMF model. On short timescales, the condition $\chi \ll 1$ is sufficient to ensure that plasmalike oscillations occur, while the much more stringent condition that $\chi \ll 2A\omega_{\rm pl}$ is required to ensure that the quantum pressure does not disperse the bicluster. As before, such conditions can be reexpressed in terms of energetics where they assume the form

$$\begin{aligned}\left|\frac{E_Q}{U_{\rm cl}}\right| &\ll 1 \quad \text{(short times)}, \\ \left|\frac{E_Q}{\langle V_{\rm eff}\rangle_\rho}\right| &\ll 1 \quad \text{(long times)}.\end{aligned} \tag{16}$$

We emphasize that while the above analysis uses a sinusoidal velocity profile as an initial condition, the results are not overly

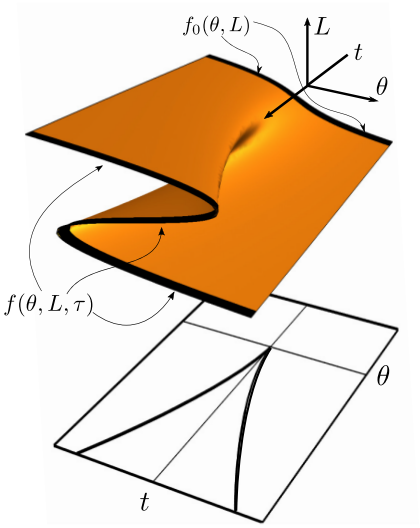

FIG. 6. The formation of a cusp catastrophe: illustration of how a line of initial data in phase space (i.e., a vanishingly thin water-bag distribution) is folded over by the dynamics. Projecting down onto the θ-t plane produces a cusp-shaped envelope on which the density of trajectories diverges. This cusp catastrophe is structurally stable against perturbations and hence occurs generically without the need for special initial conditions. In the case of the bicluster, this folding occurs simultaneously at two symmetric points around the ring.

sensitive to this choice. This parallels the classical case, where a thin, but finite, spread in the momentum of an initial water-bag distribution still leads to the clustering phenomenon discussed above. Likewise, in the quantum case, deviations from the initial conditions chosen above do not have a dramatic effect on the dynamics.

VI. NONEQUILIBRIUM PHASE DIAGRAM

We have already highlighted the fact that systems with LRI take an anomalously long time to come to equilibrium and, therefore, rather than equilibrium states, they are characterized by their QSS. This motivates the out-of-equilibrium phase diagram presented in Fig. 1 which we now explain.

The horizontal axis measures the effective Planck constant χ and the vertical axis measures the initial amplitude of the perturbation from equilibrium due to plasma oscillations. This is equivalent to a dependence on the initial energy of the system. As we are working with a closed system with conserved energy, we may interpret this behavior in the microcanonical ensemble as a proxy for temperature in the canonical ensemble. We emphasize, however, that the bicluster itself is *not* predicted by a canonical treatment, i.e., a system at equilibrium with a heat bath [74]. Rather, this behavior is inherently nonequilibrium and driven by the long-range interacting nature of the HMF model.

To distinguish the possible regimes, it useful to return to Fig. 5, where results are shown first for $A\omega_{\rm pl}$ fixed as χ is tuned [Figs. 5(a)–5(c)], and subsequently for χ fixed as $A\omega_{\rm pl}$ is tuned [Figs. 5(c)–5(f)]. In the first three figures, the most prominent feature is the changing timescale, which is a consequence of Eq. (11), and in particular the dependence of $\omega_{k=\pm1}$ on χ. Additionally, it is clear that the amplitude of modulations is dramatically different between the three figures, and this is most easily understood on energetic grounds. Initially, all three simulations have all of their energy stored as $T_{\rm cl} = \frac{1}{4}A^2\omega_{\rm pl}^2$. In each case, however, the energetic cost of density modulations is very different. In Fig. 5(a), the system behaves essentially as a free-Schrödinger equation which forms a standing wave, such that $\rho_{\rm max} \lesssim A$, while in contrast both Figs. 5(b) and 5(c) are driven at least partially by the interplay between linear plasma oscillations and nonlinear effects as evidenced by the excitation of a π-periodic density wave. The consequences are markedly different, however, in that the density modulations in Fig. 5(b) are a perturbation about a homogeneous background, whereas in Fig. 5(c) they are the $\mathcal{O}(1)$ effect that dominates the density profile, and which signals the onset of nonlinear effects.

In Figs. 5(c)–5(f), we can see the emergence of the wave version of the cusp catastrophe as $A\omega_{\rm pl}$ is made larger and larger. This enhances nonlinear effects allowing them to dominate the free-Schrödinger dispersion of the quantum pressure. Eventually, a clear bimodal cusplike profile emerges, which signals the validity of the time-averaged treatment, and by association the presence of violent relaxation.

With these features in hand, we may construct a nonequilibrium phase diagram shown in Fig. 1. Note that our initial conditions are limited to the linear regime so that two well-separated timescales exist and we can perform a multiscale analysis. The crossover between the biclustered regime and the plasma oscillation regime occurs when $\chi \approx 2A\omega_{\rm pl}$. This is predicted by Eq. (15) and confirmed by the emergence of $\mathcal{O}(1)$ density fluctuations, but the absence of interference effects, in Fig. 5(c). The crossover between the plasma-dominated and free-Schrödinger regimes is found by considering Eq. (11), and we take $\chi \approx 1$. Plotting these, as in Fig. 1, we see that the free-Schrödinger regime does not overlap with the bicluster regime for any combination of χ and $A\omega_{\rm pl}$.

VII. WAVE CATASTROPHES

The cusp-shaped caustics seen in Figs. 2 and 4 result from (imperfect) focusing of classical trajectories, and they are described by Thom's famous catastrophe theory [87–89]. The utility of this theory is that, for each dimension, structurally stable singularities only take on certain universal shapes. Structural stability implies stability against perturbations and hence these objects occur in a wide range of physical phenomena without the need for special symmetry or fine tuning. This universality also extends into the wave or quantum realm where catastrophes give rise to wave patterns known as wave catastrophes or diffraction integrals [93]. Using a path integral approach provides a rather well-defined connection between the classical and quantum dynamics which we now discuss; details can be found in Appendix E.

Catastrophes are organized into a hierarchy specified by their codimension, with the higher catastrophes containing the lower ones. The simplest is the fold which is generated by the cubic function $S_f(C_1, s) = C_1 s + s^3$, while the cusp, which is made of two folds, is generated by a quartic function $S_c(C_1, C_2; s) = C_1 s + C_2 s^2 + s^4$. The parameters $\{C_1, C_2\}$ are

known as control parameters: the fold has one, whereas the cusp has two. In the present problem these are the spatial and temporal coordinates, while the state variable s parametrizes paths (e.g., the initial angles θ_0 around the ring at $\tau = 0$, see Fig. 4 and also Appendix E). In more physical language, a generating function is an action and its saddles give rise to the classical paths via the principle of stationary action $\partial S/\partial s = 0$. Catastrophes are associated with *coalescing saddles*. The fold, being cubic, has two possible stationary points which coalesce on the caustic itself at $C_1 = 0$. The cusp has three possible stationary points: these coalesce in pairs as one crosses either of the two fold lines specified by $C_1 = \pm\sqrt{8/27}(-C_2)^{3/2}$, and the most singular point is the tip of the cusp at $C_1 = C_2 = 0$ where all three stationary points coalesce together.

The fact that a catastrophe can be expressed in terms of an action provides a route to quantization motivated by the Feynman path integral prescription. Here, one sums over all paths, not just the classical ones, and the amplitude associated with each path is $\exp(iS/\hbar)$. In this way, one obtains the wave catastrophes [93]

$$\Psi(\mathbf{C}) = \frac{1}{\sqrt{\hbar}} \int_{-\infty}^{\infty} e^{iS(\mathbf{C};\mathbf{s})/\hbar}\, d\mathbf{s}, \tag{17}$$

which are the universal wave functions replacing the divergent classical catastrophes. In the case of the fold, the cubic action gives rise to the Airy function $\mathrm{Ai}(x)$ [94]:

$$\begin{aligned}\Psi_f(C_1) &= \frac{1}{\sqrt{\hbar}} \int_{-\infty}^{\infty} e^{i(C_1 s + s^3)/\hbar}\, ds \\ &= \frac{2\pi}{3^{1/3}\hbar^{1/6}}\, \mathrm{Ai}\left(\frac{C_1}{3^{1/3}\hbar^{2/3}}\right).\end{aligned} \tag{18}$$

This implies that as $\hbar$ is varied, the overall amplitude of the fold caustic diverges as $\hbar^{-1/6}$ while the fringe spacing vanishes as $\hbar^{2/3}$. The exponent $1/6$ is known as the Arnold index and the exponent $2/3$ is known as the Berry index.

For the cusp one obtains

$$\Psi_c(C_1,C_2) = \frac{1}{\sqrt{\hbar}} \int_{-\infty}^{\infty} e^{i(C_1 s + C_2 s^2 + s^4)/\hbar}\, ds \tag{19}$$

$$= \frac{1}{\hbar^{1/4}} \mathrm{Pe}\left(\frac{C_2}{\hbar^{1/2}}, \frac{C_1}{\hbar^{3/4}}\right), \tag{20}$$

where

$$\mathrm{Pe}(a,b) = \int_{-\infty}^{\infty} e^{i(bt + at^2 + t^4)}\, dt \tag{21}$$

is the Pearcey function [115] which is a two-dimensional complex-valued function that is tabulated in mathematical handbooks [116]. We can read off the Arnold index for the cusp as being $1/4$ and the two Berry indices are $1/2$ and $3/4$. The cusp caustic generated by classical paths (obeying $\partial\Phi_c/\partial s = 0$) is plotted in Fig. 7(a) and the Pearcey function in Fig. 7(b).

By comparing Fig. 7(b) with Figs. 3, 5, and 8 we indeed identify the characteristic Pearcey pattern as must be the case on the grounds of structural stability [89]. Thus, the new length scales and timescales introduced by quantum effects in the HMF problem are of universal origin and have nontrivial scaling properties that differ from naive expectations

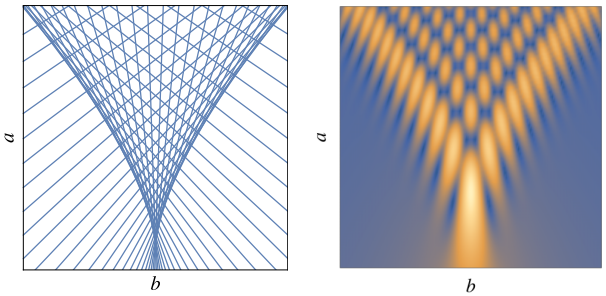

(a) Cusp catastrophe (b) Pearcey function

FIG. 7. Classical trajectories in two dimensions will generically form cusp-shaped caustics where the density of trajectories diverges, as shown in (a). In the wave or quantum theory interference removes the singularity and replaces it with a universal wave function, the Pearcey function $\mathrm{Pe}(a,b)$, which is valid in the immediate locale of the caustic. In (b) we plot $|\mathrm{Pe}(a,b)|$. Note that this function contains interesting subwavelength features such as vortices at its nodes. (a) Cusp catastrophe. (b) Pearcey function.

based on the Schrödinger equation. Replacing $\hbar$ in the above formulas by χ shows that the magnitude of the spatial density modulations scale as $|\Psi_c|^2 \sim \chi^{-1/2}$, while the length scales and timescales vary as $\sim \chi^{-3/4}$ and $\sim \chi^{-1/2}$, respectively.

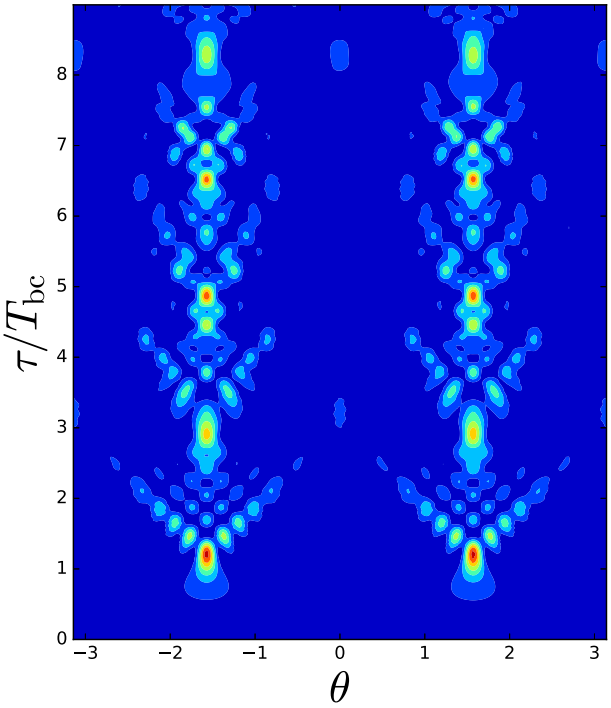

FIG. 8. Quantum biclusters: dynamics of the density profile $\rho(\theta,\tau)$ for repulsive interactions ($\epsilon > 0$) with initial conditions $\rho_0 = 1/2\pi$ and $v_0 = A\omega_{\mathrm{pl}} \cos\theta$. This simulation used $A\omega_{\mathrm{pl}} = 0.01$, $\chi = 0.005$, and included Fourier components up to $k_{\max} = 58$. The timescale is in units of the classical bicluster formation time $T_{\mathrm{bc}} = \mathcal{O}([A\omega_{\mathrm{pl}}]^{-1})$ which is two orders of magnitude larger than the inverse plasma frequency $\omega_{\mathrm{pl}}^{-1}$ relevant in the attractive case.

These results hold close to the origin of each cluster; further away nonuniversal effects creep in (finite system size and interference between Pearcey functions). In particular, in Fig. 8 we see well-defined Pearcey functions at the first clustering events but as time progresses the interference patterns become altered, which occurs both because of interference with the tails of the earlier Pearcey functions and also because the underlying classical cusps become narrower with time [76].

VIII. COMMUTATIVITY OF THE THERMODYNAMIC AND CLASSICAL LIMITS

The noncommutativity of the $N \to \infty$ and $t \to \infty$ limits for systems with LRIs is well known [117], and gives rise to the characteristic feature that if $N \to \infty$ first a nonequilibrium state will never relax to Maxwell-Boltzmann equilibrium. Furthermore, in single-particle quantum mechanics there is an analogous situation for the $\hbar \to 0$ and $t \to \infty$ limits, such that completely different results are obtained in the semiclassical and adiabatic limits [118] and also in quantum systems whose classical limit is chaotic [119]. We shall now discuss whether the $N \to \infty$ and $\hbar \to 0$ limits commute in order to complete the final link between these three important limits.

A significant hint comes from comparing the classical and quantum Euler equations [Eqs. (3) and (7), respectively] and noting that the former is obtained from the full Vlasov equation (2) via the zero-temperature approximation. The zero-temperature approximation ignores thermal fluctuations of the momentum $f(\theta, L) \approx \rho(\theta)\delta[v(\theta) - L]$ and hence gives rise to a well-defined velocity profile v. The same effect is realized in the quantum case by a different mechanism: BEC gives rise to a well-defined phase $S(\theta)$ and hence a well-defined velocity profile via $v = \partial_\theta S$. In the limit $\chi \to 0$ of Eq. (7) we obtain exactly the classical Euler equations (3).

This is interesting because for finite time, the classical equations of motion provide an exact description of a quantum system in the $\hbar \to 0$ limit [119], while the Vlasov equation (2), which is a mean field approximation at finite N, provides an exact description of the classical dynamics in the thermodynamic ($N \to \infty$) limit [102]. Additionally, motivated by work on boson stars [111], Chavanis has argued that Eq. (6) is exact in the thermodynamic limit [104], presumably when restricted to Bose-condensed initial conditions.

Considering a generic quantum state as an initial condition leads to a noncommutativity of limits as illustrated in Fig. 9. In particular, taking the classical limit $\hbar \to 0$, followed by the thermodynamic limit $N \to \infty$, leads to an exact description in terms of the full Vlasov equation. By contrast, if the GGPE captures the leading order behavior in the $N \to \infty$ limit, at least for initially Bose-condensed states, then the Euler equations are obtained; these are only a particular (zero-temperature) limit of the Vlasov equation. This suggests that the recovery of the full Vlasov equation requires features beyond the GGPE, the most obvious of which are phase fluctuations. We note in this context that Chavanis has proposed using the Wigner function to obtain a more complete description of the quantum dynamics [120].

Finally, we note that both $\chi \to 0$ and $N \to \infty$ both cause the density of states of the full quantum many-body spectrum to diverge, and so may be expected to yield similar results.

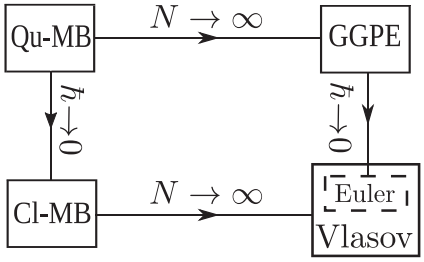

FIG. 9. Schematic depiction of noncommutativity of the thermodynamic $N \to \infty$, and classical $\hbar \to 0$ limits for the finite time dynamics of pure quantum states. The sequence $\hbar \to 0$ followed by $N \to \infty$ takes us from the quantum to classical many-body descriptions and then to the Vlasov equation which gives an exact description of the classical dynamics in the thermodynamic limit. Conversely, if the GGPE captures the leading order dynamical behavior in the thermodynamic limit, then the sequence $N \to \infty$ followed by $\hbar \to 0$ leads to the classical Euler equations, which emerge from the Vlasov equation in the zero-temperature approximation.

The interplay between the three limits $\hbar \to 0$, $t \to \infty$, and $N \to \infty$ for long-range interacting systems is an interesting, and to the authors' knowledge open, problem, and is an obvious avenue of investigation for quantum QMB systems with LRI in general. Its resolution may help shed light on what lessons learned from the study of classical systems with LRI can be carried over into the quantum regime.

IX. CONCLUSIONS AND FUTURE PROSPECTS

Motivated by ongoing success in the laboratory creating atomic and molecular systems with LRI, we have made a preliminary study of violent relaxation in a quantum system. This nonergodic dynamical process is a signature of LRI and leads to the formation of slowly evolving patterns with rich and universal structure rather than to the more standard featureless equilibrium state. Although we investigated the dynamics in a specific model, namely, the HMF model, it is known to reproduce many of the generic features of many-body systems with LRI.

By choosing initial conditions whose long-time propagation is well understood in the classical limit, we were able to isolate the role played by the quantum pressure in modifying the dynamics. The consequences for attractive interactions ($\epsilon < 0$) are fairly straightforward; whereas the classical self-focusing forms cusp-shaped caustics in the θ-τ plane where the density diverges, these are replaced by smooth but oscillating Pearcey wave catastrophes in the quantum dynamics. Similar structures have been seen (although they are often not identified as wave catastrophes) in other studies on condensates, both theoretical and experimental, such as BECs hitting obstacles [121], atom optics with BECs [122–124], and self-trapping in polariton BECs [84]. The underlying connection is nonergodic dynamics. Indeed, wave catastrophes are expected to be a universal feature of quantum dynamics in mean field or close to mean field regimes [125], and more rigorous mathematical analysis of nonlinear Schrödinger equations demonstrates this to be true provided the nonlinearity obeys certain constraints [126–128]. A key implication of the appearance of wave

catastrophes in the present problem is the emergence of new spatial and temporal scales that are not present in the classical problem and which scale in a nontrivial way as the effective Planck's constant χ is varied.

The repulsive ($\epsilon > 0$) dynamics also features cusp caustics although in this case the cusps come in pairs, or biclusters, and the timescale for their formation is generally much longer than in the attractive case. The bicluster has special significance because it is an example of a QSS, i.e., a slowly evolving nonequilibrium state that is a paradigm of LRI. As in the attractive case, the biclusters are smoothed by interference and become Pearcey functions. Deeper in the quantum regime, zero-point motion becomes dominant and also shifts the timescales for cluster formation and can even stabilize some states against clustering. The bicluster is more sensitive to quantum pressure than the attractive monocluster and the reduced Planck's constant χ must be surprisingly small before classical behavior emerges; specifically, the long-time criterion is given by $\chi \ll A\omega_{\rm pl}$, where $A\omega_{\rm pl}$ is the amplitude of the velocity fluctuations ("plasma" waves) in the initial state. At zero temperature, one can construct a nonequilibrium phase diagram characterizing the QSS as a function of just χ and $A\omega_{\rm pl}$ which are the two dimensionless quantities specifying the problem.

In addition to investigating the dynamics, we point out that there is a lack of commutation between the thermodynamic ($N \to \infty$) and classical ($\chi \to 0$) limits. Performing the $\chi \to 0$ limit first and then $N \to \infty$ leads to the Vlasov equation, whereas the opposite order leads to the Euler equations. The latter equations are a special case of the former, corresponding to the zero-temperature limit. We hope that in the future someone will take up the challenge this presents by including non-mean-field quantum states that go beyond the Gross-Pitaevskii theory (at least for finite N) and thus examine the implications this has for thermalization.

The HMF model provides a simple arena in which to investigate the essential features of LRI. Atoms trapped in optical cavities come close to realizing the HMF model [60] and display a symmetry breaking transition from a homogeneous to an ordered density [54–62] that has been observed experimentally [32] and which is essentially the same phenomenon as clustering. Although the atom-cavity system is intrinsically open, and hence includes noise and friction, it would be interesting to see if there are regimes, e.g., in very high-finesse cavities, where quantum pressure can dominate other sources of noise and stabilize the system against ordering. Another possible realization of this work is in "closed" XY-type spin models such as those that can be realized with cold Rydberg gases and ensembles of polar molecules [97–99]. Although the interactions in these systems are not infinite ranged, they can easily extend over the entire sample. Yet another quantum system with LRI, perhaps the most advanced from the experimental point of view [1–12], are dipolar BECs. The collapse instability has already been observed in these "quantum ferrofluids" [3,4], but it would be interesting to see whether they also display violent relaxation in a geometry where the interactions are predominantly repulsive.

We close by emphasizing that the wave catastrophes (Pearcey functions) studied in this paper are universal features of dynamics. They obey self-similar scaling laws and can therefore be regarded as nonequilibrium generalizations of phase transitions [125,129]. We hope to expand on this line of inquiry in the future, both for short- and long-range interacting systems.

ACKNOWLEDGMENTS

We gratefully acknowledge G. Morigi for bringing the HMF model to our attention, and Y. Levin and J. Barré for helping us understand its classical dynamics. Useful insights from both Y.L. and J.B. were made possible by interactions at ICTP, and both D.O. and R.P. thank them for their hospitality. We also thank R. Dingwall for useful comments on our manuscript, and the OIST school on coherent quantum dynamics which facilitated our interaction. This research was funded by the Natural Sciences and Engineering Research Council of Canada (NSERC) and the Government of Ontario.

APPENDIX A: SINUSOIDAL MEAN FIELD POTENTIAL

In Sec. II we claim that $\Phi(\theta,\tau)$ always takes the form of a sinusoid. This result may seem remarkable at first glance but in fact follows from a well-known and very simple result. Expanding $\rho(\theta,\tau) = \sum_k \hat{\rho}_k(\tau)e^{ik\theta}$, and writing $\Phi(\theta,\tau) = \mathrm{Re}\int_{-\pi}^{\pi} \rho(\phi,\tau)e^{i(\theta-\phi)}d\theta$ one can easily see that $\Phi(\theta,\tau) = 2\pi\,\mathrm{Re}\hat{\rho}_1(\tau)e^{i\theta}$. In general, $\hat{\rho}_k(\tau) = M(\tau)e^{i\varphi(\tau)}$, where $M(\tau)$ and $\varphi(\tau)$ are two real-valued functions determined by solving for the evolution of the full density profile $\rho(\theta,\tau)$. Simple algebra yields

$$\Phi(\theta,\tau) = M(\tau)\cos[\theta - \varphi(\tau)] \tag{A1}$$

as claimed in the main text. This derivation applies to both the quantum and classical Euler equations and can be easily extended to the Vlasov equation by treating a generic phase space density $f(\theta,L,\tau)$ as a linear combination of zero-temperature ones.

APPENDIX B: VALIDITY OF THE GROSS-PITAEVSKII TREATMENT

It is often stated that Bose condensation in one-dimensional systems is forbidden due to phase fluctuations, even at zero temperature [109]. Formally, Bose condensation implies spontaneous symmetry breaking of the global, and continuous, U(1) symmetry which can be expressed in terms of the field operator as $\hat{\Psi} \to e^{i\theta}\hat{\Psi}$, and according to the Mermin-Wagner theorem [107,108], symmetry breaking is forbidden in one-dimensional systems. However, this theorem does not apply in finite systems such as a ring of finite radius R where the long wavelength fluctuations which destroy the condensate are cut off by the finite system size. Furthermore, the Mermin-Wagner theorem assumes short-range interactions and so it does not apply in the presence of LRIs, as evidenced by the fact that the one-dimensional HMF model, quantum or classical, exhibits critical phenomena such as the paramagnetic-ferromagnetic transition [74].

In typical atomic gases the interatomic potential $V(\mathbf{r} - \mathbf{r}')$ is deep and falls off asymptotically as r^{-6}, being of the isotropic van der Waals type, which is considered short range from a statistical mechanics point of view [130]. In

order to provide a low energy description consistent with the Hartree approximation, $V(\mathbf{r}-\mathbf{r}')$ must be replaced by a pseudopotential $g\delta(\mathbf{r}-\mathbf{r}')$, where $g = 4\pi\hbar^2 a_s/m$, a_s being the s-wave scattering length [131]. This reduces the integral in Φ to a purely local nonlinearity $\propto|\Psi|^2$ such that the equation of motion for Ψ becomes the usual Gross-Pitaevskii equation [105,106]. By contrast, if the potential is long ranged and gently varying, like the sinusoidal potential in the HMF model, it is neither necessary nor possible to replace it by a δ-function pseudopotential and one instead retains the integral in Φ. The Gross-Pitaevskii equation then takes the form of the integrodifferential equation, or GGPE, given in Eq. (6). This form of GGPE has previously been successfully employed to treat dipolar Bose gases [132–134] and has been rigorously justified in Ref. [112].

In the presence of long-range interactions, it is the high-density regime where Gross-Pitaevskii theory applies. A classic example of this is the charged Bose gas where the criterion for weak correlation is $a_0(N/V)^{1/3} \gg 1$, where $a_0 = 4\pi\epsilon_0\hbar^2/mq^2$ is the Bohr radius associated with the Coulomb interaction between particles of charge q [110]. In other words, the interactions are weak if the Bohr radius is large in comparison to the interparticle spacing. A related problem is provided by boson stars where rigorous analysis has demonstrated that the ground state energy asymptotes to the Hartree value in the thermodynamic limit [111]. The high density regime is realized naturally in the $N\to\infty$ limit, and so it is reasonable to assume that a Gross-Pitaevskii treatment is justified for a system of indistinguishable bosons interacting via LRI.

APPENDIX C: NUMERICAL METHOD

To solve the evolution of the GGPE we use the momentum space representation of Eq. (C1):

$$i\chi\partial_\tau a_k = \frac{\chi^2}{2}k^2 a_k + \mathrm{sgn}(\epsilon)\Phi_{kk'}a_{k'} := \widetilde{H}_{kk'}a_{k'}, \quad \text{(C1a)}$$

$$\Phi_{kk'} = \frac{1}{2}(\mathbf{M}\delta_{k+1,k'} + \mathbf{M}^*\delta_{k,k'+1}), \quad \text{(C1b)}$$

$$\mathbf{M} = \sum_{k\in\mathbb{Z}} a_k^* a_{k+1} = \int_{-\pi}^{\pi} |\Psi(\tau,\theta)|^2 e^{i\theta}d\theta. \quad \text{(C1c)}$$

This approach is advantageous because, unlike a generic two-body potential, the cosine potential only couples adjacent momentum modes. This leads to a tridiagonal pseudo-Hamiltonian $\widetilde{H}_{kk'}(\tau)$ defined in Eq. (C1a), whose time dependence is inherited from the evolution of the order parameter by way of the mean field potential. The pseudo-Hamiltonian is truncated at $\pm k_{\max}$ and a second-order implicit integration scheme based on the Dyson series (described below) is used to evolve forward in time.

Given some state $a_k(\tau_n)$ and time τ_n we first define a time evolution operator $U_{kk'}[\tau_n,\Delta\tau]$ given explicitly by

$$U(\tau_n,\Delta\tau) = 1 - i\Delta\tau\widetilde{H}_{kk'}(\tau_n), \quad \text{(C2)}$$

where $\widetilde{H}_{kk'}$ is the pseudo-Hamiltonian appearing in Eq. (C1) and the time step is sufficiently small so as not to invalidate Von Neumann error analysis (i.e., $\Delta\tau < 1/2k_{\max}^2$). The zeroth order approximation of $a_k(\tau_{n+1})$ is taken to be

$$a_k^{(0)}(\tau_{n+1}) = U_{kk'}(\tau_n,\Delta_\tau)a_{k'}(\tau_n). \quad \text{(C3)}$$

Proceeding iteratively, the mth approximation is found by solving the equation

$$U_{kk'}^{(m-1)}\left(\tau_{n+1}, -\frac{\Delta\tau}{2}\right)a_{k'}^{(m)}(\tau_{n+1}) = U_{kk'}\left(\tau_n,\frac{\Delta\tau}{2}\right)a_{k'}(\tau_n), \quad \text{(C4)}$$

where $U^{(m-1)}$ uses the $(m-1)$th approximation of $a_k(\tau_{n+1})$. This process is repeated until the overlap between successive states is unity within one part per million. Explicit schemes were also tested, and were found to give monotonically increasing error in the norm of Ψ; successful simulation of long-time behavior considered in this paper (i.e., bicluster) requires an implicit scheme.

Finally, we note that to simulate the semiclassical behavior of the bicluster, it is necessary to include an unexpectedly large number of Fourier components. This is related to representing the small amplitude plasma wave $v = A\omega_{\mathrm{pl}}\sin\theta$ in the GGPE form. In particular, one must Taylor expand $\exp[iS/\chi]$. Since $v = \partial_\theta S$ we have $S = \mathcal{O}(A\omega_{\mathrm{pl}})$. As is discussed in the main text, classical-like behavior emerges when $A\omega_{\mathrm{pl}}/\chi \gg 1$, and to obtain an accurate approximation of the wave function's Fourier transform requires that $(A\omega_{\mathrm{pl}})^{k_{\max}}/(k_{\max}!) \ll 1$ where $k_{\max}$ is the largest Fourier component in the simulation.

APPENDIX D: CLASSICAL DESCRIPTION OF THE FORMATION OF THE BICLUSTER

For repulsive interactions, linearized dynamics describing $\{\hat{v}_{|k|=1},\hat{\rho}_{|k|=1}\}$ are oscillatory; following Ref. [76] we refer to this excitation as a plasma wave. For the initial conditions we choose $v_1(\theta,0) = A\omega_{\mathrm{pl}}\cos\theta$ and $\rho(\theta,0) = 1/2\pi$, where $A \ll 1$, corresponding to a uniform density plus a small position-dependent velocity modulation $v_1(\theta) = A\omega_{\mathrm{pl}}\cos\theta$. In direct analogy with Eq. (11), the solutions to the linearized equations of motion with these initial conditions are [76]

$$\rho_1 = -\frac{A}{2\pi}\sin(\omega_{\mathrm{pl}}\tau)\sin\theta,\ v_1 = A\,\omega_{\mathrm{pl}}\cos(\omega_{\mathrm{pl}}\tau)\cos\theta, \quad \text{(D1)}$$

where $\omega_{\mathrm{pl}} := \omega_1 = 1/\sqrt{2}$ denotes the plasma wave's frequency. As will be shown below, unlike for attractive interactions, the formation of the bicluster is not driven directly by the rapidly oscillating mean field potential, but rather by a slowly evolving effective potential V_{eff} induced by time-averaged linear plasma oscillations.

As we first saw in Fig. 2, the bicluster forms very slowly in comparison to the plasma period and this suggests a multiple scales analysis [76]. Consequently, we consider $v(\theta,\tau) = v_1(\theta,\tau) + Au(\theta,\mathcal{T})$ where $\mathcal{T} = A\tau$ is $\mathcal{O}(1)$ when the fast time τ is $\mathcal{O}(1/A\omega_{\mathrm{pl}})$; note this hierarchy is only present for $A \ll 1$. Inserting this expression into Eq. (3b), and averaging over

many plasma oscillations, leads us to

$$A^2\partial_{\mathcal{T}}u - \underbrace{\frac{\omega_{\rm pl}^2A^2}{2}\sin(2\theta)\,\cos^2(\omega_{\rm pl}\tau)}_{v_1\partial_\theta v_1} + A^2u\partial_\theta u + \omega_{\rm pl}^2A^2[\cos\theta\partial_\theta u - u\sin\theta]\cos(\omega_{\rm pl}\tau) = \underbrace{\int_{-\pi}^{\pi}\rho(\theta',\tau)\sin(\theta-\theta')d\theta' - \frac{\partial v_1}{\partial\tau}}_{\mathcal{L}}$$

$$\text{time averaged} \Rightarrow \partial_{\mathcal{T}}u + u\partial_\theta u = -\langle v_1\partial_\theta v_1\rangle_{\mathcal{T}} := -\frac{1}{A^2}\partial_\theta V_{\rm eff}(\theta) \quad \text{where} \quad V_{\rm eff}(\theta) = \left[\frac{A^2\omega_{\rm pl}^2}{8}\cos 2\theta\right]. \tag{D2}$$

In going from the first line to second line, we have used the fact that the convolution on the right-hand side depends only on the first Fourier component of the density $\hat{\rho}_{k=\pm1}$ and consequently the quantity $\mathcal{L}$ vanishes at all times [135] because it satisfies the linearized equations of motion. This gives a remarkably simple result [75,76]: the slow velocity field $u(\theta,\mathcal{T})$ obeys a Euler equation driven by $V_{\rm eff}(\theta)$ [compare with Eq. (3b), the original Euler equation obeyed by the full velocity field]. $V_{\rm eff}$ is derived from the square of the plasma wave and hence corresponds to a potential with two minima around the ring, giving rise to two symmetric clustering points. Furthermore, there is negligible back-action on the plasma wave by the slow dynamics: $V_{\rm eff}$ is invariant under $\theta \to \theta+\pi$, and consequently only influences $\hat{\rho}_k$ and $\hat{v}_k$ for k even. We therefore expect the linear dynamics of the first Fourier component to continue to be a good approximation even at late times.

The first appearance of the bicluster state can be estimated by considering Eq. (D2), whose characteristics are Jacobi elliptic functions. Near a minimum of $V_{\rm eff}$ these are approximately cosine functions, and we can approximate $V_{\rm eff} \approx \frac{A^2\omega_{\rm pl}^2}{4}(\theta-\theta_{\rm min})^2$. This identifies the frequency of the bicluster oscillation in the original fast time coordinate as $\omega_{\rm eff} = A\omega_{\rm pl}/\sqrt{2}$. Consequently, the first bicluster will appear at one quarter the oscillator period $T_{\rm bc} = \pi/2\omega_{\rm eff} = \pi/\sqrt{2}A\omega_{\rm pl}$ [76].

APPENDIX E: UNIVERSALITY IN SELF-FOCUSING

Pearcey functions can be expected as a generic consequence of self-focusing in coherent quantum systems. The reasons behind this are most easily understood in the case of linear wave equations, however, the same underlying ideas generalize for sufficiently weak nonlinear effects. Importantly, the HMF model's nonlinearity acts essentially as a linear, albeit time-dependent, background potential, which is relatively insensitive to the local structure of the wave function, and therefore its dynamics is well modeled by linear theory.

First, let us consider the one-dimensional linear Schrödinger equation

$$i\hbar\partial_t\psi = -\frac{\hbar^2}{2}\partial_x^2\psi + V(x)\psi, \tag{E1}$$

with initial data $\psi(x,0) = \psi_0(x) = A(x)\exp[i\varphi(x)/\hbar]$. The solutions of this equation may be expressed via the integral equation

$$\psi(x,t) = \int dx' K(x';x,t)\psi_0(x') = f(t)\int dx' A(x')e^{i[S_{\rm cl}(x';x,t)+\phi(x')]/\hbar}, \tag{E2}$$

where we have used the fact that the propagator may be expressed in terms of the classical action via $K(x';x,t) = f(t)\exp[iS_{\rm cl}(x';x,t)/\hbar]$ [136]. In the limit that $\hbar\to0$, the above integral is dominated by the stationary points (with respect to x') of what we will now refer to as the generating function $\Phi = S_{\rm cl}+\phi$.

The integral in Eq. (E2) is over all paths labeled by their initial positions x' (see Fig. 4 for an illustration of the paths.) We interpret x and t as *control parameters* of the function $\Phi(x';x,t)$, and for a given choice of x and t we can generically expect the stationary points of Φ to be locally quadratic in x'. If, however, we consider *all* values of x and t, then it is generic that pairs of stationary points will coalesce leaving the function Φ looking locally cubic (hereafter referred to as a fold), and furthermore these cubic points may coalesce to give locally quartic behavior $\Phi\propto(x'-y')^4$ (hereafter referred to as a cusp). Remarkably, it is *not* generic that these quartic points may coalesce when one varies two control parameters (in this case x and t) [89], and therefore these three possibilities (saddle, fold, cusp) are exhaustive in a two-dimensional control space.

The coalescing of saddles is in direct correspondence with self-focusing behavior in the classical dynamics. This can be understood as follows: a saddle represents a classical trajectory, and a coalescing of saddles represents the focusing of two trajectories. Catastrophe theory guarantees us that when focusing occurs in a two-dimensional control space, we need only consider folds and cusps. In an associated wave theory such as the HMF model's GGPE, this structure is inherited via an Airy and Pearcey function structure, respectively.

This can be understood by taking Eq. (E2) and transforming the control variables $(x,t)\to(C_1,C_2)$ and introducing $s = (\kappa/\hbar)^{1/4}(x'-y')$ (where $\kappa = \Phi^{(4)}|_{y'}/4!$) such that $\Phi(s;y,\tau)$ assumes its *normal form* [137]. For the cusp catastrophe this is $\Phi(s;C_1,C_2) = \hbar(s^4+C_2s^2+C_1s)$ and this form is valid when the control parameters (C_1,C_2) [or equivalently (x,t)] are close to the cusp point or fold line. One can then expand $A(x')$ about $s=0$ and assuming that $A(x') = A_0+\mathcal{O}(s)$, and likewise that $f(t)\approx f_0$ in the vicinity of the cusp this leads to the local form of the wave function [116]

$$\psi(C_1,C_2) \sim f_0A_0\left(\frac{\kappa}{\hbar}\right)^{1/4}\int ds\exp[i(s^4+C_2s^2+C_1s)] = f_0A_0\left(\frac{\kappa}{\hbar}\right)^{1/4}\mathrm{Pe}(C_2,C_1). \tag{E3}$$

Similar considerations give Airy functions in coordinates perpendicular to the fold lines.

Importantly, wave catastrophes are *robust* against both perturbations in the initial data, and the precise details of the

wave equation. This is the statement of structural stability upon which catastrophe theory is built. This provides a justification for identifying the structures in Figs. 3, 5(e), 5(f), and 8 as Pearcey functions, and this claim is further vindicated by the fact that in the classical theory these same structures are well understood to result from the pileup of trajectories.

Finally, we comment on the robustness of these caustic structures even in the presence of stronger local nonlinearities such as in the GPE. One might expect that the universality discussed above would be destroyed by a term such as $|\psi|^2\psi$ since $|\psi|^2 \sim \mathcal{O}(1/\sqrt{\hbar})$ near a cusp point. Surprisingly, however, rigorous mathematical studies have demonstrated that even in this case the linear theory presented above is trustworthy in the vicinity of the caustic for surprisingly large nonlinearities. This is true both for Airy-function behavior near a fold catastrophe [126,128], and Pearcey-function behavior near a cusp catastrophe [127]. The fact that these structures are robust, even against a local nonlinearity suggests, that linear analysis should certainly hold for the much milder nonlocal GGPE employed in this work.

---

[1] A. Griesmaier, J. Werner, S. Hensler, J. Stuhler, and T. Pfau, Phys. Rev. Lett. **94**, 160401 (2005).

[2] T. Lahaye, T. Koch, B. Fröhlich, M. Fattori, J. Metz, A. Griesmaier, S. Giovanazzi, and T. Pfau, Nature (London) **448**, 672 (2007).

[3] T. Lahaye, J. Metz, B. Fröhlich, T. Koch, M. Meister, A. Griesmaier, T. Pfau, H. Saito, Y. Kawaguchi, and M. Ueda, Phys. Rev. Lett. **101**, 080401 (2008).

[4] T. Koch, T. Lahaye, J. Metz, B. Fröhlich, A. Griesmaier, and T. Pfau, Nat. Phys. **4**, 218 (2008).

[5] Q. Beaufils, R. Chicireanu, T. Zanon, B. Laburthe-Tolra, E. Marèchal, L. Vernac, J.-C. Keller, and O. Gorceix, Phys. Rev. A **77**, 061601(R) (2008).

[6] M. Lu, N. Q. Burdick, S. H. Youn, and B. L. Lev, Phys. Rev. Lett. **107**, 190401 (2011).

[7] B. Pasquiou, G. Bismut, E. Marèchal, P. Pedri, L. Vernac, O. Gorceix, and B. Laburthe-Tolra, Phys. Rev. Lett. **106**, 015301 (2011).

[8] K. Aikawa, A. Frisch, M. Mark, S. Baier, A. Rietzler, R. Grimm, and F. Ferlaino, Phys. Rev. Lett. **108**, 210401 (2012).

[9] H. Kadau, M. Schmitt, M. Wenzel, C. Wink, T. Maier, I. Ferrier-Barbut, and T. Pfau, Nature (London) **530**, 194 (2016).

[10] I. Ferrier-Barbut, H. Kadau, M. Schmitt, M. Wenzel, and T. Pfau, Phys. Rev. Lett. **116**, 215301 (2016).

[11] L. Chomaz, R. M. W. van Bijnen, D. Petter, G. Faraoni, S. Baier, J. H. Becher, M. J. Mark, F. Wächtler, L. Santos, and F. Ferlaino, Nat. Phys. **14**, 442 (2018).

[12] M. Wenzel, F. Böttcher, T. Langen, I. Ferrier-Barbut, and T. Pfau, Phys. Rev. A **96**, 053630 (2017).

[13] A. Chotia, B. Neyenhuis, S. A. Moses, B. Yan, J. P. Covey, M. Foss-Feig, A. M. Rey, D. S. Jin, and J. Ye, Phys. Rev. Lett. **108**, 080405 (2012).

[14] B. Yan, S. A. Moses, B. Gadway, J. P. Covey, K. R. A. Hazzard, A. M. Rey, D. S. Jin, and J. Ye, Nature (London) **501**, 521 (2013).

[15] M. J. Martin, M. Bishof, M. D. Swallows, X. Zhang, C. Benko, J. von Stecher, A. V. Gorshkov, A. M. Rey, and J. Ye, Science **341**, 632 (2013).

[16] K. R. A. Hazzard, B. Gadway, M. Foss-Feig, B. Yan, S. A. Moses, J. P. Covey, N. Y. Yao, M. D. Lukin, J. Ye, D. S. Jin, and A. M. Rey, Phys. Rev. Lett. **113**, 195302 (2014).

[17] P. Richerme, A. Lee, C. Senko, J. Smith, M. Foss-Feig, S. Michalakis, A. V. Gorshkov, and C. Monroe, Nature (London) **511**, 198 (2014).

[18] S. A. Moses, J. P. Covey, M. T. Miecnikowski, B. Yan, B. Gadway, J. Ye, and D. S. Jin, Science **350**, 659 (2015).

[19] K. Kim, M.-S. Chang, R. Islam, S. Korenblit, L.-M. Duan, and C. Monroe, Phys. Rev. Lett. **103**, 120502 (2009).

[20] J. W. Britton, B. C. Sawyer, A. C. Keith, C.-C. J. Wang, J. K. Freericks, H. Uys, M. J. Biercuk, J. J. John, and J. Bollinger, Nature (London) **484**, 489 (2012).

[21] S. Korenblit, D. Kafri, W. C. Campbell, R. Islam, E. E. Edwards, Z.-X. Gong, G.-D. Lin, L.-M. Duan, J. Kim, K. Kim, and C. Monroe, New J. Phys. **14**, 095024 (2012).

[22] R. Islam, C. Senko, W. Campbell, S. Korenblit, J. Smith, A. Lee, E. E. Edwards, C.-C. J. Wang, J. K. Freericks, and C. Monroe, Science **340**, 583 (2013).

[23] R. Heidemann, U. Raitzsch, V. Bendkowsky, B. Butscher, R. Löw, L. Santos, and T. Pfau, Phys. Rev. Lett. **99**, 163601 (2007).

[24] D. Comparat and P. Pillet, J. Opt. Soc. Am. B **27**, A208 (2010).

[25] A. Schwarzkopf, R. E. Sapiro, and G. Raithel, Phys. Rev. Lett. **107**, 103001 (2011).

[26] P. Schauß, M. Cheneau, M. Endres, T. Fukuhara, S. Hild, A. Omran, T. Pohl, C. Gross, S. Kuhr, and I. Bloch, Nature (London) **491**, 87 (2012).

[27] G. Günter, H. Schempp, M. Robert-de Saint-Vincent, V. Gavryusev, S. Helmrich, C. Hofmann, S. Whitlock, and M. Weidemüller, Science **342**, 954 (2013).

[28] H. Schempp, G. Günter, S. Wüster, M. Weidemüller, and S. Whitlock, Phys. Rev. Lett. **115**, 093002 (2015).

[29] D. Barredo, H. Labuhn, S. Ravets, T. Lahaye, A. Browaeys, and C. S. Adams, Phys. Rev. Lett. **114**, 113002 (2015).

[30] H. Labuhn, D. Barredo, S. Ravets, S. De Léséleuc, T. Macrì, T. Lahaye, and A. Browaeys, Nature (London) **534**, 667 (2016).

[31] A. T. Black, H. W. Chan, and V. Vuletić, Phys. Rev. Lett. **91**, 203001 (2003).

[32] K. Baumann, C. Guerlin, F. Brennecke, and T. Esslinger, Nature (London) **464**, 1301 (2010).

[33] R. Mottl, F. Brennecke, K. Baumann, R. Landig, T. Donner, and T. Esslinger, Science **336**, 1570 (2012).

[34] R. Landig, F. Brennecke, R. Mottl, T. Donner, and T. Esslinger, Nat. Commun. **6**, 7046 (2015).

[35] R. Landig, L. Hruby, N. Dogra, M. Landini, R. Mottl, T. Donner, and T. Esslinger, Nature (London) **532**, 476 (2016).

[36] J. Lèonard, A. Morales, P. Zupancic, T. Esslinger, and T. Donner, Nature (London) **543**, 87 (2017).

[37] J. S. Douglas, H. Habibian, C.-L. Hung, A. V. Gorshkov, H. J. Kimble, and D. E. Chang, Nat. Photonics **9**, 326 (2015).

[38] A. Gonzàlez-Tudela, C. L. Hung, D. E. Chang, J. I. Cirac, and H. J. Kimble, Nat. Photonics **9**, 320 (2015).

[39] E. Shahmoon, P. Grišins, H. P. Stimming, I. Mazets, and G. Kurizki, Optica **3**, 725 (2016).

[40] D. Porras and J. I. Cirac, Phys. Rev. Lett. **92**, 207901 (2004).
[41] S. Gopalakrishnan, B. L. Lev, and P. M. Goldbart, Phys. Rev. Lett. **107**, 277201 (2011).
[42] K. R. A. Hazzard, S. R. Manmana, M. Foss-Feig, and A. M. Rey, Phys. Rev. Lett. **110**, 075301 (2013).
[43] P. Hauke and L. Tagliacozzo, Phys. Rev. Lett. **111**, 207202 (2013).
[44] J. Eisert, M. van den Worm, S. R. Manmana, and M. Kastner, Phys. Rev. Lett. **111**, 260401 (2013).
[45] J. Schachenmayer, B. P. Lanyon, C. F. Roos, and A. J. Daley, Phys. Rev. X **3**, 031015 (2013).
[46] T. Graß and M. Lewenstein, EPJ Quantum Technol. **1**, 8 (2014).
[47] R. M. W. van Bijnen and T. Pohl, Phys. Rev. Lett. **114**, 243002 (2015).
[48] M. F. Maghrebi, Z.-X. Gong, and A. V. Gorshkov, Phys. Rev. Lett. **119**, 023001 (2017).
[49] J. Zeiher, R. van Bijnen, P. Schauß, S. Hild, J. Choi, T. Pohl, I. Bloch, and C. Gross, Nat. Phys. **12**, 1095 (2016).
[50] A. W. Glaetzle, R. M. W. van Bijnen, P. Zoller, and W. Lechner, Nat. Commun. **8**, 15813 (2017).
[51] D. O'Dell, S. Giovanazzi, G. Kurizki, and V. M. Akulin, Phys. Rev. Lett. **84**, 5687 (2000).
[52] S. Giovanazzi, G. Kurizki, I. E. Mazets, and S. Stringari, Europhys. Lett. **56**, 1 (2001).
[53] G. Kurizki, S. Giovanazzi, D. O'Dell, and A. I. Artemiev, in *Dynamics and Thermodynamics of Systems with Long Range Interactions*, Lecture Notes in Physics (Springer, Berlin, 2002), pp. 369–403.
[54] P. Domokos, P. Horak, and H. Ritsch, J. Phys. B: At., Mol. Opt. Phys. **34**, 187 (2001).
[55] P. Domokos and H. Ritsch, Phys. Rev. Lett. **89**, 253003 (2002).
[56] J. K. Asbóth, P. Domokos, H. Ritsch, and A. Vukics, Phys. Rev. A **72**, 053417 (2005).
[57] D. Nagy, G. Kónya, G. Szirmai, and P. Domokos, Phys. Rev. Lett. **104**, 130401 (2010).
[58] J. Keeling, M. J. Bhaseen, and B. D. Simons, Phys. Rev. Lett. **105**, 043001 (2010).
[59] H. Ritsch, P. Domokos, F. Brennecke, and T. Esslinger, Rev. Mod. Phys. **85**, 553 (2013).
[60] S. Schütz and G. Morigi, Phys. Rev. Lett. **113**, 203002 (2014).
[61] S. Schütz, S. B. Jäger, and G. Morigi, Phys. Rev. Lett. **117**, 083001 (2016).
[62] T. Keller, V. Torggler, S. B. Jäger, S. Schütz, H. Ritsch, and G. Morigi, New J. Phys. **20**, 025004 (2018).
[63] J. Binney and S. Tremaine, *Galactic Dynamics* (Princeton University Press, Princeton, NJ, 2011), pp. 289–291.
[64] D. Lynden-Bell, Mon. Not. R. Astron. Soc. **136**, 101 (1967).
[65] Y. Y. Yamaguchi, Phys. Rev. E **78**, 041114 (2008).
[66] Y. Levin, R. Pakter, and T. N. Teles, Phys. Rev. Lett. **100**, 040604 (2008).
[67] R. Pakter and Y. Levin, Phys. Rev. Lett. **106**, 200603 (2011).
[68] T. N. Teles, Y. Levin, and R. Pakter, Mon. Not. R. Astron. Soc.: Lett. **417**, L21 (2011).
[69] A. Campa, T. Dauxois, and S. Ruffo, Phys. Rep. **480**, 57 (2009).
[70] Y. Levin, R. Pakter, F. B. Rizzato, T. N. Teles, and F. P. C. Benetti, Phys. Rep. **535**, 1 (2014).
[71] Y. Y. Yamaguchi, J. Barré, F. Bouchet, T. Dauxois, and S. Ruffo, Phys. A (Amsterdam) **337**, 36 (2004).
[72] K. Jain, F. Bouchet, and D. Mukamel, J. Stat. Mech. (2007) P11008.
[73] M. Antoni and S. Ruffo, Phys. Rev. E **52**, 2361 (1995).
[74] T. Dauxois, V. Latora, and A. Rapisarda, in *Dynamics and Thermodynamics of Systems with Long Range Interactions*, Lecture Notes in Physics (Springer, Berlin, 2002), pp. 458–487.
[75] J. Barré, F. Bouchet, T. Dauxois, and S. Ruffo, Phys. Rev. Lett. **89**, 110601 (2002).
[76] J. Barré, F. Bouchet, T. Dauxois, and S. Ruffo, Eur. Phys. J. B. **29**, 577 (2002).
[77] F. Staniscia, P. H. Chavanis, and G. De Ninno, Phys. Rev. E **83**, 051111 (2011).
[78] F. Brennecke, T. Donner, S. Ritter, T. Bourdel, M. Köhl, and T. Esslinger, Nature (London) **450**, 268 (2007).
[79] Y. Colombe, T. Steinmetz, G. Dubois, F. Linke, D. Hunger, and J. Reichel, Nature (London) **450**, 272 (2007).
[80] S. Slama, S. Bux, G. Krenz, C. Zimmermann, and P. W. Courteille, Phys. Rev. Lett. **98**, 053603 (2007).
[81] K. W. Murch, K. L. Moore, S. Gupta, and D. M. Stamper-Kurn, Nat. Phys. **4**, 561 (2008).
[82] M. Wolke, J. Klinner, H. H. Keßler, and A. Hemmerich, Science **337**, 75 (2012).
[83] A. Goldberg, A. Al-Qasimi, and D. H. J. O'Dell, arXiv:1609.05602.
[84] L. Dominici, M. Petrov, M. Matuszewski, D. Ballarini, M. De Giorgi, D. Colas, E. Cancellieri, B. Silva Fernández, A. Bramati, G. Gigli, A. Kavokin, F. Laussy, and D. Sanvitto, Nat. Commun. **6**, 8993 (2015).
[85] V. I. Arnold, S. F. Shandarin, and Y. B. Zeldovich, Geophys. Astrophys. Fluid Dyn. **20**, 111 (1982).
[86] J. Feldbrugge, R. van de Weygaert, J. Hidding, and J. Feldbrugge, J. Cosmol. Astropart. Phys. 05 (2018) 027.
[87] R. Thom, *Structural Stability and Morphogenesis* (Benjamin, San Francisco, 1975).
[88] V. I. Arnol'd, Russ. Math. Survs. **30**, 1 (1975).
[89] T. Poston and I. Stewart, *Catastrophe Theory and Its Applications*, Dover Books on Mathematics (Dover, New York, 1978).
[90] Y. B. Zeldovich, Astron. Astrophys. **5**, 84 (1970).
[91] T. Dauxois, P. Holdsworth, and S. Ruffo, Eur. Phys. J. B **16**, 659 (2000).
[92] F. Leyvraz, M.-C. Firpo, and S. Ruffo, J. Phys. A: Math. Gen. **35**, 4413 (2002).
[93] M. Berry, Adv. Phys. **25**, 1 (1976).
[94] M. V. Berry, *Les Houches Lecture Series Session XXXV* (North-Holland, Amsterdam, 1981), pp. 458–487.
[95] M. Kac, G. E. Uhlenbeck, and P. C. Hemmer, J. Math. Phys. **4**, 216 (1963).
[96] Where the kinetic energy of each rotor is included.
[97] R. Barnett, D. Petrov, M. Lukin, and E. Demler, Phys. Rev. Lett. **96**, 190401 (2006).
[98] H. Yu, W. M. Liu, and C. Lee, arXiv:0910.4922.
[99] L. Carr, D. DeMille, R. Krems, and J. Ye, New J. Phys. **11**, 055049 (2009).
[100] H. Spohn, in *Large Scale Dynamics of Interaction*, 1st ed., edited by E. H. Lieb, W. Beiglbock, T. Regge, R. P. Geroch, and W. Thirring (Springer, Berlin, 1992).
[101] The Vlasov equation constitutes a mean field equation because it deals exclusively with the averaged particle density $f(\theta, L, t)$. Whereas the full Boltzmann equation has knowledge of particle-particle correlations via the collision integral, this is neglected in the Vlasov equation. Finite N corrections that would appear as collisional terms on the right-hand side of

Eq. (2) are suppressed and in the case of the HMF model one can show analytically that these are $o(1/N)$ [117], while numerical evidence for the HMF model suggests a suppression of $\mathcal{O}(1/N^{1.7})$ [71].
[102] W. Braun and K. Hepp, Commun. Math. Phys. **56**, 101 (1977).
[103] Y. Nakayama and R. Boucher, *Introduction to Fluid Mechanics* (Wiley, New York, 1997), pp. 197–205.
[104] P.-H. Chavanis, J. Stat. Mech.: Theory Exp. (2011) P08003.
[105] L. Pitaevskii and S. Stringari, *Bose-Einstein Condensation*, International Series of Monographs on Physics (Clarendon, Oxford, 2003).
[106] C. Pethick and H. Smith, *Bose-Einstein Condensation in Dilute Gases* (Cambridge University Press, Cambridge, 2002).
[107] N. D. Mermin and H. Wagner, Phys. Rev. Lett. **17**, 1133 (1966).
[108] S. Coleman, Commun. Math. Phys. **31**, 259 (1973).
[109] C. Mora and Y. Castin, Phys. Rev. A **67**, 053615 (2003).
[110] L. L. Foldy, Phys. Rev. **124**, 649 (1961).
[111] E. H. Lieb and H.-T. Yau, Astrophys. J. **323**, 140 (1987).
[112] A. Triay, SIAM J. Math. Anal. **50**, 33 (2018).
[113] J. M. Burgers, *Advances in Applied Mechanics*, Vol. 1 (Elsevier, Amsterdam, 1948), pp. 171–199.
[114] P. Miller, *Applied Asymptotic Analysis*, Graduate Studies in Mathematics (American Mathematical Society, Providence, RI, 2006).
[115] T. Pearcey, Philos. Mag. J. Sci. **37**, 311 (1946).
[116] F. Olver, D. Lozier, R. Boisvert, and C. Clark, *NIST Handbook of Mathematical Functions*, Vol. 5 (Cambridge University Press, Cambridge, 2010), p. 966.
[117] F. Bouchet and T. Dauxois, Phys. Rev. E **72**, 045103 (2005).
[118] M. V. Berry, J. Phys. A: Math. Gen. **17**, 1225 (1984).
[119] D. Delande, Quantum chaos in atomic physics, in *Coherent Atomic Matter Waves: 27 July–27 August 1999*, edited by R. Kaiser, C. Westbrook, and F. David (Springer, Berlin, 2001), pp. 415–479.
[120] P.-H. Chavanis, J. Stat. Mech.: Theory Exp. (2011) P08002.
[121] I. Carusotto, S. X. Hu, L. A. Collins, and A. Smerzi, Phys. Rev. Lett. **97**, 260403 (2006).
[122] W. Rooijakkers, S. Wu, P. Striehl, M. Vengalattore, and M. Prentiss, Phys. Rev. A **68**, 063412 (2003).
[123] J. H. Huckans, I. B. Spielman, B. L. Tolra, W. D. Phillips, and J. V. Porto, Phys. Rev. A **80**, 043609 (2009).
[124] S. Rosenblum, O. Bechler, I. Shomroni, R. Kaner, T. Arusi-Parpar, O. Raz, and B. Dayan, Phys. Rev. Lett. **112**, 120403 (2014).
[125] J. Mumford, W. Kirkby, and D. H. J. O'Dell, J. Phys. B: At., Mol. Opt. Phys. **50**, 044005 (2017).
[126] R. Carles, *Semi-classical Analysis for Nonlinear Schrödinger Equations* (World Scientific, Singapore, 2008), pp. 121–125.
[127] R. Haberman and R. Sun, Stud. Appl. Math. **72**, 1 (1985).
[128] J. K. Hunter and J. B. Keller, Wave Motion **9**, 429 (1987).
[129] S. Helmrich, A. Arias, and S. Whitlock, arXiv:1605.08609.
[130] T. Dauxois, S. Ruffo, E. Arimondo, and M. Wilkens, *Dynamics and Thermodynamics of Systems with Long Range Interactions*, Lecture Notes in Physics (Springer, Berlin, 2008).
[131] K. Huang, *Statistical Mechanics* (Wiley, New York, 1987).
[132] L. Santos, G. V. Shlyapnikov, P. Zoller, and M. Lewenstein, Phys. Rev. Lett. **85**, 1791 (2000).
[133] S. Yi and L. You, Phys. Rev. A **63**, 053607 (2001).
[134] D. H. J. O'Dell, S. Giovanazzi, and C. Eberlein, Phys. Rev. Lett. **92**, 250401 (2004).
[135] The much weaker criterion of (nearly) vanishing on average $\langle\mathcal{L}\rangle_{\mathcal{T}}$ is sufficient for the associated multiscale analysis to remain valid.
[136] J. J. Sakurai, *Modern Quantum Mechanics* (Addison-Wesley, Reading, MA, 1994).
[137] This is the analog of the method of steepest descent for saddles, where the normal form is a $\Phi(s) \sim \hbar[\frac{1}{2}s^2 + \mathcal{O}(s^3)]$ and results in a Gaussian integral.

"Such, in the month of August 1834, was my first chance interview with that singular and beautiful phenomenon which I have called the Wave of Translation"'

—John F. Scott Russell

CHAPTER 3

Solitary Waves in the HMF Model: Exact Solutions of the GGPE

Ryan Plestid, and D.H.J. O'Dell
Balancing long-range interactions and quantum pressure: solitons in the HMF model
Phys. Rev. E **100**, 022216; doi:10.1103/PhysRevE.100.022216

In this paper we explain how to determine exact stationary states of the HMF model's GGPE by mapping the model's non-linear equations onto a well known linear equation whose solutions are tabulated as special functions (Mathieu functions). We discover that for certain parameters there are an infinite set of non-trivial stationary solutions generalizing the results for the ground state obtained by Chavanis [82].

We identify each of these states as solitary waves in the limit that $\chi \to 0$. In this limit the solutions are found to become highly localized, being trapped by their own mean-field potential into a region whose spatial extent is $\sim \mathcal{O}(\chi)$. We are able to provide analytic formulae describing the solitons in this same limit by leveraging known and tabulated asympotitc formulae for the Mathieu functions. Using the same small-χ behaviour we are able to calculate the linearized normal mode spectrum and we establish that the full tower of solitons is asymptotically stable in the $\chi \to 0$ limit.

Finally, we note that the analytic features of the following paper are put to extensive use in Chapter 4 where they are used to contruct beyond-mean-field states for the HMF model's full many-body ground state.

Our major focuses in this chapter are as follows

- How can the HMF model's non-linear eigenvalue problem be mapped onto a known linear eigenvalue problem?
- Can the stationary states of the HMF model's GGPE be identified as solitary waves (i.e. solitons)?
- Are these solitons stable with respect to to small perturbations?
- Can we determine analytic solutions in the small χ limit for the full set of solitary waves?

Balancing long-range interactions and quantum pressure: Solitons in the Hamiltonian mean-field model

Ryan Plestid [1,2,*] and D. H. J. O'Dell [1,†]

[1] *Department of Physics and Astronomy, McMaster University, 1280 Main St. W., Hamilton, Ontario, Canada L8S 4M1*

[2] *Perimeter Institute for Theoretical Physics, 31 Caroline St. N., Waterloo, Ontario, Canada N2L 2Y5*

(Received 9 May 2019; revised manuscript received 25 July 2019; published 19 August 2019)

The Hamiltonian mean-field (HMF) model describes particles on a ring interacting via a cosine interaction, or equivalently, rotors coupled by infinite-range XY interactions. Conceived as a generic statistical mechanical model for long-range interactions such as gravity (of which the cosine is the first Fourier component), it has recently been used to account for self-organization in experiments on cold atoms with long-range optically mediated interactions. The significance of the HMF model lies in its ability to capture the universal effects of long-range interactions and yet be exactly solvable in the canonical ensemble. In this work we consider the quantum version of the HMF model in one dimension and provide a classification of all possible stationary solutions of its generalized Gross-Pitaevskii equation (GGPE), which is both nonlinear and nonlocal. The exact solutions are Mathieu functions that obey a nonlinear relation between the wave function and the depth of the mean-field potential, and we identify them as bright solitons. Using a Galilean transformation these solutions can be boosted to finite velocity and are increasingly localized as the mean-field potential becomes deeper. In contrast to the usual local GPE, the HMF case features a tower of solitons, each with a different number of nodes. Our results suggest that long-range interactions support solitary waves in a novel manner relative to the short-range case.

DOI: 10.1103/PhysRevE.100.022216

I. INTRODUCTION

Solitary waves are one of the most distinctive consequences of nonlinearity and result from a balance between dispersion and nonlinear forces. Their defining property is shape-preserving (i.e., dispersionless) propagation, as first noted in 1834 by J. Scott Russell when he observed them on the Edinburgh and Glasgow Union Canal [1]. The phenomenon has subsequently been extensively studied in classical hydrodynamics [2–5] and also in light propagating in optical fibers [6–11] and Bose-Einstein condensates (BECs) formed in dilute atomic gases. In the latter case, quantum pressure (quantum zero point motion) provides the stabilizing dispersion against collapse. Bright [12–17], dark [18–25], and dark-bright [26,27] varieties of solitary wave have all been observed in BECs.

In integrable systems solitary waves are guaranteed to survive collisions with one another, and are then referred to as *solitons*, i.e., elastically scattering and shape-preserving wave packets. Well-known examples occur in the Korteweg-de Vries equation [28–30], Sine-Gordon equation [28,29,31], and the nonlinear Schrödinger or Gross-Pitaevskii equation (GPE) [29,30,32]. The nonlinearity in all these wave equations appears as a local term that depends only on the wave function at the same point. For example, the GPE has a cubic term $g\Psi(\mathbf{x},t)|\Psi(\mathbf{x},t)|^2$ where g parameterizes the sign and magnitude of the self-coupling. However, there exist physical systems where long-range interactions (LRIs) lead to a *nonlocal* nonlinearity that can also support solitary waves. This is the case in nonneutral plasmas [33], where there is a net Coulomb $1/r$ interaction, in the Calogero-Sutherland (CS) model [34–36], where particles interact via a $1/r^2$ potential, and in dipolar BECs [37–44], where dipole-dipole interactions lead to $1/r^3$ interactions. Nonlocal interactions also occur in optical systems, such as those mediated by thermal conduction [45–49], and their consequences have been observed experimentally [50,51]. The CS model is integrable and hence supports true solitons [52–55], whereas nonneutral plasmas are not integrable systems and only support solitary waves. Dipolar BECs display an instability where the attractive part of the interaction can cause the system to collapse [40]; far from the instability solitary waves are predicted to collide elastically and thus behave as solitons, whereas close to the instability the collisions become inelastic due to the emission of phonons [56]. In the BEC literature it is common not to distinguish solitons from solitary waves and thus we use the terms somewhat interchangeably in this paper.

In dipolar BECs solitons are usually analyzed using a generalized Gross-Pitaevskii equation (GGPE), which is an integro-differential equation that incorporates the nonlocal nonlinearity through a Hartree-type mean-field term of the form $\Psi(\mathbf{x},t)\int V(\mathbf{x}-\mathbf{x}')|\Psi(\mathbf{x}',t)|^2\,d\mathbf{x}'$ [56–61]. This approach has recently been put on a rigorous mathematical footing [62,63]; for reviews of nonlocal nonlinear Schrödinger equations we refer the reader to Refs. [64] and [65]. It has also been suggested that the Manakov equations [66] (which describe both two-component BECs [67] and randomly birefringent light in optical fibers [68,69]) can give rise to a so-called algebraic nonlinearity provided the system is prepared

*plestird@mcmaster.ca
†dodell@mcmaster.ca

with a specific set of initial conditions [70]. Integral terms can also appear in the equations describing the motion of vortices in superfluids at finite temperatures; they arise, for example, from the mutual friction between a solitary wave along a vortex and its surrounding flow [71].

Another physically important class of nonlocal nonlinearity is found in self-gravitating systems. In particular, compact yet stable astrophysical objects made of bosons and known as "Bose stars" have been hypothesized [72,73]. These can be identified as solitons if the attraction due to gravity is balanced by quantum pressure [74]. The realization that dark matter in the universe may be bosonic and cold enough to Bose condense into such Bose stars has driven considerable interest in these systems [75–81]. For the most part these studies use the nonrelativistic Schrödinger-Newton (also known as the Schrödinger-Poisson) equations [82,83], which result in a GGPE similar in form to both the GGPE used for dipolar BECs and also the equation to be studied in this paper. We also note in passing that laboratory analogues of the Schrödinger-Newton system have been proposed in the form of atomic BECs with a $1/r$ interaction provided by laser-induced dipole-dipole interactions [84,85].

The focus of the present paper is the Hamiltonian mean-field (HMF) model [86] which describes N particles of mass m living on a ring. They have positions $\theta_i \in (-\pi, \pi]$, angular momenta L_i, and interact via a pairwise cosine potential of strength ϵ giving the Hamiltonian

$$H = \sum_i \frac{L_i^2}{2I} + \frac{\epsilon}{N} \sum_{i<j} \cos(\theta_i - \theta_j), \tag{1}$$

where $I = mR^2$ is the moment of inertia for a ring of radius R. Since every particle interacts with every other due to the long-range nature of the interactions, a factor of $1/N$ is explicitly included to make the energy extensive (often termed the Kac prescription [87]). The cosine potential can be thought of as the first nonconstant term in a Fourier series expansion of a gravity- or Coulomb-like $1/r$ interaction around the ring, but without the singularity at $r = 0$ that otherwise complicates the treatment of such potentials. Another way to view the HMF model is as a system of N rotors interacting via an infinite range XY interaction. If $\epsilon > 0$ the particle interactions are repulsive at small distances, or equivalently, the rotors experience an antiferromagnetic coupling and hence prefer to antialign. If instead $\epsilon < 0$ the interactions are attractive-ferromagnetic and the rotors prefer to align. The average magnetization of the rotors along an axis specified by its angle φ to the vertical is given by $\langle \cos(\theta - \varphi) \rangle = (1/N) \sum_i \cos(\theta_i - \varphi)$, and this quantity serves as an order parameter for a symmetry-breaking phase transition (clustering transition) which occurs in the attractive case at low temperatures [88]. In this paper we focus on the attractive-ferromagnetic case.

The HMF model was originally written as a toy model, and its significance lies in the fact that it is simple and yet able to capture many of the general qualitative properties of systems with LRI; for reviews see Refs. [88–90]. However, more recently it was realized that cold atomic gases trapped in high-finesse optical cavities can directly realize the HMF model [up to an additional term of the form $\cos(\theta_i + \theta_j)$] [91]. Here the long-range interactions are electromagnetic in origin and mediated by optical cavity modes that can extend over the entire gas. Ongoing experiments [92–97], many with BECs, have demonstrated symmetry breaking and self-organization in the atomic density distribution that is described by the HMF model [91,98–101].

One of the most striking properties of systems with LRI has long been appreciated by the astrophysics community: the two-body relaxation time (also known as the Chandrasekhar relaxation time) to thermodynamic (Boltzmann-Gibbs) equilibrium, diverges with the number of particles $t_{\text{relax}} \sim N t_{\text{cross}}/10 \log[N]$, where t_{cross} is the typical time for a particle to cross the system [102]. Thus, in the thermodynamic limit $N \to \infty$ the system never achieves thermodynamic equilibrium. Nevertheless, when a self-gravitating system is disturbed from equilibrium the common mean-field potential that arises from the long-range nature of gravity becomes time dependent and can drive a rapid, collisionless relaxation mechanism known as violent relaxation whose timescale does not depend on the number of particles. This efficiently mixes phase space [102], but the process is nonergodic and the resulting quasistationary state is not the equilibrium state predicted by the microcanonical ensemble. However, coarse graining of the phase space distribution function by a macroscopic observer averages over the increasingly fine structures that develop during collisionless relaxation and in this way conventional statistical mechanics approaches can be applied [90,103–105]. The HMF model has been shown to display violent relaxation [106–109], as well as other generic consequences of LRI, including spontaneous symmetry breaking in low dimensions, i.e., the clustering phase transition mentioned above (LRI violate the Mermin-Wagner theorem), and the so-called "core-halo" statistics observed at late times in gravitational dynamics simulations [90,104,105].

The HMF model can be extended to describe quantum systems with LRI if we replace the kinetic energy term in Eq. (1) by its quantum operator $-\frac{\hbar^2}{2mR^2}\partial_{\theta_i}^2$, and the system is then equivalent to an infinite range $O(2)$ quantum rotor model [110–114]. Motivation for studying the quantum problem comes both from cold atom experiments and the Bose star picture of dark matter mentioned above. The equilibrium states of the quantum HMF model have been examined in Refs. [115,116] and the dynamics, including violent relaxation, were recently studied in Ref. [117], where it was found that the automatic coarse graining of phase space at the level of Planck's constant h can strongly modify the relaxation in the deep quantum regime. Furthermore, in its quantum form the HMF model bears a resemblance to the CS model mentioned above, which, when defined on a finite domain with periodic boundary conditions, has a pairwise interaction $V(\theta_i - \theta_j) = 1/\sin^2(\theta_i - \theta_j)$. Like the HMF model, the CS model has a periodic infinite range interaction. This connection is relevant in the present context because the CS model supports true solitons. The HMF model is not thought to be exactly integrable, but intriguingly, classical long-range interacting many-body systems are known to be described (exactly in the $N \to \infty$ limit [118]) by the Vlasov equation. Vlasov

dynamics *are integrable* for a on-dimensional system [119], such as the HMF model.[1] Furthermore, the classical (i.e., $\hbar \to 0$) limit of the GGPE corresponds to the "zero-temperature" limit of the Vlasov equation [108,109,117]. Therefore, although the HMF model is not exactly integrable, its classical dynamics are nearly integrable due to the structure of the Vlasov equation. We speculate that the "pseudo-integrability" extends also to the GGPE and may allow the solitary waves (bright solitons) presented here to scatter elastically.

Our goal in this work is to study solitary waves in the quantum HMF model with attractive-ferromagnetic interactions. We focus on the model's associated GGPE, appropriate for describing the dynamics of a Bose condensed state (the HMF model, despite its name, describes a many-body system: to obtain a GGPE we assume all the particles occupy the same quantum state). We find that the exact solutions to this equation are Mathieu functions that satisfy a nonlinear self-consistency relation. As the interaction strength tends to infinity the number of these solutions also becomes infinite and we identify them as bright solitons each with a different number of nodes. Both the large number of solutions and the fact they have nodes makes them unusual when compared to the standard local GPE case [32]. We attribute these differences to the LRI themselves and hypothesize that this might be a generic feature.

This paper is organized as follows: In Sec. II we introduce the GGPE for the HMF model. In Sec. III we show how to find the full set of exact stationary solutions to the GGPE via a self-consistent Mathieu equation, and in Sec. IV we boost these solutions to finite velocity to obtain traveling waves. In Sec. V we explore the regime in which the solutions can be considered as bright solitons and discuss the parametric dependence of the stationary solutions on Planck's constant. Next we discuss the asymptotic behavior of these solutions and derive useful analytic expressions. In Sec. VI we study their stability at leading order in the strong coupling regime by linearizing the equations of motion and analyzing the mode spectrum. Finally, in Sec. VII we summarize our work and discuss future directions of investigation.

II. GENERALIZED GROSS-PITAEVSKII EQUATION

An atomic BEC with short-range interactions is described by the standard GPE with a local cubic nonlinearity [121]

$$i\hbar\frac{\partial\Psi}{\partial t} = \left[-\frac{\hbar^2}{2m}\nabla^2 + V_{\text{ext}}(\mathbf{x}) + gN|\Psi|^2\right]\Psi, \tag{2}$$

where N is the number of atoms, $\Psi(\mathbf{x},t)$ is the condensate wave function normalized to unity: $\int_{-\infty}^{\infty}|\Psi|^2\,d\mathbf{x} = 1$, $V_{\text{ext}}(\mathbf{x})$ is a possible external potential, e.g., a harmonic trap or periodic optical lattice potential, and the coupling constant g parameterizes the interatomic interactions (usually of the van der Waals type). Any stationary solution to this equation can be found in the usual way by putting $\Psi(\mathbf{x},t) = \psi(\mathbf{x})\exp[-i\mu t/\hbar]$, giving

$$\mu\psi = \left[-\frac{\hbar^2}{2m}\nabla^2 + V_{\text{ext}}(\mathbf{x}) + gN|\psi|^2\right]\psi. \tag{3}$$

If this were a linear Schrödinger equation, the eigenvalue μ would be the energy E of the state ψ. However, due to the nonlinearity of the GPE μ is in fact the chemical potential which is the change in energy associated with adding a particle to the system: $\mu = \partial E/\partial N$ [121]. In a waveguide configuration, where the BEC is tightly trapped in the x and y directions but untrapped along the z direction, the problem becomes effectively one-dimensional. Specializing further to the case of attractive interactions ($g < 0$), the stationary GPE has the bright soliton solution

$$\psi_0(z) = \psi_0(0)\frac{1}{\cosh(z/\sqrt{2}\xi)}, \tag{4}$$

where $\rho_0 = |\psi_0(0)|^2$ is the central density and $\xi = 1/\sqrt{2m|g|\rho_0}$ is a characteristic length called the healing length [121]. In the optical soliton literature this solution is called the *fundamental soliton* and the coordinate z is replaced by $z - vt$ representing a shape-preserving waveform propagating at the group velocity v (there is also a multiplicative phase factor we shall not specify here) [11].

By contrast, the LRI in the HMF model lead to a *nonlocal nonlinearity* [116,117]. The HMF model lives on a ring so that the wave function obeys periodic boundary conditions $\Psi(\theta,t) = \Psi(\theta+2\pi,t)$, and it also does not include an explicit potential $V_{\text{ext}}(\mathbf{x})$. Fixing the interactions to be attractive (i.e., $\epsilon < 0$), the HMF model's GGPE can be written in reduced variables as

$$i\chi\frac{\partial\Psi}{\partial\tau} = \left[-\frac{\chi^2}{2}\frac{\partial^2}{\partial\theta^2} - \Phi(\theta,\tau)\right]\Psi, \tag{5a}$$

$$\text{where}\quad \Phi(\theta,\tau) = \int_{-\pi}^{\pi}\rho(\theta',\tau)\cos(\theta-\theta')\,d\theta' \tag{5b}$$

is a nonlocal Hartree potential that depends on the integral over the angular probability density $\rho(\theta,\tau) = |\Psi(\theta,\tau)|^2$. We have introduced the quantities $\tau = t\times\sqrt{\frac{|\epsilon|}{mR^2}}$ and χ, the latter of which plays the role of a dimensionless Planck's constant:

$$\chi = \frac{\hbar}{\sqrt{mR^2|\epsilon|}}. \tag{6}$$

Note that χ depends on the magnitude of the interaction strength $|\epsilon|$.

The seemingly complicated integro-differential equation given in Eq. (5) can be simplified by expanding the probability density in its Fourier components $\rho(\theta') = \sum\hat{\rho}_k e^{ik\theta'}/2\pi$. We see that Φ depends only on $\hat{\rho}_{\pm1}$, which we can write in all generality as $\hat{\rho}_{\pm1} := M(\tau)\exp[\mp i\varphi(\tau)]$. From this it follows that the Hartree potential takes the remarkably simple form

$$\Phi(\theta,\tau) = M(\tau)\cos[\theta-\varphi(\tau)]. \tag{7}$$

The physical significance of this result is that all the individual two-body XY potentials of the many-body theory are replaced in the Gross-Pitaevskii theory by a single collective potential $\Phi(\theta,\tau)$ which retains the same XY form (a cosine) but breaks the angular symmetry by picking out a particular direction

[1] Furthermore, the infinite set of Casimir invariants for the Vlasov equation can mimic the effects of integrability for higher dimensional systems with LRI; see, e.g., Ref. [120].

specified by $\varphi(\tau)$ along which the magnetization is $M(\tau)$. Furthermore, because $M(\tau)$ is the coefficient of the ± 1 terms in the Fourier expansion of the probability density, we can always project it out from the angular probability distribution via the integral

$$M(\tau) = \int_{-\pi}^{\pi} \rho(\theta, \tau) \cos(\theta - \varphi)\, d\theta, \tag{8}$$

which is the continuous version of the definition of the magnetization given in the Introduction, $M = \langle \cos(\theta - \varphi) \rangle = (1/N) \sum_i \cos(\theta_i - \varphi)$.

The stationary states $\Psi(\theta, \tau) = \psi(\theta) \exp[-i\mu\tau/\chi]$ of the GGPE satisfy the equation

$$-\frac{\chi^2}{2} \frac{\partial^2 \psi}{\partial \theta^2} + (-\mu - M[\psi] \cos\theta)\psi = 0, \tag{9}$$

where we have taken advantage of the fact that in the stationary case we can define our coordinates such that $\varphi = 0$. As for the case of contact interactions, the eigenvalue μ is not the same as the energy $E = \langle \psi | H | \psi \rangle$ of the state ψ associated with Hamiltonian given in Eq. (1), but is the chemical potential.

The stationary GGPE given in Eq. (9) has the same form as the Mathieu equation [122]

$$\frac{\partial^2 w}{\partial z^2} + [a - 2q \cos(2z)]w = 0, \tag{10}$$

whose solutions are Mathieu functions. These are denoted $\mathrm{ce}_n(z; q)$ and $\mathrm{se}_n(z; q)$ and have eigenvalues $a = A_n(q)$ and $B_n(q)$, respectively. In general, Mathieu functions also depend on a second parameter, which physically is the quasimomentum. However, here the quasimomentum is fixed to be zero by the periodic boundary conditions imposed by the ring.

There is a crucial difference between the standard Mathieu equation and the GGPE. Whereas the former corresponds to a linear problem where the "depth parameter" q of the cosine potential takes a fixed specified value, in our problem the depth of the cosine potential is the magnetization $M[\psi]$ which is a functional of the wave function and so depends on the solution itself. In other words, we have a nonlinear eigenvalue problem which, remarkably, has eigenvectors that are Mathieu functions obeying a linear equation but which must be supplemented by the self-consistency condition

$$M[\psi] = \int_{-\pi}^{\pi} |\psi(\theta')|^2 \cos(\theta')\, d\theta'. \tag{11}$$

We note that this is simply a restatement of Eq. (8) for a density $\rho(\theta) = |\psi(\theta)|^2$ that is independent of time.

An analogous situation occurs in cavity-QED where atoms are trapped in an optical cavity pumped by a laser [123–128]. The laser light forms a standing (or traveling [129,130]) wave inside the cavity which the atoms experience as a sinusoidal potential via the optical dipole interaction. The atoms' center-of-mass wave function is therefore also determined by the Mathieu equation. However, the interaction acts back on the light which sees the atoms as a refractive medium. This backaction shifts the cavity's resonance frequency, and hence controls the amount of laser light that can enter the cavity, by an amount that depends on the overlap between the atomic density distribution and the optical mode. In this way the atomic density profile affects the depth of the sinusoidal potential which in turn affects the atomic density profile. The problem is therefore nonlinear and also leads to a Mathieu equation with a parameter q that must be determined self-consistently from the atomic wave function like in Eq. (11). One effect of this nonlinearity is the appearance of curious loops in the band structure that are not present in the linear problem and which can lie in the band gaps [124,131].

Band gap loops also occur in the problem of a BEC in an optical lattice of fixed depth, i.e., Eq. (2) with $V_{\mathrm{ext}}(x) = V_0 \cos(kx)$, where the nonlinearity comes purely from interatomic interactions modeled by the cubic nonlinearity. This situation has been investigated both experimentally [132] and theoretically [133–138] where it is found that the loops correspond to two different types of solutions: periodic trains of solitons, i.e., spatially extended solutions [136,138], and localized band gap solitons [137]. Despite their localization, these latter solitons can have one or more nodes. In the HMF problem we also have a cosine potential but it is limited to a single period by the periodicity of the ring. This fixes the quasimomentum to zero and hence collapses the band structure to the center of the Brillouin zone. Still, we shall find analogous solutions to localized band gap solitons as will be described below.

III. SELF-CONSISTENT MATHIEU FUNCTIONS

To convert between the GGPE given in Eq. (9) and the standard form of the Mathieu equation given in Eq. (10) we make the identifications[2] $\theta = 2(z + \pi/2)$ and $\partial_z^2 = 4\partial_\theta^2$. Multiplying both sides of Eq. (10) by a factor of $-\chi^2/8$ we find

$$\mu = \frac{\chi^2}{8} a \quad \text{and} \quad M = \frac{\chi^2}{4} q. \tag{12}$$

The solutions we require are the ones that are 2π-periodic in the angle θ, and these correspond to ce_{2n} and se_{2n} with $n \geqslant 0$ an integer.

To find self-consistent solutions of the GGPE we use the following algorithm:

(1) We first treat q as a fixed parameter like in the usual linear theory of Mathieu functions. Taking a given Mathieu function of fixed n and q (which we denote q_n) we compute $M(q_n)$ using Eq. (11) where $\psi = \mathrm{ce}_n(z; q_n)/\sqrt{\pi}$ or $\psi = \mathrm{se}_{n+1}(z; q_n)/\sqrt{\pi}$ and $z = (\theta - \pi)/2$.

(2) Next, we obtain $\chi(q_n)$ by using Eq. (12), which gives $\chi(q_n) = \sqrt{4M(q_n)/q_n}$.

(3) The above two steps are repeated a large number of times for different values of q to obtain a map between χ and q. This must be done separately for each Mathieu function (each value of n).

(4) Although we have treated q as a parameter upon which χ depends, in reality the situation is reversed with q_n being determined self-consistently in terms of χ. We therefore invert the map $\chi(q_n)$ to find $q_n(\chi; \aleph)$ where we have introduced the

[2] The shift in coordinates is equivalent to a negative value of q and accounts for the attractive nature of the interparticle interaction.

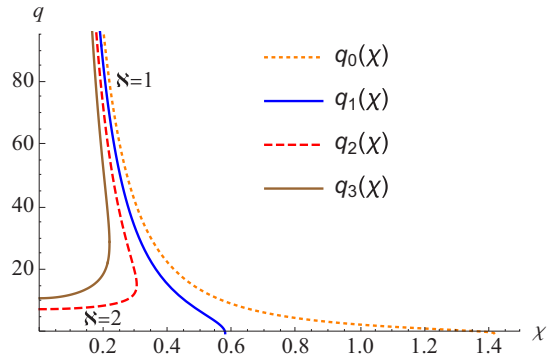

FIG. 1. Self-consistent values of the potential depth, as parameterized by q, as a function of χ for the first four stationary solutions: this plot shows which Mathieu functions satisfy both Eq. (9) and the self-consistency condition (11). Using Eq. (13) we can then find explicit expressions for the stationary state $\psi_n(\theta;\chi,\aleph)$. The parameter $\aleph$ labels the different branches of $q_n(\chi;\aleph)$. Note that both $n=2$ and $n=3$ have two branches as the function turns back on itself. This is a generic feature for $n \geqslant 2$.

integer $\aleph$ to label different branches of the function in the case that $\chi(q_n)$ is not invertible. The results are shown in Fig. 1.

Noting that Mathieu functions are conventionally normalized on the unit circle such that $\int |\mathrm{ce}_n(\theta)|^2 d\theta = \pi$, and $\int |\mathrm{se}_n(\theta)|^2 d\theta = \pi$, we define our stationary states as

$$\psi_n(\theta;\chi,\aleph) = \frac{1}{\sqrt{\pi}} \begin{cases} \mathrm{ce}_n\left[\frac{\theta-\pi}{2}; q_n(\chi;\aleph)\right] & n \text{ even} \\ \mathrm{se}_{n+1}\left[\frac{\theta-\pi}{2}; q_n(\chi;\aleph)\right] & n \text{ odd} \end{cases} \tag{13}$$

where $q_n(\chi;\aleph)$ is obtained via the algorithm outlined above. In Figs. 2 and 3 we plot some examples of these stationary solutions for $\chi = 0.5$ and $\chi = 0.05$, respectively, where in the latter case both branches of solutions exist, so we have chosen the $\aleph = 1$ branch. We see that n gives the number of nodes.

According to its definition in Eq. (6), χ decreases as the magnitude of the (attractive) interaction strength $|\epsilon|$ increases, and hence the $\aleph = 1$ branch solutions correspond most naturally to bright solitons: from Fig. 1 we see that as χ decreases the potential, as parameterized by q, becomes deeper and the states are more tightly bound as can be seen by comparing Fig. 2 with 3 (see Sec. V for further justification that these are really localized solutions). By contrast, the $\aleph = 2$ branch corresponds to shallower potentials which vary only slightly with χ. This branch continuously passes to negative χ (not shown in Fig. 3) corresponding to repulsive interactions, which shows that the repulsive HMF model can also support stationary states; however, we emphasize that these states

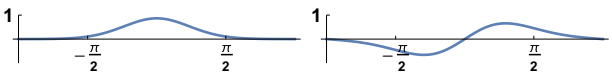

FIG. 2. Plots of the two self-consistent stationary solutions to the GGPE [Eqs. (5a) and (5b)] that exist at $\chi = 0.5$. They are the $n=0$ and $n=1$ states, where n gives the number of modes. The solutions are periodic with period 2π.

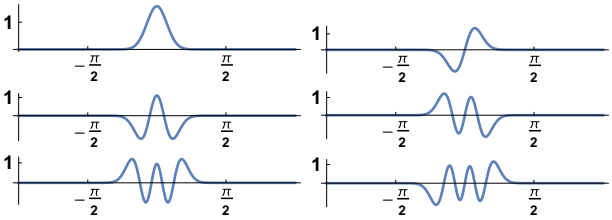

FIG. 3. Plots of the first six self-consistent stationary solutions to the GGPE for $\chi = 0.05$. These solutions all lie on the upper branch of Fig. 1, i.e., $\psi_n(\theta;\chi,\aleph=1)$ where $n \in \{0,1,2,3,4,5\}$. Note that even for moderately small values of χ the first few stationary states are quite well localized, and upon a Galilean transformation to finite velocity can be interpreted as solitary wave solutions. All states are periodic with period 2π.

generally have smaller values of q and are less localized than their attractive interacting counterparts.

The first two solutions, ψ_0 and ψ_1, have only a single branch and are shown in Fig. 2. For weak interactions ($\chi \gg 1$) ones finds that q is zero so that the self-consistent Hartree cosine potential is zero. These solutions then correspond to ordinary sine waves (although, as shown in Fig. 4, for $\chi > \sqrt{2}$ the energy eigenvalue or chemical potential corresponding to ψ_0 takes the value $\mu = 0$, and thus this is a trivial solution corresponding to an infinite wavelength, i.e., a flat density profile). However, at a critical value of χ, which is different for each solution, the Hartree potential switches on and the solutions evolve continuously into Mathieu functions. For ψ_0 this occurs at $\chi = \sqrt{2}$ [116], and for ψ_1 it occurs at $\chi = 1/\sqrt{3}$. The higher solutions behave differently, as can be seen from Fig. 1. In their case each solution again switches on below a critical value χ, but q takes on a finite value at the point each solution appears (and which immediately splits into two branches).

With the knowledge of the dependence of the q_n's upon χ depicted in Fig. 1 we can straightforwardly obtain physical quantities such as the chemical potentials and magnetizations

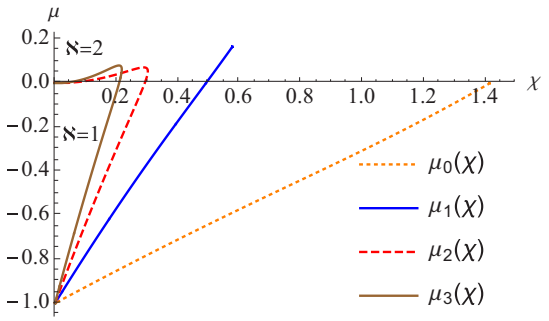

FIG. 4. The eigenvalues μ of the GGPE as a function of χ for the first four stationary solutions. μ_0 and μ_1 abruptly appear at critical values of $\chi = \sqrt{2}$ and $\chi = 1/\sqrt{3}$, respectively; for larger values of χ the self-consistent Hartree cosine potential is zero (i.e., $q = 0$), and the solutions ψ_0 and ψ_1 are ordinary sine waves so we have not plotted that portion of their eigenvalues. Like in Fig. 1, $\aleph = 1$ and $\aleph = 2$ label the two branches of the higher solutions.

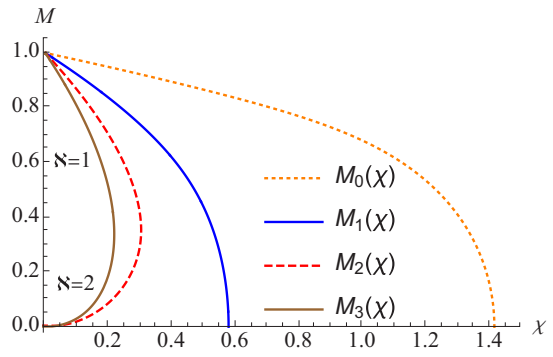

FIG. 5. The magnetization M as a function of χ for the first four stationary solutions. With the exception of the two lowest states, the solutions have two branches labeled by $\aleph = 1$ and $\aleph = 2$ like in the earlier figures. Treating the magnetization as an order parameter signifying a clustering or ordering phase transition which breaks the angular symmetry of the system, we see that this transition is second order (continuous), at least in the lowest two states. The fact that a phase transition occurs in a 1D system is a special feature of LRI.

of all the stationary states. These are plotted in Figs. 4 and 5, respectively. Each chemical potential $\mu_n = \partial E_n/\partial N$ gives the change in energy of its respective state $E_n = \langle\psi_n|H|\psi_n\rangle$ when a particle is added to the system. From Fig. 4 we see that the gaps between the different μ_n vanish linearly as $\chi \to 0$, so that all μ_n tend to the common value of -1. However, the rate at which they approach this limit is higher the higher the state so that the largest gap is between μ_0 and μ_1.

Although the chemical potential is sensitive to the clustering or ordering phase transition that occurs at the critical value of χ, it is the magnetization which is usually taken as the order parameter for the transition [88]. In particular, examining the behavior of the magnetization M_0 of the lowest state in Fig. 4, we see that when the coupling is weak ($\chi \gg 1$) the magnetization is zero but at the critical value $\chi = \sqrt{2}$ it begins to take on finite values indicating a second order (continuous) phase transition. Similar behavior is found for M_1. However, the behavior of the magnetization of the higher states is more complicated; nevertheless the $\aleph = 1$ branches of these states, which correspond to bright solitons, tend to full magnetization $M = 1$ in the strong coupling regime $\chi \ll 1$.

The results given in this section generalize those obtained by Chavanis [116] for the ground state of the quantum HMF model. In particular, the approach described above allows one to classify *all possible* stationary states of the GGPE. They are labeled by their number of nodes n, and their depth parameter $q_n(\chi;\aleph)$. Furthermore, while the approach followed in Ref. [116] gives an expansion for the small q properties of the ground state $\psi_0(\theta;\chi)$, as well as the leading order result in the strong-coupling regime $\chi \ll 1$, the approach followed here is valid for all values of χ and, upon computation of $q_n(\chi)$, provides an analytic expression for $\psi_n(\theta)$. The standard large and small q asymptotics of the Mathieu functions [122] can then be used to obtain analytic approximations for $q_n(\chi;\aleph = 1)$.

The fact that the GGPE admits a tower of stationary solutions $\psi_n(\theta;\chi,\aleph)$, each labeled by its number of nodes n and branch $\aleph$, is quite distinct from the case of the local GPE where there is only a single stationary bright soliton solution, i.e., the nodeless fundamental soliton given in Eq. (4). In particular, the GGPE's tower of stationary solutions should not be confused with the so-called "higher order solitons" found in the local GPE which can display multiple peaks and nodes at certain instants of time [6,11,139]. These higher order solitons are time-dependent combinations of the fundamental and do not correspond to the individual stationary solutions we describe above. Indeed, as famously shown by Zakharov and Shabat [140], the inverse scattering transform method can be applied to the local GPE and in general gives rise to a nonlinear superposition of multiple fundamental solitons and continuous waves (see p. 21 in Ref. [9] and p. 245 in Ref. [11] for a summary of these results).

IV. BOOSTED SOLUTIONS

The same solutions as already described for the stationary case can be transformed to traveling waves with velocity v by performing a Galilean boost:

$$\psi_n(\theta)e^{-i\mu_n\tau/\chi} \to \psi_n(\theta - v\tau)e^{iv\theta/\chi}\, e^{-i(\mu_n+v^2/2)\tau/\chi}. \quad (14)$$

In order that these wave functions still satisfy the periodic boundary conditions we require that $v/\chi = n$ with $n \in \mathbb{Z}$. The existence and classification of these wave functions is the main result of our work. In the next section we will see when they can be considered to be solitary waves.

V. EMERGENCE OF SOLITONS AT STRONG COUPLING

Having established the existence of nontrivial stationary and traveling waves we will now argue that the crucial solitonic property of localization emerges in the strong-coupling regime $\chi \ll 1$. Finally, we show how in this same limit an explicit asymptotic series for the depth parameter $q_n(\chi)$ can be obtained.

A. Localization in the strong-coupling regime

In the limit of strong coupling the Hartree mean-field potential is deep relative to the kinetic energy, and the magnetization can be expected to saturate to unity. It then follows via the relation $q = 4M/\chi^2$ that this limit corresponds to large values of q, and we will see that this is indeed the case.

As $q \to \infty$ the eigenvalues, A and B, of the Mathieu equation display the well-known asymptotic behavior as a function of q [122],

$$\left.\begin{matrix} A_n(q) \\ B_{n+1}(q) \end{matrix}\right\} \sim -2q\left[1 - \frac{1}{\sqrt{q}}(2n+1) + O\left(\frac{1}{q}\right)\right], \quad (15)$$

from which we can identify that the low-lying states are bound within a deep well[3] whose minimum is spontaneously chosen

[3] The spectrum is that of a harmonic oscillator with anharmonic corrections occurring at $O(1/q)$.

around the ring. There are two classical turning points:

$$\theta^{\pm}_{\text{turn}} \sim \pm\frac{(4n+2)^{1/2}}{q^{1/4}} + O\left(\frac{1}{q^{1/2}}\right). \tag{16}$$

At distances $|\theta| \gtrsim 2\theta^{+}_{\text{turn}}$ the wave function is exponentially suppressed and consequently the state is localized in a region around the mean-field potential's minimum (as can be seen in Fig. 3). The size of this region shrinks with q and shows that localized stationary states emerge in the strong-coupling regime, and, by Galilean invariance, so too do finite-velocity traveling solitons. Thus, we identify the solutions as solitary waves because they can be arbitrarily localized and their shape is determined by a competition between quantum dispersion and a classical mean-field potential, Φ, which is the source of the nonlinearity in Eq. (5).

We may quantify the regime in which soliton-like solutions appear by estimating a critical value $q_n^{(c)}$ above which the stationary state is sufficiently narrow to be considered localized relative to the spatial extent of the unit circle. Demanding that $\theta^{+}_{\text{turn}} < \pi/4$ implies that for q satisfying

$$q \gtrsim q_c(n) = \frac{64}{\pi^4}(2n+1)^2 \approx \frac{2}{3}(2n+1)^2, \tag{17}$$

or equivalently[4] for χ satisfying

$$\chi \lesssim \frac{\pi^2/8}{2n+1} \approx \frac{1.23}{2n+1}, \tag{18}$$

the stationary states discussed above are well localized.

From Eq. (16) we see that for fixed n the stationary states' widths tends to zero and are localized within an interval of size $\Delta\theta \sim O(1/q^{1/4})$ centered about the minimum of the mean-field potential. This suggests approximating the cosine potential as a quadratic potential well, and a thorough analysis reveals that this can be done provided the turning point structure of the problem is preserved. The stationary solutions in this regime are parabolic cylinder functions [141–144]:

$$\psi_n(\theta;q) \sim \left[\frac{\sqrt{q}}{2\pi(n!)^2}\right]^{1/4} \begin{cases} D_n(\zeta) & n \text{ even} \\ \cos\left(\frac{1}{2}\theta\right) D_n(\zeta) & n \text{ odd} \end{cases}, \tag{19}$$

where $\zeta = 2q^{1/4}\sin(\theta/2)$ [see Eqs. (A4) and (A5) for a more extensive discussion].

B. Magnetization and Hartree potential depth in the strong coupling regime

We seek to compute the magnetization

$$M(q_n) = \int_{-\pi}^{\pi} d\theta\, |\psi_n(\theta;q)|^2 \cos\theta \tag{20}$$

in the strong coupling regime. Expanding the wave function in terms of parabolic cylinder functions, and changing variables to $\zeta = 2q^{1/4}\sin(\theta/2)$, we obtain

$$M(q) = \int_{-2q^{1/4}}^{2q^{1/4}} \frac{d\zeta}{q^{1/4}} \left[\frac{1-\frac{\zeta^2}{2\sqrt{q}}}{\sqrt{1-\frac{\zeta^2}{4\sqrt{q}}}}\right] |\psi_n(\zeta;q)|^2. \tag{21}$$

[4] Taking $M \sim O(1)$ as $q \to \infty$.

A Taylor expansion of $(1-\frac{\zeta^2}{2\sqrt{q}})/\sqrt{1-\frac{\zeta^2}{4\sqrt{q}}}$ and knowledge of integrals of the form

$$I^{(k)}_{n,m} = \int_{-\infty}^{\infty} d\zeta\, D_n(\zeta) D_m(\zeta) \zeta^k \tag{22}$$

allows one to compute asymptotic expressions for the magnetization as a function of q, the details of which can be found in Appendix A. We find

$$M(q_n) \sim 1 - \frac{1}{\sqrt{q}}\left[\frac{2n+1}{2}\right] + O\left(\frac{1}{q^{3/2}}\right). \tag{23}$$

This equation applies to the branches of solutions labeled by $\aleph = 1$ in Fig. 1.

With this result we may now compute $\chi_n(q) = \sqrt{4M/q}$, which can subsequently be inverted yielding

$$q_n(\chi;\aleph=1) \sim \frac{4}{\chi^2}\left[1 - \frac{2n+1}{4}\chi - \frac{(2n+1)^2}{32}\chi^2\right], \tag{24}$$

where, again, $\aleph = 1$ denotes the branch of $q_n(\chi)$ to which our asymptotic analysis applies.

The above asymptotic analysis is only sensible provided that χ is sufficiently small such that dispersive effects are weak relative to the mean-field Hartree potential. Quantitatively we require that Eq. (18) is satisfied; for $n = 0$ and $n = 1$ this occurs for values of $\chi \lesssim 1$.

C. Energy in the strong coupling regime

An analytic expression for the energy of a solitary wave can also be obtained in the small-χ limit. The energy functional (i.e., Hamiltonian) for the HMF model is

$$\begin{aligned}\mathcal{E} &= \int \psi^*\left[-\frac{1}{2}\chi^2\partial_\theta^2\right]\psi\, d\theta - \frac{1}{2}M[\psi]^2 \\ &= \mu_n + \frac{1}{2}M[\psi_n]^2,\end{aligned} \tag{25}$$

where in the second equality we have used Eq. (9). The small-χ behavior of the magnetization M is given by Eqs. (23) and (24),

$$M \sim 1 - \frac{2n+1}{4}\chi, \tag{26}$$

while the chemical potential's behavior can be found by using the large-q asymptotics of $a_n \sim -2q + (4n+2)\sqrt{q}$, which, when written in terms of χ, gives

$$\begin{aligned}\mu_n &= \frac{\chi^2}{8} \times a_n \sim \frac{\chi^2}{2}[-2q(\chi) + (4n+2)\sqrt{q(\chi)}] \\ &\sim -1 + \frac{3}{4}(2n+1)\chi.\end{aligned} \tag{27}$$

Thus we have

$$\mathcal{E}_n \sim -\frac{1}{2} + \frac{2n+1}{4}\chi, \tag{28}$$

such that the energy increases linearly with n at leading order in χ; a nonperturbative graph of the energy's n dependence can be obtained by combining the curves plotted in Figs. 4 and 5.

VI. LINEAR STABILITY ANALYSIS

In order to understand whether the solitary waves analyzed in the previous two sections are stable, we study their linearized equations of motion in the soliton's rest frame. Since we identify these solutions as being solitary waves in the limit that $\chi \to 0$, and since for $n \geqslant 2$ the solutions exist only for small values of χ, we restrict our analysis to the $\aleph = 1$ branch of solutions in the limit that $\chi \to 0$ such that a large-q expansion is justified.

We consider stability of the soliton solutions with respect to perturbations of the Bogoliubov form

$$\Psi(\theta,\tau) = [\psi_n(\theta) + \delta\psi_n(\theta,\tau)]e^{-i\mu\tau/\chi}, \tag{29}$$

$$\delta\psi_n(\theta,\tau) = \sum_\alpha U_\alpha(\theta)e^{-i\omega_\alpha\tau/\chi} + V_\alpha^*(\theta)e^{i\omega_\alpha^*\tau/\chi}, \tag{30}$$

which have real frequencies if the unperturbed solution is stable, and complex frequencies if it is dynamically unstable [32]. Substituting this ansatz into Eq. (5), working to first order in U_α and V_α^*, and collecting terms varying in time as $e^{-i\omega_\alpha\tau/\chi}$ and $e^{i\omega_\alpha^*\tau/\chi}$, respectively, one finds the following coupled equations for the normal modes:

$$\omega U(\theta) = (\widehat{H}_n - \mu_n)U(\theta) - \Phi(\theta)\psi_n(\theta), \tag{31}$$

$$-\omega V(\theta) = (\widehat{H}_n - \mu_n)V(\theta) - \Phi(\theta)\psi_n(\theta), \tag{32}$$

where we have used the reality of the soliton, $\psi_n^* = \psi_n$ (since we are in the rest frame of the solitary wave). The subscript α has been left implicit, $\widehat{H}_n = -\frac{1}{2}\chi^2\partial_\theta^2 - M[\psi_n]\cos\theta$, and we define the linearized mean-field potential as

$$\Phi(\theta) = \int_{-\pi}^{\pi}[U(\theta') + V(\theta')]\psi_n(\theta')\cos(\theta-\theta')\,d\theta'. \tag{33}$$

It is convenient to decompose both $U(\theta)$ and $V(\theta)$ in terms of the set of Mathieu functions orthogonal to ψ_n, which we will denote by $\{\phi_m\}$. Note that these solutions are complete and satisfy the *linear* equation

$$\widehat{H}_n\phi_m = -\tfrac{1}{2}\chi^2\phi_m'' + M[\psi_n]\cos(\theta)\,\phi_m = \lambda_m\phi_m, \tag{34}$$

where λ_m is related to the eigenvalue a_m of Eq. (10) via $\lambda_m = \chi^2 a_m/8$ [cf. Eq. (12)]. Importantly, $M[\psi_n]$ is the magnetization induced by the soliton solution ψ_n and is independent of ϕ_m. Explicitly, we have $U(\theta) = \sum_m u_m\phi_m(\theta)$ and $V(\theta) = \sum_m v_m\phi_m(\theta)$ where u_m and v_m are c-numbers and $m \neq n$. This final condition ensures that our linear operator is diagonalizable [145].

To find the frequencies $\{\omega_\alpha\}$, we take Eqs. (31) and (32) and operate on both sides with $\int d\theta\phi_m(\theta)$. By virtue of the orthogonality relations $\int\phi_m\phi_\ell\,d\theta = \delta_{m\ell}$ and $\int\phi_m\psi_n\,d\theta = 0$, this projects out the mth element of $\{\phi_m\}$ and allows us to express Eq. (31) in terms of the coefficients u_ℓ and v_ℓ via

$$\omega u_m = (\lambda_m - \mu_n)u_m - \sum_{\ell\neq n}F_{m\ell}(u_\ell + v_\ell), \tag{35a}$$

$$-\omega v_m = (\lambda_m - \mu_n)v_m - \sum_{\ell\neq n}F_{m\ell}(u_\ell + v_\ell), \tag{35b}$$

where the quantity $F_{m\ell}$ is defined as

$$F_{m\ell} = \mathcal{I}^C_{\ell,n}\mathcal{I}^C_{m,n} + \mathcal{I}^S_{\ell,n}\mathcal{I}^S_{m,n}, \tag{36}$$

and where the integrals $\mathcal{I}^C_{\ell,n}$ and $\mathcal{I}^S_{\ell,n}$ are defined in terms of the mean-field solutions via

$$\mathcal{I}^C_{m,n} = \int_{-\pi}^{\pi}\phi_m(\theta)\psi_n(\theta)\cos\theta\,d\theta, \tag{37a}$$

$$\mathcal{I}^S_{m,n} = \int_{-\pi}^{\pi}\phi_m(\theta)\psi_n(\theta)\sin\theta\,d\theta. \tag{37b}$$

We may interpret $F_{m\ell}$ as a matrix operator acting on the vector $(u+v)_\ell$ such that the equations can be cast in the form

$$\omega_n\begin{pmatrix}u\\v\end{pmatrix} = \frac{1}{\sqrt{q}}\begin{pmatrix}\mathcal{D}_n - \mathcal{F}_n & -\mathcal{F}_n\\ \mathcal{F}_n & -(\mathcal{D}_n - \mathcal{F}_n)\end{pmatrix}\begin{pmatrix}u\\v\end{pmatrix}. \tag{38}$$

Here $\mathcal{D}_n$ is a diagonal matrix with $\mathcal{D}_n^{m,m} = \sqrt{q}(\lambda_m - \mu_n)$ along the diagonal, while the matrix elements of $\mathcal{F}$ are related to those of F via $\mathcal{F}_{m\ell} = \sqrt{q}F_{m\ell}$. Physically, $\mathcal{D}_n$ tells us whether an orthogonal Mathieu function ϕ_m has a larger or smaller eigenvalue (chemical potential) as compared to the soliton ψ_n. The matrix $\mathcal{F}_n$ is the mode-to-mode coupling induced indirectly by the soliton.

Explicit expressions for the matrix elements $F_{m\ell}$ and $\mathcal{D}_n^{m,m}$ can be obtained in the large-q (i.e., small-χ) regime. As outlined in Appendix B, by making large-q expansions of the integrals $\mathcal{I}^C_{m,n}$ and $\mathcal{I}^S_{m,n}$, then at $O(1/\sqrt{q})$ only $\mathcal{I}^S_{m,n}$ contributes to $F_{m\ell}$ with the explicit (leading order) formula being

$$\mathcal{I}^S_{m,n} \sim \frac{1}{q^{1/4}}(\sqrt{n+1}\,\delta_{m,n+1} + \sqrt{n}\,\delta_{m,n-1}). \tag{39}$$

Higher order terms connect states with $m = n\pm 2$, $m = n\pm 3$, etc. Likewise, to find the large-q behavior of $\mathcal{D}_n$, we can use the large-q asymptotic formula for the eigenvalues of the Mathieu equation [122]:

$$\mu_n \sim \frac{\chi^2(q_n)}{8}\left\{-2q + 2(2n+1)\sqrt{q} + \frac{1}{8}[(2n+1)^2+1]\right\}, \tag{40}$$

$$\lambda_m \sim \frac{\chi^2(q_n)}{8}\left\{-2q + 2(2m+1)\sqrt{q} + \frac{1}{8}[(2m+1]^2+1)\right\}. \tag{41}$$

Notice that both λ_m and μ_n are multiplied by the same value of χ^2, which corresponds to the soliton's self-consistent depth parameter q_n. At leading order this implies that $\mathcal{D}_n^{m,\ell} \sim 2(m-n)\delta_{\ell,m}$, and that all of $\mathcal{F}_n$'s nonvanishing entries are contained within a 2×2 block composed of $\ell, m = n\pm1$ (unless $n=0$) given by

$$\begin{pmatrix}n & \sqrt{n(n+1)}\\ \sqrt{n(n+1)} & n+1\end{pmatrix}. \tag{42}$$

This implies that in the strong-coupling regime the perturbations about the soliton are *weakly interacting*, with the exception of the two Mathieu modes whose eigenvalues are closest to the soliton's chemical potential. These two modes actually couple with a strength that is $O(n)$ such that solitons with a higher number of nodes mediate stronger interactions than those with fewer nodes. By contrast, if $n=0$ (i.e., if we are perturbing around the lowest energy soliton), then intermode coupling does not exist at $O(1/\sqrt{q})$ and $\mathcal{F}_n$ is diagonal at leading order, having all vanishing entries except

for $\mathcal{F}_n^{11} = 1$. We focus now on $n \geqslant 1$ after which we will return to $n = 0$ as a special case.

By rewriting Eq. (38) in terms of $u + v$ and $u - v$, it can be easily seen that the eigenvalues of the above matrix equation are determined by the condition that

$$\mathrm{Det}\big[q\omega_n^2 \mathbb{1} - \big(\mathcal{D}_n^2 - 2\mathcal{F}_n\mathcal{D}_n\big)\big] = 0. \tag{43}$$

The spectrum of $\mathcal{D}_n^2 - 2\mathcal{F}_n\mathcal{D}_n$ is the same as that of $\mathcal{D}_n^2$ except for the two eigenvalues that are determined (for $n \geqslant 1$) by the 2×2 matrix

$$\begin{pmatrix} 4n+4 & -4\sqrt{n(n+1)} \\ 4\sqrt{n(n+1)} & -4n \end{pmatrix}, \tag{44}$$

whose eigenvalues are independent of n and given by $\lambda_1{=}0$ and $\lambda_2 = 4$. We thereby find that the entire spectrum is positive, indicating stability, except for one entry which is marginal at this order, being neither positive nor negative.

To elucidate the stability of the mode corresponding to λ_1 we must calculate subdominant corrections to $\mathcal{I}^S$, and $\lambda_m - \mu_n$. This can be achieved using first-order perturbation theory for which we need the eigenvector corresponding to λ_1 at leading order, which is given by

$$v_1 = (\sqrt{n/(2n+1)}, \sqrt{(n+1)/(2n+1)})^T. \tag{45}$$

If we denote the subdominant corrections as $\delta\mathcal{D}_n$ and $\delta\mathcal{F}_n$ (such that $\mathcal{D}_n \to \mathcal{D}_n + q^{-1/2}\delta\mathcal{D}_n$ and $\mathcal{F}_n \to \mathcal{F}_n + q^{-1/2}\delta\mathcal{F}_n$) then, the first-order perturbative correction to the eigenvalue is given by

$$\lambda_1 \sim \frac{1}{\sqrt{q}} v_1^T [\{\mathcal{D}_n, \delta\mathcal{D}_n\} - 2(\delta\mathcal{F}_n\mathcal{D}_n + \mathcal{F}_n\delta\mathcal{D}_n)]v_1, \tag{46}$$

where the curly braces denote an anticommutator. Using Eqs. (40) and (41) we find for $\delta\mathcal{D}_n$

$$\delta D_n = \begin{pmatrix} \frac{1}{4}(10n+4) & 0 \\ 0 & \frac{1}{4}(-6-10n) \end{pmatrix}. \tag{47}$$

The relevant matrix elements of $\mathcal{F}$ are $\mathcal{F}_{\ell m}$ with $\ell, m = n \pm 1$ which can be represented as a 2×2 matrix

$$\delta\mathcal{F} = \begin{pmatrix} -\frac{3}{4}n^2 & -\frac{3}{8}\sqrt{n(n+1)}(2n+1) \\ -\frac{3}{8}\sqrt{n(n+1)}(2n+1) & -\frac{3}{4}(1+n)^2 \end{pmatrix} \tag{48}$$

such that

$$\lambda_1 \sim \frac{1}{\sqrt{q}} \times \frac{n(1+n)}{2n+1} \quad \text{for} \quad n \geqslant 1. \tag{49}$$

Thus, for $n \geqslant 1$ all of the eigenvalues λ are positive definite, such that ω_m is always real, and the solitons are dynamically stable. The typical frequencies are given by $\omega_m \sim \frac{2}{\sqrt{q}}$ $|m-n| \sim \chi|m-n|$, while the smallest frequency is parametrically smaller being given by $\omega_1 = \pm\sqrt{\lambda_1/q} \sim O(\chi^{3/2})$.

As mentioned above, the case of the $n = 0$ is different. Here the zeroth eigenvector is $v_1 = (1, 0)^T$, and it turns out that its eigenvalue is small $\lambda_1 \sim O(1/q)$, If we define the matrix $M = \mathcal{D}_n^2 - 2\mathcal{F}_n\mathcal{D}_n$, then we have that

$$M = \begin{pmatrix} M_{11} & 0 & M_{13} \\ 0 & M_{22} & 0 \\ M_{31} & 0 & M_{33} \end{pmatrix}, \tag{50}$$

where the zeros stem from the fact that $\mathcal{I}^C_{0,m} = 0$ if m is odd. As we will soon see, M_{13} and M_{31} are both $O(1/\sqrt{q})$ while M_{33} is $O(1)$, and we can therefore calculate the correction to λ_1 within second-order perturbation theory

$$\lambda_1 \sim M_{11} + \frac{M_{13}M_{31}}{M_{11} - M_{33}} + O(q^{-3/2}) \quad \text{for} \quad n = 0. \tag{51}$$

Explicit formula for M_{11}, M_{13}, and M_{31} in terms of $\mathcal{I}^S_{0,m}$ and $\Delta_m = \lambda_m - \mu_0$ are given by

$$M_{11} = q\Delta_1^2 - 2q\Delta_1\mathcal{I}^S_{0,1}\mathcal{I}^S_{0,1}, \tag{52}$$

$$M_{13} = -2q\Delta_3\mathcal{I}^S_{0,1}\mathcal{I}^S_{0,3}, \tag{53}$$

$$M_{31} = -2q\Delta_1\mathcal{I}^S_{0,1}\mathcal{I}^S_{0,3}, \tag{54}$$

$$M_{33} = q\Delta_3^2 - 2q\Delta_3\mathcal{I}^S_{0,3}\mathcal{I}^S_{0,3}. \tag{55}$$

The large q behavior of Δ_m can be found by using Eq. (28.8.1) of Ref. [122] and the next-to-next-to leading order expression for $\chi(q_n)$ given in Eq. (A18). To compute $\mathcal{I}^S_{0,m}$ we make use of Eqs. (28.8.3) to (28.8.7) from [122] at next-to-next-to leading order accuracy. At the level of accuracy required to compute λ_1 the results are

$$q^{1/4}\mathcal{I}^S_{0,1} \sim 1 - \frac{3}{8\sqrt{q}} - \frac{19}{256q}, \tag{56}$$

$$q^{1/4}\mathcal{I}^S_{0,3} \sim -\frac{3\sqrt{3/2}}{8\sqrt{q}}, \tag{57}$$

$$\sqrt{q}\Delta_1 \sim 2 - \frac{3}{2\sqrt{q}} + \frac{3}{16q}, \tag{58}$$

$$\sqrt{q}\Delta_3 \sim 6. \tag{59}$$

Substituting these expressions into Eqs. (52) to (55) we find

$$M_{11} \sim \frac{13}{32q} + O\left(\frac{1}{q^{3/2}}\right), \tag{60}$$

$$M_{13} \sim \frac{9\sqrt{3/2}}{2\sqrt{q}} + O\left(\frac{1}{q}\right), \tag{61}$$

$$M_{31} \sim \frac{3\sqrt{3/2}}{2\sqrt{q}} + O\left(\frac{1}{q}\right), \tag{62}$$

$$M_{33} \sim 36 + O\left(\frac{1}{q^{1/2}}\right). \tag{63}$$

Then, using Eq. (51), we arrive at

$$\lambda_1 \sim \frac{1}{8q} \quad \text{for} \quad n = 0. \tag{64}$$

Thus, the $n = 0$ soliton is also stable (as it must be since it is the lowest energy stationary state). Curiously, while all of the other solitons' smallest normal mode frequencies are $O(\chi^{3/2})$, the ground state's lowest lying normal mode frequency is actually $O(\chi^2)$ since $\omega_1 = \sqrt{\lambda_1/q} \sim O(\chi^2)$.

VII. CONCLUSIONS

We have shown that the GGPE for the HMF model admits exact solutions in the form of Mathieu functions complemented by a self-consistency condition on the depth of the Hartree potential they generate. These solutions can be

boosted to finite speeds (providing the phase associated with the flow satisfies the periodic boundary conditions). In the strong coupling regime ($\chi \ll 1$) the solutions can be arbitrarily highly localized, and thus we interpret them as bright solitons. A linear stability analysis in the same strong coupling regime shows that they are stable against perturbations when the interactions are attractive.

The fact that the solutions: (1) arise in a periodic potential, (2) are localized, and (3) come in towers with increasing numbers of nodes, means that they have properties in common with gap solitons [137]. However, the periodic potential in the HMF case is self-generated, whereas in the standard gap soliton case the periodic potential is imposed externally. Furthermore, in contrast to the bright soliton solutions of the standard GPE which are stabilized by a $|\psi|^2\psi$ nonlinearity, the HMF model's solitons are stabilized by a nonlocal nonlinearity $\Phi[\psi](\theta) = M[\psi]\cos\theta$, where the depth is given by the magnetization $M[\psi]$; see Eq. (5b).

The approach followed in this work not only allows us to identify solitary wave solutions, but also to find and classify all possible stationary states for both attractive and repulsive interactions at arbitrary coupling strength (we focused on the attractive case). Furthermore, in the strong coupling limit the self-consistency condition can be developed analytically in an asymptotic series so as to provide a completely explicit analytic solution. Given that exact solutions of nonlinear models are few and far between, this illustrates once again that the HMF model is rather special even though it is not thought to be integrable.

One possible reason for the existence of a richer family of solutions (i.e., the tower of solutions) in comparison to the standard short-range attractive system, where the GPE supports a single nodeless bright soliton [i.e., the fundamental soliton given in Eq. (4)], is that the self-consistency condition in the latter case is much more restrictive: both the depth and shape must match. By contrast, in the HMF case the mean-field potential is generated by the coherent addition of the microscopic cosine (XY) interactions and thus inherits a cosine form where only the depth needs to be self-consistently determined. We conjecture that this coherent addition across the sample is a generic feature of LRIs and suggests that such systems deserve closer examination as a potential setting for solitons.

An interesting future direction of research would be to study collisional properties of the bright solitons (solitary waves) identified in this work and to determine if they are true solitons (i.e., do they collide elastically). As sketched in the introduction, systems with LRI can be expected to behave similarly to integrable systems. A numerical study of soliton dynamics in the HMF model would be a natural testing ground for this idea.

Another extension of the present work concerns the quantum phase transition predicted by the HMF model's GGPE due to a spontaneous breaking of translational invariance at the critical value of $\chi = \sqrt{2}$ [116]. The GGPE does not include the effects of quantum fluctuations, and these may inhibit this spontaneous symmetry breaking. However, our exact solutions can serve as the building blocks of more sophisticated quantum states that are required for studying the role of quantum fluctuations. These effects will be discussed elsewhere [146].

ACKNOWLEDGMENTS

We thank Dmitry Pelinovsky, Robert Dingwall, Wyatt Kirkby, and Thomas Bland for helpful discussions. This research was funded by the Natural Sciences and Engineering Research Council of Canada (NSERC) and the Government of Ontario. Support is also acknowledged from the Perimeter Institute for Theoretical Physics. Research at the Perimeter Institute is supported by the Government of Canada through the Department of Innovation, Science and Economic Development and by the Province of Ontario through the Ministry of Research and Innovation.

APPENDIX A: ASYMPTOTIC ANALYSIS OF THE SELF-CONSISTENT MAGNETIZATION

We are interested in calculating the magnetization

$$\begin{aligned} M_n(\chi) &= \int_{-\pi}^{\pi} d\theta |\psi_n(\theta;\chi)|^2 \cos\theta \\ &= \int_{-\pi}^{\pi} d\theta |\psi_n(\theta;\chi)|^2 \left(1 - 2\sin^2\frac{\theta}{2}\right) \\ &= 1 - 2\int_{-\pi}^{\pi} d\theta |\psi_n(\theta;\chi)|^2 \sin^2\frac{\theta}{2} \end{aligned}$$

in the strong coupling regime where $\chi \ll 1$. We must consider the cases of n even and n odd separately due to their definition in terms of either even or odd Mathieu functions, which we repeat here for convenience:

$$\psi_n(\theta;\chi,\aleph) = \frac{1}{\sqrt{\pi}} \begin{cases} \mathrm{ce}_n\left[\frac{\theta-\pi}{2}; q_n(\chi;\aleph)\right] & n \text{ even} \\ \mathrm{se}_{n+1}\left[\frac{\theta-\pi}{2}; q_n(\chi;\aleph)\right] & n \text{ odd.} \end{cases} \tag{A1}$$

The strong coupling regime is equivalent to $q \gg 1$ in the conventional Mathieu equation. When applied to the HMF model, this means that one can study the regime in which $q \gg 1$, compute the magnetization and by extension $\chi(q) = \sqrt{4M(q)/q}$, and then invert this expression to find how q depends on χ.

Consequently, it is convenient for computational purposes to consider q, rather than χ as a fixed parameter, and later invert the relationship between them as described above. Integrals such as Eq. (A1) are conveniently analyzed by transforming to the coordinate $\zeta = 2q^{1/4}\sin\frac{\theta}{2}$; doing so we find [as in Eq. (21)]

$$M_n(q) = 1 - \frac{1}{2\sqrt{q}} \int_{-2q^{1/4}}^{2q^{1/4}} \frac{d\zeta}{q^{1/4}} |\psi_n(\zeta;q)|^2 \frac{\zeta^2}{\sqrt{1 - \frac{\zeta^2}{4\sqrt{q}}}}. \tag{A2}$$

For the purposes of obtaining an asymptotic series in $1/\sqrt{q}$ we can extend the limits of integration to $\pm\infty$,

$$M_n(q) \sim 1 - \frac{1}{2\sqrt{q}} \int_{-\infty}^{\infty} \frac{d\zeta}{q^{1/4}} |\psi_n(\zeta;q)|^2 \frac{\zeta^2}{\sqrt{1 - \frac{\zeta^2}{4\sqrt{q}}}}, \tag{A3}$$

where $\sim$ denotes an asymptotically small error as $q \to \infty$ [122]. We can then expand the square root in the denominator

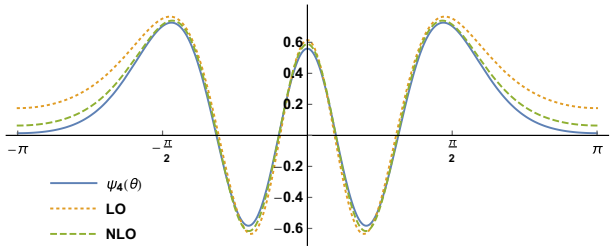

FIG. 6. Comparison of the $n = 4$ exact solitary wave $\psi_n(\theta, q)$ for $q = \frac{2}{3}(2n+1)^2 = 54$. LO denotes the leading-order Sips expansion Eqs. (A4) and (A5), and NLO denotes the approximation including next-to-leading order terms. As we can see, the Sips expansion becomes accurate even at only moderately large values of q. For $q = (2n+1)^2 = 81$ the exact and NLO curves become virtually indistinguishable.

in a Taylor series and use the large-q behavior of the stationary solutions $\psi_n(\zeta; q)$.

In the limit of large q both $\mathrm{ce}_n(z; q)$ and $\mathrm{se}_n(z; q)$ can be expanded in terms of parabolic cylinder functions [122,141–144]. This is easy to understand, since for n fixed and $q \to \infty$ the classical turning points coalesce at the minimum of the cosine potential. Therefore the states are constrained to live arbitrarily close to the potential's minimum and a harmonic approximation is justified. To ensure that the turning point structure is maintained the expansion is carried out using $\xi = 2q^{1/4}\cos z$ rather than the naive choice of $z - \pi/2$. Explicitly, Sips's expansion of the Mathieu functions in terms of parabolic cylinder functions assumes the form [122]

$$\mathrm{ce}_n(z; q) \sim \widehat{C}_n(q)[\widehat{U}_n(\xi; q) + \widehat{V}_n(\xi; q)], \tag{A4}$$

$$\mathrm{se}_{n-1}(z; q) \sim \widehat{S}_n(q)\sin(z)[\widehat{U}_n(\xi; q) - \widehat{V}_n(\xi; q)], \tag{A5}$$

where $U_m(\xi; q)$ and $V_m(\xi; q)$ are given at next-to-leading order [i.e., suppressing terms of $O(q)$] by

$$\widehat{U}_n(\xi; q) \sim D_n(\xi) + \frac{1}{64\sqrt{q}}\left[\frac{n!}{(n-4)!}D_{n-4}(\xi) - D_{n+4}(\xi)\right], \tag{A6}$$

$$\widehat{V}_n(\xi; q) \sim \frac{1}{16\sqrt{q}}[n(1-n)D_{n-2}(\xi) - D_{n+2}(\xi)], \tag{A7}$$

where $D_n = D_n(\xi)$ are the parabolic cylinder functions of order n, and the normalization constants are given by

$$\widehat{C}_n(q) \sim \left[\frac{\pi\sqrt{q}}{2(n!)^2}\right]^{1/4}\left[1 + \frac{(2n+1)}{8\sqrt{q}} + O\left(\frac{1}{q}\right)\right]^{-1/2}, \tag{A8}$$

$$\widehat{S}_n(q) \sim \left[\frac{\pi\sqrt{q}}{2(n!)^2}\right]^{1/4}\left[1 - \frac{(2n+1)}{8\sqrt{q}} + O\left(\frac{1}{q}\right)\right]^{-1/2}. \tag{A9}$$

The accuracy of the Sips expansion even for relatively modest values of q is illustrated in Fig. 6.

Since we have a series solution to $\psi_n(\zeta; q)$ in terms of parabolic cylinder functions, and we are interested in computing integrals $\int |\psi_n|^2 \zeta^k d\zeta$, we ultimately require knowledge of integrals of the form

$$I^{(k)}_{m,n} = \int_{-\infty}^{\infty} D_m(\xi) D_n(\xi) \xi^k d\xi. \tag{A10}$$

Then using the recursion relation [144]

$$I^{(k)}_{m,n} = I^{(k-1)}_{m+1,n} + I^{(k-1)}_{m,n+1} - (k-1)I^{(k-2)}_{m,n}, \tag{A11}$$

we arrive at the following identities:

$$I^{(0)}_{m,n} = n!\sqrt{2\pi} \times \delta_{m,n}, \tag{A12}$$

$$I^{(1)}_{m,n} = n!\sqrt{2\pi} \times [(n+1)\delta_{m,n+1} + \delta_{m+1,n}], \tag{A13}$$

$$I^{(2)}_{m,n} = n!\sqrt{2\pi} \times [(n+2)(n+1)\delta_{m,n+2} + (2n+1)\delta_{m,n} + \delta_{m+2,n}], \tag{A14}$$

$$I^{(4)}_{n,n} = n!\sqrt{2\pi} \times 3(2n^2 + 2n + 1). \tag{A15}$$

Armed with these details, we may now attack the integral in Eq. (A3). First, we note that by Eq. (A1) that in using Eqs. (A4) and (A5) we must make the substitution $z \to (\theta + \pi)/2$, which in turn implies that $\xi \to \zeta = 2q^{1/4}\sin(\theta/2)$ and $\sin z \to \cos(\theta/2)$. Expressing all functions in terms of ζ and then performing a Taylor expansion yields

$$M_n(q) \sim 1 - \int_{-\infty}^{\infty} \frac{d\zeta}{q^{1/4}}\left[\frac{1}{\sqrt{\pi}}\right]^2 [\widehat{U}_n(\zeta) \pm \widehat{V}_n(\zeta)]^2 \left[\left(\frac{\pi\sqrt{q}}{2(n!)^2}\right)^{1/4}\right]^2 \left(1 \mp \frac{2n+1}{8\sqrt{q}}\right) \times \left(\frac{1}{2\sqrt{q}}\zeta^2 \pm \frac{1}{16q}\zeta^4\right), \tag{A16}$$

where the upper sign corresponds to n even and the lower sign to n odd. Using Eqs. (A12) to (A14), the integral may then be expressed in terms of $I^{(k)}_{m,n}$ as

$$\begin{aligned} M_n(q) &\sim 1 - \frac{1}{n!\sqrt{2\pi}}\left\{\frac{1}{2\sqrt{q}}I^{(2)}_{n,n} \pm \frac{1}{16q}\left[I^{(4)}_{n,n} + n(1-n)I^{(2)}_{n,n-2} - I^{(2)}_{n,n+2} - (2n+1)I^{(2)}_{n,n}\right]\right\} + O\left(\frac{1}{q^{3/2}}\right) \\ &= 1 - \frac{1}{2\sqrt{q}}[2n+1] \mp \frac{1}{16q}[3(2n^2+2n+1) + n(1-n) - (n+1)(n+2) - (2n+1)^2] + O\left(x\frac{1}{q^{3/2}}\right) \\ &= 1 - \frac{1}{2\sqrt{q}}[2n+1] + O\left(\frac{1}{q^{3/2}}\right). \end{aligned} \tag{A17}$$

Having obtained the magnetization in terms of the auxiliary parameter q, we now compute $\chi(q)$ and find at next-to-next-to leading order

$$\chi(q_n) = \sqrt{\frac{4M_n(q)}{q}} \sim \frac{2}{\sqrt{q}}\left[1 - \frac{1}{\sqrt{q}}\frac{2n+1}{4} - \frac{1}{q}\frac{(2n+1)^2}{32}\right], \tag{A18}$$

which may in turn be inverted to find

$$q_n(\chi;\aleph=1) \sim \frac{4}{\chi^2}\left[1 - \frac{2n+1}{4}\chi - \frac{(2n+1)^2}{32}\chi^2\right] \tag{A19}$$

as claimed in the main text. The branch labeled by $\aleph = 1$ is the appropriate one since we took the auxiliary variable q to be large.

APPENDIX B: DEFINITION AND ASYMPTOTICS OF THE INTEGRALS $\mathcal{I}^C_{m,n}$ AND $\mathcal{I}^S_{m,n}$

The following integrals appear in Eq. (36):

$$\mathcal{I}^C_{m,n} = \int_{-\pi}^{\pi} \phi_m(\theta)\psi_n(\theta)\cos\theta\, d\theta, \tag{B1}$$

$$\mathcal{I}^S_{m,n} = \int_{-\pi}^{\pi} \phi_m(\theta)\psi_n(\theta)\sin\theta\, d\theta, \tag{B2}$$

where ψ_n is the stationary state [given by a Mathieu function with depth parameter $q(\chi)$] around which fluctuations take place, and ϕ_m is a Mathieu function orthogonal[5] to ψ_m.

Note that both ψ_n and ψ_m, being Mathieu functions, are strictly even or odd, and so $\mathcal{I}^C_{m,n} = 0$ identically if $m+n$ is odd, while $\mathcal{I}^S_{m,n} = 0$ identically if $m+n$ is even. We can compute these integrals order-by-order in $1/\sqrt{q}$ by re-expressing them in terms of $\zeta = 2q^{1/4}\sin\frac{\theta}{2}$. For the sine integral we find

$$\mathcal{I}^S_{m,n} = \int_{-2q^{1/4}}^{2q^{1/4}} \left[\frac{d\zeta}{q^{1/4}\left(1-\frac{\zeta^2}{4\sqrt{q}}\right)}\right]\phi_m(\zeta;q)\psi_n(\zeta;q) \times \left[\frac{\zeta}{q^{1/4}}\sqrt{1-\frac{\zeta^2}{4\sqrt{q}}}\right]. \tag{B3}$$

[5] The functions $\{\psi_m\}$ satisfy the (rescaled) linear Mathieu equation $-\frac{\chi^2}{2}\phi_m'' - M[\psi_n]\cos\theta\phi_m = \lambda_m\phi_m$.

Next, using the asymptotic formulas for Mathieu functions, Eqs. (A4) and (A5), and working at leading order in $1/\sqrt{q}$ we find

$$\begin{aligned}\mathcal{I}^S_{m,n} &\sim \int_{-2q^{1/4}}^{2q^{1/4}} d\zeta\,\frac{\zeta}{\sqrt{q}}\left\{\frac{1}{\sqrt{\pi}}\left[\frac{\pi\sqrt{q}}{2(n!)^2}\right]^{1/4} D_n(\zeta)\right\} \\ &\quad\times\left\{\frac{1}{\sqrt{\pi}}\left[\frac{\pi\sqrt{q}}{2(m!)^2}\right]^{1/4} D_m(\zeta)\right\} \\ &= \frac{1}{q^{1/4}}\frac{1}{\sqrt{2\pi m!n!}} I^{(1)}_{n,m} \\ &= \frac{1}{q^{1/4}}[\sqrt{n+1}\delta_{m,n+1} + \sqrt{n}\delta_{m+1,n}],\end{aligned} \tag{B4}$$

where we have made use of Eq. (A13) to move between the second and third equalities. For Eq. (48) we require $\mathcal{I}^S_{m,n}$ with $m = n \pm 1$ at next-to-leading order, to calculate $\delta\mathcal{F}$. These are given by

$$\mathcal{I}^S_{n+1,n} = q^{1/4}\left[\sqrt{n+1} - \frac{3(n+1)}{8\sqrt{q}}\right], \tag{B5}$$

$$\mathcal{I}^S_{n-1,n} = q^{1/4}\left[n - \frac{3n}{8\sqrt{q}}\right]. \tag{B6}$$

Next, turning our attention to the cosine integral we find

$$\mathcal{I}^C_{m,n} = \int_{-2q^{1/4}}^{2q^{1/4}} \left[\frac{d\zeta}{q^{1/4}\left(1-\frac{\zeta^2}{4\sqrt{q}}\right)}\right]\phi_m(\zeta;q)\psi_n(\zeta;q) \times\left[1-\frac{\zeta^2}{2\sqrt{q}}\right]. \tag{B7}$$

When re-expressed in terms of parabolic cylinder functions, we see that the $O(1)$ piece vanishes ($\int D_m D_n\, d\zeta = 0$ for $m \neq n$), and the remaining integral ($\int D_m D_n \zeta^2/\sqrt{q}\, d\zeta$) is $O(1/\sqrt{q})$. This implies that

$$I^C_{m,n} \sim O\left(\frac{1}{\sqrt{q}}\right). \tag{B8}$$

This is subdominant to the sine integral $I^S_{m,n} \sim O(1/q^{1/4})$ and so can be neglected at leading order as claimed in the main text.

[1] J. S. Russell, Report on waves, *Report of the 14th Meeting of the British Association for the Advancement of Science, York* (John Murray, London, 1844), pp. 311–390.

[2] P. G. Drazin and R. S. Johnson, *Solitons: An Introduction* (Cambridge University Press, Cambridge, 1989).

[3] M. Tanaka, The stability of solitary waves, Phys. Fluids **29**, 650 (1986).

[4] Z. Wang, Stability and dynamics of two-dimensional fully nonlinear gravity-capillary solitary waves in deep water, J. Fluid Mech. **809**, 530 (2016).

[5] W. Y. Duan, Z. Wang, B. B. Zhao, R. C. Ertekin, and J. W. Kim, Steady solution of the velocity field of steep solitary waves, Appl. Ocean Res. **73**, 70 (2018).

[6] L. F. Mollenauer, R. H. Stolen, and J. P. Gordon, Experimental Observation of Picosecond Pulse Narrowing and Solitons in Optical Fibers, Phys. Rev. Lett. **45**, 1095 (1980).

[7] J. P. Gordon, Interaction forces among solitons in optical fibers, Opt. Lett. **8**, 596 (1983).

[8] Y. Kodama and K. Nozaki, Soliton interaction in optical fibers, Opt. Lett. **12**, 1038 (1987).

[9] A. Hasegawa, *Optical Solitons in Fibers* (Springer, Berlin, 1989).

[10] Y. S. Kivshar and B. Luther-Davies, Dark optical solitons: Physics and applications, Phys. Rep. **298**, 81 (1998).

[11] L. F. Mollenauer and J. P. Gordon, *Solitons in Optical Fibers* (Academic Press, New York, 2006).

[12] K. E. Strecker, G. B. Partridge, A. G. Truscott, and R. G. Hulet, Formation and propagation of matter-wave soliton trains, Nature (London) **417**, 150 (2002).

[13] L. Khaykovich, F. Schreck, G. Ferrari, T. Bourdel, J. Cubizolles, L. D. Carr, Y. Castin, and C. Salomon, Formation of a matter-wave bright soliton, Science **296**, 1290 (2002).

[14] S. L. Cornish, S. T. Thompson, and C. E. Wieman, Formation of Bright Matter-Wave Solitons during the Collapse of Attractive Bose-Einstein Condensates, Phys. Rev. Lett. **96**, 170401 (2006).

[15] A. L. Marchant, T. P. Billam, T. P. Wiles, M. M. H. Yu, S. A. Gardiner, and S. L. Cornish, Controlled formation and reflection of a bright solitary matter-wave, Nat. Commun. **4**, 1865 (2013).

[16] G. D. McDonald, C. C. N. Kuhn, K. S. Hardman, S. Bennetts, P. J. Everitt, P. A. Altin, J. E. Debs, J. D. Close, and N. P. Robins, Bright Solitonic Matter-Wave Interferometer, Phys. Rev. Lett. **113**, 013002 (2014).

[17] P. Medley, M. A. Minar, N. C. Cizek, D. Berryrieser, and M. A. Kasevich, Evaporative Production of Bright Atomic Solitons, Phys. Rev. Lett. **112**, 060401 (2014).

[18] S. Burger, K. Bongs, S. Dettmer, W. Ertmer, K. Sengstock, A. Sanpera, G. V. Shlyapnikov, and M. Lewenstein, Dark Solitons in Bose-Einstein Condensates, Phys. Rev. Lett. **83**, 5198 (1999).

[19] J. Denschlag, J. E. Simsarian, D. L. Feder, C. W. Clark, L. A. Collins, J. Cubizolles, L. Deng, E. W. Hagley, K. Helmerson, W. P. Reinhardt, S. L. Rolston, B. I. Schneider, and W. D. Phillips, Generating solitons by phase engineering of a Bose-Einstein condensate, Science **287**, 97 (2000).

[20] Z. Dutton, M. Budde, C. Slowe, and L. V. Hau, Observation of quantum shock waves created with ultra-compressed slow light pulses in a Bose-Einstein condensate, Science **293**, 663 (2001).

[21] G.-B. Jo, J.-H. Choi, C. A. Christensen, T. A. Pasquini, Y.-R. Lee, W. Ketterle, and D. E. Pritchard, Phase-Sensitive Recombination of Two Bose-Einstein Condensates on an Atom Chip, Phys. Rev. Lett. **98**, 180401 (2007).

[22] P. Engels and C. Atherton, Stationary and Nonstationary Fluid Flow of a Bose-Einstein Condensate through a Penetrable Barrier, Phys. Rev. Lett. **99**, 160405 (2007).

[23] A. Weller, J. P. Ronzheimer, C. Gross, J. Esteve, M. K. Oberthaler, D. J. Frantzeskakis, G. Theocharis, and P. G. Kevrekidis, Experimental Observation of Oscillating and Interacting Matter Wave Dark Solitons, Phys. Rev. Lett. **101**, 130401 (2008).

[24] S. Stellmer, C. Becker, P. Soltan-Panahi, E.-M. Richter, S. Dörscher, M. Baumert, J. Kronjäger, K. Bongs, and K. Sengstock, Collisions of Dark Solitons in Elongated Bose-Einstein Condensates, Phys. Rev. Lett. **101**, 120406 (2008).

[25] J. J. Chang, P. Engels, and M. A. Hoefer, Formation of Dispersive Shock Waves by Merging and Splitting Bose-Einstein Condensates, Phys. Rev. Lett. **101**, 170404 (2008).

[26] C. Becker, S. Stellmer, P. Soltan-Panahi, S. Dörscher, M. Baumert, E.-M. Richter, J. Kronjäger, K. Bongs, and K. Sengstock, Oscillations and interactions of dark and dark-bright solitons in Bose-Einstein condensates, Nat. Phys. **4**, 496 (2008).

[27] C. Hamner, J. J. Chang, P. Engels, and M. A. Hoefer, Generation of Dark-Bright Soliton Trains in Superfluid-Superfluid Counterflow, Phys. Rev. Lett. **106**, 065302 (2011).

[28] A. C. Scott, F. Y. F. Chu, and D. W. McLaughlin, The soliton: A new concept in applied science, Proc. IEEE **61**, 1443 (1973).

[29] A. Scott, *Nonlinear Science: Emergence and Dynamics of Coherent Structures* (Oxford University Press, Oxford, 2003).

[30] C. Klein and J.-C. Saut, IST versus PDE, a comparative study, arXiv:1409.2020 (2014).

[31] M. Hudak, J. Tothova, and O. Hudak, Inverse scattering method I. Methodological part with an example: Soliton solution of the Sine-Gordon equation, doi: 10.13140/RG.2.2.35000.65287.

[32] C. J. Pethick and H. Smith, *Bose-Einstein Condensation in Dilute Gases* (Cambridge University Press, Cambridge, 2002).

[33] R. C. Davidson, *Physics of Nonneutral Plasmas* (World Scientific, Singapore, 2001).

[34] F. Calogero, Solution of the one-dimensional n-body problem with quadratic and/or inversely quadratic pair potentials, J. Math. Phys. **12**, 419 (1971).

[35] B. Sutherland, Exact results for a quantum many-body problem in one dimension, Phys. Rev. A **4**, 2019 (1971).

[36] B. Sutherland, Exact results for a quantum many-body problem in one dimension. II, Phys. Rev. A **5**, 1372 (1972).

[37] L. Santos, G. V. Shlyapnikov, P. Zoller, and M. Lewenstein, Bose-Einstein Condensation in Trapped Dipolar Gases, Phys. Rev. Lett. **85**, 1791 (2000).

[38] A. Griesmaier, J. Werner, S. Hensler, J. Stuhler, and T. Pfau, Bose-Einstein Condensation of Chromium, Phys. Rev. Lett. **94**, 160401 (2005).

[39] T. Lahaye, T. Koch, B. Fröhlich, M. Fattori, J. Metz, A. Griesmaier, S. Giovanazzi, and T. Pfau, Strong dipolar effects in a quantum ferrofluid, Nature (London) **448**, 672 (2007).

[40] T. Koch, T. Lahaye, J. Metz, B. Fröhlich, A. Griesmaier, and T. Pfau, Stabilization of a purely dipolar quantum gas against collapse, Nat. Phys. **4**, 218 (2008).

[41] Q. Beaufils, R. Chicireanu, T. Zanon, B. Laburthe-Tolra, E. Marèchal, L. Vernac, J.-C. Keller, and O. Gorceix, All-optical production of chromium Bose-Einstein condensates, Phys. Rev. A **77**, 061601(R) (2008).

[42] T. Lahaye, C. Menotti, L. Santos, M. Lewenstein, and T. Pfau, The physics of dipolar bosonic quantum gases, Rep. Prog. Phys. **72**, 126401 (2009).

[43] M. Lu, N. Q. Burdick, S. H. Youn, and B. L. Lev, Strongly Dipolar Bose-Einstein Condensate of Dysprosium, Phys. Rev. Lett. **107**, 190401 (2011).

[44] K. Aikawa, A. Frisch, M. Mark, S. Baier, A. Rietzler, R. Grimm, and F. Ferlaino, Bose-Einstein Condensation of Erbium, Phys. Rev. Lett. **108**, 210401 (2012).

[45] N. I. Nikolov, D. Neshev, O. Bang, and W. Z. Królikowski, Quadratic solitons as nonlocal solitons, Phys. Rev. E **68**, 036614 (2003).

[46] W. Królikowski, O. Bang, N. I. Nikolov, J. Wyller, J. J. Rasmussen, and D. Edmundson, Modulational instability, solitons and beam propagation in spatially nonlocal nonlinear media, J. Opt. B **6**, S288 (2004).

[47] N. I. Nikolov, D. Neshev, W. Królikowski, O. Bang, J. J. Rasmussen, and P. L. Christiansen, Attraction of nonlocal dark optical solitons, Opt. Lett. **29**, 286 (2004).

[48] Q. Kong, Q. Wang, and W. Królikowski, Analytical theory of dark nonlocal solitons, Opt. Lett. **35**, 2152 (2010).

[49] W. Chen, M. Shen, Q. Kong, J. Shi, Q. Wang, and W. Królikowski, Interactions of nonlocal dark solitons under competing cubic-quintic nonlinearities, Opt. Lett. **39**, 1764 (2014).

[50] A. Dreischuh, D. N. Neshev, D. E. Petersen, O. Bang, and W. Królikowski, Observation of Attraction between Dark Solitons, Phys. Rev. Lett. **96**, 043901 (2006).

[51] C. Conti, A. Fratalocchi, M. Peccianti, G. Ruocco, and S. Trillo, Observation of a Gradient Catastrophe Generating Solitons, Phys. Rev. Lett. **102**, 083902 (2009).

[52] A. P. Polychronakos, Waves and Solitons in the Continuum Limit of the Calogero-Sutherland Model, Phys. Rev. Lett. **74**, 5153 (1995).

[53] I. Andrić, V. Bardek, and L. Jonke, Solitons in the Calogero-Sutherland collective-field model, Phys. Lett. B **357**, 374 (1995).

[54] D. Sen and R. K. Bhaduri, Applications of the collective field theory for the Calogero-Sutherland model, Ann. Phys. **260**, 203 (1997).

[55] V. Bardek, J. Feinberg, and S. Meljanac, Density waves in the Calogero model—Revisited, Ann. Phys. **325**, 691 (2010).

[56] M. J. Edmonds, T. Bland, D. H. J. O'Dell, and N. G. Parker, Exploring the stability and dynamics of dipolar matter-wave dark solitons, Phys. Rev. A **93**, 063617 (2016).

[57] P. Pedri and L. Santos, Two-Dimensional Bright Solitons in Dipolar Bose-Einstein Condensates, Phys. Rev. Lett. **95**, 200404 (2005).

[58] J. Cuevas, B. A. Malomed, P. G. Kevrekidis, and D. J. Frantzeskakis, Solitons in quasi-one-dimensional Bose-Einstein condensates with competing dipolar and local interactions, Phys. Rev. A **79**, 053608 (2009).

[59] B. B. Baizakov, S. M. Al-Marzoug, and H. Bahlouli, Interaction of solitons in one-dimensional dipolar Bose-Einstein condensates and formation of soliton molecules, Phys. Rev. A **92**, 033605 (2015).

[60] K. Pawlowski and K. Rzazewski, Dipolar dark solitons, New J. Phys. **17**, 105006 (2015).

[61] T. Bland, M. J. Edmonds, N. P. Proukakis, A. M. Martin, D. H. J. O'Dell, and N. G. Parker, Controllable nonlocal interactions between dark solitons in dipolar condensates, Phys. Rev. A **92**, 063601 (2015).

[62] A. Triay, Derivation of the dipolar Gross-Pitaevskii energy, SIAM J. Math. Anal. **50**, 33 (2018).

[63] A. Eychenne and N. Rougerie, On the stability of 2D dipolar Bose-Einstein condensates arXiv:1809.07085 (2018).

[64] M. J. Ablowitz and Z. H. Musslimani, Integrable nonlocal nonlinear equations, Stud. Appl. Math. **139**, 7 (2017).

[65] M. Ablowitz, I. Bakirtas, and B. Ilan, Wave collapse in a class of nonlocal nonlinear Schrödinger equations, Physica D **207**, 230 (2005).

[66] S. V. Manakov, On the theory of two-dimensional stationary self-focusing of electromagnetic waves, Zh. Eksp. Tecr. Fiz. **65**, 505 (1973) [Sov. Phys.-JETP **38**, 248 (1974)].

[67] P. G. Kevrekidis and D. J. Frantzeskakis, Solitons in coupled nonlinear Schrödinger models: A survey of recent developments, Rev. Phys. **1**, 140 (2016).

[68] S. G. Evangelides, L. F. Mollenauer, J. P. Gordon, and N. S. Bergano, Polarization multiplexing with solitons, J. Lightwave Technol. **10**, 28 (1992).

[69] P. K. A. Wai and C. R. Menyuk, Polarization decorrelation in optical fibers with randomly varying birefringence, Opt. Lett. **19**, 1517 (1994).

[70] J. Yang, Physically significant nonlocal nonlinear Schrödinger equation and its soliton solutions, Phys. Rev. E **98**, 042202 (2018).

[71] R. A. Van Gorder, Quantum Hasimoto transformation and nonlinear waves on a superfluid vortex filament under the quantum local induction approximation, Phys. Rev. E **91**, 053201 (2015).

[72] P. Jetzer, Boson stars, Phys. Rep. **220**, 163 (1992).

[73] F. E. Schunck and E. W. Mielke, General relativistic boson stars, Class. Quantum Grav. **20**, R301 (2003).

[74] E. Seidel and W.-M. Suen, Formation of Solitonic Stars through Gravitational Cooling, Phys. Rev. Lett. **72**, 2516 (1994).

[75] S. Khlebnikov, Short-scale gravitational instability in a disordered Bose gas, Phys. Rev. D **62**, 043519 (2000).

[76] A. Elgart and B. Schlein, Mean field dynamics of boson stars, Commun. Pure Appl. Math. **60**, 500 (2007).

[77] P. Sikivie and Q. Yang, Bose-Einstein Condensation of Dark Matter Axions, Phys. Rev. Lett. **103**, 111301 (2009).

[78] O. Erken, P. Sikivie, H. Tam, and Q. Yang, Cosmic axion thermalization, Phys. Rev. D **85**, 063520 (2012).

[79] H.-Y. Schive, T. Chiueh, and T. Broadhurst, Cosmic structure as the quantum interference of a coherent dark wave, Nat. Phys. **10**, 496 (2014).

[80] D. G. Levkov, A. G. Panin, and I. I. Tkachev, Relativistic Axions from Collapsing Bose Stars, Phys. Rev. Lett. **118**, 011301 (2017).

[81] D. G. Levkov, A. G. Panin, and I. I. Tkachev, Gravitational Bose-Einstein Condensation in the Kinetic Regime, Phys. Rev. Lett. **121**, 151301 (2018).

[82] I. M. Moroz, R. Penrose, and P. Tod, Spherically-symmetric solutions of the Schrödinger-Newton equations, Class. Quantum Grav. **15**, 2733 (1998).

[83] M. Bahrami, A. Großardt, S. Donadi, and A. Bassi, The Schrödinger-Newton equation and its foundations, New J. Phys. **16**, 115007 (2014).

[84] D. O'Dell, S. Giovanazzi, G. Kurizki, and V. M. Akulin, Bose-Einstein Condensates with $1/r$ Interatomic Attraction: Electromagnetically Induced "Gravity," Phys. Rev. Lett. **84**, 5687 (2000).

[85] S. Giovanazzi, G. Kurizki, I. E. Mazets, and S. Stringari, Collective excitations of a "gravitationally" self-bound Bose gas, Europhys. Lett. **56**, 1 (2001).

[86] M. Antoni and S. Ruffo, Clustering and relaxation in Hamiltonian long-range dynamics, Phys. Rev. E **52**, 2361 (1995).

[87] M. Kac, G. E. Uhlenbeck, and P. C. Hemmer, On the van der Waals theory of the vapor-liquid equilibrium. I. Discussion of a one-dimensional model, J. Math. Phys. **4**, 216 (1963).

[88] T. Dauxois, V. Latora, and A. Rapisarda, The Hamiltonian mean field model: From dynamics to statistical mechanics and back, *Dynamics and Thermodynamics of Systems with Long-Range Interactions*, Lecture Notes in Physics, Vol. 602 (Springer, Berlin, 2002), pp. 458–487.

[89] A. Campa, T. Dauxois, and S. Ruffo, Statistical mechanics and dynamics of solvable models with long-range interactions, Phys. Rep. **480**, 57 (2009).

[90] Y. Levin, R. Pakter, F. B. Rizzato, Ta. N. Teles, and F. P. C. Benetti, Nonequilibrium statistical mechanics of systems with long-range interactions, Phys. Rep. **535**, 1 (2014).

[91] S. Schütz and G. Morigi, Prethermalization of Atoms Due to Photon-Mediated Long-Range Interactions, Phys. Rev. Lett. **113**, 203002 (2014).

[92] A. T. Black, H. W. Chan, and V. Vuletić, Observation of Collective Friction Forces due to Spatial Self-Organization of Atoms: From Rayleigh to Bragg Scattering, Phys. Rev. Lett. **91**, 203001 (2003).

[93] K. Baumann, C. Guerlin, F. Brennecke, and T. Esslinger, Dicke quantum phase transition with a superfluid gas in an optical cavity, Nature (London) **464**, 1301 (2010).

[94] R. Mottl, F. Brennecke, K. Baumann, R. Landig, T. Donner, and T. Esslinger, Roton-type mode softening in a quantum gas with cavity-mediated long-range interactions, Science **336**, 1570 (2012).

[95] J. Léonard, A. Morales, P. Zupancic, T. Esslinger, and T. Donner, Supersolid formation in a quantum gas breaking a continuous translational symmetry, Nature (London) **543**, 87 (2017).

[96] J. G. Cosme, C. Georges, A. Hemmerich, and L. Mathey, Dynamical Control of Order in a Cavity-BEC System, Phys. Rev. Lett. **121**, 153001 (2018).

[97] R. M. Kroeze, Y. Guo, V. D. Vaidya, J. Keeling, and B. L. Lev, Spinor Self-Ordering of a Quantum Gas in a Cavity, Phys. Rev. Lett. **121**, 163601 (2018).

[98] S. Schütz, S. B. Jäger, and G. Morigi, Thermodynamics and dynamics of atomic self-organization in an optical cavity, Phys. Rev. A **92**, 063808 (2015).

[99] S. Schütz, S. B. Jäger, and G. Morigi, Dissipation-Assisted Prethermalization in Long-Range Interacting Atomic Ensembles, Phys. Rev. Lett. **117**, 083001 (2016).

[100] T. Keller, S. B. Jäger, and G. Morigi, Phases of cold atoms interacting via photon-mediated long-range forces, J. Stat. Mech. (2017) 064002.

[101] T. Keller, V. Torggler, S. B. Jäger, S. Schütz, H. Ritsch, and G. Morigi, Quenches across the self-organization transition in multimode cavities, New J. Phys. **20**, 025004 (2018).

[102] J. Binney and S. Tremaine, *Galactic Dynamics* (Princeton University Press, Princeton, 2011).

[103] D. Lynden-Bell, Statistical mechanics of violent relaxation in stellar systems, Mon. Not. R. Astron. Soc. **136**, 101 (1967).

[104] Y. Y. Yamaguchi, One-dimensional self-gravitating sheet model and Lynden-Bell statistics, Phys. Rev. E **78**, 041114 (2008).

[105] R. Pakter and Y. Levin, Core-Halo Distribution in the Hamiltonian Mean-Field Model, Phys. Rev. Lett. **106**, 200603 (2011).

[106] T. Dauxois, P. Holdsworth, and S. Ruffo, Violation of ensemble equivalence in the antiferromagnetic mean-field XY model, Eur. Phys. J. B **16**, 659 (2000).

[107] F. Leyvraz, M.-C. Firpo, and S. Ruffo, Violation of ensemble equivalence in the antiferromagnetic mean-field XY model, J. Phys. A **35**, 4413 (2002).

[108] J. Barré, F. Bouchet, T. Dauxois, and S. Ruffo, Out-of-Equilibrium States as Statistical Equilibria of an Effective Dynamics in a System with Long-Range Interactions, Phys. Rev. Lett. **89**, 110601 (2002).

[109] J. Barré, F. Bouchet, T. Dauxois, and S. Ruffo, Birth and long-time stabilization of out-of-equilibrium coherent structures, Eur. Phys. J. B **29**, 577 (2002).

[110] J. Ye, S. Sachdev, and N. Read, Solvable Spin Glass of Quantum Rotors, Phys. Rev. Lett. **70**, 4011 (1993).

[111] T. K. Kopeć, Infinite-range-interaction M-component quantum spin glasses: Statics and dynamics in the large-M limit, Phys. Rev. B **50**, 9963 (1994).

[112] N. Read, S. Sachdev, and J. Ye, Landau theory of quantum spin glasses of rotors and Ising spins, Phys. Rev. B **52**, 384 (1995).

[113] M. P. Kennett, C. Chamon, and J. Ye, Aging dynamics of quantum spin glasses of rotors, Phys. Rev. B **64**, 224408 (2001).

[114] S. Sachdev, *Quantum Phase Transitions* (Cambridge University Press, Cambridge, 2011).

[115] P.-H. Chavanis, The quantum HMF model: I. Fermions, J. Stat. Mech. (2011) P08002.

[116] P.-H. Chavanis, The quantum HMF model: II. Bosons, J. Stat. Mech. (2011) P08003.

[117] R. Plestid, P. Mahon, and D. H. J. O'Dell, Violent relaxation in quantum fluids with long-range interactions, Phys. Rev. E **98**, 012112 (2018).

[118] W. Braun and K. Hepp, The Vlasov dynamics and its fluctuations in the 1/n limit of interacting classical particles, Commun. Math. Phys. **56**, 101 (1977).

[119] S. Ogawa and Y. Y. Yamaguchi, Linear response theory in the Vlasov equation for homogeneous and for inhomogeneous quasistationary states, Phys. Rev. E **85**, 061115 (2012).

[120] A. Patelli and S. Ruffo, General linear response formula for non integrable systems obeying the Vlasov equation, Eur. Phys. J. D **68**, 329 (2014).

[121] L. Pitaevskii and S. Stringari, *Bose-Einstein Condensation*, International Series of Monographs on Physics (Clarendon Press, Oxford, 2003).

[122] G. Wolf, Mathieu functions and Hills equation, in *NIST Handbook of Mathematical Functions*, edited by F. W. J. Olver, D. W. Lozier, R. F. Boisvert, and C. W. Clark (Cambridge University Press, Cambridge, 2010), Vol. 5, p. 966.

[123] B. Prasanna Venkatesh, M. Trupke, E. A. Hinds, and D. H. J. O'Dell, Atomic Bloch-Zener oscillations for sensitive force measurements in a cavity, Phys. Rev. A **80**, 063834 (2009).

[124] B. Prasanna Venkatesh, J. Larson, and D. H. J. O'Dell, Band-structure loops and multistability in cavity QED, Phys. Rev. A **83**, 063606 (2011).

[125] B. P. Venkatesh and D. H. J. O'Dell, Bloch oscillations of cold atoms in a cavity: Effects of quantum noise, Phys. Rev. A **88**, 013848 (2013).

[126] H. Keßler, J. Klinder, B. Prasanna Venkatesh, Ch. Georges, and A. Hemmerich, *In situ* observation of optomechanical Bloch oscillations in an optical cavity, New J. Phys. **18**, 102001 (2016).

[127] Ch. Georges, J. Vargas, H. Keßler, J. Klinder, and A. Hemmerich, Bloch oscillations of a Bose-Einstein condensate in a cavity-induced optical lattice, Phys. Rev. A **96**, 063615 (2017).

[128] M. D. Lee, S. D. Jenkins, Y. Bronstein, and J. Ruostekoski, Stochastic electrodynamics simulations for collective atom response in optical cavities, Phys. Rev. A **96**, 023855 (2017).

[129] J. Goldwin, B. P. Venkatesh, and D. H. J. O'Dell, Backaction-Driven Transport of Bloch Oscillating Atoms in Ring Cavities, Phys. Rev. Lett. **113**, 073003 (2014).

[130] M. Samoylova, N. Piovella, G. R. M. Robb, R. Bachelard, and Ph. W. Courteille, Synchronization of Bloch oscillations by a ring cavity, Opt. Express **23**, 14823 (2015).

[131] M. Coles and D. Pelinovsky, Loops of energy bands for Bloch waves in optical lattices, Stud. Appl. Math. **128**, 300 (2012).

[132] B. Eiermann, Th. Anker, M. Albiez, M. Taglieber, P. Treutlein, K.-P. Marzlin, and M. K. Oberthaler, Bright Bose-Einstein Gap Solitons of Atoms with Repulsive Interaction, Phys. Rev. Lett. **92**, 230401 (2004).

[133] B. Wu and Q. Niu, Nonlinear Landau-Zener tunneling, Phys. Rev. A **61**, 023402 (2000).

[134] J. C. Bronski, L. D. Carr, B. Deconinck, and J. N. Kutz, Bose-Einstein Condensates in Standing Waves: The Cubic Nonlinear Schrödinger Equation with a Periodic Potential, Phys. Rev. Lett. **86**, 1402 (2001).

[135] B. Wu and Q. Niu, Superfluidity of Bose-Einstein condensate in an optical lattice: Landau-Zener tunnelling and dynamical instability, New J. Phys. **5**, 104 (2003).

[136] M. Machholm, C. J. Pethick, and H. Smith, Band structure, elementary excitations, and stability of a Bose-Einstein condensate in a periodic potential, Phys. Rev. A **67**, 053613 (2003).

[137] P. J. Y. Louis, E. A. Ostrovskaya, C. M. Savage, and Y. S. Kivshar, Bose-Einstein condensates in optical lattices: Band-gap structure and solitons, Phys. Rev. A **67**, 013602 (2003).

[138] M. Machholm, A. Nicolin, C. J. Pethick, and H. Smith, Spatial period doubling in Bose-Einstein condensates in an optical lattice, Phys. Rev. A **69**, 043604 (2004).

[139] J. Satsuma and N. Yajima, Initial value problems of one-dimensional self-modulation of nonlinear waves in dispersive media, Prog. Theor. Phys. Supp. **55**, 284 (1974).

[140] V. E. Zakharov and A. B. Shabat, Exact theory of two-dimensional self-focusing and one-dimensional self-modulation of waves in nonlinear media, Sov. Phys. JETP **34**, 62 (1972).

[141] R. Sips, Representation asymptotique des fonctions de Mathieu et des fonctions d'onde spheroidales, Trans. Am. Math. Soc. **66**, 93 (1949).

[142] R. Sips, Représentation asymptotique des fonctions de Mathieu et des fonctions sphéroidales. II, Trans. Am. Math. Soc. **90**, 340 (1959).

[143] R. B. Dingle and H. J. W. Müller, Asymptotic expansions of Mathieu functions and their characteristic numbers, J. Reine Angew. Math. **211**, 11 (1962).

[144] D. Frenkel and R. Portugal, Algebraic methods to compute Mathieu functions, J. Phys. A **34**, 3541 (2001).

[145] Y. Castin, Bose-Einstein condensates in atomic gases: Simple theoretical results, in *Coherent Atomic Matter Waves*, edited by R. Kaiser, C. Westbrook, and F. David (Springer, Berlin, 2001), pp. 1–136.

[146] R. Plestid and J. Lambert (unpublished).

"...if fluctuations dominate the mean value, then mean field theory will become unreliable and potentially quite wrong. Now use mean field theory to predict its own demise."

— Leo Kadanoff

CHAPTER 4

Centre of Mass Fluctuations and the Many-Body Ground State

Ryan Plestid, and James Lambert
Quantum fluctuations vs. long-range interactions: the failure of mean-field theory in the quantum HMF model
To be submitted to Phys. Rev. E.

Long-range interacting systems are well described by mean-field theory both classically and quan tum mechanically. It is often claimed that mean-field theory is exact in the $N \to \infty$ limit for long range interacting systems. This has important implications for the HMF model because mean-field theory predicts that, for attractive interactions (i.e. $\epsilon < 0$), the model exhibits a quantum phase transition. This can be seen most easily by taking the Hartree energy for $\epsilon < 0$

$$\mathcal{E} = \int \mathrm{d}\theta \frac{\chi^2}{2} |\partial \Psi|^2 - \frac{1}{2} \int \mathrm{d}\theta \mathrm{d}\theta' |\Psi|^2(\theta) |\Psi|^2(\theta') \cos(\theta - \theta') \tag{4.1}$$

and inserting the ansatz $\psi = (2\pi)^{-1/2}(a_0 + \sqrt{2} a_1 \cos\theta)$ where $a_0 = \sqrt{(1 - 2|a_1|^2)}$ such that $\int \mathrm{d}\theta |\psi|^2 = 1$ with a_0 real. Then, the energy can be written as

$$\mathcal{E} = \frac{\chi^2}{2} a_1^2 - 2(a_0 a_1)^2 = (\chi^2 - 2) a_1^2 + 4 a_1^4 \tag{4.2}$$

which is the canonical form of the Landau free-energy for a second order phase transition. Therefore, as was first pointed out by Chavanis, mean-field theory predicts a second order phase transition at $\chi = \sqrt{2}$ for the HMF model with attractive interactions.

This agrees with the analysis of the previous paper in terms of Mathieu functions where the above analysis can be generalized to obtain an asymptotic expansion for ψ_0 in the vicinity of $\chi = \sqrt{2}$. Since the Hartree ansatz is expected to be accurate at $T = 0$ and so this would suggest that the model exhibits a quantum phase transition.

The GGPE does not include quantum fluctuations, rather, it results from a Hartree ansatz for the ground state wavefunction $\Psi(\theta_1, \theta_2, ..., \theta_N) = \prod_i \psi(\theta_i)$; we will call these states Hartree states. This restriction, which forces the candidate wavefunction to be a product state, is artifically imposed and it remains a logical possibility that non-product states may have lower energies. For instance, for $\chi < \sqrt{2}$, ψ_n spontaneously breaks the HMF model's $O(2)$ symmetry by selecting a position of maximum density. This necessarily implies that there exists of a continuous family of states all of which have degenerate energy, and so it is reasonable to expect that some linear combination of these product states may have a lower energy than any of the product states indivdually.

Our major focus in this paper is to determine if such a coherent super position of product states can realize a lower energy state with a restored $O(2)$ symmetry. If this is the case then at zero temperature the HMF model will not exhibit a quantum phase transition. The main focuses of this paper are:

- Is $O(2)$ symmetry broken in the HMF model?
- How do finite-N corrections influence the HMF model's symmetry breaking pattern?
- What are the consequences of our results for finite temperatures?

Quantum fluctuations inhibit symmetry breaking in the HMF model

Ryan Plestid[1, 2, *] and James Lambert[1, †]

[1] *Department of Physics & Astronomy, McMaster University, 1280 Main St. W., Hamilton, Ontario, Canada*
[2] *Perimeter Institute for Theoretical Physics, 31 Caroline St. N., Waterloo, Ontario, Canada*

(Dated: June 4, 2019)

It is widely believed that mean-field theory is exact for a wide-range of classical long-range interacting systems. Is this also true once quantum fluctuations have been accounted for? As a test case we study the Hamiltonian Mean Field (HMF) model for a system of indistinguishable bosons which is predicted (according to mean-field theory) to undergo a second-order quantum phase transition at zero temperature. The ordered phase is characterized by a spontaneously broken $O(2)$ symmetry, which, despite occurring in a one-dimensional model, is not ruled out by the Mermin-Wagner theorem due to the presence of long-range interactions. Nevertheless, a spontaneously broken symmetry implies gapless Goldstone modes whose large fluctuations can restore broken symmetries. In this work, we study the influence of quantum fluctuations by projecting the Hamiltonian onto the continuous subspace of symmetry breaking mean-field states. We find that the energetic cost of gradients in the center of mass wavefunction inhibit the breaking of the $O(2)$ symmetry, but that the energetic cost is very small — scaling as $\mathcal{O}(1/N^2)$. Nevertheless, for any finite N, no matter how large, this implies that the ground state has a restored $O(2)$ symmetry. Implications for the finite temperature phases, and classical limit, of the HMF model are discussed.

Systems with long-range interactions lie beyond the scope of traditional statistical mechanics [1–3]. They can exhibit ensemble inequivalence [1, 2, 4–6], divergent relaxation time scales (scaling as $t \gtrsim \log N$ for N particles) [7], and non-ergodic dynamics that lead to late-time states that disagree with the microcanonical ensemble [8–15] (preferring instead Lynden-Bell [16], or core-halo statistics [3, 17, 18]). While these features were first appreciated in the context of self-gravitating systems [16, 19], it has become increasingly clear that peculiarities of gravitational systems (such as negative specific heat [20] and the gravothermal heat catastrophe [21]) are special cases of a broader statistical theory of long-range interacting systems [1–3].

One important feature of long-range interactions is that fluctuations can be suppressed to such a degree that continuous symmetries can be spontaneously broken even in one-dimensional systems [1, 2, 22–26]. This can be understood in the context of lattice models by considering the coordination number of each lattice site. Long-range interactions lead to large coordination numbers, which is equivalent to considering the lattice in some effective dimension $d_{\text{eff}} > d$. Given that fluctuations are well known to be suppressed in high dimensional systems it is not surprising that long-range interactions can achieve the same effect. Mathematically the presence of long-range interactions invalidates the Mermin-Wagner theorem [27], and its inapplicability is what allows for spontaneous symmetry breaking in a low-dimensional long-range interacting system [2, 24, 26].

There is an extensive literature concerning the validity of mean-field theory for long-range interacting systems. For instance, in the classical literature, it has been rigorously proven [28] (i.e. with bounded error) that a long-range interacting system's exact dynamics are well approximated by a mean-field collisionless-Boltzmann (i.e. Vlasov) equation (see e.g. [3] or [7]). This approximation is valid on time scales of order $t \lesssim \mathcal{O}(\log N)$. Therefore, in the $N \to \infty$ limit, it is often said that the collisionless-Boltzmann equation (i.e. mean-field theory) is exact [3, 7, 28]. Similar claims exist for equilibrium physics. For instance, Lieb was able to rigorously bound the difference between a self-gravitating bosonic star's ground state energy and its Hartree energy, and showed that this difference vanishes in the thermodynamic limit [29]. Similarly, it is well known that long-range interacting spin models have mean-field critical exponents [23], and it was conjectured that their free-energy is also identical to that derived via a mean-field (meaning all-to-all interacting) model [30]. Subsequent studies supported this idea for long-range interacting spin systems [31–34], while more recent work has revealed disagreements between the all-to-all and power-law decaying models in a limited region of parameter space [35–37].

The success of all-to-all models in describing the thermodynamics of long-range interacting systems has led to them being an essential building block upon which modern statistical theories of long-range interacting systems are built. Examples include (for a review see [2]) the Emery-Blume-Griffiths model [4], the mean-field ϕ^4 model [38–40], and the Hamiltonian Mean Field (HMF) model [41].

Since its proposal in 1995 [41] the HMF model has been perhaps the most influential toy model in the long-range interacting community. Originally proposed as a simplified model of self-gravitating systems, it has emerged as a paradigmatic starting point, and tool, for understanding generic features of long-range interacting systems. While all-to-all (i.e. mean field) models were motivated above by appealing to equilibrium physics, they turn out to also capture dynamical behavior . The HMF model can be used as a tool for understanding chaos [42–

* plestird@mcmaster.ca
† lambej3@mcmaster.ca

45], violent relaxation [10, 17, 46–49], core-halo statistics [3, 17, 18], and other quasi-stationary states [10–12, 46] in long-range interacting systems. The HMF model exhibits a second order phase transition associated with the spontaneous breaking of a continuous $[O(2)]$ symmetry [1, 41]. The HMF model's canonical partition function can be calculated exactly in the classical limit, and exhibits ensemble equivalence with the microcanonical ensemble.

The HMF model describes particles of unit mass, on a circle of unit radius, interacting via a pairwise cosine potential. When quantized for N indistinguishable bosons, the HMF model is defined by the Hamiltonian [50]

$$\hat{H}_{\text{HMF}} = \sum_i \frac{\chi^2}{2}\frac{\partial^2}{\partial\theta_i^2} - \frac{1}{N}\sum_{i<j}\cos(\theta_i - \theta_j)\ . \tag{1}$$

Here χ is a dimensionless Planck's constant[1] and we have chosen the case of the attractive HMF model as indicated by the negative sign of the potential. The $\frac{1}{N}$ scaling in front of the cosine interaction, known as the Kac prescription [51], preserves extensivity of the Hamiltonian, and is a consequence of the peculiar thermodynamic limit for long-range interacting systems ($N \to \infty$ with system size, and χ held fixed [2, 50, 52]). Equation (1) can also be interpreted as a describing a lattice of $O(2)$ quantum rotors interacting with one another via all-to-all interactions with θ_i labeling the angle of each rotor on the lattice.

As mentioned above, classically (in the limit $\chi \to 0$) the model undergoes a thermal clustering transition [1] characterized by the order parameter

$$\mathbf{M} = \langle\cos\theta\rangle\hat{\mathbf{x}} + \langle\sin\theta\rangle\hat{\mathbf{y}}\ , \tag{2}$$

which, for $\mathbf{M} \neq 0$, implies a spontaneously broken $O(2)$ symmetry. This transition is second-order, and is driven by thermal fluctuations. At high temperatures, $T > T_c$, the system is homogeneous, and $\mathbf{M} = 0$. For low temperatures, $T < T_c$, the system spontaneously breaks its underlying $O(2)$ symmetry.

In addition to mimicking certain dynamical features of self-gravitating bosons [50] Eq. (1) is also closely related to a handful of quantum systems that can be realized in the lab. For instance, cold atoms loaded into optical cavities can realize the generalized HMF model, which is identical to Eq. (1) up to terms of the form $\sum_{i<j}\cos[\theta_i - \theta_j]$ [53, 54]. If, in the rotor interpretation of the model, the sum in Eq. (1) is restricted to be nearest neighbor rotors then it can be shown that this nearest-neighbor quantum rotor model offers a low energy description of bosons in an optical lattice [55] (i.e. a coupled set of Bose-Josephson junctions). Likewise a spin-S Heisenberg ladder with anti-ferromagnetic coupling can realize the $O(3)$ nearest neighbor quantum rotor model [55]. We would expect an infinite-range rotor model such as Eq. (1) to reproduce the physics of rotors with long-range (i.e. polynomially decaying $1/|r_i - r_j|^\alpha$ with $\alpha < 1$) couplings as can be engineered in trapped ion systems [56–58].

Chavanis undertook the first study of the model's bosonic [50] (and fermionic [59]) equilibrium phase diagram. Using a Hartree ansatz, one finds that for $\chi < \sqrt{2}$ the lowest Hartree-energy state also spontaneously breaks the $O(2)$ symmetry, becoming a delta-function in the limit that $\chi \to 0$. For $\chi > \sqrt{2}$ it is found that the gradient energy for a single-particle wavefunction is no longer compensated for by the gain in interaction energy; this leads to a homogeneous ground state. Both of these two behaviors connect smoothly with the model's limiting cases: For $\chi \to 0$ this agrees with the $T \to 0$ prediction of the classical HMF model. For $\chi \to \infty$ we recover an ideal Bose gas in a finite volume, the ground state of which is indeed a homogeneous product state.

Recently, the HMF model has been considered as a quantum dynamical system. The quantum analogue of certain classical behaviors, such as violent relaxation, and the formation of quasi stationary states has been studied [48]. Interestingly, classical instabilities related to the formation of bi-clusters [10, 11] have been found to be stabilized by quantum (kinetic) pressure [48]. The HMF model's Gross-Pitaevskii equation has also been found to admit exactly solvable solitary wave solutions [60]. In fact, the Hartree states considered by Chavanis [50] may be considered as a special case of these solutions.

In this paper we make use of the exact solutions of [60] to systematically study whether quantum effects beyond mean-field theory can modify the HMF model's symmetry breaking pattern at zero temperature. In particular, the mean-field (i.e. Hartree) prediction of a spontaneously broken $[O(2)]$ symmetry suggests a highly degenerate ground state; if there is one ground state $|\Theta\rangle$ with its center of mass at Θ, then there must be continuous manifold of such states $\{|\Theta'\rangle\}$ with $\Theta' \in [-\pi, \pi)$. This is reminiscent, for instance, of spinor Bose-Einstein condensates, whose exact ground state is a continuous quantum superposition of mean-field solutions [61, 62]; we term these states *continuous cat states* (CCS). In our example, such states would correspond to fluctuations of the center of mass, or, equivalently of a low-lying Goldstone excitation related to the broken $O(2)$ symmetry.

We focus on computing matrix elements of the Hamiltonian between different Hartree states, $\langle\Theta|\,\hat{H}_{\text{HMF}}\,|\Theta'\rangle$. Translational invariance, and parity, ensures that these matrix elements can depend only on the difference $|\Theta - \Theta'|$. Then, since the Hartree states tend towards delta functions, we can expect a delta-expansion (in terms of derivatives of the Dirac-delta function) to provide a good approximation of their behavior. Projecting the Hamiltonian onto this subset of states and using this expansion we may then infer whether or not quantum fluctuations of the center of mass raise, or lower, the energy.

Viewing the HMF model as archetypal of long-range interacting systems, it is natural to study how the

[1] For a ring of radius R, with particles of mass, m, and a prefactor of ϵ multiplying the cosine interaction $\chi = \hbar/\sqrt{mR^2\epsilon}$.

model's phase diagram is modified by quantum effects. Mapping out the phase diagram for the HMF model in the $\chi - T$ plane is a natural, and important, addition to the cannon of literature surrounding the HMF model. In this paper we take the first step towards this goal by studying the role of quantum fluctuations at zero temperature.

The rest of the paper is dedicated to calculating the energetic cost (or profit) of center of mass fluctuations as sketched above. In Section I we review the Hartree analysis for the HMF model [50, 60] which will serve as a starting point for our analysis. In Section II we calculate matrix elements of the Hamiltonian between different CCS. In Section III we develop a large-N asymptotic series for the energy of a given CCS. Then, in Section IV we obtain explicit expressions for the energy at leading order in χ; this allows us to determine the symmetry breaking properties of the ground state. Finally, in Section V we summarize our results and suggest future directions for the quantum HMF model.

I. MEAN FIELD THEORY

Mean-field theory for the bosonic HMF model at zero temperature is equivalent to a product-state ansatz for the ground state. Taking $|\Psi\rangle = \bigotimes |\psi\rangle$, with $|\psi\rangle$ a single particle state leads to an energy functional $\mathcal{E}[\psi] = \langle\Psi| \hat{H}_{\text{HMF}} |\Psi\rangle$. Minimizing this energy with respect to the single particle wavefunctions, $\delta\mathcal{E}/\delta\psi = 0$ then leads to a self-consistent eigenvalue problem [60]

$$-\frac{1}{2}\partial_\theta^2\psi_H + M\cos\theta\psi_H = \mu\psi_H \tag{3}$$

where μ is the chemical potential, and M is the aforementioned order parameter of Eq. (2); in the Hartree theory, M must be determined self-consistently. Equation (3) is exactly soluble, and its solutions can be expressed in terms of Mathieu functions [60, 63]

$$\psi_H(\theta) = \frac{1}{\sqrt{\pi}}\text{ce}_0\left(\tfrac{\theta-\pi}{2}; q[\chi]\right) , \tag{4}$$

where $q(\chi)$ is the depth-parameter of the Mathieu equation [63], whose dependence on χ can be determined by solving the self-consistency condition

$$q = \frac{4M}{\chi^2} \tag{5}$$

In this context, the magnetization may be thought of as a function of q, and is defined via the integral

$$M(q) = \frac{1}{\pi}\int_{-\pi}^{\pi}\left[\text{ce}_0\left(\tfrac{\theta-\pi}{2}; q\right)\right]^2\cos\theta \ . \tag{6}$$

Solving Eq. (3), one finds that for $\chi > \sqrt{2}$ the magnetization vanishes, $M = 0$, and that the lowest energy wavefunction is homogeneous i.e. $\psi_H = 1/\sqrt{2\pi}$ [50]. Furthermore, a Bogoliubov theory of fluctuations about this ground state can be constructed, and it can be easily checked that the quantum depletion of the ground state $\sum_{k\neq 0}\langle a_k^\dagger a_k\rangle_{T=0}$ (with a_k the atomic ladder operator) is finite, being given by $\sum_{k\neq 0}\sinh^2\theta_k$ with $\sinh^2\theta_k = \frac{1}{2}\left(\sqrt{1-2\delta_{k,\pm1}/\chi^2}-1\right)$.

For $\chi < \sqrt{2}$ one finds instead that $M \neq 0$ and the ground state wavefunction begins to acquire non-zero curvature, with the explicit wave-function being give by Eq. (4). The transition between the spatially homogeneous ground state and the spatially localized ground state can be viewed as a quantum phase transition associated with the spontaneous breaking of translational invariance; the transition is predicted to be second order.

This simplified analysis then predicts that there is a degenerate manifold of ground states, given by $|\Theta; N\rangle = \bigotimes |\psi_H;\Theta\rangle$ where Θ labels the wavefunction's center of mass (COM), such that $\psi_H(\theta-\Theta) = \langle\theta|\psi_H;\Theta\rangle$ is peaked at $\theta = \Theta$. For this kind of mean-field analysis to be self-consistent, however, we require that quantum fluctuations of the COM are small *a posteori*. Because the clustered phase is characterized by a spontaneously broken continuous symmetry, we must then consider fluctuations of gapless excitations corresponding to the shift symmetry $\Theta \to \Theta + \Delta\Theta$.

II. CENTER OF MASS FLUCTUATIONS

We can study the importance of COM fluctuations by considering a CCS

$$|\mathfrak{f}; N\rangle = \int \mathrm{d}\Theta\ \mathfrak{f}(\Theta)\,|\Theta; N\rangle \tag{7}$$

where $\mathfrak{f}$ is the COM wavefunction, such that $|\mathfrak{f}; N\rangle$ is a coherent superposition of product states centered about Θ. The product states

$$|\Theta; N\rangle = \bigotimes_{i=1}^{N}|\psi_H;\Theta\rangle \tag{8}$$

are composed of single particle wavefunctions, centered at Θ, $\psi_H(\theta-\Theta) = \langle\theta|\psi_H;\Theta\rangle$, that minimize the Hartree (i.e. mean-field) energy.

The case of $\mathfrak{f} \propto \delta(\Theta)$ corresponds to a Hartree state (localized about a single COM) whereas if $\mathfrak{f}(\Theta)$ is independent of Θ then this state has a restored translational invariance. To test whether or not quantum fluctuations restore translational symmetry we can compute the average energy of a CCS. We are therefore interested in minimizing the energy-per-particle

$$E[\mathfrak{f}] = \frac{1}{N}\langle\mathfrak{f}; N|\,\hat{H}_{\text{HMF}}\,|\mathfrak{f}; N\rangle \ . \tag{9}$$

Because of the system's translational invariance, we can guarantee that the resulting functional can be diagonalized in momentum space

$$E[\mathfrak{f}] = \sum_k \hat{E}(k)|\hat{\mathfrak{f}}(k)|^2, \tag{10}$$

where $\mathfrak{f}(\Theta) = \sum_k \mathrm{e}^{\mathrm{i}k\Theta}\hat{\mathfrak{f}}(k)/\sqrt{2\pi}$. Studying the variational problem $\delta\hat{E}/\delta\mathfrak{f} = 0$ is equivalent to minimizing $\hat{E}(k)|\mathfrak{f}(k)|^2$ subject to the constraint that $\langle\mathfrak{f};N|\mathfrak{f};N\rangle = 1$; we can therefore conclude without any loss of generality that the minimum energy COM wavefunction will be of the form $\mathfrak{f}_k(\Theta) = \mathrm{e}^{\mathrm{i}k\Theta}$ with $k \in \mathbb{Z}$.

It will be useful to introduce the functions

$$\mathcal{T}_H(y) = \frac{\chi^2}{2}\int \mathrm{d}\theta\partial\psi_H^*(\theta - \tfrac{1}{2}y)\partial\psi_H(\theta + \tfrac{1}{2}y) \tag{11}$$

and

$$\begin{aligned}\mathcal{V}_H(y) = \frac{1}{2}\int \mathrm{d}\theta\mathrm{d}\theta'\psi_H^*(\theta - \tfrac{1}{2}y)\psi_H^*(\theta' - \tfrac{1}{2}y)\\ \times\cos(\theta-\theta')\psi_H(\theta + \tfrac{1}{2}y)\psi_H(\theta' + \tfrac{1}{2}y)\ ,\end{aligned} \tag{12}$$

with $y = \Theta - \Theta'$. Throughout our analysis we will find that the Hamiltonian's matrix elements between two Hartree states $\langle\Theta_2;N|\,\hat{H}\,|\Theta_1;N\rangle$ can be expressed in terms of derivatives of the above functions evaluated at zero separation. With this in mind we introduce the following notation

$$\mathcal{V}_H^{(n)} = \partial_y^n\mathcal{V}_H(y)\Big|_{y=0} \text{ and } \mathcal{T}_H^{(n)} = \partial_y^n\mathcal{T}_H(y)\Big|_{y=0}\ . \tag{13}$$

Explicitly, the functions $\mathcal{V}_H(y)$ and $\mathcal{T}_H(y)$ are related to the the matrix elements of the kinetic, $\hat{T} = \sum_i \frac{1}{2m}\hat{p}_i^2$, and potential, $\hat{V} = -\frac{1}{N}\sum_{ij}\cos\Big(\hat{\theta}_i - \hat{\theta}_j\Big)$, operators via

$$\frac{1}{N}\langle\Theta_1;N|\,\hat{T}\,|\Theta_2;N\rangle = \mathcal{T}_H(y)O(y;N-1) \tag{14}$$

$$\frac{1}{N}\langle\Theta_1;N|\,\hat{V}\,|\Theta_2;N\rangle = -\mathcal{V}_H(y)\Big[\frac{N(N-1)}{N^2}\Big]O(y;N-2) \tag{15}$$

where we define the overlap

$$O(y;\aleph) = \langle\Theta_1;\aleph|\Theta_2;\aleph\rangle = [\langle\psi_H;\Theta_1|\psi_H;\Theta_2\rangle]^{\aleph}\ , \tag{16}$$

(with $\aleph = N,\ N-1,$ or, $N-2$), in terms of the coordinate difference $y = \Theta_1 - \Theta_2$. Introducing the COM coordinate $x = \frac{1}{2}(\Theta_1 + \Theta_2)$ we can write

$$E[\mathfrak{f}] = \int_{-\pi}^{\pi}\int_{-\pi}^{\pi}\mathrm{d}x\mathrm{d}y\ \mathfrak{f}^*\left(x - \tfrac{1}{2}y\right)\ \mathfrak{f}\left(x + \tfrac{1}{2}y\right)\ \Big[\mathcal{T}_H(y)O(y;N-1) - \mathcal{V}_H(y)\big[1 - \tfrac{1}{N}\big]O(y;N-2)\Big]\ , \tag{17}$$

from which we can immediately see that

$$\hat{E}(k) = \int_{-\pi}^{\pi}\mathrm{d}y\ \mathrm{e}^{-\mathrm{i}ky}\Big[\mathcal{T}_H(y)O(y;N-1) - \mathcal{V}_H(y)\big[1 - \tfrac{1}{N}\big]O(y;N-2)\Big]\ . \tag{18}$$

Note that in both Eqs. (17) and (18) all of the derivatives from the full many body Hamiltonian Eq. (1) appear in the functions $\mathcal{T}_H(y)$ and $\mathcal{V}_H(y)$ and they do not act directly on the COM wavefunction.

III. LARGE-N EXPANSION

We are ultimately interested in the thermodynamic limit ($N \to \infty$ with χ held fixed [50, 52]), and in particular whether sub-leading corrections in $1/N$ can modify the symmetry breaking pattern at zero temperature. To study this limit we develop an expansion that relies on the $\aleph$-body overlap, $O(y;\aleph)$, being tightly peaked for $\aleph \gg 1$. Because $O(y;\aleph) = [\langle\psi_H;\Theta_1|\psi_H;\Theta_2\rangle]^{\aleph}$ can be written as an exponentiated single particle overlap, this will be true even for moderately peaked single-particle overlaps. In the clustered phase, provided $\chi \lesssim 1$, the overlap between two Hartree states, $|\Theta_1;\aleph\rangle$ and $|\Theta_2;\aleph\rangle$, admits a δ-expansion of the form

$$O(y;\aleph) = \frac{1}{|C(\aleph,\chi)|^2}\left[\delta(y) + \sum_{p>0}\frac{\mathcal{K}_p(\chi)}{\aleph^p}\delta^{(2p)}(y)\right]\ . \tag{19}$$

We use this to develop a systematic expansion in $1/N$ by considering a perturbative expansion of the COM wavefunction

$$\mathfrak{f} = C(N,\chi)\Big(\mathfrak{f}_0 + \frac{1}{N}\mathfrak{f}_1 + \frac{1}{N^2}\mathfrak{f}_2 + ...\Big). \tag{20}$$

The multiplicative constant $C(N,\chi)$ is chosen such that $\langle\mathfrak{f}_0,\mathfrak{f}_0\rangle = \int\mathfrak{f}_0^*(x)\mathfrak{f}_0(x)\mathrm{d}x = 1$, which ensures that $\langle\mathfrak{f};N|\mathfrak{f};N\rangle = 1$ at leading order[2]. To maintain this normalization order by order in $1/N$ we impose the following

[2] The physical state overlap $\langle\mathfrak{f}|\mathfrak{f}\rangle$ differs from the L^2 inner product, $\langle\mathfrak{f},\mathfrak{f}\rangle$ at $\mathcal{O}(1/N)$ i.e. $\langle\mathfrak{f}|\mathfrak{f}\rangle = \langle\mathfrak{f},\mathfrak{f}\rangle + \mathcal{O}(1/N)$.

constraints on the COM wavefunction

$$\langle \mathfrak{f}_0, \mathfrak{f}_0\rangle = 1 \tag{21}$$

$$2\mathrm{Re}\langle \mathfrak{f}_1, \mathfrak{f}_0\rangle = \mathcal{K}_1\langle \mathfrak{f}_0^{(1)}, \mathfrak{f}_0^{(1)}\rangle \tag{22}$$

$$\langle \mathfrak{f}_1, \mathfrak{f}_1\rangle + 2\mathrm{Re}\langle \mathfrak{f}_0, \mathfrak{f}_2\rangle = \mathcal{K}_1\ 2\mathrm{Re}\langle \mathfrak{f}_1^{(1)}, \mathfrak{f}_0^{(1)}\rangle - \mathcal{K}_2\langle \mathfrak{f}_0^{(2)}, \mathfrak{f}_0^{(2)}\rangle \tag{23}$$

which can be derived using Eq. (19) and identity Eq. (A5). Note that, as above, the inner product $\langle \mathfrak{f}_i, \mathfrak{f}_j\rangle = \int \mathrm{d}x \mathfrak{f}_i^*(x)\mathfrak{f}_j(x)$ is the L^2 inner product, and should not be confused with the state overlap $\langle \mathfrak{f}|\mathfrak{f}\rangle$.

These normalization constraints play an important role in the calculation of the energy as discussed in Appendix B. Due to non-trivial correlations between $\mathfrak{f}_1$ and $\mathfrak{f}_0$, expanding $\hat{E}(k)$ directly will not tell us how the energy $E[\mathfrak{f}]$ depends on the wavefunction $\mathfrak{f}$. Rather, one must expand $\mathfrak{f}$ and $\hat{E}(k)$ concurrently.

$$\hat{E}(k) = \frac{1}{|C(N,\chi)|^2}\left[\hat{E}_0 + \frac{1}{N}\hat{E}_1 + \frac{1}{N^2}\hat{E}_2 + \ ...\ \right], \tag{24}$$

where $\hat{E}_0 = E_H$, with $E_H = \mathcal{T}_H^{(0)} - \mathcal{V}_H^{(0)}$ the Hartree energy. We find that $\hat{E}$ is given by

$$\hat{E}(k)|\mathfrak{f}(k)|^2 = \hat{E}_0|\mathfrak{f}_0|^2 + \frac{1}{N}\left[\hat{E}_1|\mathfrak{f}_0|^2 + 2\hat{E}_0\mathrm{Re}\ \mathfrak{f}_0^*\mathfrak{f}_1\right] + \frac{1}{N^2}\left[\hat{E}_2|\mathfrak{f}_0|^2 + \hat{E}_1|\mathfrak{f}_1|^2 + 2\hat{E}_0\mathrm{Re}\ \mathfrak{f}_0^*\mathfrak{f}_2\right]. \tag{25}$$

By using Eqs. (21) to (23), the above expression can be simplified such that $E[\mathfrak{f}] = \sum_k \hat{E}(k)|\mathfrak{f}(k)|^2$ can be written as

$$E[\mathfrak{f}] = E_0 + \frac{E_2}{N^2}\langle \mathfrak{f}_0^{(1)}, \mathfrak{f}_0^{(1)}\rangle + \mathcal{O}\left(\frac{1}{N^3}\right) \tag{26}$$

or at the same level of accuracy

$$E[\mathfrak{f}] = E_0 + \frac{E_2}{N^2}\langle \mathfrak{f}^{(1)}, \mathfrak{f}^{(1)}\rangle + \mathcal{O}\left(\frac{1}{N^3}\right) \tag{27}$$

Equation (27) controls the symmetry breaking in the HMF model. Naively, the term E_2 is irrelevant in the thermodynamic limit [being $\mathcal{O}(1)$], however, because the leading order term predicts a degenerate ground state, the small $\mathcal{O}\big(1/N^2\big)$ perturbation $\hat{E}_2$ dictates the symmetry breaking pattern of the ground state. The sign of E_2 dictates whether in-homogeneity (i.e. non-zero values of k) raises or lowers the energy of a CCS, and is consequently indicative of whether or not quantum fluctuations can destroy the localized (magnetized) phase. The full details of our calculation can be found in Appendix B, however for brevity's sake we simply quote the leading order contribution for each quantity

$$E_0 = E_H + \frac{1}{N}[\mathcal{T}_H^{(2)} - \mathcal{V}_H^{(2)} - \tfrac{1}{2}\mathcal{T}_H^{(0)}] + \mathcal{O}\left(\frac{1}{N^2}\right), \tag{28}$$

and

$$E_2 = [\mathcal{K}_1^2 - 6\mathcal{K}_2][\mathcal{T}_H^{(2)} - \mathcal{V}_H^{(2)}] - \mathcal{K}_1[\mathcal{T}_H^{(0)} - 2\mathcal{V}_H^{(0)}]\ . \tag{29}$$

The fact that gradient corrections vanish at $\mathcal{O}(1/N)$ is a consequence of a cancellation between the $\hat{E}_1|\mathfrak{f}_0|^2$ and $2\hat{E}_0\mathrm{Re}\ \mathfrak{f}_0^*\mathfrak{f}_1$ in Eq. (25). This cancellation is not accidental, and is discussed in greater detail in Appendix B 4

IV. STRONG COUPLING REGIME

To determine whether these fluctuations can restore translational invariance we can study a point in parameter space deep within the clustered phase $\chi \lesssim 1$ and see if quantum fluctuations can lead to a translationally invariant COM wavefunction (i.e. $\mathfrak{f} = 1/\sqrt{2\pi}$). For this to occur $\hat{E}_2$ must be positive such that $k = 0$ is energetically preferred.

Although left implicit until now, the parameters $\mathcal{K}_1(\chi)$, and $\mathcal{K}_2(\chi)$ are themselves functions of χ as are the derivatives of the CCS energies $\mathcal{V}_H^{(n)}(\chi)$ and $\mathcal{T}_H^{(n)}(\chi)$. These functions are determined exactly in terms of integrals Eqs. (11) and (12) involving the Hartree ground state $\psi_H(\theta;\chi)$ (whose χ dependence is determined by Eq. (3)). To test whether quantum fluctuations of the COM can restore the spontaneously broken symmetry it is sufficient to restrict our attention to small but finite values of χ satisfying $\chi \ll \sqrt{2}$.

Both $\mathcal{K}_1$ and $\mathcal{K}_2$ are determined by $O(y;N,\chi)$. As argued in the appendix, for small values of χ this can be well approximated by (see Appendix C)

$$O(y;\aleph) \approx \left[\frac{I_0\big(\sqrt{q}\cos\frac{y}{2}\big)}{I_0\big(\sqrt{q}\big)}\right]^{\aleph} \tag{30}$$

where $I_0(z)$ is the modified Bessel function of the first kind and q is an auxiliary depth parameter related to the mean-field magnetization, M, and χ via $q = \sqrt{4M/\chi}$. We are interested in finding a delta-expansion for $O(y)$ and are thus interested in integrals of the form $\int_\pi^\pi O(y)f(y)\ \mathrm{d}y$. For $1 \lesssim y \lesssim \pi$ the overlap is exponentially small [i.e. $\mathcal{O}\big(\mathrm{e}^{-\sqrt{q}}\big)$] so we can neglect this contribution to the integral. For moderate values of y we can then use the large argument expansion of the modified Bessel functions $I_0(z) \sim \mathrm{e}^{-z}/\sqrt{2\pi z}$ leading to

$$O(y;\aleph) \sim \exp\left\{\aleph\left[\tfrac{4}{\chi}(1-\tfrac{1}{8}\chi)\sin^2\tfrac{y}{4} - \tfrac{1}{2}\log\cos\tfrac{y}{2}\right]\right\}\ . \tag{31}$$

Using this exponential form, the integrals we are interested in studying can then be approximated using Watson's Lemma

$$\int \mathrm{e}^{-\aleph G(y)} f(y)\mathrm{d}y \sim \sqrt{\frac{2\pi}{\aleph G^{(2)}}}\sum_p \frac{f^{(2p)}}{(2p)!!\big[\aleph G^{(2)}\big]^p}, \tag{32}$$

where the bracketed superscripts denote the $2p^{\text{th}}$ derivative of the function evaluated at $y = 0$. For $O(y;\aleph)$ we

have

$$G^{(2)} = \frac{1}{2\chi} - \frac{3}{16}. \tag{33}$$

We can then read off overall prefactor of Eq. (20)

$$|C(N,\chi)|^2 = \sqrt{\frac{2\pi}{NG^{(2)}}} = 2\sqrt{\frac{\pi\chi}{N}}\left[1 + \frac{3\chi}{32}\right] \tag{34}$$

and the coefficients $\mathcal{K}_1$ and $\mathcal{K}_2$ which are given at next-to-leading order

$$\mathcal{K}_1 \sim \chi + \frac{3\chi^2}{8} \qquad \mathcal{K}_2 \sim \frac{\chi^2}{2} + \frac{3\chi^3}{8} \tag{35}$$

Next, using Eq. (C6) for the Mathieu functions, we can derive the small-χ behavior of the CCS-functionals and their derivatives.

$$\mathcal{T}_H^{(0)} \sim \frac{\chi}{4} \qquad \mathcal{T}_H^{(2)} \sim -\frac{3}{8} \tag{36}$$

$$\mathcal{V}_H^{(0)} \sim \frac{1}{2} - \frac{\chi}{4} \qquad \mathcal{V}_H^{(2)} \sim -\frac{1}{2\chi} + \frac{3}{8}. \tag{37}$$

Note that we need the sub-leading corrections to $\mathcal{T}_H^{(0)}$ and $\mathcal{T}_H^{(2)}$ because they are the same order as $\mathcal{T}_H^{(0)}$ and $\mathcal{T}_H^{(2)}$.

Including these terms we find that $\mathcal{O}(\chi)$ contribution vanishes, but the $\mathcal{O}(\chi^2)$ contribution does not. We finally arrive at

$$\hat{E}_2 \sim \frac{3\chi^2}{8} + \mathcal{O}(\chi^3)\,. \tag{38}$$

This tell us that that curvature of the COM wavefunction is energetically unfavorable such that the system prefers a homogeneous CCS over a clumped one. Thus, quantum fluctuations corresponding to Goldstone modes restore the spontaneously broken translational invariance. The lowest energy state, at all finite values of N (no matter how large), is given by

$$|\mathrm{GS}\rangle_{\mathrm{CCS}} = \frac{1}{\sqrt{2\pi}}\int_{-\pi}^{\pi} \mathrm{d}\Theta\,|\Theta\rangle + \mathcal{O}\left(\frac{1}{N}\right)\,. \tag{39}$$

As was alluded to earlier, this is reminiscent of spinor Bose-Einstein condensates, whose exact ground state is known to be a CCS that is formally identical to Eq. (39) [61, 62].

V. DISCUSSION AND CONCLUSIONS

Quantum fluctuations of Goldstone modes can play an important role in determining the zero temperature behavior of a long-range interacting system. In the example studied here, properties of the ground state such as its symmetry breaking pattern are left undetermined at the level of mean-field theory due to a high level of degeneracy in the energy spectrum. Previous work on Bose stars suggests that this degeneracy is a generic consequence of long-range interactions [29]. In the case of the HMF model, we find that this degeneracy is only lifted at $\mathcal{O}(1/N^2)$ for any finite N (no matter how large). At zero-temperature this has the striking consequence of leading to a restored $O(2)$ symmetry in the ground state.

At finite N, the system is gapped, $\Delta = 3\chi^2/8N^2$, with excitations corresponding to departures from a homogeneous COM wavefunction. In the $N \to \infty$ limit the system becomes gapless, such that $|\mathrm{GS}\rangle_{\mathrm{CCS}}$ becomes embedded in a highly degenerate manifold of states, almost all of which break the model's underlying $O(2)$ symmetry. This is reminiscent of the behavior of spin-1/2 chains, where a rotationally invariant singlet ground state is separated at finite N from a triplet excitation that breaks rotation invariance. In the $N \to \infty$ limit the gap closes and the singlet becomes embedded in a degenerate ground state manifold whose low lying excitations are triplets [64] in analogy with the clumping excitations in the HMF.

This discussion is interesting, because the HMF model's classical partition function can be calculated *exactly* in the $N \to \infty$ limit, and exhibits a thermally driven second order phase transition [2, 41]; at low temperatures the system breaks the $O(2)$ symmetry. Thus, our observation that quantum fluctuations can restore the $O(2)$ symmetry leaves open two logical possibilities that are compatible with the exact classical results [41]:

1. The limit $\chi \to 0$ is singular, and the classically ordered phase exists only for χ strictly equal to zero such that for $\chi > 0$ quantum fluctuations completely inhibit ordering at all temperatures.

2. The HMF model exhibits a re-entrant phase wherein at finite temperature, for small values of χ the $O(2)$ symmetry is broken. Interpreting the $O(2)$ symmetry as a translational invariance for particles on a ring, this is reminiscent of inverse melting which is known to exist in certain spin models [65, 66].

Schematic phase diagrams for each of these two scenarios are sketched in Fig. 1. The determination of which of these two possibilities is born out by the HMF model is beyond the scope of this paper, however a definitive answer to this question should be attainable via path integral Monte Carlo studies.

The fact that the symmetry of the ground state is protected by feeble gradient corrections to the energy of the COM wavefunction suggests that the $T \to 0$ limit is non-trivial. Since deformations of the COM wavefunction should be the lowest energy excitations[3], our analysis suggests that the low-temperature behavior of the HMF model will be controlled by the parameter $\alpha = \beta\chi^2/N^2$;

[3] Single particle excitations will have an energy per particle of $\mathcal{O}(1/N)$, while deformations of the single particle wavefunction $\psi_H \to \psi_H + \delta\psi$ lead to an energy per-particle that is $\mathcal{O}(1)$.

a cursory examination of this quantity clearly indicates that the limit of $\beta \to 0$ (i.e. zero temperature) does not commute with $\chi \to 0$, and, more importantly, $N \to \infty$. Viewing deformations of the COM wavefunction as low-lying excitations (all of which break the $O(2)$ symmetry) it is conceivable that at finite temperatures it could be entropically favorable to macroscopically excite these degrees of freedom and break the $O(2)$ symmetry. In contrast, one may expect that if feeble quantum fluctuations can inhibit symmetry breaking at zero temperature, they will continue to be able to do so at finite temperature.

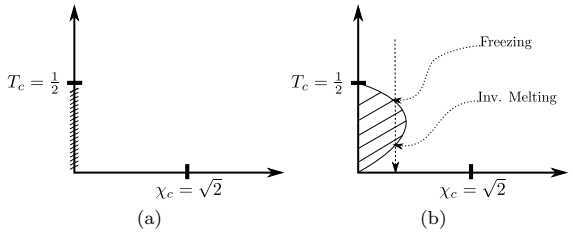

FIG. 1: Two possible resolutions of our result and the exact classical calculation. The limit $\chi \to 0$ could be singular such that symmetry breaking (hashed lines) is only possible for $\chi = 0$ (a). Alternatively, a re-entrant phase could appear at finite temperature (b). We identify this possibility as analogous to inverse melting, as indicated by the line of decreasing temperature at fixed χ. The parameters corresponding to classical and quantum (mean-field) symmetry breaking are marked with thick black lines.

In summary we find that quantum fluctuations due to Goldstone modes can substantially alter the symmetry breaking pattern of the HMF model. The energetic cost to excite a non-homogeneous center of mass wavefunction vanishes in the thermodynamic limit, suggesting that finite temperature effects could substantially alter our predictions. While we have provided an analytic study of the HMF model's ground state, our approach is necessarily approximate and we have only included COM fluctuations. A numerical investigation into both the finite temperature and zero temperature (i.e. ground state) properties of the system is a natural extension of this work, and is the most important next step in the study of the HMF model.

VI. ACKNOWLEDGEMENTS

We would like to thank Dr. Sung-Sik Lee for suggestions, discussions, and encouragement. This work was supported by funds from the National Science and Engineering Research Council (NSERC) of Canada. Support is also acknowledged from the Perimeter Institute for Theoretical Physics. Research at the Perimeter Institute is supported by the Government of Canada through the Department of Innovation, Science and Economic Development and by the Province of Ontario through the Ministry of Research and Innovation.

Appendix A: Delta function identities

In Appendix B we frequently encounter integrals of the form

$$\int \mathrm{d}x\mathrm{d}y \delta^{(2n)}(y) g(x - y/2) f(x + y/2) h(y) \ , \tag{A1}$$

and in this appendix we provide a short derivation of a useful identity Eq. (A9). We may first, however, study the simpler case of

$$\int \mathrm{d}x\mathrm{d}y \delta^{(2)}(y) g(x - y/2) f(x + y/2). \tag{A2}$$

In this case we must integrate by parts twice to pull the derivative off of the delta function. This gives

$$\begin{aligned} &= \int \mathrm{d}x\mathrm{d}y \delta(y) \frac{1}{4}[g'' f + f'' g - 2g' f'] \\ &= \int \mathrm{d}x \frac{1}{4}[g''(x) f(x) + f''(x) g(x) - 2g'(x) f'(x)] \\ &= -\int \mathrm{d}x g'(x) f'(x). \end{aligned} \tag{A3}$$

This generalizes naturally. If we denote $\partial^m [g\left(x - \frac{1}{2}y\right) f\left(x + \frac{1}{2}y\right)] = \mathcal{G}_m(\alpha, \beta)$ then the generalized identity is

$$\begin{aligned} \int \mathrm{d}x \ \mathcal{G}_{2m}(x, x) &= (-1)^m \int \mathrm{d}x \ g^{(m)}(x) f^{(m)}(x) \\ &= \langle \bar{g}^{(m)}, f^{(m)} \rangle. \end{aligned} \tag{A4}$$

Applying this result to a delta-function leads to

$$\begin{aligned} &= \int \mathrm{d}x\mathrm{d}y \ \delta^{(2n)}(y) g\left(x - \tfrac{1}{2}y\right) f\left(x + \tfrac{1}{2}y\right) \\ &= \int \mathrm{d}x\mathrm{d}y \ \delta(y) \partial_y^{2n} \left[g\left(x + \tfrac{1}{2}y\right) f\left(x - \tfrac{1}{2}y\right)\right] \\ &= (-1)^n \int \mathrm{d}x \ g^{(n)}(x) f^{(n)}(x). \end{aligned} \tag{A5}$$

Finally, when including an additional function in the integrand, we simply distribute the derivatives and find

$$\begin{aligned} &= \int \mathrm{d}x\mathrm{d}y \ \delta^{(2n)}(y) g\left(x - \tfrac{1}{2}y\right) f\left(x + \tfrac{1}{2}y\right) h(y) \\ &= \int \mathrm{d}x\mathrm{d}y \ \delta(y) \partial_y^{2n} \left[g\left(x + \tfrac{1}{2}y\right) f\left(x - \tfrac{1}{2}y\right) h(y)\right] \\ &= \int \mathrm{d}x\mathrm{d}y \ \delta(y) \sum_m \binom{2n}{m} \mathcal{G}_m(\alpha, \beta) \partial_y^{2n-m} h(y) \ . \end{aligned} \tag{A6}$$

Because $h(y)$ is an even function, all of the odd-derivatives vanish leading to

$$\int \mathrm{d}x\mathrm{d}y \ \delta(y) \sum_m \binom{2n}{2m} \mathcal{G}_m(\alpha, \beta) \partial_y^{2(n-m)} h(y) \tag{A7}$$

Now we can perform the integration over y

$$\begin{aligned}&\sum_m \binom{2n}{2m} \int \mathrm{d}x\mathrm{d}y\ \delta(y)\mathcal{G}_{2m}(\alpha,\beta)h^{(2m-2n)}(y)\\ =&\sum_m \binom{2n}{2m} \left[\partial_y^{2(n-m)}h(y)\right]_{y=0}\int \mathrm{d}x\ \mathcal{G}_{2m}(x,x).\end{aligned} \tag{A8}$$

Now using Eq. (A4) we arrive at

$$\begin{aligned}&\int \mathrm{d}x\mathrm{d}y\ \delta^{(2n)}(y) g\left(x-\tfrac{1}{2}y\right) f\left(x+\tfrac{1}{2}y\right) h(y)\\ &\quad=\sum_m \binom{2n}{2m}(-1)^m\langle \bar{g}^{(m)}, f^{(m)}\rangle h_0^{(2n-2m)}\ ,\end{aligned} \tag{A9}$$

where $h_0^{(2n-2m)} = \partial_y^{2(n-m)}h(y)|_{y=0}$. In calculations throughout this paper $f\left(x+\frac{1}{2}y\right) = \mathfrak{f}_a\left(x+\frac{1}{2}y\right)$ and $g\left(x-\frac{1}{2}y\right) = \mathfrak{f}_b^*\left(x-\frac{1}{2}y\right)$ such that $\langle \bar{g}^{(m)}, f^{(m)}\rangle = \langle \mathfrak{f}_b^{(m)}, \mathfrak{f}_a^{(m)}\rangle$.

Appendix B: Large-N Asymptotics for the Energy

In Eqs. (28) and (29) we quote results for ground state energy shift E_0, and the COM wavefunction's gradient energy E_2. In this appendix we derive these results.

We begin by considering the kinetic energy

$$\begin{aligned}T[\mathfrak{f}] &= \frac{1}{N}\langle \mathfrak{f}; N|\,\hat{T}\,|\mathfrak{f}; N\rangle\\ &= \int \mathrm{d}x\mathrm{d}y\, \mathfrak{f}^*\left(x-\tfrac{1}{2}y\right)\mathfrak{f}\left(x+\tfrac{1}{2}y\right)\mathcal{T}_H(y)O(y;N-1)\end{aligned}$$

Notice that the overlap has had a particle removed since we are computing the expectation value of a single-particle operator. Because of our COM wavefunction normalization this means we will find an overall prefactor of $|C(N)|^2/|C(N-1)|^2 = \sqrt{N/(N-1)}$. Leading to

$$\begin{aligned}T[\mathfrak{f}] =&\sqrt{\frac{N}{N-1}}\int \mathrm{d}x\mathrm{d}y\,\mathcal{T}_H(y)\\ &\times\sum_{a,b}\frac{1}{N^{a+b}}\mathfrak{f}_a^*\left(x-\tfrac{1}{2}y\right)\mathfrak{f}_b\left(x+\tfrac{1}{2}y\right)\\ &\times\sum_p\frac{\mathcal{K}_p}{N^p}\frac{1}{\left(1-\frac{1}{N}\right)^p}\delta^{(2p)}(y).\end{aligned}$$

where we have used $|C(N)/C(N-1)|^2 = \sqrt{N/(N-1}$ It is convenient to ignore the prefactor and work with the integral defined above directly. To simplify our analysis we introduce a re-scaled kinetic energy.

$$\widetilde{T}[\mathfrak{f}] = \sqrt{\frac{N}{N-1}}T[\mathfrak{f}]\ , \tag{B1}$$

such that

$$\begin{aligned}\widetilde{T}[\mathfrak{f}] =& \int \mathrm{d}x\mathrm{d}y\sum_{a,b}\frac{1}{N^{a+b}}\mathfrak{f}_a^*\left(x-\tfrac{1}{2}y\right)\mathfrak{f}_b\left(x+\tfrac{1}{2}y\right)\\ &\times\mathcal{T}_H(y)\sum_p\frac{\mathcal{K}_p}{N^p}\frac{1}{\left(1-\frac{1}{N}\right)^p}\delta^{(2p)}(y).\end{aligned} \tag{B2}$$

If we next consider the potential energy a similar expression may be defined. Starting with

$$\begin{aligned}V[\mathfrak{f}] =& \int \mathrm{d}x\mathrm{d}y\ \mathfrak{f}^*\left(x-\tfrac{1}{2}y\right)\mathfrak{f}\left(x+\tfrac{1}{2}y\right)\\ &\times\mathcal{V}_H\left(1-\frac{1}{N}\right)\langle\Theta_1; N-2|\Theta_2; N-2\rangle\ ,\end{aligned} \tag{B3}$$

we have

$$\begin{aligned}V[\mathfrak{f}] =& \int \mathrm{d}x\mathrm{d}y\ \sum_{a,b}\frac{1}{N^{a+b}}\ \mathfrak{f}_a^*(x-\tfrac{1}{2}y)\mathfrak{f}_b(x+\tfrac{1}{2}y)\\ &\times\mathcal{V}_H(y)\times\left(1-\frac{1}{N}\right)\left|\frac{C(N)}{C(N-2)}\right|^2\\ &\times\sum_p\frac{\mathcal{K}_p}{N^p}\frac{1}{\left(1-\frac{2}{N}\right)^p}\ \delta^{(2p)}(y)\end{aligned} \tag{B4}$$

As before we may use $|C(N)/C(N-2)|^2 = \sqrt{\frac{N}{N-2}}$ and introduce the function

$$\widetilde{V}[\mathfrak{f}] = \sqrt{\frac{N(N-1)^2}{N^2(N-2)}}\widetilde{V}[\mathfrak{f}]\ , \tag{B5}$$

such that

$$\begin{aligned}\widetilde{V}[\mathfrak{f}] =& \int \mathrm{d}x\mathrm{d}y\ \sum_{a,b}\frac{1}{N^{a+b}}\ \mathfrak{f}_a^*(x-\tfrac{1}{2}y)\mathfrak{f}_b(x+\tfrac{1}{2}y)\\ &\times\mathcal{V}_H(y)\sum_p\frac{\mathcal{K}_p}{N^p}\frac{1}{\left(1-\frac{2}{N}\right)^p}\ \delta^{(2p)}(y)\end{aligned} \tag{B6}$$

Notice that the expressions for $\widetilde{T}$ and $\widetilde{V}$ are nearly identical beyond cosmetic changes such as $\mathcal{T}_H \leftrightarrow \mathcal{V}_H$, save for one exception. The sum over p has a factor of $1/(1-m/N)^p$ where $m=1$ for $\widetilde{T}$ and $m=2$ for $\widetilde{V}$; this effect enters first at $\mathcal{O}\big(1/N^2\big)$ via the term

$$\frac{1}{N^2}m\mathcal{K}_1\delta^{(2)}(y)\quad m=1 \text{ or } 2 \tag{B7}$$

At this level of accuracy we therefore have (omitting the explicit arguments of $x\pm\frac{1}{2}y$ for brevity's sake)

$$\widetilde{T}[\mathfrak{f}] = \int \mathrm{d}x\mathrm{d}y \left[\mathfrak{f}_0^*\mathfrak{f}_0 + \frac{1}{N}(\mathfrak{f}_1^*\mathfrak{f}_0 + \mathfrak{f}_0^*\mathfrak{f}_1) + \frac{1}{N^2}(\mathfrak{f}_2^*\mathfrak{f}_0 + \mathfrak{f}_0^*\mathfrak{f}_2 + \mathfrak{f}_1^*\mathfrak{f}_1)\right] \times \mathcal{T}_H(y)\left[\delta(y) + \frac{1}{N}\mathcal{K}_1\delta^{(2)}(y) + \frac{1}{N^2}\left(\mathcal{K}_2\delta^{(4)}(y) + \mathcal{K}_1\delta^{(2)}(y)\delta^{(2)}(y)\right)\right] \tag{B8}$$

$$\widetilde{V}[\mathfrak{f}] = \int \mathrm{d}x\mathrm{d}y \left[\mathfrak{f}_0^*\mathfrak{f}_0 + \frac{1}{N}(\mathfrak{f}_1^*\mathfrak{f}_0 + \mathfrak{f}_0^*\mathfrak{f}_1) + \frac{1}{N^2}(\mathfrak{f}_2^*\mathfrak{f}_0 + \mathfrak{f}_0^*\mathfrak{f}_2 + \mathfrak{f}_1^*\mathfrak{f}_1)\right] \times \mathcal{V}_H(y)\left[\delta(y) + \frac{1}{N}\mathcal{K}_1\delta^{(2)}(y) + \frac{1}{N^2}\left(\mathcal{K}_2\delta^{(4)}(y) + 2\mathcal{K}_1\delta^{(2)}(y)\delta^{(2)}(y)\right)\right] \tag{B9}$$

1. Kinetic energy

At leading order the only contribution to the kinetic energy is given by,

$$\begin{aligned}\widetilde{T}_0 &= \int \mathrm{d}x\mathrm{d}y\, \mathfrak{f}_0^*\mathfrak{f}_0\delta(y)\mathcal{T}_H(y)\\ &= \mathcal{T}_H^{(0)}\end{aligned} \tag{B10}$$

At next leading order we have,

$$\begin{aligned}\widetilde{T}_1 &= \int \mathrm{d}x\mathrm{d}y\, \left(\mathfrak{f}_1^*\mathfrak{f}_0 + \mathfrak{f}_0^*\mathfrak{f}_1\right)\delta(y)\\ &\quad + \int \mathrm{d}x\mathrm{d}y\, \mathfrak{f}_0^*\mathfrak{f}_0\mathcal{K}_1\delta^{(2)}(y)\\ &= 2\,\mathrm{Re}\langle\mathfrak{f}_0,\mathfrak{f}_1\rangle + \mathcal{K}_1\sum_{n=0}^{1}\binom{2}{2n}(-1)^n\langle\mathfrak{f}_0^{(n)},\mathfrak{f}_0^{(n)}\rangle\mathcal{T}_H^{(2-2n)}\\ &= 2\,\mathrm{Re}\langle\mathfrak{f}_0,\mathfrak{f}_1\rangle\mathcal{T}_H^{(0)} - \mathcal{K}_1\langle\mathfrak{f}_0^{(1)},\mathfrak{f}_0^{(1)}\rangle\mathcal{T}_H^{(0)} + \mathcal{K}_1\mathcal{T}_H^{(2)}\\ &= \mathcal{K}_1\mathcal{T}_H^{(2)}\end{aligned}$$

where we have used Eq. (A9), and in going to the final equality, we have imposed the normalization condition Eq. (22).

At next-to-next-to leading order we have

$$\begin{aligned}\widetilde{T}_2 &= \int \mathrm{d}x\mathrm{d}y\, \left(\mathfrak{f}_0^*\mathfrak{f}_2 + \mathfrak{f}_2^*\mathfrak{f}_0 + \mathfrak{f}_1^*\mathfrak{f}_1\right)\delta(y)\mathcal{T}_H(y)\\ &\quad + \int \mathrm{d}x\mathrm{d}y\, \left(\mathfrak{f}_0^*\mathfrak{f}_1 + \mathfrak{f}_1^*\mathfrak{f}_0\right)\mathcal{K}_1\delta^{(2)}(y)\mathcal{T}_H(y)\\ &\quad + \int \mathrm{d}x\mathrm{d}y\mathfrak{f}_0^*\mathfrak{f}_0\mathcal{K}_2\delta^{(4)}(y)\mathcal{T}_H(y)\\ &\quad + \int \mathrm{d}x\mathrm{d}y\mathfrak{f}_0^*\mathfrak{f}_0\mathcal{K}_1\delta^{(2)}(y)\mathcal{T}_H(y)\end{aligned} \tag{B11}$$

using Eq. (A9) and

$$\begin{aligned}\widetilde{T}_2 &= 2\,\mathrm{Re}\langle\mathfrak{f}_0,\mathfrak{f}_2\rangle\mathcal{T}_H^{(0)} + \langle\mathfrak{f}_1,\mathfrak{f}_1\rangle\mathcal{T}_H^{(0)}\\ &\quad + 2\mathcal{K}_1\,\mathrm{Re}\langle\mathfrak{f}_0,\mathfrak{f}_1\rangle\mathcal{T}_H^{(2)} - 2\mathcal{K}_1\,\mathrm{Re}\langle\mathfrak{f}_0^{(1)},\mathfrak{f}_1^{(1)}\rangle\mathcal{T}_H^{(0)}\\ &\quad + \mathcal{K}_2\mathcal{T}_H^{(4)} - 6\mathcal{K}_2\langle\mathfrak{f}_0^{(1)},\mathfrak{f}_0^{(1)}\rangle\mathcal{T}_H^{(2)} + \mathcal{K}_2\langle\mathfrak{f}_0^{(2)},\mathfrak{f}_0^{(2)}\rangle\mathcal{T}_H^{(0)}\\ &\quad + \mathcal{K}_1\mathcal{T}_H^{(2)} - \mathcal{K}_1\langle\mathfrak{f}_0^{(1)},\mathfrak{f}_0^{(1)}\rangle\mathcal{T}_H^{(0)}\end{aligned} \tag{B12}$$

Summing all of the terms, and imposing the normalization conditions from Eqs. (21) to (23), we find

$$\begin{aligned}\widetilde{T}_2 &= \mathcal{K}_2\mathcal{T}_H^{(4)} + \mathcal{K}_1\mathcal{T}_H^{(2)}\\ &\quad + \left(\left[\mathcal{K}_1^2 - 6\mathcal{K}_2\right]\mathcal{T}_H^{(2)} - \mathcal{K}_1\mathcal{T}_H^{(0)}\right)\langle\mathfrak{f}_0^{(1)},\mathfrak{f}_0^{(1)}\rangle\end{aligned} \tag{B13}$$

In conclusion we find

$$\widetilde{T}_0 = \mathcal{T}_H^{(0)} \tag{B14}$$

$$\widetilde{T}_1 = \mathcal{K}_1\mathcal{T}_H^{(2)} \tag{B15}$$

$$\begin{aligned}\widetilde{T}_2 &= \mathcal{K}_2\mathcal{T}_H^{(4)} + \mathcal{K}_1\mathcal{T}_H^{(2)}\\ &\quad + \left(\left[\mathcal{K}_1^2 - 6\mathcal{K}_2\right]\mathcal{T}_H^{(2)} - \mathcal{K}_1\mathcal{T}_H^{(0)}\right)\langle\mathfrak{f}_0^{(1)},\mathfrak{f}_0^{(1)}\rangle\end{aligned} \tag{B16}$$

Using $T = (1 - \frac{1}{2N} + \frac{3}{8N^2})\widetilde{T}$ we then find

$$T_0 = \widetilde{T}_0 \tag{B17}$$

$$T_1 = \widetilde{T}_1 - \frac{1}{2}\widetilde{T}_0 \tag{B18}$$

$$T_2 = \widetilde{T}_2 - \frac{1}{2}\widetilde{T}_1 + \frac{3}{8}\widetilde{T}_0 \tag{B19}$$

2. Potential Energy

The calculation for $\widetilde{V}_n$ largely parallels that of $\widetilde{T}_n$.

$$\begin{aligned}\widetilde{V}_0 &= \int \mathrm{d}x\mathrm{d}y\, \mathfrak{f}_0^*\mathfrak{f}_0\mathcal{V}_H(y)\delta(y)\\ &= \mathcal{V}_H^{(0)}\langle\mathfrak{f}_0,\mathfrak{f}_0\rangle = \mathcal{V}_H^{(0)}\end{aligned} \tag{B20}$$

$$\begin{aligned}\widetilde{V}_1 &= \int \mathrm{d}x\mathrm{d}y\, \mathfrak{f}_0^*\mathfrak{f}_0\mathcal{V}_H(y)\mathcal{K}_1\delta^{(2)}(y)\\ &\qquad + [\mathfrak{f}_0^*\mathfrak{f}_1 + \mathfrak{f}_1^*\mathfrak{f}_0^*]\mathcal{V}_H(y)\delta(y)\\ &= \mathcal{V}_H^{(2)} + 2\mathrm{Re}\langle\mathfrak{f}_0,\mathfrak{f}_1\rangle\mathcal{V}_H^{(0)} - \mathcal{K}_1\langle\mathfrak{f}_0^{(1)},\mathfrak{f}_0^{(1)}\rangle\mathcal{V}_H^{(0)}\\ &= \mathcal{V}_H^{(2)}\end{aligned} \tag{B21}$$

where we have used the COM wavefunction's normalization constraint Eq. (22).

We then find

$$\begin{aligned}\widetilde{V}_2 = &\int \mathrm{d}x\mathrm{d}y\ \mathfrak{f}_0^*\mathfrak{f}_0\mathcal{V}_H(y)\Big[\mathcal{K}_2\delta^{(4)}(y) + 2\mathcal{K}_1\delta^{(2)}(y)\Big] \\ &+ \int \mathrm{d}x\mathrm{d}y\ [\mathfrak{f}_0^*\mathfrak{f}_1 + \mathfrak{f}_1^*\mathfrak{f}_0^*]\mathcal{V}_H(y)\mathcal{K}_1\delta^{(2)}(y) \\ &+ \int \mathrm{d}x\mathrm{d}y\ [\mathfrak{f}_1^*\mathfrak{f}_1 + \mathfrak{f}_0^*\mathfrak{f}_2 + \mathfrak{f}_2^*\mathfrak{f}_0]\mathcal{V}_H(y)\delta(y)\ .\end{aligned} \tag{B22}$$

Notice the factor of $2\mathcal{K}_1\delta^{(2)}(y)$ in contrast to the factor of $\mathcal{K}_1\delta^{(2)}(y)$ found in Eq. (B11).

As before, we will address each term in the calculation separately,

$$\begin{aligned}&= 2\mathrm{Re}\langle\mathfrak{f}_0,\mathfrak{f}_2\rangle\mathcal{V}_H^{(0)} + \langle\mathfrak{f}_1,\mathfrak{f}_1\rangle\mathcal{V}_H^{(0)} \\ &+ 2\mathcal{K}_1\Big[\mathcal{V}_H^{(2)} - \langle\mathfrak{f}_0^{(1)},\mathfrak{f}_0^{(1)}\rangle\mathcal{V}_H^{(0)}\Big] \\ &+ \mathcal{K}_2\Big[\mathcal{V}_H^{(4)} - 6\langle\mathfrak{f}_0^{(1)},\mathfrak{f}_0^{(1)}\rangle\mathcal{V}_H^{(2)} + \langle\mathfrak{f}_0^{(2)},\mathfrak{f}_0^{(2)}\rangle\mathcal{V}_H^{(0)}\Big] \\ &+ \mathcal{K}_1\Big[(2\mathrm{Re}\langle\mathfrak{f}_0,\mathfrak{f}_1\rangle)\mathcal{V}_H^{(2)} - (2\mathrm{Re}\langle\mathfrak{f}_0^{(1)},\mathfrak{f}_1^{(1)}\rangle)\mathcal{V}_H^{(0)}\Big]\end{aligned} \tag{B23}$$

Adding all of these terms together, and making use of the normalization conditions Eqs. (21) to (23) we find

$$\begin{aligned}\widetilde{V}_2 = &\mathcal{K}_2\mathcal{V}_H^{(4)} + 2\mathcal{K}_1\mathcal{V}_H^{(2)} \\ &+ \Big(\big[\mathcal{K}_1^2 - 6\mathcal{K}_2\big]\mathcal{T}_H^{(2)} - \mathcal{K}_1\mathcal{T}_H^{(0)}\Big)\langle\mathfrak{f}_0^{(1)},\mathfrak{f}_0^{(1)}\rangle\end{aligned} \tag{B24}$$

This leads finally to

$$\widetilde{V}_0 = \mathcal{V}_H^{(0)} \tag{B25}$$

$$\widetilde{V}_1 = \mathcal{K}_1\mathcal{V}_H^{(2)} \tag{B26}$$

$$\begin{aligned}\widetilde{V}_2 = &\mathcal{K}_2\mathcal{V}_H^{(4)} + 2\mathcal{K}_1\mathcal{V}_H^{(2)} \\ &+ \Big(\big[\mathcal{K}_1^2 - 6\mathcal{K}_2\big]\mathcal{V}_H^{(2)} - 2\mathcal{K}_1\mathcal{V}_H^{(0)}\Big)\langle\mathfrak{f}_0^{(1)},\mathfrak{f}_0^{(1)}\rangle.\end{aligned} \tag{B27}$$

Lastly we can use the formula $V = (1+\frac{1}{N^2})\widetilde{V} + \mathcal{O}\big(1/N^3\big)$ to find

$$V_0 = \widetilde{V}_0 \qquad V_1 = \widetilde{V}_1 \qquad V_2 = \widetilde{V}_2 + \widetilde{V}_0\ . \tag{B28}$$

3. Total Energy

Recall that $E[\mathfrak{f}] = T[\mathfrak{f}] - V[\mathfrak{f}]$. Let us focus first on the shift of the ground state energy. We find, at leading order,

$$\delta E_0 \approx \frac{1}{N}\Big[\mathcal{T}_H^{(2)} - \mathcal{V}_H^{(2)} - \frac{1}{2}\mathcal{T}_H^{(0)}\Big]. \tag{B29}$$

For the gradient energy of the COM wavefunction, we find (again at leading order)

$$\begin{aligned}\hat{E}_2 \approx &\big[\mathcal{K}_1^2 - 6\mathcal{K}_2\big]\Big[\mathcal{T}_H^{(2)} - \mathcal{V}_H^{(2)}\Big] \\ &- \mathcal{K}_1\Big[\mathcal{T}_H^{(0)} - 2\mathcal{V}_H^{(0)}\Big]\ .\end{aligned} \tag{B30}$$

As emphasized in the main text this is the mean result of our work and demonstrates that quantum fluctuations of the COM can lower the energy of a CCS state.

4. Cancellations Due to Normalization Conditions

In the previous section we found that terms such as $\langle\mathfrak{f}_0^{(1)},\mathfrak{f}_0^{(1)}\rangle$ were absent at $\mathcal{O}(1/N)$, and likewise terms such as $\langle\mathfrak{f}_0^{(2)},\mathfrak{f}_0^{(2)}\rangle$ were absent at $\mathcal{O}\big(1/N^2\big)$. In this section we outline that this is not an accidental cancellation, but is a direct consequence of the normalization conditions Eqs. (21) to (23).

To derive Eqs. (21) to (23) we demand that $\langle\mathfrak{f};N|\mathfrak{f};N\rangle = 1$, and that this normalization is maintained order-by-order in $1/N$. The exact expression for the overlap is given by

$$\langle\mathfrak{f}|\mathfrak{f}\rangle = \int \mathrm{d}x\mathrm{d}y\mathfrak{f}\left(x-\tfrac{1}{2}y\right)\mathfrak{f}^*\left(x+\tfrac{1}{2}y\right)O(y;N)\ . \tag{B31}$$

At leading order, using the delta-expansion of $O(y;N)$ this is equivalent to demanding that

$$\langle\mathfrak{f}_0,\mathfrak{f}_0\rangle := \int_{-\pi}^{\pi}\mathfrak{f}_0^*(x)\mathfrak{f}_0(x)\mathrm{d}x = 1\ , \tag{B32}$$

which is Eq. (21). At $\mathcal{O}(1/N)$ we find instead

$$\langle\mathfrak{f}|\mathfrak{f}\rangle = \langle\mathfrak{f}_0,\mathfrak{f}_0\rangle + \frac{1}{N}\Big[2\mathrm{Re}\langle\mathfrak{f}_0,\mathfrak{f}_1\rangle - \mathcal{K}_1\langle\mathfrak{f}_0^{(1)},\mathfrak{f}_0^{(1)}\rangle\Big]. \tag{B33}$$

By requiring that this correction at $\mathcal{O}(1/N)$ vanish we arrive at Eq. (22). Similarly, at $\mathcal{O}\big(1/N^2\big)$ we have

$$\langle\mathfrak{f}|\mathfrak{f}\rangle = \langle\mathfrak{f}_0,\mathfrak{f}_0\rangle + \frac{1}{N}[(2\mathrm{Re}\langle\mathfrak{f}_0,\mathfrak{f}_1\rangle) - \mathcal{K}_1\langle\mathfrak{f}_0^{(1)},\mathfrak{f}_0^{(1)}\rangle] + \frac{1}{N^2}[\mathcal{K}_2\langle\mathfrak{f}_0^{(2)},\mathfrak{f}_0^{(2)}\rangle - \mathcal{K}_1(2\mathrm{Re}\langle\mathfrak{f}_0^{(1)},\mathfrak{f}_1^{(1)}\rangle) + 2\mathrm{Re}\langle\mathfrak{f}_0,\mathfrak{f}_2\rangle + \langle\mathfrak{f}_1,\mathfrak{f}_1\rangle]\ . \tag{B34}$$

Our third normalization condition, Eq. (23), then follows from the requirement that the bracketed term of $\mathcal{O}\big(1/N^2\big)$ must vanish.

Importantly, this exact same combination of terms is

guaranteed to appear in our calculations of $E[\mathfrak{f}]$. This is most clearly illustrated at $\mathcal{O}(1/N)$. Let us consider just the term

$$\begin{aligned}&\int \mathrm{d}x\mathrm{d}y\ \mathcal{K}_1\delta^{(2)}(y)\mathfrak{f}_0\mathfrak{f}_0^*\mathcal{V}_H(y)\\&=\mathcal{K}_1\mathcal{V}_H^{(2)}-\mathcal{K}_1\mathcal{V}_H^{(0)}\langle\mathfrak{f}_0^{(1)},\mathfrak{f}_0^{(1)}\rangle\ .\end{aligned}\tag{B35}$$

Notice that when the derivatives act on the function $\mathfrak{f}_0$ it gives the same result as the normalization condition, but with an overall prefactor of $\mathcal{V}_H^{(0)}$. The same prefactor will also appear in the term

$$\begin{aligned}&\int \mathrm{d}x\mathrm{d}y\ \delta(y)[\mathfrak{f}_0(\alpha)\mathfrak{f}_1^*(\beta)+\mathfrak{f}_1(\alpha)\mathfrak{f}_0^*(\beta)]\mathcal{V}_H(y)\\&=\mathcal{V}_H^{(0)}(2\mathrm{Re}\langle\mathfrak{f}_0,\mathfrak{f}_1\rangle)\ ,\end{aligned}\tag{B36}$$

where we have used $\alpha=x-\frac{1}{2}y$, and $\beta=x+\frac{1}{2}y$ for shorthand. Upon addition of these two terms, we will have the combination that corresponds to Eq. (22). This happens when *all* of the derivatives from the delta-expansion act on $\mathfrak{f}_0$; this leaves no derivatives left-over to act on $\mathcal{V}_H(y)$ and this ensures that the prefactor appearing in front of $\mathcal{K}_n\langle\mathfrak{f}_0^{(n)},\mathfrak{f}_0^{(n)}\rangle$ is $\mathcal{V}_H^{(0)}$. This is why the gradient corrections to the COM wavefunction's energy appear at $\mathcal{O}\big(1/N^2\big)$ as opposed to $\mathcal{O}(1/N)$ as may be naively expected. The same cancellation occurs at $\mathcal{O}\big(1/N^2\big)$ but precludes terms of the form $\langle\mathfrak{f}_0^{(2)},\mathfrak{f}_0^{(2)}\rangle$.

Appendix C: Many-body overlap functions

In the body of the main text we claimed that the functions $O(y;\aleph)$ could be expanded in the large $\aleph$ limit in a "delta-expansion"

$$O(y;\aleph)=\frac{1}{|C(\aleph,\chi)|^2}\left[\delta(y)+\sum_{p>0}\frac{\mathcal{K}_p(\chi)}{\aleph^p}\delta^{(2p)}(y)\right]\ .\tag{C1}$$

In this section we will justify this claim by making use of the properties of the Hartree wavefunctions $\psi_H(\theta)$. The results obtained in this section will allow us to obtain explicit expressions for $\mathcal{K}_1$, and $\mathcal{K}_2$ in Appendix D. As noted before, the $\aleph$-body overlap can be re-written as an exponentiated overlap of the Hartree states

$$O(y;\aleph)=\big[\ \langle\psi_H;\ x-\tfrac{1}{2}y|\psi_H;\ x+\tfrac{1}{2}y\rangle\ \big]^{\aleph},\tag{C2}$$

where

$$\begin{aligned}&\langle\psi_H;\ x-\tfrac{1}{2}y|\psi_H;\ x+\tfrac{1}{2}y\rangle\\&=\int\mathrm{d}\theta\psi_H^*(\theta-[x-\tfrac{1}{2}y])\psi_H(\theta-[x+\tfrac{1}{2}y])\\&=\int\mathrm{d}\theta\psi_H(\theta+\tfrac{1}{2}y)\psi_H(\theta-\tfrac{1}{2}y)\ ,\end{aligned}\tag{C3}$$

and, where we have used the fact that $\psi_H(\theta)$ is real. The form of the Hartree wavefunctions are known: they are given by appropriately scaled and shifted Mathieu functions, with an auxiliary parameter $q(\chi)$ that can be determined exactly

$$\psi_H(\theta)=\frac{1}{\sqrt{\pi}}\mathrm{ce}_0\big(\tfrac{1}{2}(\theta-\pi);q(\chi)\ \big)\ .\tag{C4}$$

Thus, we have

$$\begin{aligned}&\langle\psi_H;\ x-\tfrac{1}{2}y|\psi_H;\ x+\tfrac{1}{2}y\rangle\\&=\frac{1}{\pi}\int\mathrm{d}\theta\ \mathrm{ce}_0(\tfrac{1}{2}\theta;q)\mathrm{ce}_0(\tfrac{1}{2}(\theta+y);q)\ .\end{aligned}\tag{C5}$$

Now for $\chi\ll 1$ we have that $q\sim 1/\chi^2$ such that q is very large. In this regime the Mathieu functions are well approximated by parabolic cylinder functions, D_n, via Sips' expansion [63]

$$\mathrm{ce}_0(z;q)\sim C_0(q)[U_0(\xi;q)+V_0(\xi;q)]\tag{C6}$$

$$C_0(q)\sim\left[\frac{\pi\sqrt{q}}{2}\right]^{1/4}\left[1+\frac{1}{8\sqrt{q}}\right]^{-1/2}\tag{C7}$$

$$U_0(\xi\ ;q)\sim D_0(\xi)-\frac{1}{4\sqrt{q}}D_4(\xi)\tag{C8}$$

$$V_0(\xi\ ;q)\sim-\frac{1}{16\sqrt{q}}D_2(\xi)\tag{C9}$$

$$\tag{C10}$$

such that

$$\mathrm{ce}_0(z;\ q)\sim\left[\frac{\pi\sqrt{q}}{2}\right]^{1/4}D_0(\xi)+\mathcal{O}\left(\frac{1}{\sqrt{q}}\right)\tag{C11}$$

Introducing the variables $\zeta=2q^{1/4}\sin\frac{\theta}{2}$ we then find

$$\begin{aligned}\psi_H(\theta;\chi)&\sim\left[\frac{\sqrt{q}}{2\pi}\right]^{1/4}D_0(\zeta)+\mathcal{O}\left(\frac{1}{\sqrt{q}}\right)\\&=\left[\frac{q}{(2\pi)^2}\right]^{1/8}\mathrm{e}^{-\sqrt{q}\sin^2\frac{\theta}{2}}+\mathcal{O}\left(\frac{1}{\sqrt{q}}\right).\end{aligned}\tag{C12}$$

Using the leading order behaviour for ψ_H, the overlap can be expressed as a Bessel function

$$\begin{aligned}&\langle\psi_H;\ x-\tfrac{1}{2}y|\psi_H;\ x+\tfrac{1}{2}y\rangle\\&=\int_0^{2\pi}\mathrm{d}\theta\psi_H^*(\theta-\tfrac{1}{2}y;\chi)\psi_H(\theta+\tfrac{1}{2}y;\chi)\\&\sim\left[\frac{q}{(2\pi)^2}\right]^{1/4}\int_0^{2\pi}\mathrm{d}\theta\mathrm{e}^{-\sqrt{q}\sin^2\frac{x-y/2}{2}}\mathrm{e}^{-\sqrt{q}\sin^2\frac{x+y/2}{2}}\\&=\left[\frac{q}{(2\pi)^2}\right]^{1/4}\int_0^{2\pi}\mathrm{d}\theta\mathrm{e}^{\sqrt{q}\left(1-\cos x\cos\frac{y}{2}\right)}\\&=\frac{I_0(\sqrt{q}\cos\frac{y}{2})}{\sqrt{2\pi q^{1/2}}\mathrm{e}^{\sqrt{q}}}\end{aligned}\tag{C13}$$

where $I_0(z)$ is the modified Bessel function of the first kind [63]. At the same order of accuracy we can instead write

$$\langle \psi_H;\ x-\tfrac{1}{2}y|\psi_H;\ x+\tfrac{1}{2}y\rangle \sim \frac{I_0(\sqrt{q}\cos\frac{y}{2})}{I_0(\sqrt{q})}\ , \tag{C14}$$

which is exact for $y=0$. For most values of y we can use a large-argument expansion for the Bessel function $I_0(z)\sim \mathrm{e}^z/\sqrt{2\pi z}$. For values of y such that $\sqrt{q}\cos\frac{y}{2}\sim\mathcal{O}(1)$ it follows that $I_0(y)\sim\mathcal{O}(1)$ and so the overlap is $\mathcal{O}\big(q^{1/4}\mathrm{e}^{-\sqrt{q}}\big)$.

When considering integrals on the interval $y\in[-\pi,\pi]$ it is therefore justifiable to neglect contributions from this exponentially suppressed region. Then, on the remainder of the interval, we can use the large-argument expansion of the Bessel function as a global approximation. This allows us to re-write the overlap as

$$\begin{aligned}&\langle \psi_H;\ x-\tfrac{1}{2}y|\psi_H;\ x+\tfrac{1}{2}y\rangle\\ &\sim \exp\Big[2\sqrt{q}\sin^2\tfrac{y}{4}-\tfrac{1}{2}\log\cos\tfrac{y}{2}+\mathcal{O}\Big(\tfrac{1}{\sqrt{q}}\Big)\Big]\end{aligned} \tag{C15}$$

By extension the $\aleph$-body overlap assumes the form

$$O(y;\aleph)\sim\exp\big\{\aleph\big[2\sqrt{q}\sin^2\tfrac{y}{4}-\tfrac{1}{2}\log\cos\tfrac{y}{2}\big]\big\}\ , \tag{C16}$$

where we have neglected terms of $\mathcal{O}\big(1/\sqrt{q}\big)$ or smaller. Trading q for χ via $q\sim 4\chi^{-2}(1-\chi/4)$, we find at the same order of accuracy

$$O(y;\aleph)\sim \mathrm{e}^{\aleph\left[\left(\frac{4}{\chi}-\frac{1}{2}\right)\sin^2\frac{y}{4}-\frac{1}{2}\log\cos\frac{y}{2}\right]}\ . \tag{C17}$$

Appendix D: Small χ expansions

As noted in the main text, $\mathcal{T}_H(y)$'s leading order behavior as a function of χ is important. We would like to compute $\mathcal{T}_H^{(0)}$ and $\mathcal{T}_H^{(2)}$ and we will make use of Sips' expansion for the ground state wavefunctions Eq. (C6)

$$\psi_H(x)\sim\left[\frac{\sqrt{q}}{2\pi}\right]^{1/4}\left[D_0(\zeta)-\frac{1}{16\sqrt{q}}\mathfrak{D}(\zeta)\right]\ , \tag{D1}$$

where $\zeta=2q^{1/4}\sin\frac{\theta}{2}$, and

$$\mathfrak{D}(\zeta)=D_0(\zeta)+D_2(\zeta)+\frac{1}{4}D_4(\zeta)\ . \tag{D2}$$

We are interested in

$$\mathcal{T}_H(y)=\frac{\chi^2}{2}\int \mathrm{d}x\left[\frac{\mathrm{d}}{\mathrm{d}x}\psi_H(x-\tfrac{1}{2}y)\right]\left[\frac{\mathrm{d}}{\mathrm{d}x}\psi_H(x+\tfrac{1}{2}y)\right]\ . \tag{D3}$$

It will be useful to have the following identities

$$\frac{\mathrm{d}\zeta_\pm}{\mathrm{d}x}=q^{1/4}\cos\left(\frac{x\pm\frac{1}{2}y}{2}\right)=q^{1/4}\left(1-\frac{\zeta_\pm^2}{4\sqrt{q}}\right)^{1/2} \tag{D4}$$

$$\frac{\mathrm{d}^2\zeta_\pm}{\mathrm{d}x^2}=-\frac{q^{1/4}}{2}\left(\frac{x\pm\frac{1}{2}y}{2}\right)=-\frac{q^{1/4}}{4}\zeta_\pm\ , \tag{D5}$$

where $\zeta_\pm=\zeta(x\pm\frac{1}{2}y)$ with which we can re-express Eq. (D3) as

$$\begin{aligned}\mathcal{T}_H(y)=-\frac{\chi^2}{2}\sqrt{q}\int\frac{\mathrm{d}\zeta}{q^{\frac{1}{4}}\sqrt{1-\frac{\zeta^2}{4\sqrt{q}}}}\left(1-\frac{\zeta_-^2}{4\sqrt{q}}\right)^{1/2}\\ \times\left(1-\frac{\zeta_+^2}{4\sqrt{q}}\right)^{1/2}\psi_H'(\zeta_-)\psi_H'(\zeta_+)\ .\end{aligned} \tag{D6}$$

At leading order in $1/\sqrt{q}$ we have

$$\mathcal{T}_H(y)\sim-\frac{\chi^2}{2}\sqrt{q}\int\frac{\mathrm{d}\zeta}{\sqrt{2\pi}}D_0'(\zeta_-)D_0'(\zeta_+)\ . \tag{D7}$$

This leads immediately to the result

$$\begin{aligned}\mathcal{T}_H^{(0)}&\sim-\frac{\chi^2}{2}\sqrt{q}\int\frac{\mathrm{d}\zeta}{\sqrt{2\pi}}D_0'(\zeta)D_0'(\zeta)\\ &=-\frac{\sqrt{q}}{8}\chi^2\ .\end{aligned} \tag{D8}$$

Next, to calculate $\mathcal{T}_H^{(2)}$ we must act with $\frac{\mathrm{d}^2}{\mathrm{d}y^2}$ on Eq. (D7). A useful identity is

$$\begin{aligned}&\frac{\mathrm{d}^2}{\mathrm{d}y^2}[f(\zeta_-)g(\zeta_+)+f(\zeta_+)g(\zeta_-)]\\ &=\left[\frac{\mathrm{d}^2\zeta_+}{\mathrm{d}y^2}+\frac{\mathrm{d}^2\zeta_-}{\mathrm{d}y^2}\right][f'g+g'f]\\ &\quad+4\frac{\mathrm{d}\zeta_+}{\mathrm{d}y}\frac{\mathrm{d}\zeta_-}{\mathrm{d}y}f'g'\\ &\quad+\left[\left(\frac{\mathrm{d}\zeta_+}{\mathrm{d}y}\right)^2\left(\frac{\mathrm{d}\zeta_-}{\mathrm{d}y}\right)^2\right][f''g+g''f]\ .\end{aligned} \tag{D9}$$

which, holds when $y=0$. We can insert this identity underneath the integral after acting with the derivative operator. This will give us an integral representation for $\mathcal{T}_H^{(2)}:=\mathcal{T}_H''(y=0)$. Using the explicit forms of the derivatives,

$$\frac{\mathrm{d}\zeta_\pm}{\mathrm{d}y}=\pm\frac{q^{1/4}}{2}\left(1-\frac{\zeta_\pm^2}{4\sqrt{q}}\right)^{1/2} \tag{D10}$$

$$\frac{\mathrm{d}^2\zeta_\pm}{\mathrm{d}y^2}=-\frac{\zeta}{16}\ , \tag{D11}$$

we find

$$\begin{aligned}\mathcal{T}_H^{(2)}&\sim-q\frac{\chi^2}{2}\int\frac{\mathrm{d}\zeta}{\sqrt{2\pi}}2[D_0'D_0'-2D_0'''D_0']\\ &=2q\chi^2\int\frac{\mathrm{d}\zeta}{\sqrt{2\pi}}D_0''D_0''\\ &=\frac{3q\chi^2}{32}.\end{aligned} \tag{D12}$$

where we have used the leading order approximation for $\mathrm{d}\zeta_\pm/\mathrm{d}y$ and neglected the contribution from terms

proportional to $\mathrm{d}^2\zeta_\pm/\mathrm{d}^2 y$ because they are subleading. To obtain the second equality we integrated by parts, however at higher orders in $1/\sqrt{q}$ one needs to be careful to keep track of factors of ζ^2 in the integrand.

When calculating $\mathcal{V}_H^{(0)}$ and $\mathcal{V}_H^{(2)}$ we need to work beyond leading order, because the leading order piece cancels in Eq. (29). We are interested in

$$\mathcal{V}_H(y) = \frac{1}{2}\int \mathrm{d}x_1\mathrm{d}x_2 \psi_H(x_1+\tfrac{y}{2})\psi_H(x_1-\tfrac{y}{2}) \times \psi_H(x_2+\tfrac{y}{2})\psi_H(x_2-\tfrac{y}{2})\cos(x_1-x_2) \tag{D13}$$

which can be re-written as

$$\mathcal{V}_H(y) = \frac{1}{2}\big[I_C(y)^2 + I_S(y)^2\big] \tag{D14}$$

$$I_C(y) = \int \mathrm{d}x \psi_H(x+\tfrac{y}{2})\psi_H(x-\tfrac{y}{2})\cos(x) \tag{D15}$$

$$I_S(y) = \int \mathrm{d}x \psi_H(x+\tfrac{y}{2})\psi_H(x-\tfrac{y}{2})\sin(x) \tag{D16}$$

Importantly $I_S(0)=0$, $I_S'(0)=0$, and $I_C'(0)$ such that

$$\mathcal{V}_H^{(0)} = \frac{1}{2}I_C^2(0) \quad \text{and} \quad \mathcal{V}_H^{(2)} = I_C(0)I_C''(0)\ , \tag{D17}$$

so we can focus exclusively on the integral $I_C(y)$. Rewriting this in terms of ζ and keeping only terms to order $1/\sqrt{q}$ we arrive at

$$I_C(y) = \frac{1}{\sqrt{2\pi}}\bigg[\int D_0(\zeta_-)D_0(\zeta_+)\Big(1-\frac{3\zeta^2}{8\sqrt{q}}\Big)\mathrm{d}\zeta - \frac{1}{16\sqrt{q}}\int D_0(\zeta_-)\mathfrak{D}(\zeta_+) + D_0(\zeta_+)\mathfrak{D}(\zeta_-)\mathrm{d}\zeta\bigg] \tag{D18}$$

Evaluating at $y=0$ sets $\zeta_\pm = \zeta$ and we find

$$I_C(0) = \frac{1}{\sqrt{2\pi}}\bigg[\int D_0(\zeta)D_0(\zeta)\Big(1-\frac{3\zeta^2}{8\sqrt{q}}\Big)\mathrm{d}\zeta - \frac{1}{8\sqrt{q}}\int D_0(\zeta)\mathfrak{D}(\zeta)\mathrm{d}\zeta\bigg] = 1-\frac{1}{2\sqrt{q}} \tag{D19}$$

To find $I_C''(0)$ we must act on Eq. (D18) with $\frac{\mathrm{d}^2}{\mathrm{d}y^2}$. Being careful to retain sub-leading terms we find

$$\begin{aligned} I_C''(0) &= -\frac{\sqrt{q}}{\sqrt{2\pi}}\bigg[\int \frac{D_0'D_0' - D_0''D_0}{2}\Big(1-\frac{5\zeta^2}{8\sqrt{q}}\Big)\mathrm{d}\zeta \\ &\quad + \frac{2}{\sqrt{2\pi}}\int D_0'D_0\frac{\zeta}{16}\mathrm{d}\zeta - \frac{1}{8\sqrt{q}}\int D_0'\mathfrak{D}'\mathrm{d}\zeta\bigg] \\ &= -\frac{\sqrt{q}}{4}\Big(1-\frac{3}{4\sqrt{q}}\Big) \end{aligned} \tag{D20}$$

Using $\mathcal{V}_H^{(0)} = \frac{1}{2}[I_C(0)]^2$, $\mathcal{V}_H^{(2)} = I_C''(0)I_C(0)$, and the small-$\chi$ behavior of q [60],

$$q \sim \frac{4}{\chi^2}\Big[1-\frac{\chi}{4}+\mathcal{O}\big(\chi^2\big)\Big] \tag{D21}$$

we then find

$$\begin{aligned} \mathcal{V}_H^{(0)} &= \frac{1}{2}\Big[1-\frac{1}{\sqrt{q}}+\mathcal{O}\Big(\frac{1}{q}\Big)\Big] && \text{(D22)}\\ &= \frac{1}{2}\Big[1-\frac{\chi}{2}+\mathcal{O}\big(\chi^2\big)\Big] \\ \mathcal{V}_H^{(2)} &= -\frac{\sqrt{q}}{4}\Big[1-\frac{5}{16\sqrt{q}}+\mathcal{O}\Big(\frac{1}{q}\Big)\Big] && \text{(D23)}\\ &= -\frac{1}{2\chi}\Big[1-\frac{3\chi}{4}+\mathcal{O}\big(\chi^2\big)\Big] \\ \mathcal{T}_H^{(0)} &= \chi^2\times\frac{\sqrt{q}}{8}\Big[1+\mathcal{O}\Big(\frac{1}{\sqrt{q}}\Big)\Big] && \text{(D24)}\\ &= \frac{\chi}{4}[1+\mathcal{O}(\chi)] \\ \mathcal{T}_H^{(2)} &= \chi^2\times\Big(-\frac{3q}{32}\Big)\Big[1+\mathcal{O}\Big(\frac{1}{\sqrt{q}}\Big)\Big] && \text{(D25)}\\ &= -\frac{3}{8}[1+\mathcal{O}(\chi)]\ . \end{aligned}$$

[1] T. Dauxois, S. Ruffo, E. Arimondo, and M. Wilkens, *Dynamics and Thermodynamics of Systems with Long Range Interactions*, Lecture Notes in Physics (Springer

Berlin Heidelberg, 2008).
[2] A. Campa, T. Dauxois, and S. Ruffo, Phys. Rep. **480**, 57 (2009), arXiv:0907.0323.
[3] Y. Levin, R. Pakter, F. B. Rizzato, T. N. Teles, and F. P. C. Benetti, Physics Reports **535**, 1 (2014).
[4] J. Barré, D. Mukamel, and S. Ruffo, Phys. Rev. Lett. **87**, 30601 (2001).
[5] L. Casetti and M. Kastner, Physica A: Statistical Mechanics and its Applications **384**, 318 (2007).
[6] M. Kastner, Phys. Rev. Lett. **104**, 240403 (2010), arXiv:1003.2347 [cond-mat.stat-mech].
[7] H. Spohn, *Large Scale Dynamics of Interaction*, 1st ed., edited by W. H. Lieb , Elliot,(Princeton), Beiglbock, Wolf, (Heidelberg), Regge, Tullio, (Universita Torino), Geroch, Robert, (Chicago), Thirring, Walter (Springer-Verlag, Berlin, Germany, 1992).
[8] S. Goldstein, S. Cuperman, and M. Lecar, Monthly Notices of the Royal Astronomical Society **143**, 209 (1969).
[9] M. Lecar and L. Cohen, "Numerical experiments on lynden-bell's statistics," in *Gravitational N-Body Problem: Proceedings of the Iau Colloquium No. 10 Held in Cambridge, England August 12–15, 1970*, edited by M. Lecar (Springer Netherlands, Dordrecht, 1972) pp. 262–275.
[10] J. Barré, F. Bouchet, T. Dauxois, and S. Ruffo, Phys. Rev. Lett. **89**, 110601 (2002).
[11] J. Barré, F. Bouchet, T. Dauxois, and S. Ruffo, Eur. Phys. J. B. **29**, 577 (2002).
[12] Y. Y. Yamaguchi, J. Barré, F. Bouchet, T. Dauxois, and S. Ruffo, Physica A: Statistical Mechanics and its Applications **337**, 36 (2004).
[13] Y. Yamaguchi, Phys. Rev. E **78**, 041114 (2008).
[14] M. Joyce and T. Worrakitpoonpon, Phys. Rev. E **84**, 011139 (2011).
[15] Y. Y. Yamaguchi and S. Ogawa, Phys. Rev. E **92**, 042131 (2015).
[16] D. Lynden-Bell, Mon. Not. R. Astron. Soc. **136**, 101 (1967).
[17] R. Pakter and Y. Levin, Phys. Rev. Lett. **106**, 200603 (2011).
[18] T. N. Teles, Y. Levin, and R. Pakter, Monthly Notices of the Royal Astronomical Society: Letters **417**, L21 (2011).
[19] J. Binney and S. Tremaine, *Galactic dynamics* (Princeton university press, 2011) pp. 289–291.
[20] D. Lynden-Bell, Physica A Statistical Mechanics and its Applications **263**, 293 (1999), arXiv:cond-mat/9812172 [cond-mat.stat-mech].
[21] D. Lynden-Bell and R. Wood, Monthly Notices of the Royal Astronomical Society **138**, 495 (1968).
[22] F. J. Dyson, Comm. Math. Phys. **12**, 91 (1969).
[23] M. E. Fisher, S.-k. Ma, and B. G. Nickel, Phys. Rev. Lett. **29**, 917 (1972).
[24] P. Bruno, Phys. Rev. Lett. **87**, 137203 (2001).
[25] D. Peter, S. Müller, S. Wessel, and H. P. Büchler, Phys. Rev. Lett. **109**, 025303 (2012), arXiv:1203.1624 [cond-mat.quant-gas].
[26] M. F. Maghrebi, Z.-X. Gong, and A. V. Gorshkov, Phys. Rev. Lett. **119**, 023001 (2017).
[27] N. D. Mermin and H. Wagner, Phys. Rev. Lett. **17**, 1133 (1966).
[28] W. Braun and K. Hepp, Commun. Math. Phys. **56**, 101 (1977).
[29] E. H. Lieb and H.-T. Yau, Astrophys. J. **323**, 140 (1987).
[30] S. A. Cannas, A. C. N. de Magalhães, and F. A. Tamarit, Phys. Rev. B **61**, 11521 (2000).
[31] A. Campa, A. Giansanti, and D. Moroni, Phys. Rev. E **62**, 303 (2000).
[32] F. Tamarit and C. Anteneodo, Phys. Rev. Lett. **84**, 208 (2000).
[33] J. Barré, F. Bouchet, T. Dauxois, and S. Ruffo, Journal of Statistical Physics **119**, 677 (2005).
[34] A. Campa and P.-H. Chavanis, Journal of Statistical Mechanics: Theory and Experiment **2010**, P06001 (2010).
[35] T. Mori, Phys. Rev. E **82**, 060103 (2010).
[36] T. Mori, Phys. Rev. E **84**, 031128 (2011).
[37] T. Mori, Journal of Statistical Mechanics: Theory and Experiment **2013**, P10003 (2013).
[38] I. Hahn and M. Kastner, The European Physical Journal B - Condensed Matter and Complex Systems **50**, 311 (2006).
[39] A. Campa and S. Ruffo, Physica A: Statistical Mechanics and its Applications **369**, 517 (2006).
[40] A. Campa, S. Ruffo, and H. Touchette, Physica A: Statistical Mechanics and its Applications **385**, 233 (2007).
[41] M. Antoni and S. Ruffo, Phys. Rev. E **52**, 2361 (1995).
[42] V. Latora, A. Rapisarda, and S. Ruffo, Physica D: Nonlinear Phenomena **131**, 38 (1999), classical Chaos and its Quantum Manifestations.
[43] F. Ginelli, K. A. Takeuchi, H. Chaté, A. Politi, and A. Torcini, Phys. Rev. E **84**, 066211 (2011).
[44] T. Manos and S. Ruffo, Transport Theory and Statistical Physics **40**, 360 (2011), arXiv:1006.5341 [nlin.CD].
[45] L. H. M. Filho, M. A. Amato, and T. M. Rocha Filho, Journal of Statistical Mechanics: Theory and Experiment **3**, 033204 (2018), arXiv:1704.02678 [cond-mat.stat-mech].
[46] J. Barr, F. Bouchet, T. Dauxois, S. Ruffo, and Y. Y. Yamaguchi, Physica A: Statistical Mechanics and its Applications **365**, 177 (2006), fundamental Problems of Modern Statistical Mechanics.
[47] W. Ettoumi and M.-C. Firpo, Journal of Physics A: Mathematical and Theoretical **44**, 175002 (2011), 15 pages.
[48] R. Plestid, P. Mahon, and D. H. J. O'Dell, Phys. Rev. E **98**, 012112 (2018), arXiv:1610.01582.
[49] G. Giachetti and L. Casetti, arXiv e-prints (2019), arXiv:1902.02436 [cond-mat.stat-mech].
[50] P. Chavanis, J. Stat. Mech. Theory Exp. **2011**, P08003 (2011).
[51] M. Kac, G. E. Uhlenbeck, and P. Hemmer, Journal of Mathematical Physics **4** (1963).
[52] J. Barr and F. Bouchet, Comptes Rendus Physique **7**, 414 (2006), statistical mechanics of non-extensive systems.
[53] S. Schütz and G. Morigi, Phys. Rev. Lett. **113**, 203002 (2014).
[54] T. Keller, V. Torggler, S. B. Jger, S. Schtz, H. Ritsch, and G. Morigi, New Journal of Physics **20**, 025004 (2018).
[55] S. Sachdev, *Quantum Phase Transitions* (Cambridge University Press, 2000).
[56] K. Kim, M.-S. Chang, R. Islam, S. Korenblit, L.-M. Duan, and C. Monroe, Phys. Rev. Lett. **103**, 120502 (2009).
[57] J. Zeiher, J.-y. Choi, A. Rubio-Abadal, T. Pohl, R. van Bijnen, I. Bloch, and C. Gross, Phys. Rev. X **7**, 041063 (2017).
[58] R. Islam, C. Senko, W. C. Campbell, S. Korenblit, J. Smith, A. Lee, E. E. Edwards, C.-C. J. Wang, J. K. Freericks, and C. Monroe, Science **340**, 583 (2013).
[59] P. Chavanis, J. Stat. Mech. Theory Exp. **2011**, P08002 (2011).

[60] R. Plestid and D. H. J. O'Dell, arXiv e-prints (2018), arXiv:1810.02420 [nlin.PS].
[61] T.-L. Ho and S. K. Yip, Phys. Rev. Lett. **84**, 4031 (2000).
[62] Y. Castin and C. Herzog, Comptes Rendus de l'Acadmie des Sciences - Series IV - Physics **2**, 419 (2001), arXiv:cond-mat/0012040.
[63] F. Olver, D. Lozier, R. Boisvert, and C. Clark, *NIST Handbook of mathematical functions*, Vol. 5 (Cambridge University Press, 2010) p. 966.
[64] A. Auerbach, *Interacting electrons and quantum magnetism* (Springer Science & Business Media, 2012).
[65] N. Schupper and N. M. Shnerb, Phys. Rev. E **72**, 046107 (2005).
[66] M. Sellitto, Phys. Rev. B **73**, 180202 (2006).

"Generalizing the HMF model to the quantum regime is the natural next step in the systematic exploration of the properties of this model since its introduction in 1995."

— Pierre Henri Chavanis

CHAPTER 5

Conclusions and Outlook

In this thesis we have laid out three preliminary studies of the HMF model's quantum behaviour. Our workhorse has been the GGPE which assumes that the model's ground state is a product state with no correlations. In Chapter 2 we outlined the dynamical consequences of the GGPE and found that many of the HMF model's classical dynamical features are reproduced within the quantum regime, but that quantum pressure ultimately disfavours focussing; often the features of the dynamics can be understood in terms of universal diffraction integrals. These effects were most pronounced in the case of repulsive interactions where late-time focussing can be inhibited entirely by quantum pressure, even when the short-time dynamics are largely unaffected by the quantum pressure. We learned that the $\chi \to 0$, $t \to \infty$, and $N \to \infty$ limits likely do not commute with one another.

In Chapter 3 we found exact solutions to the HMF model's GGPE. We focussed on the attractive case, however the same methods are readily applied to the case of attractive interactions. We developed a systematic asymptotic expansion for these solutions in the limit of $\chi \to 0$, and studied the linear stability of the solitary waves. We found that the long-range interactions in the HMF model were able to support not just a single solitary wave (as in the typical GPE) but many such solutions.

Finally, in Chapter 4 using the analytic solutions developed in Chapter 3 we explored the role of quantum fluctuations in determining the symmetry breaking pattern within the HMF model. We focussed on gapless (i.e. Goldstone) modes corresponding to translations of the centre of mass. We systematically computed the matrix elements of the Hamiltonian between Hartree states with different centre of mass wavefunctions, and ultimately found that it was energetically favourable to restore the $O(2)$ symmetry via quantum fluctuations. However, the energetic cost of breaking the $O(2)$ symmetry

was found to vanish in the $N \to \infty$ limit, and so, much as in Chapter 1, subtle questions related to the commutativity of the $N \to \infty$, $\chi \to 0$, and $T \to 0$ limits naturally arose. Nevertheless, our result firmly establishes that quantum fluctuations can invalidate mean-field theory in a LRI-MB system, contrary to conventional wisdom.

These three papers are only the first few steps towards a better understanding of the HMF model's quantum behaviour, and by extension of quantum LRI-MB systems more generally. From where we stand today there are a few different directions that one could explore to help further our understanding of quantum LRI-MB systems.

5.1 Path Integral Monte Carlo

A natural next-step from Chapter 4 is to understand the phase diagram of the HMF model in the full $\chi - T$ plane. In Chapter 4 we conjecture some possible behaviors that could exist, and we strongly advocate for a full path integral worm Monte Carlo (or other method appropriate for many-body Bose systems) to take place. Determining if the model exhibits a re-entrant phase would be the primary objective of such a study.

5.2 Low-energy effective description

A complimentary direction moving forward would be to develop a low-energy effective theory that is capable of describing the HMF model at low temperatures in the hopes of learning how to develop a universal low-energy descirption of a wide class of long-ranged models. In short-range systems local effective field theories and the renormalization group provide a convenient scheme for understanding the low-energy behaviour of a system without recourse to its underlying microphysical details. Rather, knowing only the relvant low-energy excitations and the symmetries that govern them, an effective theory can be constructed using a derivative expansion. Unlike for short-range interactions, a LRI-MB system is likely to be described by a *non-local* effective theory. Consequently there is no universal derivative expansion to be carried out. Since the HMF model is relatively tractable, it may be possible to study its low-energy excitations directly, and to develop an effective theory in terms of those excitations. The Path integral Monte Carlo approach outlined above would provide an immediate testing ground for any such predictions.

5.3 Cavity Realization of the HMF Model

Finally, it would be of great interest to realize the HMF model in the lab. The most likely route to doing so would be using a cavity-mediated interaction, much like the one discussed in [58]. So far there only exist proposals for the generalized HMF model (defined on a torus rather than the unit circle). It is likely possible to realize the HMF model by including additional cavity modes, perhaps by using circularly polarized light. If this were possible, then such a set-up would realize a quantum simulation of the HMF model, naturally complimenting the approaches outlined above. This would then make the HMF model a bonafide sandbox for LRI-MB physics in the quantum regime.

Bibliography

[1] N. D. Mermin and H. Wagner. "Absence of Ferromagnetism or Antiferromagnetism in One- or Two-Dimensional Isotropic Heisenberg Models". In: *Phys. Rev. Lett.* 17 (22 1966), pp. 1133–1136.

[2] S. Coleman. "There are no Goldstone bosons in two dimensions". In: *Comm. Math. Phys.* 31.4 (1973), pp. 259–264.

[3] J. Goldstone. "Field theories with « Superconductor » solutions". In: *Il Nuovo Cimento (1955-1965)* 19.1 (1961), pp. 154–164.

[4] J. Barré, D. Mukamel, and S. Ruffo. "Inequivalence of Ensembles in a System with Long-Range Interactions". In: *Phys. Rev. Lett.* 87 (2001), p. 30601.

[5] A. Campa, T. Dauxois, and S. Ruffo. "Statistical mechanics and dynamics of solvable models with long-range interactions". In: *Phys. Rep.* 480.3-6 (2009), pp. 57–159.

[6] Lapo Casetti and Michael Kastner. "Partial equivalence of statistical ensembles and kinetic energy". In: *Physica A: Statistical Mechanics and its Applications* 384.2 (2007), pp. 318 –334.

[7] T. Dauxois, S. Ruffo, E. Arimondo, and M. Wilkens. *Dynamics and Thermodynamics of Systems with Long Range Interactions*. Lecture Notes in Physics. Springer Berlin Heidelberg, 2008.

[8] W. Braun and K. Hepp. "The Vlasov dynamics and its fluctuations in the $1/N$ limit of interacting classical particles". In: *Commun. Math. Phys.* 56.2 (1977), pp. 101–113.

[9] H. Spohn. *Large scale dynamics of interacting particles*. Texts and monographs in physics. Springer-Verlag, 1991.

[10] P. H. Chavanis. "Dynamics and thermodynamics of systems with long-range interactions: interpretation of the different functionals". In: *AIP Conference Proceedings* 970.1 (2008), pp. 39–90.

[11] Y. Levin, R. Pakter, F. B. Rizzato, T. N. Teles, and F. P. C. Benetti. "Nonequilibrium statistical mechanics of systems with long-range interactions". In: *Physics Reports* 535.1 (2014), pp. 1 –60.

[12] Ryan Plestid, Perry Mahon, and D. H. J. O'Dell. "Violent relaxation in quantum fluids with long-range interactions". In: *Phys. Rev. E* 98 (1 2018), p. 012112.

[13] J. Barré, F. Bouchet, T. Dauxois, and S. Ruffo. "Out-of-Equilibrium States as Statistical Equilibria of an Effective Dynamics in a System with Long-Range Interactions". In: *Phys. Rev. Lett.* 89.11 (2002), p. 110601.

[14] AS Eddington. "The internal constitution of the stars". In: *The Observatory* 43 (1920), pp. 341–358.

[15] Donald Lynden-Bell. "Statistical Mechanics of Violent Relaxation in Stellar Systems". In: *Mon. Not. R. Astron. Soc.* 136 (1967), pp. 101–121.

[16] D. Lynden-Bell and R. Wood. "The gravo-thermal catastrophe in isothermal spheres and the onset of red-giant structure for stellar systems". In: *Monthly Notices of the Royal Astronomical Society* 138 (1968), p. 495.

[17] T. Padmanabhan. "Statistical mechanics of gravitating systems". In: *Physics Reports* 188.5 (1990), pp. 285 –362.

[18] D. Lynden-Bell. "Negative specific heat in astronomy, physics and chemistry". In: *Physica* A263 (1999), pp. 293–304.

[19] J. Binney and S. Tremaine. *Galactic dynamics*. Princeton university press, 2011, pp. 289–291.

[20] A. A. Vlasov. "On vibrational properties of electron gas". In: *Zh. ETF* 8.3 (1938), p. 291.

[21] L. D. Landau. "On the vibrations of the electronic plasma". In: *J. Phys.(USSR)* 10 (1946). [Zh. Eksp. Teor. Fiz.16,574(1946)], pp. 25–34.

[22] A. A. Vlasov. "The vibrational properties of an electron gas". In: *Usp. Fiz. Nauk* 93.11 (1967), pp. 444–470.

[23] J. A. S. Lima, R. Silva, and Janilo Santos. "Plasma oscillations and nonextensive statistics". In: *Phys. Rev. E* 61 (3 2000), pp. 3260–3263.

[24] R. Fitzpatrick. *Plasma Physics: An Introduction*. Taylor & Francis, 2014.

[25] Freeman J. Dyson. "Existence of a phase-transition in a one-dimensional Ising ferromagnet". In: *Comm. Math. Phys.* 12.2 (1969), pp. 91–107.

[26] Michael E. Fisher, Shang-keng Ma, and B. G. Nickel. "Critical Exponents for Long-Range Interactions". In: *Phys. Rev. Lett.* 29 (14 1972), pp. 917–920.

[27] K. Kim, M.-S. Chang, R. Islam, S. Korenblit, L.-M. Duan, and C. Monroe. "Entanglement and Tunable Spin-Spin Couplings between Trapped Ions Using Multiple Transverse Modes". In: *Phys. Rev. Lett.* 103 (2009), p. 120502.

[28] S. Korenblit, D. Kafri, W. C. Campbell, R. Islam, E. E. Edwards, Z.-X. Gong, G.-D. Lin, L.-M. Duan, J. Kim, K. Kim, and C. Monroe. "Quantum Simulation of Spin Models on an Arbitrary Lattice with Trapped Ions". In: *New J. Phys.* 14 (2012), p. 095024.

[29] J. Schachenmayer, B. P. Lanyon, C. F. Roos, and A. J. Daley. "Entanglement Growth in Quench Dynamics with Variable Range Interactions". In: *Phys. Rev. X* 3 (3 2013), p. 031015.

[30] R. Islam, C. Senko, W.C. Campbell, S. Korenblit, J. Smith, A. Lee, E. E. Edwards, C.-C. J. Wang, J. K. Freericks, and C. Monroe. "Emergence and Frustration of Magnetic Order with Variable-Range Interactions in a Trapped Ion Quantum Simulator". In: *Science* 340 (2013), p. 583.

[31] Philip Richerme, Zhe-Xuan Gong, Aaron Lee, Crystal Senko, Jacob Smith, Michael Foss-Feig, Spyridon Michalakis, Alexey V. Gorshkov, and Christopher Monroe. "Non-local propagation of correlations in long-range interacting quantum systems". In: *arXiv e-prints*, arXiv:1401.5088 (2014), arXiv:1401.5088.

[32] Z.-X. Gong, M. F. Maghrebi, A. Hu, M. L. Wall, M. Foss-Feig, and A. V. Gorshkov. "Topological phases with long-range interactions". In: *Phys. Rev. B* 93 (4 2016), p. 041102.

[33] L. Santos, G. V. Shlyapnikov, P. Zoller, and M. Lewenstein. "Bose-Einstein Condensation in Trapped Dipolar Gases". In: *Phys. Rev. Lett.* 85 (9 2000), pp. 1791–1794.

[34] D. O'Dell, S. Giovanazzi, G. Kurizki, and V. M. Akulin. "Bose-Einstein Condensates with 1/r Interatomic Attraction: Electromagnetically Induced "Gravity"". In: *Phys. Rev. Lett.* 84 (2000), p. 5687.

[35] P. Pedri and L. Santos. "Two-Dimensional Bright Solitons in Dipolar Bose-Einstein Condensates". In: *Phys. Rev. Lett.* 95 (20 2005), p. 200404.

[36] A. Griesmaier, J. Werner, S. Hensler, J. Stuhler, and T. Pfau. "Bose-Einstein Condensation of Chromium". In: *Phys. Rev. Lett.* 94 (16 2005), p. 160401.

[37] S. Yi and L. You. "Trapped condensates of atoms with dipole interactions". In: *Phys. Rev. A* 63 (5 2001), p. 053607.

[38] D. H. J. O'Dell, S. Giovanazzi, and C. Eberlein. "Exact Hydrodynamics of a Trapped Dipolar Bose-Einstein Condensate". In: *Phys. Rev. Lett.* 92 (25 2004), p. 250401.

[39] K. Pawlowski and K. Rzazewski. "Dipolar dark solitons". In: *New J. Phys.* 17 (2015), p. 105006.

[40] S. Giovanazzi, G. Kurizki, I. E. Mazets, and S. Stringari. "Collective excitations of a" gravitationally" self-bound Bose gas". In: *Europhys. Lett.* 56 (2001), p. 1.

[41] G. Kurizki, S. Giovanazzi, D. O'Dell, and A. I. Artemiev. "New Regimes in Cold Gases via Laser-induced Long-Range Interactions". In: *Dyn. Thermodyn. Syst. with Long-Range Interact.* Lecture Notes in Physics. Springer Berlin Heidelberg, 2002, pp. 369–403.

[42] R. Heidemann, U. Raitzsch, V. Bendkowsky, B. Butscher, R. Löw, L. Santos, and T. Pfau. "Evidence for coherent collective Rydberg excitation in the strong blockade regime". In: *Phys. Rev. Lett.* 99 (2009), p. 163601.

[43] D. Comparat and P. Pillet. "Dipole blockade in a cold Rydberg atomic sample". In: *J. Opt. Soc. Am. B* 27 (2010), A208.

[44] A. Schwarzkopf, R. E. Sapiro, and G. Raithel. "Imaging spatial correlations of Rydberg excitations in cold atom clouds". In: *Phys. Rev. Lett.* 107 (2011), p. 103001.

[45] P. Schauß, M. Cheneau, M. Endres, T. Fukuhara, S. Hild, A. Omran, T. Pohl, C. Gross, S. Kuhr, and I. Bloch. "Observation of spatially ordered structures in a two-dimensional Rydberg gas". In: *Nature (London)* 491 (2012), p. 87.

[46] H. Schempp, G. Günter, S. Wüster, M. Weidemller, and S. Whitlock. "Correlated Exciton Transport in Rydberg-Dressed-Atom Spin Chains". In: *Phys. Rev. Lett.* 115 (2015), p. 093002.

[47] D. Barredo, H. Labuhn, S. Ravets, T. Lahaye, A. Browaeys, and C. S. Adams. "Coherent Excitation Transfer in a Spin Chain of Three Rydberg Atoms". In: *Phys. Rev. Lett.* 114 (11 2015), p. 113002.

[48] J. Zeiher, R. van Bijnen, P. Schauß, S. Hild, J. Choi, T. Pohl, I. Bloch, and C. Gross. "Many-body interferometry of a Rydberg-dressed spin lattice". In: *Nat. Phys.* 12 (2016), p. 1095.

[49] H. Labuhn, D. Barredo, S. Ravets, S. De Léséleuc, T. Macrì, T. Lahaye, and A. Browaeys. "Tunable two-dimensional arrays of single Rydberg atoms for realizing quantum Ising models". In: *Nature (London)* 534 (2016), p. 667.

[50] A. T. Black, H. W. Chan, and V. Vuletić. "Observation of Collective Friction Forces due to Spatial Self-Organization of Atoms: From Rayleigh to Bragg Scattering". In: *Phys. Rev. Lett.* 91 (2003), p. 203001.

[51] A. T. Black, H. W. Chan, and V. Vuletić. "Observation of Collective Friction Forces due to Spatial Self-Organization of Atoms: From Rayleigh to Bragg Scattering". In: *Phys. Rev. Lett.* 91 (2003), p. 203001.

[52] D. Porras and J. I. Cirac. "Effective Quantum Spin Systems with Trapped Ions". In: *Phys. Rev. Lett.* 92 (2004), p. 207901.

[53] Y. Colombe, T. Steinmetz, G. Dubois, F. Linke, D. Hunger, and J. Reichel. "Strong atom-field coupling for Bose-Einstein condensates in an optical cavity on a chip". In: *Nature* 450 (2007), p. 272.

[54] K Baumann, C. Guerlin, F Brennecke, and T. Esslinger. "Dicke quantum phase transition with a superfluid gas in an optical cavity". In: *Nature (London)* 464 (2010), p. 1301.

[55] Ferdinand Brennecke, Tobias Donner, Stephan Ritter, Thomas Bourdel, Michael Köhl, and Tilman Esslinger. "Cavity QED with a Bose-Einstein condensate". In: *Nature* 450.7167 (2007), pp. 268–271.

[56] R. Mottl, F. Brennecke, K. Baumann, R. Landig, T. Donner, and T. Esslinger. "Roton-Type Mode Softening in a Quantum Gas with Cavity-Mediated Long-Range Interactions". In: *Science* 336.6088 (2012), pp. 1570–1573.

[57] Helmut Ritsch, Peter Domokos, Ferdinand Brennecke, and Tilman Esslinger. "Cold atoms in cavity-generated dynamical optical potentials". In: *Rev. Mod. Phys.* 85 (2 2013), pp. 553–601.

[58] Stefan Schütz and Giovanna Morigi. "Prethermalization of Atoms Due to Photon-Mediated Long-Range Interactions". In: *Phys. Rev. Lett.* 113 (20 2014), p. 203002.

[59] A. Campa, A. Giansanti, G. Morigi, and Labini F.S. *Dynamics and thermodynamics of systems with long-range interactions: theory and experiments : Assisi, Italy, 4-8 July 2007*. AIP conference proceedings. American Institute of Physics, 2008.

[60] R. Mottl, F. Brennecke, K. Baumann, R. Landig, T. Donner, and T. Esslinger. "Roton-Type Mode Softening in a Quantum Gas with Cavity-Mediated Long-Range Interactions". In: *Science* 336 (2012), p. 1570.

[61] Renate Landig, Lorenz Hruby, Nishant Dogra, Manuele Landini, Rafael Mottl, Tobias Donner, and Tilman Esslinger. "Quantum phases from competing short- and long-range interactions in an optical lattice". In: *Nature* 532 (2016), pp. 476–479.

[62] T. Dauxois, V. Latora, and A. Rapisarda. "The Hamiltonian mean field model: from dynamics to statistical mechanics and back". In: *Dyn. Thermodyn. Syst. with Long-Range Interact.* Lecture Notes in Physics. Springer Berlin Heidelberg, 2002, pp. 458–487.

[63] M. Antoni and S. Ruffo. "Clustering and relaxation in Hamiltonian long-range dynamics". In: *Phys. Rev. E* 52.3 (1995), pp. 2361–2374.

[64] Alessandro Campa, Stefano Ruffo, and Hugo Touchette. "Negative magnetic susceptibility and nonequivalent ensembles for the mean-field ϕ^4 spin model". In: *Physica A: Statistical Mechanics and its Applications* 385.1 (2007), pp. 233 –248.

[65] T. N. Teles, Y. Levin, R. Pakter, and F. B. Rizzato. "Statistical mechanics of unbound two-dimensional self-gravitating systems". In: *J. Stat. Mech.* (2010), P05007.

[66] R. Pakter and Y. Levin. "Core-Halo Distribution in the Hamiltonian Mean-Field Model". In: *Phys. Rev. Lett.* 106 (20 2011), p. 200603.

[67] T. N. Teles, Y. Levin, and R. Pakter. "Statistical mechanics of 1D self-gravitating systems: the core-halo distribution". In: *Monthly Notices of the Royal Astronomical Society: Letters* 417.1 (2011), pp. L21–L25.

[68] M. Kac, G. E. Uhlenbeck, and P.C. Hemmer. "On the van der Waals Theory of the Vapor-Liquid Equilibrium. I. Discussion of a One-Dimensional Model". In: *Journal of Mathematical Physics* 4 (1963).

[69] Vito Latora, Andrea Rapisarda, and Stefano Ruffo. "Chaos and statistical mechanics in the Hamiltonian mean field model". In: *Physica D: Nonlinear Phenomena* 131.1 (1999). Classical Chaos and its Quantum Manifestations, pp. 38 –54.

[70] Francisco Tamarit and Celia Anteneodo. "Rotators with Long-Range Interactions: Connection with the Mean-Field Approximation". In: *Phys. Rev. Lett.* 84 (2 2000), pp. 208–211.

[71] Vito Latora, Andrea Rapisarda, and Constantino Tsallis. "Non-Gaussian equilibrium in a long-range Hamiltonian system". In: *Phys. Rev. E* 64 (5 2001), p. 056134.

[72] J. Barré, F. Bouchet, T. Dauxois, and S. Ruffo. "Birth and long-time stabilization of out-of-equilibrium coherent structures". In: *Eur. Phys. J. B.* 29.4 (2002), pp. 577–591.

[73] Y. Y. Yamaguchi, J. Barré, F. Bouchet, T. Dauxois, and S. Ruffo. "Stability criteria of the Vlasov equation and quasi-stationary states of the HMF model". In: *Physica A: Statistical Mechanics and its Applications* 337.1 (2004), pp. 36 –66.

[74] A. Pluchino, V. Latora, and A. Rapisarda. "Metastable states, anomalous distributions and correlations in the HMF model". In: *Physica D: Nonlinear Phenomena* 193.1 (2004). Anomalous distributions, nonlinear dynamics, and nonextensivity, pp. 315 –328.

[75] P. H. Chavanis, J. Vatteville, and F. Bouchet. "Dynamics and thermodynamics of a simple model similar to self-gravitating systems: the HMF model". In: *The European Physical Journal B - Condensed Matter and Complex Systems* 46.1 (2005), pp. 61–99.

[76] Pierre-Henri Chavanis. "Quasi-stationary states and incomplete violent relaxation in systems with long-range interactions". In: *Physica A: Statistical Mechanics and its Applications* 365.1 (2006). Fundamental Problems of Modern Statistical Mechanics, pp. 102 –107.

[77] Andrea Antoniazzi, Duccio Fanelli, Julien Barré, Pierre-Henri Chavanis, Thierry Dauxois, and Stefano Ruffo. "Maximum entropy principle explains quasistationary states in systems with long-range interactions: The example of the Hamiltonian mean-field model". In: *Phys. Rev. E* 75 (1 2007), p. 011112.

[78] A. Pluchino, A. Rapisarda, and C. Tsallis. "Nonergodicity and central-limit behavior for long-range Hamiltonians". In: *Europhysics Letters (EPL)* 80.2 (2007), p. 26002.

[79] Andrea Antoniazzi, Francesco Califano, Duccio Fanelli, and Stefano Ruffo. "Exploring the Thermodynamic Limit of Hamiltonian Models: Convergence to the Vlasov Equation". In: *Phys. Rev. Lett.* 98 (15 2007), p. 150602.

[80] T. Manos and S. Ruffo. "Scaling with System Size of the Lyapunov Exponents for the Hamiltonian Mean Field Model". In: *Transport Theory and Statistical Physics* 40.6-7 (2011), pp. 360–381.

[81] Shun Ogawa, Aurelio Patelli, and Yoshiyuki Y. Yamaguchi. "Non-mean-field critical exponent in a mean-field model: Dynamics versus statistical mechanics". In: *Phys. Rev. E* 89 (3 2014), p. 032131.

[82] P.H. Chavanis. "The quantum HMF model: II. Bosons". In: *J. Stat. Mech. Theory Exp.* 2011.08 (2011), P08003.

[83] P.H. Chavanis. "The quantum HMF model: I. Fermions". In: *J. Stat. Mech. Theory Exp.* 2011.08 (2011), P08002.

[84] Julien Barré, David Mukamel, and Stefano Ruffo. "Ensemble Inequivalence in Mean-Field Models of Magnetism". In: *Dynamics and Thermodynamics of Systems With Long Range Interactions. Edited by T. Dauxois, S. Ruffo, E. Arimondo, and M. Wilkens., Lecture Notes in Physics, vol. 602, p.45-67.* Ed. by T. Dauxois, S. Ruffo, E. Arimondo, and M. Wilkens. Vol. 602. 2002, pp. 45–67.

[85] Thierry Dauxois, Stefano Ruffo, Ennio Arimondo, and Martin Widlkens. "Dynamics and Thermodynamics of Systems with Long-Range Interactions: An Introduction". In: *Dynamics and Thermodynamics of Systems With Long Range Interactions. Edited by T. Dauxois, S. Ruffo, E. Arimondo, and M. Wilkens., Lecture Notes in Physics, vol. 602, p.1-19.* Ed. by T. Dauxois, S. Ruffo, E. Arimondo, and M. Wilkens. Vol. 602. 2002, pp. 1–19.

[86] Julien Barré and Freddy Bouchet. "Statistical mechanics and long range interactions". In: *Comptes Rendus Physique* 7.3 (2006). Statistical mechanics of non-extensive systems, pp. 414 –421.

[87] L.D. Landau and E.M. Lifshitz. *Statistical Physics*. v. 5. Elsevier Science, 1980.

[88] Mehran Kardar. *Statistical Physics of Fields*. Cambridge University Press, 2007.

[89] E. H. Lieb and H.-T. Yau. In: *ApJ* 323 (Dec. 1987), pp. 140–144.

[90] Sergio A. Cannas, A. C. N. de Magalhães, and Francisco A. Tamarit. "Evidence of exactness of the mean-field theory in the nonextensive regime of long-range classical spin models". In: *Phys. Rev. B* 61 (17 2000), pp. 11521–11528.

[91] Julien Barré, Freddy Bouchet, Thierry Dauxois, and Stefano Ruffo. "Large Deviation Techniques Applied to Systems with Long-Range Interactions". In: *Journal of Statistical Physics* 119.3 (2005), pp. 677–713.

[92] Alessandro Campa, Andrea Giansanti, and Daniele Moroni. "Canonical solution of a system of long-range interacting rotators on a lattice". In: *Phys. Rev. E* 62 (1 2000), pp. 303–306.

[93] Alessandro Campa and Pierre-Henri Chavanis. "A dynamical stability criterion for inhomogeneous quasi-stationary states in long-range systems". In: *Journal of Statistical Mechanics: Theory and Experiment* 2010.06 (2010), P06001.

[94] Takashi Mori. "Analysis of the exactness of mean-field theory in long-range interacting systems". In: *Phys. Rev. E* 82 (6 2010), p. 060103.

[95] Takashi Mori. "Instability of the mean-field states and generalization of phase separation in long-range interacting systems". In: *Phys. Rev. E* 84 (3 2011), p. 031128.

[96] Takashi Mori. "Phase transitions in systems with non-additive long-range interactions". In: *Journal of Statistical Mechanics: Theory and Experiment* 2013.10 (2013), P10003.

[97] Yoichiro Nambu. "Quasi-Particles and Gauge Invariance in the Theory of Superconductivity". In: *Phys. Rev.* 117 (3 1960), pp. 648–663.

[98] P. Bruno. "Absence of Spontaneous Magnetic Order at Nonzero Temperature in One- and Two-Dimensional Heisenberg and XY Systems with Long-Range Interactions". In: *Phys. Rev. Lett.* 87 (13 2001), p. 137203.

[99] de Sousa, J. R. "Phase diagram in the quantum XY model with long-range interactions". In: *Eur. Phys. J. B* 43.1 (2005), pp. 93–96.

[100] Mohammad F. Maghrebi, Zhe-Xuan Gong, and Alexey V. Gorshkov. "Continuous Symmetry Breaking in 1D Long-Range Interacting Quantum Systems". In: *Phys. Rev. Lett.* 119 (2 2017), p. 023001.

[101] P. H. Chavanis. "Kinetic theory of spatially inhomogeneous stellar systems without collective effects". In: *Astronomy & Astrophysics* 556, A93 (2013), A93.

[102] Y.Y. Yamaguchi. "One-dimensional self-gravitating sheet model and Lynden-Bell statistics". In: *Phys. Rev. E* 78 (4 2008), p. 041114.

[103] C.J. Pethick and H. Smith. *Bose-Einstein Condensation in Dilute Gases*. Cambridge University Press, 2002.

[104] N. N. Bogolyubov. "On the theory of superfluidity". In: *J. Phys.(USSR)* 11 (1947). [Izv. Akad. Nauk Ser. Fiz.11,77(1947)], pp. 23–32.

[105] A.A. Abrikosov, L.P. Gorkov, and I.E. Dzyaloshinski. *Methods of Quantum Field Theory in Statistical Physics*. Dover Books on Physics Series. Dover Publications, 1975.

[106] Kerson Huang and C. N. Yang. "Quantum-Mechanical Many-Body Problem with Hard-Sphere Interaction". In: *Phys. Rev.* 105 (3 1957), pp. 767–775.

[107] C. P. Burgess. "Introduction to Effective Field Theory". In: *Ann. Rev. Nucl. Part. Sci.* 57 (2007), pp. 329–362.

[108] Eric Braaten and Agustin Nieto. "Renormalization effects in a dilute Bose gas". In: *Phys. Rev. B* 55 (13 1997), pp. 8090–8093.

[109] Eric Braaten and Agustin Nieto. "Quantum corrections to the ground state of a trapped Bose-Einstein condensate". In: *Phys. Rev.* B56 (1997), pp. 14745–14765.

[110] Jens O. Andersen and Michael Strickland. "Application of renormalization-group techniques to a homogeneous Bose gas at finite temperature". In: *Phys. Rev. A* 60 (2 1999), pp. 1442–1450.

[111] Eric Braaten, H.-W. Hammer, and Shawn Hermans. "Nonuniversal effects in the homogeneous Bose gas". In: *Phys. Rev. A* 63 (6 2001), p. 063609.

[112] Jens O Andersen. "Theory of the weakly interacting Bose gas". In: *Rev. Mod. Phys.* 76 (2004), p. 599.

[113] L.P. Pitaevskii and S. Stringari. *Bose-Einstein Condensation*. Oxford University Press, 2003.

[114] C. W. Gardiner. "A Particle number conserving Bogolyubov method which demonstrates the validity of the time dependent Gross-Pitaevskii equation for a highly condensed Bose gas". In: *Phys. Rev.* A56.2 (1997), pp. 1414–1423.

[115] T Lahaye, C Menotti, L Santos, M Lewenstein, and T Pfau. "The physics of dipolar bosonic quantum gases". In: *Reports on Progress in Physics* 72.12 (2009), p. 126401.

[116] Pierre-Henri Chavanis and Tiberiu Harko. "Bose-Einstein condensate general relativistic stars". In: *Phys. Rev. D* 86 (6 2012), p. 064011.

[117] Joshua Eby, Madelyn Leembruggen, Lauren Street, Peter Suranyi, and L. C. R. Wijewardhana. "Approximation methods in the study of boson stars". In: *Phys. Rev. D* 98 (12 2018), p. 123013.

[118] Bertram R. Levy and Joseph B. Keller. "Low-Energy Expansion of Scattering Phase Shifts for Long-Range Potentials". In: *Journal of Mathematical Physics* 4.1 (1963), pp. 54–64.

[119] Eric Braaten and H.-W. Hammer. "Universality in the three-body problem for ^{4}He atoms". In: *Phys. Rev. A* 67 (4 2003), p. 042706.

[120] Leslie L. Foldy. "Charged Boson Gas". In: *Phys. Rev.* 124 (3 1961), pp. 649–651.

[121] Elliott H. Lieb, Robert Seiringer, Jan Philip Solovej, and Jakob Yngvason. "The Quantum-Mechanical Many-Body Problem: The Bose Gas". In: *Condensed Matter Physics and Exactly Soluble Models: Selecta of Elliott H. Lieb*. Ed. by Bruno Nachtergaele, Jan Philip Solovej, and Jakob Yngvason. Berlin, Heidelberg: Springer Berlin Heidelberg, 2004, pp. 351–435.

[122] Arnaud Triay. “Derivation of the dipolar Gross-Pitaevskii energy”. In: *arXiv e-prints*, arXiv:1703.03746 (2017), arXiv:1703.03746.